An evaluation of the checkpoint kinase inhibitor V158411

Peter Stephens

A thesis submitted to Newcastle University for the degree of Doctor of Philosophy

Northern Institute for Cancer Research

August 2014

Declaration

The work presented in this thesis was carried out at the Northern Institute for Cancer Research, Newcastle University between September 2010 and September 2013. These studies represent my own original work except where they are acknowledged by name or reference.

No part of this work is being, or has been, submitted for another degree or qualification at Newcastle University or another university.

Abstract

The aim of this work was to characterise the checkpoint 1 kinase (CHK1) inhibitor V158411; its effect on DNA damage-induced checkpoint function in parallel with chemo/radio-potentiation in a panel of cell lines characterised for their CHK1 expression and activity. Furthermore, to determine the single agent cytotoxicity in a panel of cell lines; to identify potential pharmacodynamic biomarkers of CHK1 activity suitable for measuring the activity of inhibitors in the clinic; and to explore the role of p53 and identify other potential determinants of sensitivity to CHK1 inhibitors.

V158411 on its own reliably reduces CHK1^{serine296} phosphorylation and gemcitabine-mediated induction of CHK1^{serine296} phosphorylation. Single agent V158411 reduces the fraction of cancer cells in G_2 of the cell cycle and abrogates cisplatin and IR-mediated increases in the proportion of cells in G_2.

V158411 shows significant single agent activity in a number of cell lines. There was significant potentiation of ionising radiation with V158411. There was no significant chemopotentiation of either gemcitabine or cisplatin with co-administration with V158411.

p53 status was not associated with significant differences in sensitivity to single agent V158411, chemo or radiosensitisation. However, loss of DNA-PKcs or the presence of a DNA-PKcs inhibitor conferred resistance to V158411. CHK1 and DNA-PKcs mRNA levels were found to be elevated in tumour samples compared to normal tissue levels. The LC_{50} of V158411 was shown to correlate with the inducible (2 Gy IR) phosphorylation of DNA-PKc^{sserine2096} in a panel of cancer cells.

Acknowledgements

I am extremely grateful to my supervisors Nicola Curtin and Ruth Plummer for supporting me during this project, together with other members of the Clinical and Translational Research Group at the Northern Institute for Cancer Research including Fiona Middleton, Miranda Patterson, Joanne Munck, Tao Chen and James Murray. I am very grateful to Andrew Massey from Vernalis for his advice and support at all stages of this project and for the provision of V158411 by Vernalis.

I wish to express my thanks to the Sir Bobby Robson Foundation for funding my post as a Clinical Research Associate and in particular the trustees for their investment in me.

Finally, I would like to thank my wife Cate and daughter Daisy for being patient with me over the last 3 years.

Table of Contents

List of Figures

List of Tables

Glossary

5FU	5-fluorouracil
AGT	see MGMT
AML	Acute myelogenous leukaemia
ARA-C	Cytarabine
AST	Advanced solid tumours
ATM	Ataxia telangiectasia mutated
ATR	Ataxia telangiectasia mutated and Rad3-related
ATRIP	ATR-interacting protein
AUC	Area under curve
BCNU	bis-chloroethylnitrosourea (also known as carmustine)
BER	Base excision repair
CDDP	Carboplatin
CDK	Cyclin-dependent kinase
Chk1	Checkpoint 1 kinase
Chk2	Checkpoint 2 kinase
CHLF	Chinese hamster lung fibroblasts
CHO	Chinese hamster ovary
CML	Chronic myeloid leukaemia
DMF	Disease modifying factor
DNA	Deoxy-ribose nucleic acid
DDR	DNA damage response
DLT	Dose-limiting toxicity

DSB	Double-strand break repair
FCS	Foetal calf serum
GI_{50}	Growth inhibitory concentration leading to 50% cell growth inhibition
GI_{90}	Growth inhibitory concentration leading to 90% cell growth inhibition
H2AX	H2A histone family member X
HRR	Homologous recombination repair
IC_{50}	Inhibitory concentration leading to 50% cell inhibition
IC_{90}	Inhibitory concentration leading to 90% cell inhibition
ICL	Intrastrand crosslink
IHC	Immunohistochemistry
i.p.	Intraperitoneal
IR	Ionising radiation
i.v.	Intravenous
LC_{50}	Lethal concentration leading to 50% cell death
LC_{90}	Lethal concentration leading to 90% cell death
MEF	Mouse embryonic fibroblasts
MGMT	O^6-methylguanine DNA methyltransferase
MMR	Mismatch repair
MRN	Mre-11-Rad50-Nbs1
mRNA	Messenger ribose nucleic acid
MSI	Microsatellite instability
MTD	Maximum tolerated dose

NER	Nucleotide excision repair
NHEJ	Non-homologous end-joining
NSCLC	Non-small cell lung cancer
PARP	Poly (ADP-ribose) polymerase
PCR	Polymerase chain reaction
PD	Pharmacodynamic
PK	Pharmacokinetic
PKC	Protein kinase C
RER	Radiation enhancement ratio
RNR	Ribonucleotide reductase
ROS	Reactive oxygen species
RPA	Replication protein A
SCC	Squamous cell carcinoma
shRNA	Short hairpin ribose nucleic acid
siRNA	Small interfering ribose nucleic acid
SN38	Irinotecan (active metabolite)
SRB	Sulphurhodamine B
SSA	Single-strand annealing
SSB	Single-strand break
SSBR	Single-strand break repair
STR	Short tandem repeat
TGI	Tumour growth inhibition
UV	Ultraviolet
XP	Xeroderma pigmentosa

Chapter 1 Introduction

1.1 Background

DNA can be damaged by a range of exogenous and endogenous agents. In response to DNA damage the cell cycle has checkpoints under the control of regulatory proteins that allow the cell cycle to be halted and to provide time for DNA repair. This prevents the accumulation of mutations that are harmful to the cell. Unfortunately, it can also reverse the intended effects of cytotoxic and radiation therapy. Chemotherapy and radiotherapy aim to deliver lethal damage to the DNA of tumour cells. Most malignant cells appear to have a defective G_1 checkpoint and rely on their S and G_2 checkpoints for DNA repair and cell survival (Massague, 2004). The aim of targeting the S and G_2 checkpoints is to improve tumour cell kill with relative sparing of normal tissues with a functional G_1 checkpoint. Figure 1.1 describes the cell cycle and its checkpoints.

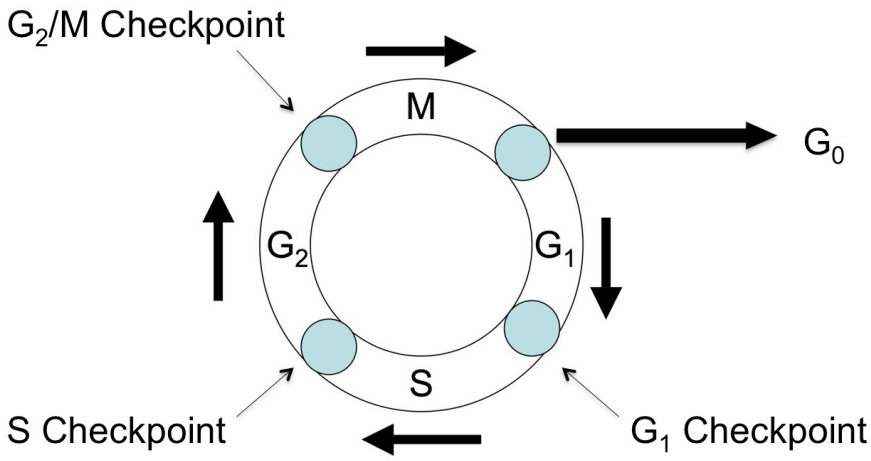

Figure 1-1 Cell cycle and checkpoints.

Progression of cell cycle and the position of G_1, S and G_2/M cell cycle checkpoints and exit point to G_0.

1.2 DNA damage and response (DDR)

Maintaining a stable genome is required for the correct function of cells and the prevention of acquisition and transmission of mutations.

There are three naturally occurring threats that lead to damage to DNA and the integrity of the genome (Hoeijmakers, 2001, Hoeijmakers, 2009).

- Environmental agents. These include ultraviolet radiation, solar ionising radiation and chemicals (e.g. aflatoxin) that are toxic to the genome.

- Endogenous products of cellular metabolism. Examples include reactive oxygen species from oxidative respiration and lipid peroxidation

- Endogenous spontaneous DNA damage due to replication errors, and nucleotides may undergo hydrolysis, methylation and demethylation.

In addition chemotherapy and therapeutic ionising radiation cause damage to DNA in a wide variety of ways.

The cell attempts to repair any damage that occurs to DNA by mounting a DNA damage response (DDR). Any attempt at DNA repair requires detection of DNA damage, transient cell cycle arrest and subsequent repair. The outcome of attempted DNA repair may be:

a) Success and the restoration of an intact genome.

b) Failure of DNA repair and the acquisition of mutations and chromosomal abnormalities that may lead to ageing or cancer

c) Failure of DNA repair and subsequent cell death.

Failure to repair DNA can result in genomic instability that is an enabling characteristic of cancer (see Figure 1-2) (Hanahan and Weinberg, 2011).

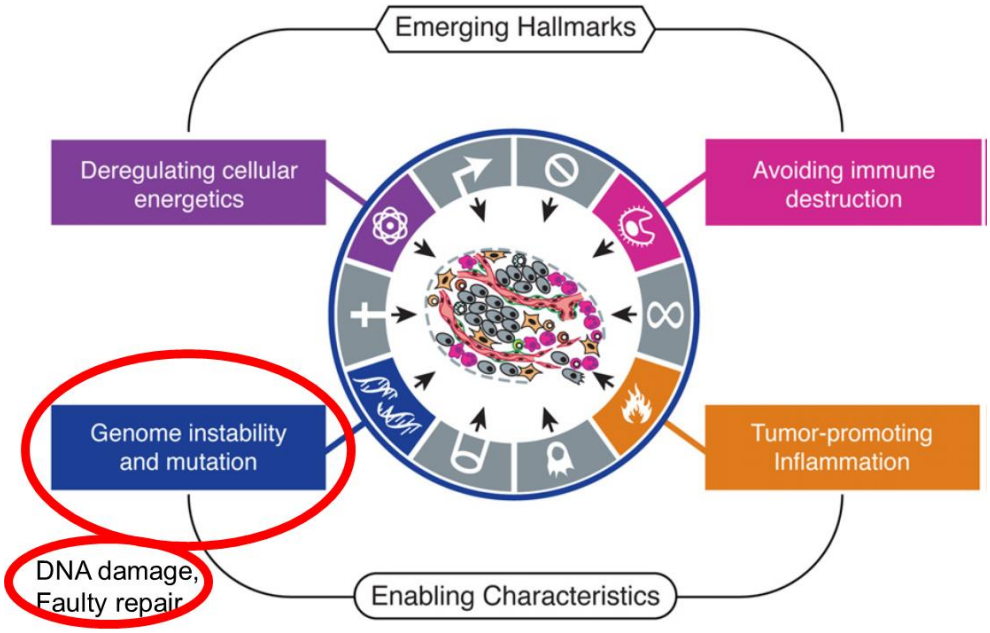

Figure 1-2 Characteristics of cancer

Characteristics of cancer demonstrating the role of DNA damage and faulty repair in carcinogenesis. Adapted from (Hanahan and Weinberg, 2011)

1.3 DNA repair

There are a variety of types of damage that can be induced in DNA and a corresponding range of different DNA repair mechanisms that deal with specific types of DNA lesion (Sehl et al., 2009, Curtin, 2012, Bouwman and Jonkers, 2012). See table 1.1 for a summary of the main DNA repair pathways.

Single strand repair

1.3.1 Direct repair

O^6-methylguanine lesions are sometimes formed naturally by incorrect methylation by s-adenosyl methionine (Tricker et al., 1991). If unrepaired these lesions are mutagenic. O^6-methylguanine DNA methyltransferase (MGMT – previously known as AGT) can repair these lesions by demethylation. Guanine can be alkylated in the O^6-position by other sources including dietary nitrosamines, nitrosated amines and bile acids (Tubbs et al., 2007). O^6-alkyl lesions are also caused by therapeutic intervention with alkylating agents (eg: the pro drugs dacarbazine and the oral agent temozolomide) and nitrosureas (BCNU/carmustine) (Saffhill et al., 1985). These lesions can be repaired by MGMT. High expression of MGMT is associated with resistance to temozolomide and carmustine (Tsuzuki et al., 1996). A schematic detailing this repair pathway is shown in Figure 1-6.

Repair Pathway	Direct Repair	BER and SSBR	NER	HRR	NHEJ	MMR
Lesion	O^6-methyl guanine	8-oxoguanine N^7-meG N^3-meA Uracil Hypoxanthine Xanthine SSB	Cyclopurines Bulky adducts 6-4 photo-products	Stalled replication forks	DNA double strand breaks	Base pair mismatches
Endogenous and environmental causes	Dietary nitrosamines Bile acids S-adenosyl methionine	Reactive oxygen species S-adenosyl methionine Environmental IR Base deamination/loss	Reactive oxygen species UV Tobacco smoke Affiatoxin	Unrepaired single strand lesions	Reactive oxygen species Environmental IR	Replication errors S-adenosyl methionine Base deamination
Therapeutic causes	Temozolomide Alkylating agents Nitrosureas	Temozolomide IR Antimetabolites Topoisomerase poisons Radiomimetics	Nitrosureas Platinum compounds	Temozolomide Topoisomerase poisons Antimetabolites	IR Topoisomerase poisons Radiomimetics	Temozolomide Nucleoside analogues

Table 1-1 DNA Repair Mechanisms

IR: ionising radiation; BER: base excision repair; SSBR: single strand break repair; NER: nucleoside excision repair; UV: ultraviolet; HRR: homologous recombination repair; NHEJ: non-homologous end joining; MMR: mismatch repair.

1.3.2 Base-excision repair (BER) and single strand break repair (SSBR)

BER is the pathway by which non-bulky damaged DNA bases are repaired (Kinsella, 2009). The process of BER leads to transient single-strand breaks (SSB), that are repaired by the downstream aspects of BER and SSBR. The bulk of DNA damage is repaired by BER because between 10000 and 100000 base lesions occur in every cell every day (Lindahl, 1993). These lesions are largely mediated by reactive oxygen species (ROS) and reactive nitrogens (Valko et al., 2006). Oxidation by ROS forms 8-oxoguanine and 5-hydroxycytosine, these 'false bases' can incorrectly pair with adenine and thymine, respectively. ROS are produced as a natural product of respiration and the inflammatory response. Other endogenous base damage may occur e.g. tRough spontaneous deamination of cytosine, aberrant methylation of the N7 position of guanine and N3 of adenine and miss-incorporation of faulty nucleotides during replication. Tumours have a high level of inflammation and hence ROS leading to more oxidative damage to DNA leading and subsequent SSBs that require repair (Halliwell, 2007).

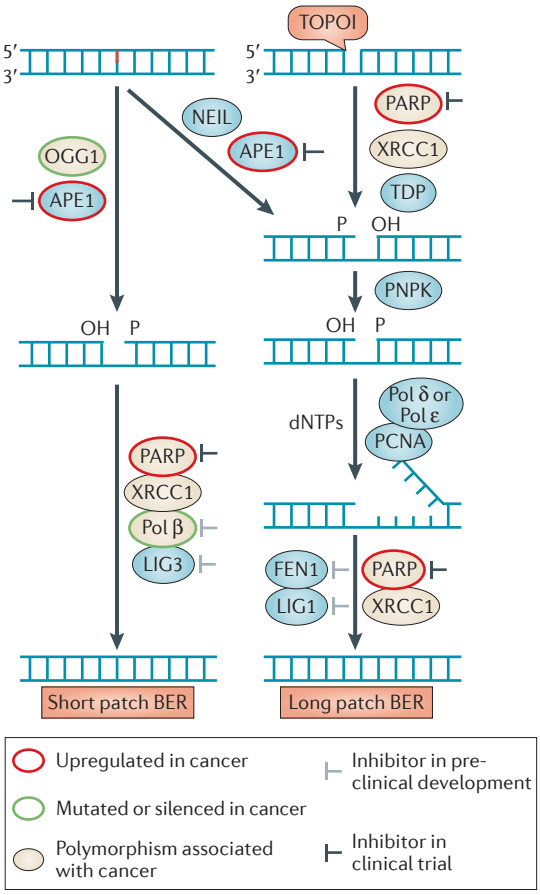

Figure 1-3 Base excision repair (BER)

Adapted from (Curtin, 2012). Two versions of BER – short patch BER predominates over long patch BER. In short patch BER a single nucleotide is replaced by DNA polymerase-β and in long patch up to 13 nucleotides can be replaced by DNA polymerase δ or ε.

The damaged bases are removed by DNA glycosylases, creating an A-P site that is the target for A-P endonuclease (O'Connor and Laval, 1991). This generates a 'nick' or SSB that is repaired by DNA polymerases and DNA ligases supported by PARP-1 (poly(ADP-ribose) polymerase 1) and PARP-2 (De Vos et al., 2012). Two forms of BER exist; short patch BER where a single nucleotide is replaced, or long patch BER where 2 to 13 nucleotides require replacing.

Exogenous damage can lead directly to SSBs. Sources of exogenous damage that can cause SSBs include ionising radiation (both natural and therapeutic mediated by ROS), alkylating chemotherapy, topoisomerase inhibitors, and anti-metabolites (thiopurines, flouropyrimidines and halogenated thymidine analogues). IR can also induce DNA strand breaks directly. Dysfunctional BER can lead to sensitivity to chemotherapy (temozolomide and alkylators) and IR.

1.3.3 Nucleotide-excision repair (NER)

NER (see Figure 1-4) involves the removal of bulky adducts that are too large to be removed by BER. Bulky adducts will distort the DNA helix so must be removed. There are 3 stages to NER; recognition of the abnormality, removal of 25-30 nucleotides in the damaged segment of DNA followed by repair of the gap in the DNA (Buschta-Hedayat et al., 1999, Naegeli and Sugasawa, 2011). Environmental stressors including UV light, tobacco smoke, aflatoxin and polycyclic aromatic hydrocarbons lead to the formation of a bulky adduct that prevents DNA transcription (Hoeijmakers, 2001). Some chemotherapy also causes DNA damage that cause interstrand and intrastrand crosslinks (ICLs) are treated in the same way as bulky adducts. Nitrosureas, and the diamine-platinum compounds cisplatin and carboplatin cause such ICLs. The bulky adducts are removed by NER. Two forms of NER occur – global genome NER and transcription coupled repair. Xeroderma pigmentosa (XP) proteins and ERCC1 are important for effective NER and ICL repair. Cells that are defective in components of the NER pathway are more sensitive to platinum-based therapy (Koberle et al., 1997).

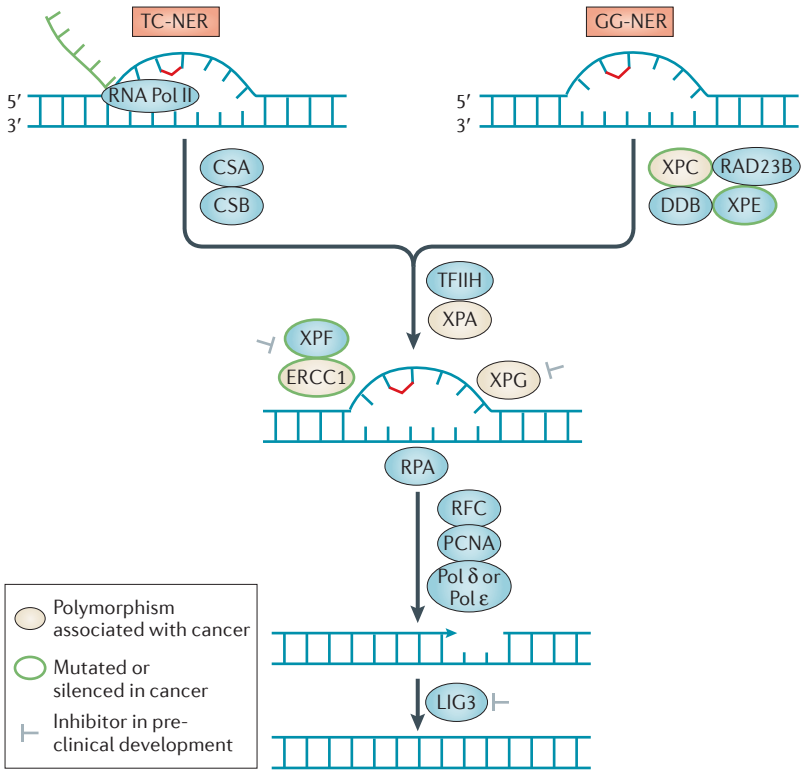

Figure 1-4 Nucleotide excision repair (NER)

Adapted from (Curtin, 2012). Two forms of exist with a final common pathway. TC-NER and GG-NER.

Double strand break (DSB) repair

DSB are relatively rare (10-50 per cell per day), but highly cytotoxic and difficult to repair (Vilenchik and Knudson, 2003). The difficulty in repairing DSBs means they are dangerous for cell viability and if unrepaired can lead to cell death; if they are incorrectly repaired they can lead to chromosomal translocations which can be a significant step in carcinogenesis (Jeggo and Lobrich, 2007).

There are two methods of DSB repair: homologous recombination repair (HRR) and non-homologous end joining (NHEJ). The choice of which pathway is used is dependent on a number of factors (Shibata et al., 2011).

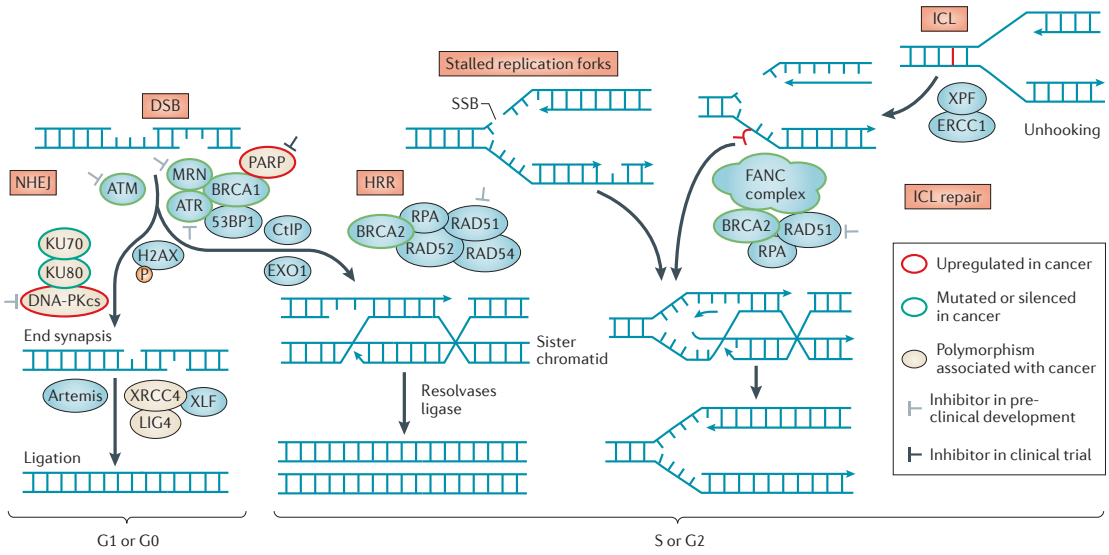

Figure 1-5 DNA double strand and interstrand crosslink repair

Adapted from (Curtin, 2012). NHEJ (non-homologous end joining) occurs during G_0 or G_1 of the cell cycle; HRR (homologous recombination repair) and ICL (interstrand cross-link) repair occur during S phase or G_2.

1.3.4 Homologous recombination repair (HRR).

HRR requires the sister chromatid to act as a template so can only repair DSBs during G_2 and S phase (Aylon et al., 2004). HRR is the preferred method of DSB repair as, if successful, it has a lower error rate than other methods. The broken ends adjacent to the DSB are resected so that overlapping single strands of DNA can invade the sister chromatid that is used as a template to repair broken DNA.

Unrepaired single strand breaks will lead to stalled replication forks. Though less common than SSBs, this scenario is very serious for a cell so requires a dedicated efficient repair mechanism. Any type of chemotherapy that can cause a single strand break can also cause stalled replication forks. Single strand breaks are converted into DSBs as the replication fork collides with the SSB. Ionising radiation and some types of chemotherapy (eg: etoposide) cause DSBs. However, platinum compounds cause intrastrand cross-links between guanine residues (5'-GG-3' and 5'-GNG-3') and adenine and guanine residues (5'-AG-3'), but no frank DSBs (Noll et al., 2006). The collision of a platinum-mediated cross-link with the replication fork will cause replication fork collapse (Annunziata and O'Shaughnessy, 2010). Failure of DSB repair leads to loss of chromosome fragments and if the wrong ends are ligated together chromosome translocations (Sehl et al., 2009).

Cells that lack functional BRCA1 or BRCA2, or other components of HRR can not perform HRR and DSB DNA repair has to be by NHEJ which is more prone to errors (see Figure 1-5). Tumours that have HRR defects are sensitive to most types of cytotoxic therapy, but are exquisitely sensitive to cross-linking agents such as platinum, IR and to topoisomerase I inhibitors. HRR is dependent on the Chk1-mediated phosphorylation of BRCA2 and RAD51 (Bahassi et al., 2008).

1.3.5 Non-homologous end-joining (NHEJ)

DNA DSBs can also be repaired by NHEJ. Such breaks can be caused directly by reactive oxygen species, IR (both natural and therapeutic) and

topoisomerase II inhibitors. IR causes approximately 1 DSB for every 25 SSBs (Nikjoo et al., 2001). NHEJ and single-strand annealing (SSA) are less accurate than HRR, but can repair DSBs that occur during G_0 and G_1 when only one copy of the DNA is available. NHEJ accounts for the repair of more than 85% of IR-mediated DSBs (Mahaney et al., 2009). NHEJ is more error prone than HRR and there is the potential for the loss or gain of nucleotides (up to 20 nucleotides can be lost or gained). NHEJ is dependent on DNA-PK, Ku70, Ku80, XRCC4 and DNA ligase IV and artemis (Takata et al., 1998, Kysela et al., 2005).

1.3.6 Mismatch repair (MMR)

Errors in replication may lead to the mismatch of bases (ie: A:C or T:G, insertion of additional nucleotides or the removal of bases (Kinsella, 2009). Insertions and deletions can lead to frame-shift mutations. Mismatches normally occur during S phase of the cell cycle. The commonest cause of base mismatches is faulty replication, but therapy with nucleoside analogues and temozolomide can also cause mismatches.

Mismatches are repaired by MMR, the mechanism of MMR is outlined in Figure 1-6. MMR recognition of lesions relies on MSH2 and MSH6 where an incorrect nucleotide has been inserted and a MSH2 and MSH3 heterodimer recognises deletions and insertions of additional nucleotides (Acharya et al., 1996). This particularly occurs in repetitive sequences (microsatellites) leading to microsatellite instability (MSI) in cells, which have defective MMR. Defects in

MMR cause tolerance to temozolomide and platinum induced DNA lesions and hence drug resistance (Irving and Hall, 2001).

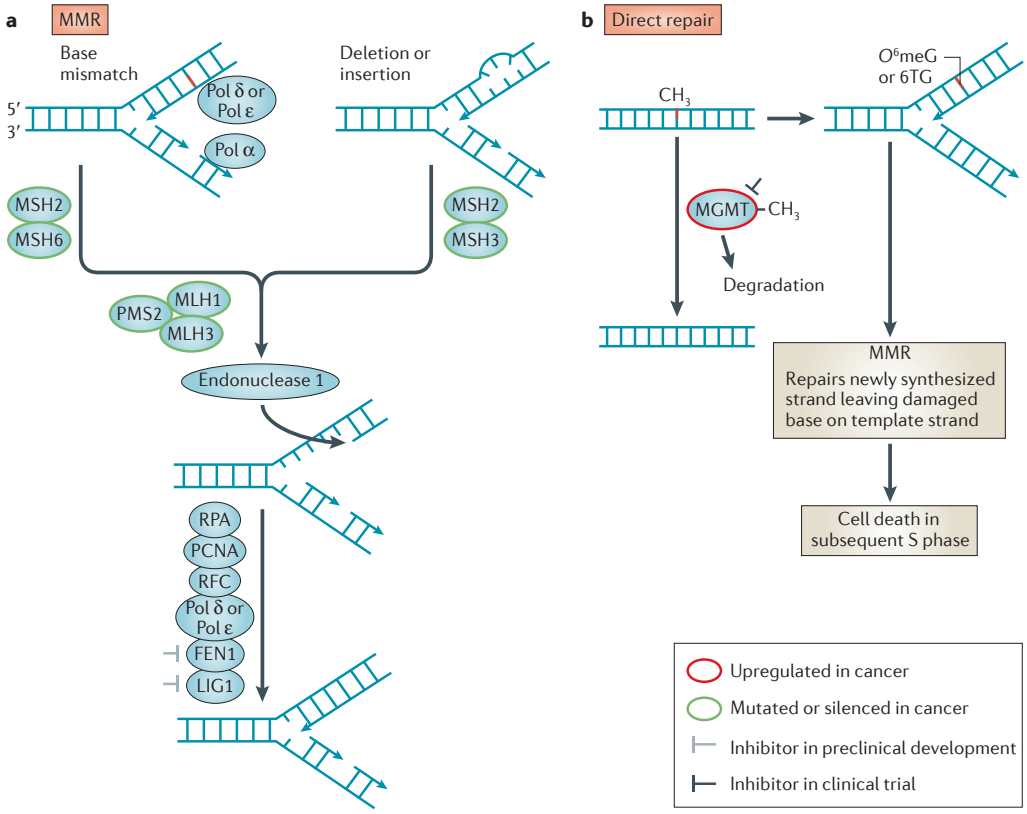

Figure 1-6 Mismatch repair (MMR) and Direct repair

Adapted from (Curtin, 2012). MMR repairs defects where incorrect base pairing has occurred and where there have been insertions or deletions. Direct repair is involved in the repair of O^6-methylguanine lesions.

1.4 Anticancer agents used in combination with CHK1 inhibitors

The subject of this thesis is the evaluation of a novel CHK1 inhibitor. Previously described CHK1 inhibitors, in pre-clinical *in vitro* and *in vivo* work and clinical trials with CHK1 inhibitors have been investigated in combination with certain types of chemotherapy, mainly antimetabolites, topoisomerase poisons and DNA cross-linking agents, and radiotherapy as described below.

1.4.1 Antimetabolites,

Antimetabolites interfere with DNA synthesis, either as inhibitors of the anabolism of deoxynucleotides or fraudulent nucleoside analogues, that may inhibit enzymes necessary to synthesise natural nucleotides or be incorporated into the DNA.

Cytarabine (also known as ARA-C) is an analogue of the nucleoside, cytosine. It competitively inhibits DNA polymerase (Kufe et al., 1984). It acts as a false nucleoside leading to partial chain termination. Ara-CTP is formed from cytarabine and then incorporated into DNA. The rate of incorporation of cytarabine into DNA correlates with the loss of clonogenic survival in pre-clinical studies in acute myelogenous leukaemia (AML). It only has an effect on proliferating cells in S phase. Cytarabine is used in acute and chronic leukaemias.

Gemcitabine is another antimetabolite deoxycytidine analogue. It is phosphorylated intracellularly by deoxycytidine kinase and phosphorylated gemcitabine depletes the cellular pools of dNTPs via the inhibition of

ribonucleotide reductase (Plunkett et al., 1995). Incorporation of gemcitabine triphosphate into DNA causes the stalling of the DNA polymerase one base beyond the incorporation site (Huang et al., 1991). This leads to partial chain termination (where DNA polymerase ε cannot extend the 3' terminus) and the stalling of replication forks. Gemcitabine is highly toxic to cells in S phase and prevents their progression into G_2. Gemcitabine is used in the treatment of pancreatic cancer, lung cancer and breast cancer. It is commonly used in combination with platinum compounds

5FU (5-fluorouracil) is an antimetabolite nucleobase that acts as a pyrimidine antagonist (Pinedo and Peters, 1988). 5FU itself is an inactive pro-drug. It enters the cell by the uracil transporter and is converted to FUdR by thymidine phosphorylase and then to FdUMP by thymidine kinase. FdUMP is converted into FdUTP; αdUMP is converted into dUTP. FdUTP and dUTP are incorporated into DNA and then excised by uracil glycosylases leading to single strand breaks in the DNA. There is an accumulation of dUMP. 5FU is also available as the oral pro-drug capecitabine. Capecitabine is not active itself but converted by carboxylesterase, cytidine deaminase and thymidine phosphorylase to form 5FU (Shewach and Lawrence, 2007). The manufacturers claim that as thymidine phosphorylase is more abundant in tumours compared to normal tissues higher final concentrations of 5FU are found in tumours following the oral administration of capecitabine. 5FU and capecitabine are the mainstays of treatment for colorectal cancer; they are also used in the treatment of upper gastrointestinal malignancy and breast cancer.

Hydroxyurea (also known as hydroxycarbamide) has been in clinical use for the treatment of leukaemias since the 1960's. It was shown to block the

incorporation of thymidine into DNA (Young and Hodas, 1964). Though this mechanism partly contributes to the cytotoxicity of hydroxyurea, its principle mechanism is inhibition of ribonucleotide reductase (RNR). RNR converts nucleoside diphosphates into deoxynucleoside diphosphates thus depleting cellular deoxynucleoside triphosphates for DNA synthesis (Xie and Plunkett, 1996). Hydroxyurea is currently used in the treatment of chronic myeloid leukaemia (CML).

1.4.2 Topoisomerase poisons

Topoisomerases modify the tertiary structure of DNA, they are essential to DNA replication as they cleave, unwind and re-ligate DNA to relieve torsional stresses in supercoiled DNA (Pommier et al., 1998a, van Maanen et al., 1988). This initiates the uncoiling of DNA to allow for transcription. Topoisomerase I and II poisons mediate their cytotoxicity in late S phase and G_2 respectively. Topoisomerase I cleaves a single strand of DNA and topoisomerase II cleaves both. Topoisomerase poisons stabilise the cleavable complex to prevent completion of the cycle, resulting in topoisomerase-associated DNA breaks. Topoisomerase I poisons cause SSB and topoisomerase II poisons DSBs.

Etoposide is a semi-synthetic member of the family of epipodophyllotoxins. Etoposide's primary mode of action is as a topoisomerase II poison (van Maanen et al., 1988, Hande, 1998). It may also inhibit mitosis by blocking microtubule assembly. Cells treated with etoposide accumulate in late S and G_2. It is used in the treatment of germ cell tumours, small cell lung cancer, sarcomas and acute leukaemias

Irinotecan, and its active metabolite SN-38, are topoisomerase I poisons (Pommier et al., 1998b). Irinotecan is a semi-synthetic derivative of camptothecin. Camptothecin is an alkaloid drug derived from the tree *Camptotheca acuminata*. Irinotecan is metabolized to the active drug SN-38 by a carboxylesterase. Cell-based pre-clinical studies often use the topoisomerase I poison camptothecin or the pro-drug SN-38 neither of which are used in clinical practice with irinotecan being used for *in vivo* studies. Irinotecan is used either alone or in combination with 5FU in the treatment of colorectal cancer. It is also used in combination with other chemotherapy in the treatment of sarcoma.

1.4.3 DNA cross-linking agents

Platinum chemotherapy (cisplatin, carboplatin and oxaliplatin) causes platinum-DNA adducts that result in intrastrand and interstrand cross-links; these prevent DNA replication and ultimately leads to apoptosis. (Raymond et al., 1998) (Siddik, 2003). Other platinum-based compounds have been used in pre-clinical research. Platinum compounds also cause mild impairment of RNA and protein synthesis. The cross-links caused by platinum chemotherapy seem to be most damaging in S phase.

Cisplatin and carboplatin are diamine-platinum compounds (Rixe et al., 1996). Both platinum based drugs act in a similar way but have differing profiles of which tumour types are sensitive or resistant. They also differ in toxicity profile; carboplatin is the most myelosuppressive, and cisplatin is associated with greater renal toxicity and ototoxicity.

Platinum chemotherapy is very widely used in upper gastrointestinal malignancy, colorectal cancer, lung cancer and germ cell malignancies. Cisplatin is also used as a radio-sensitising agent in head and neck and cervical cancer.

1.4.4 Anti-tubulin agents

The growth and contraction of tubulin fibres connecting the spindle poles with the centromeres of chromosomes is an obligatory step in the segregation of chromosomes at mitosis and thus anti-tubulin agents disrupt this process. There are two types, the vinca alkaloids, which prevent tubulin assembly, and the taxanes, which promote microtubule assembly, but then prevent the disassembly by preventing tubulin depolymerisation. Paclitaxel (Taxol™) is a taxane used in breast, ovarian and other cancers. It was originally synthesised from the bark of the yew tree. Its synthetic analogue Docetaxel (Taxotere™) is also used as a cytotoxic in breast cancer, upper gastrointestinal cancer and some types of sarcoma. There is a spindle checkpoint which delays anaphase onset if spindle defects have occurred.

1.4.5 Ionising radiation

Ionising radiation (IR) leads to DNA damage in a number of ways (Teoule, 1987). Radiation can cause a wide range of DNA damage including SSBs, DSBs, base modifications and an entity unique to radiation-induced damage known as ‘clustered damage sites’ (Harper et al., 2010). The authors

demonstrated that radiation-induced SSBs and other radiation-induced DNA damage lead to the formation of DSBs during replication and these can be quantified by RAD51 foci formation *in vitro* assays. The response to IR differs between cells that are directly targeted and 'bystander' cells (Burdak-Rothkamm and Prise, 2009). Directly targeted cells have energy-dependent IR-mediated DNA damage. Bystander cells have a different profile of response to IR, but are key recruiters of the DNA damage response via ATM and ATR.

A number of the cytotoxic therapies discussed in this section can be used as radiosensitisers. Gemcitabine, cisplatin and 5FU have been used effectively as radiosensitisers in *in vitro* and *in vivo* studies and have been used in the treatment of some tumour types (Shewach and Lawrence, 2007). Cisplatin is used widely as a radiosensitiser in the treatment of head and neck cancers, cervical cancer and in conjunction with 5FU in the treatment of oesophageal cancers. Gemcitabine is used in conjunction with radiotherapy in the treatment of pancreatic cancers. Temozolomide is used with radiation in the management of glioblastoma multiforme.

1.5 Cell cycle arrest

The cell cycle is under the control of checkpoints that trigger cell cycle arrest in response to DNA damage. The pathway depends on sensors, transducers and effectors (Zhou and Elledge, 2000). The downstream kinase and signalling cascade has been explored in the literature in great detail; however, the mechanism by which DNA damage is detected at the molecular level remains unclear (Tse et al., 2007a).

It has been shown that part of the DNA repair apparatus, Mre-11-Rad50-Nbs1 (MRN), is not only involved in the repair of broken DNA ends, but also acts as a sensor of DNA damage (Moreno-Herrero et al., 2005). This is important in the ATM pathway where MRN acts to recruit ATM to DSBs and the Nbs1 component activates ATM (Yoshiyama et al., 2013). The MRN recruits other factors including BRCA1, the mediator of DNA-damage checkpoint 1 (MDC1) and p53-binding protein (53BP1) (Shiloh, 2006). The downstream kinase cascades are explored in more detail in Chapters 1.6.4 – 1.6.7

The level of DNA damage that is required to trigger cell cycle arrest had been shown to be a single DSB based on data from yeast (Bennett et al., 1997). However, work with mammalian fibroblasts has suggested that there is a threshold below which cells are released from G_2/M arrest even if some DSBs persist (Lobrich and Jeggo, 2007). Persistent DSBs in mammalian fibroblasts have been quantified by measuring γ-H2AX foci. The threshold for cell cycle arrest is between 10-20 DSBs.

The sensitivity of the G_1 checkpoint to DNA damage is less well understood. It appears that the G_1 checkpoint has a higher sensitivity than the G_2/M

checkpoint and may even be able to respond to a single site of DNA damage (d'Adda di Fagagna et al., 2003).

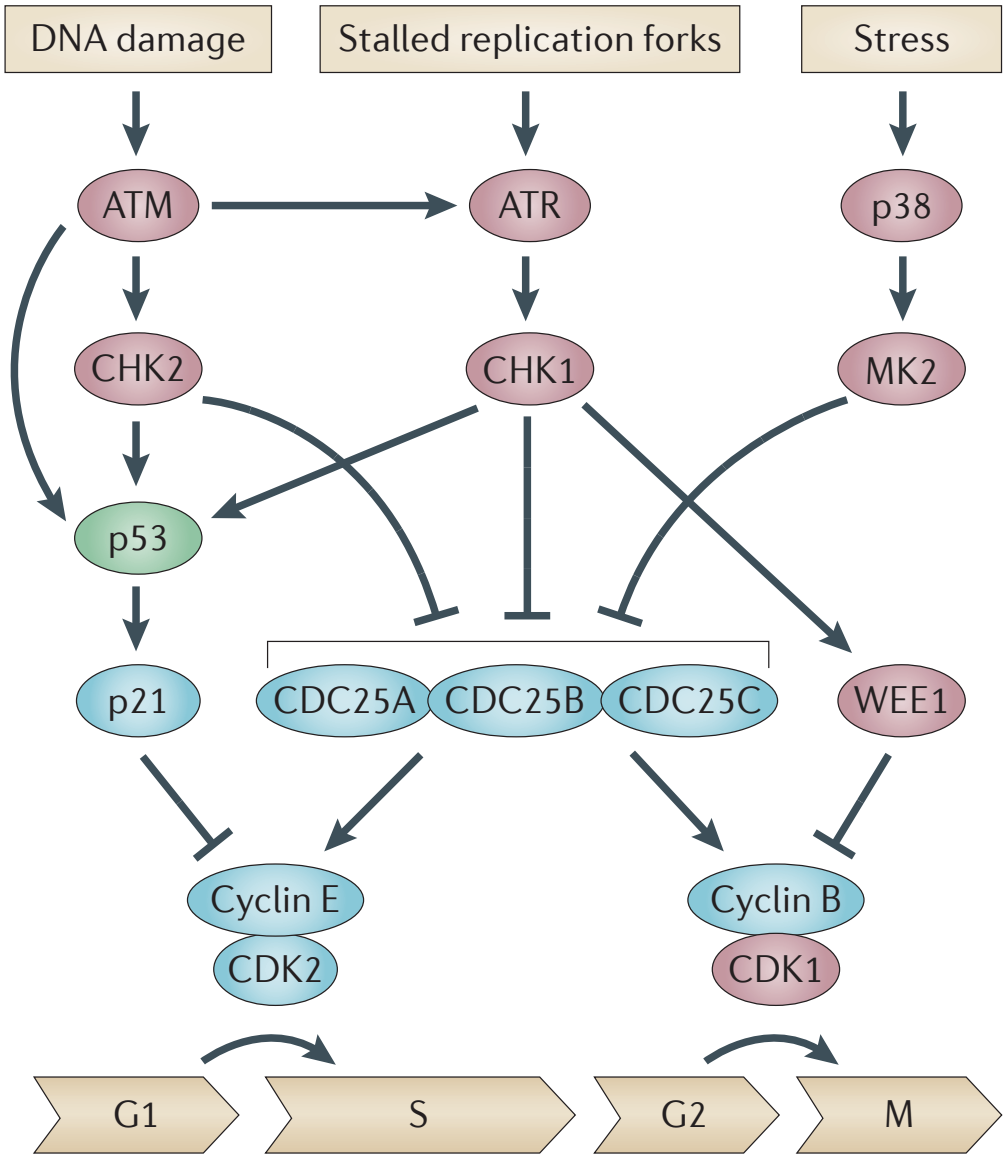

Figure 1-7 The role of ATM, ATR, CHK1 and CHK2 in the DDR

The interactions (arrows denote activation and T-bars denote inhibition) of CHK1 with p53, CDC25A, CDC25B, CDC25C and Wee1: adapted from (Bouwman and Jonkers, 2012).

1.5.1 Loss of G_1 checkpoint in cancer

Loss of G_1 cell cycle checkpoint control is common in cancers (Massague, 2004). The most well documented defects affect p53, but other defects are also important. DNA replication in G_1 is triggered by some of the CDK family.

Important elements of this pathway at G_1 include cdk2, cyclins E1 and E2 and cyclin A (Murray, 2004). Figure 1-8 demonstrates the role of cdk2 at the G_1 checkpoint, but also shows many other elements of the pathway including ATM/p53/p21 and Rb/E2/F1-3. Aberrations in any of these elements can lead to loss of G_1 cell cycle checkpoint control.

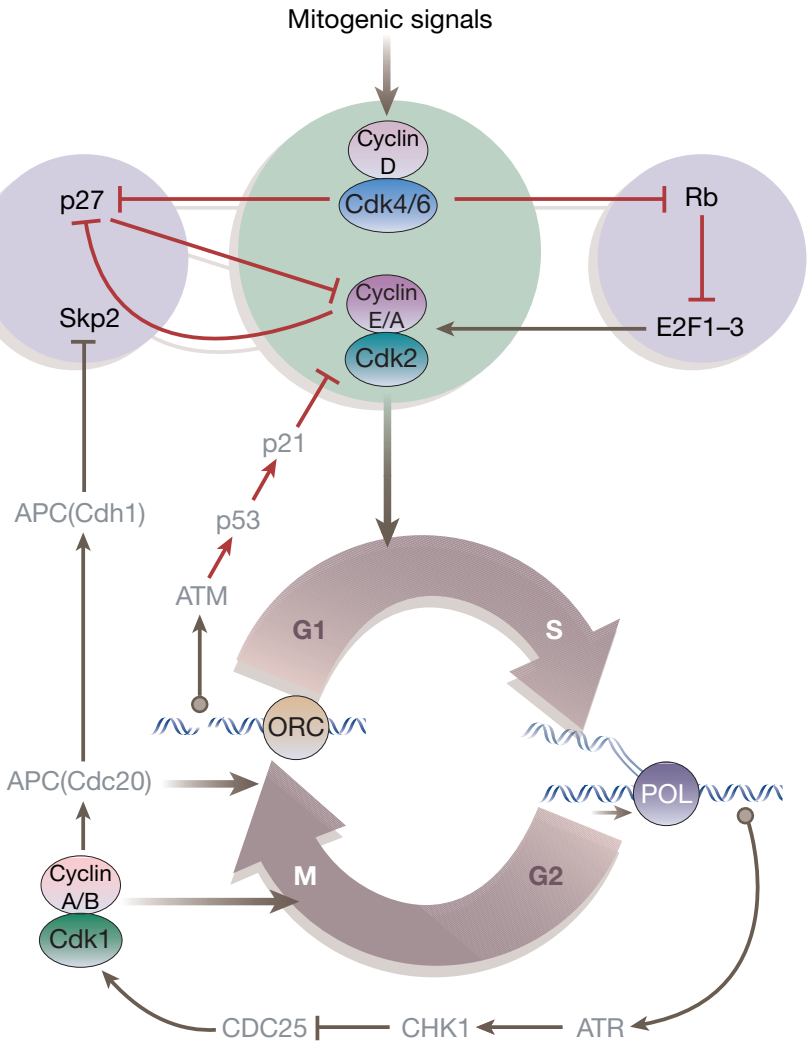

Figure 1-8 The control of G_1 cell cycle checkpoint

The control of the G1 cell cycle checkpoint and the role of cdk2/cyclinE/cyclin A, ATM/p53/p21 and Rb/E2/F1-3. Arrows denote activation and T-bars denote inhibition. Adapted from (Massague, 2004)

Loss of one cell cycle checkpoint leads to a greater dependence on other checkpoints within the cell cycle (Paulovich et al., 1997). This phenomenon has been demonstrated in a number of studies that have sought to abrogate the G_2/M checkpoint in cells with a constitutive defect in the G_1/S phase checkpoint (Powell et al., 1995, Russell et al., 1995). Therefore, cancer cells are exquisitely dependent on S and G_2 checkpoint.

p53 is a classical tumour suppressor gene; its relationship with other important components of the DNA damage response pathway is shown in Figure 1-8. DNA damage signalling and repair in G_1 is mediated by the phosphorylation and subsequent activation of repair and cell cycle proteins by ATM and the p53 tumour suppressor gene (Levine, 1997). p53 is also activated by ATM via CHK2 and directly by CHK1 (Bouwman and Jonkers, 2012). Activated p53 stimulates the expression of p21 (inhibits CDK2, CDK4 and CDK6) leading to cyclin-dependent kinase (Cdk)-mediated cell cycle arrest at both the G_1 and G_2/M checkpoints (Vogelstein et al., 2000).

1.5.2 The role of ATR and CHK1 inhibition in anti-cancer therapy

The rationale for using ATR or CHK1 inhibitors in combination with conventional cytotoxic therapy (either chemotherapy or ionising radiation) in clinical trials is as follows (see Figure 1-9). Many types of cytotoxic therapy seek to kill tumour cells by causing DNA damage leading to subsequent cell death. This affects both tumour cells and normal tissues, particularly those that are undergoing active replacement or turnover.

However, cell cycle checkpoint activation allows a window of time for DNA repair to take place. Many cancer cells lack a functional G_1 cell cycle checkpoint and so are dependent on the S and G_2 cell cycle checkpoints, which are under the control of the ATR-CHK1 pathway (Sherr, 1996, Massague, 2004). Therefore, inhibiting this pathway, in combination with conventional cytotoxic therapy, in cells lacking functional G_1 checkpoint, results in failure to arrest in response to DNA damage, accumulation of DNA damage leading to cell death. Since normal cells retain the G_1 checkpoint inhibition of the S/G_2 checkpoint with ATR or CHK1 inhibitors in combination with conventional cytotoxics should lead to preferential cytotoxicity in tumour cells.

This principle is known as synthetic lethality (Kaelin, 2005). Sometimes mutations in two individual genes may lead to a viable cell if only one mutation is present, but if mutations in both genes occur in the same cell they are lethal. This is has been extrapolated into drug development where a drug is non-toxic in normal cells, but in cancer cells with a functional mutation the presence of the drug is lethal. An example of this is PARP inhibitors which are non-toxic to normal tissues but in cancer cells with a BRCA1 or BRCA2 mutation inhibition of PARP leads to cumulative DNA damage and cell death.

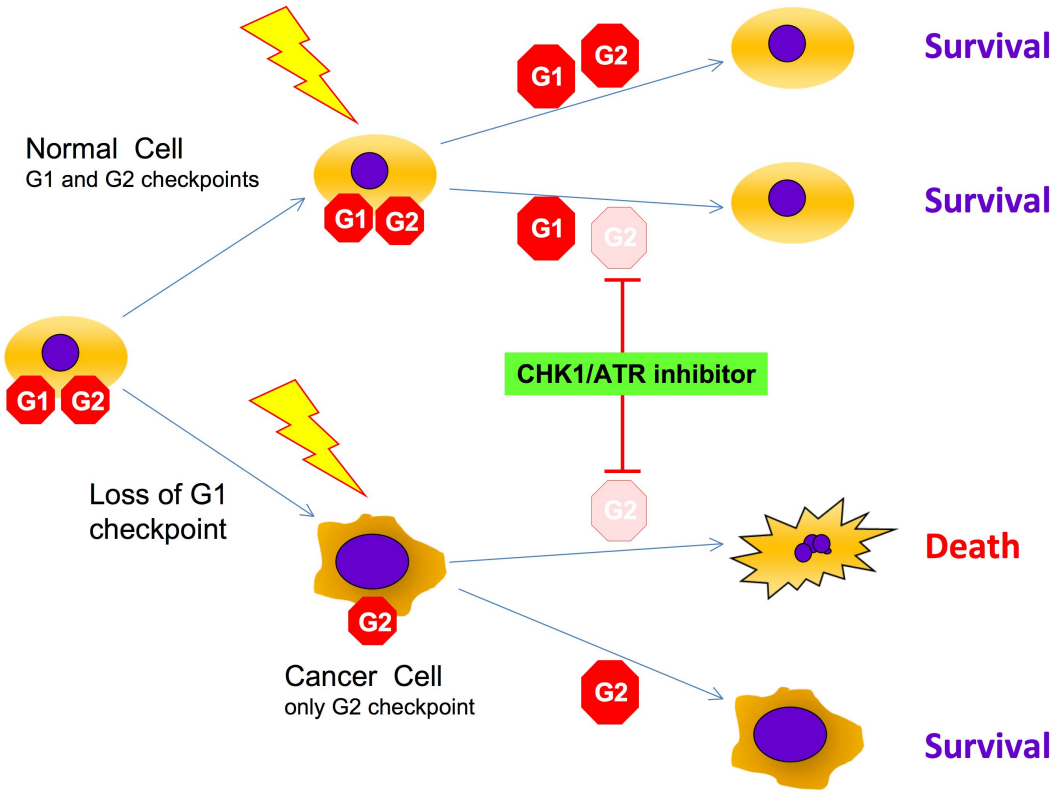

Figure 1-9 The effect of CHK1 or ATR inhibition on cancer cells with loss of the G_1 checkpoint.

Normal cells with a functional G_1 cell cycle checkpoint can pause their cell cycle following DNA damage even with exposure to a CHK1 or ATR inhibitor. Tumour cells, with a loss of a functional G_1 cell cycle checkpoint, are dependent on their G_2 cell cycle checkpoint to mediate cell cycle arrest and DNA repair following DNA damage. The addition of a CHK1 or ATR inhibitor in conjunction with a DNA damaging agent may selectively kill tumour cells over normal tissue.

1.6 Checkpoint 1 kinase (CHK1)

1.6.1 Structure and activity of CHK1

CHK1 gene is found on chromosome 11 at 11q24.2 and comprises 16 coding exons (Sanchez et al., 1997). It encodes a protein kinase that has an N-terminal kinase domain, linker, regulatory domain and C-terminal domain (Patil et al., 2013). The crystal structure was first published in 2000 by Chen et al and is shown in Figure 1-10 (Chen et al., 2000). Checkpoint 1 kinase (CHK1) is a protein kinase that has a number of roles in cell cycle regulation.

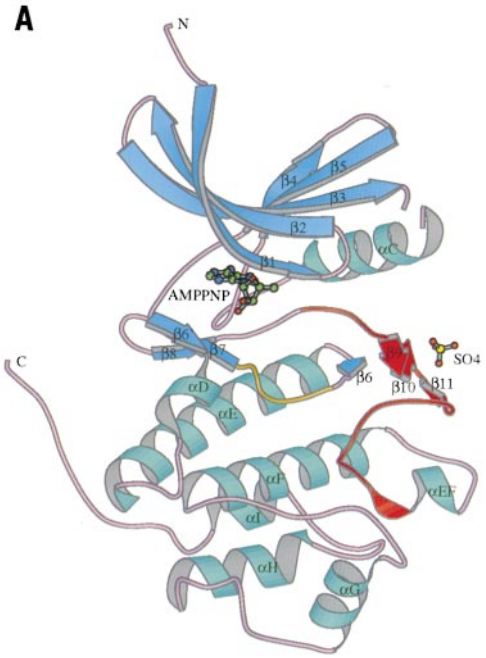

Figure 1-10 Crystal structure of CHK1 protein

Ribbon diagram of the binary structure of CHK1 with AMP-PNP. Shows α helices (blue), β strands (cyan), catalytic loop (orange) and activation loop (red). Ball and stick model of AMP-PNP. Protein termini are labelled N and C. Taken from (Chen et al., 2000).

1.6.2 Characteristics of CHK1

The characteristics and attributes of Chk1 are as follows:

- CHK1 deficiency is embryonic lethal
- CHK1 is activated by ATR
- CHK1 is activated by ATM
- CHK1 activation leads to cell cycle arrest
- CHK1 activates DNA repair via RAD51
- CHK1 activates downstream cyclin-dependent kinases
- CHK1 acts as a spindle checkpoint regulator

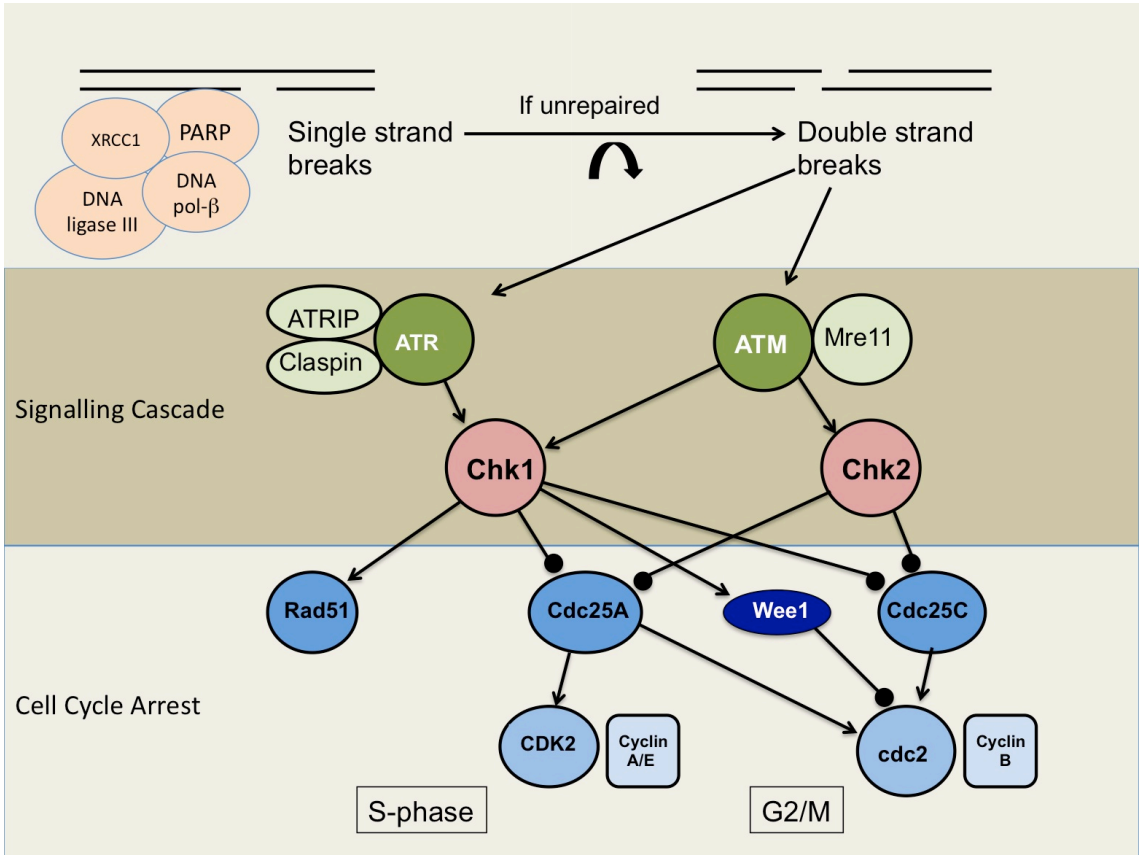

Figure 1-11 The role of ATR, ATM, CHK1 and CHK2 in cell cycle control.

The upstream activators of ATR, ATM, CHK1 and CHK2 and the downstream mediators of DNA damage-induced cell cycle checkpoints. Arrows denote activation and ball-ended-bars denote inhibition

1.6.3 CHK1 deficiency is embryonic lethal

CHK1 is a very important protein in the embryonic development of cells. Liu et al demonstrated that *Chk1*-deficient embryonic stem cells have a defective G_2/M checkpoint (Liu et al., 2000a). The cells respond in an abnormal fashion to DNA damage from ionising radiation. *Chk1* deficiency in embryonic stem cells gives rise to a proliferation defect and subsequent cell death. In mice *Chk1* deficiency is associated with peri-implantation embryonic lethality. There are no documented syndromes in humans associated with *CHK1* deficiency which suggests that it might be associated with embryonic-lethality in humans too.

1.6.4 CHK1 is activated by ATR

CHK1 can be activated by two DNA damage signalling kinases – ataxia telangiectasia mutated (ATM) and ataxia telangiectasia mutated and Rad3-related (ATR) (see Figure 1-11). Liu et al showed that ATR activates CHK1 by phosphorylation. The development of a clone of cells with defective ATR (kinase-dead) inhibited CHK1^{serine345} phosphorylation in response to UV radiation (Liu et al., 2000b). The phosphorylation of CHK1 is essential for its activation and subsequent downstream effects. Dart et al demonstrated that ATR is recruited to chromatin during S-phase within the normal cell cycle in the absence of DNA damage (Dart et al., 2004). During DNA replication there is stalling of replication forks, if the DNA damage prevents DNA polymerase and other associated enzymes completing the normal replicate process. Replication fork stalling leads to binding of replication protein A (RPA) to the exposed single strand of DNA and subsequent recruitment of ATR-interacting protein (ATRIP)

and ATR (See figure 1-12) (Liu et al., 2012). This leads to the formation of nuclear foci of ATR in conjunction with binding proteins.

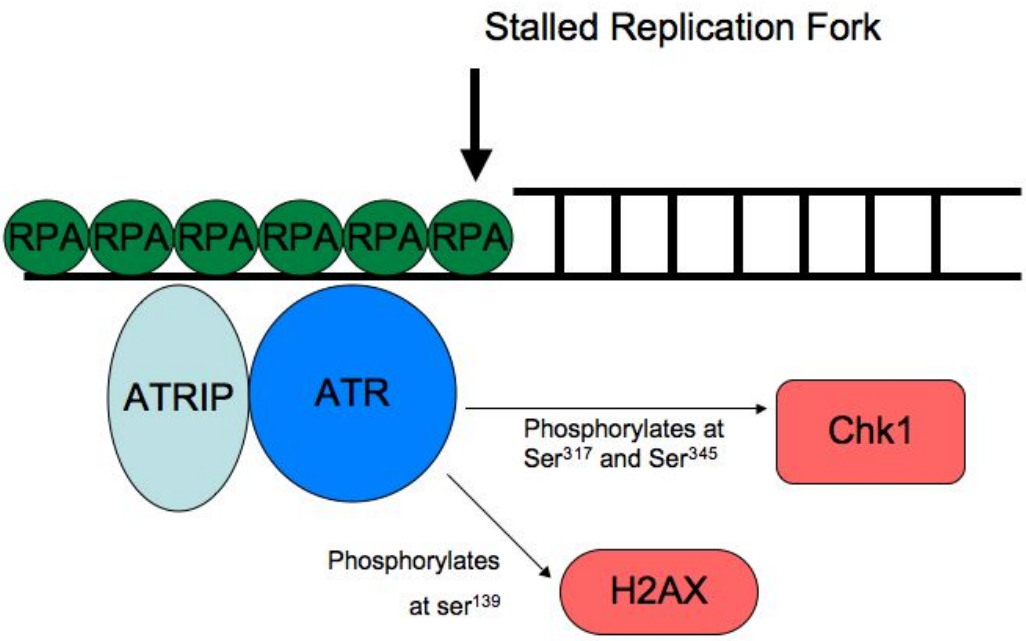

Figure 1-12 The role of ATR at the replication fork.

RPA binds to stalled replication forks. ATR associates with ATRIP and the sequestered RPA leading to its activation and phosphorylation of CHK1 at serine^{317} and serine^{345} and H2AX at serine^{319}.

ATR activates CHK1 by phosphorylating the CHK1 protein on serine^{317} and serine^{345} in an ATP-dependent process (Zhao and Piwnica-Worms, 2001). The ATR specificity of these phosphorylation events was demonstrated using HEK 293 (renal carcinoma) cells with a dominant negative kinase-active form of ATR and a parallel cell line with kinase-inactive ATR (Zhao and Piwnica-Worms, 2001). In response to hydroxyurea-induced DNA damage the activating phosphorylation of CHK1 on serine^{317} and serine^{345} was only seen in HEK 293 cells with kinase-active ATR. ATR also phosphorylates H2AX at serine^{139}.

The essential role of ATR in the phosphorylation of CHK1 has been clarified further using knockdown cell lines. Cells in which ATM is depleted have been shown to be capable of phosphorylating CHK1, but cells in which ATR is depleted show no phosphorylation of CHK1 (Jamil et al., 2008). In their studies of ATR, Jamil et al also looked at the role of MCL-1 (myeloid cell leukaemia protein – a member of the Bcl-2 family of proteins). They showed that MCL-1 appears to act as a co-regulator of ATR-mediated CHK-1 phosphorylation. Transfection-induced over-expression of MCL-1 in HeLa (cervical cancer – p53-null) and HL60 (pro-myelocytic leukaemia – p53 deleted) cells led to increased phosphorylation of CHK1 on serine^{345} by ATR and an accumulation of cells in G_2, even in the absence of DNA damage. In HeLa cells siRNA knockdown of MCL-1 abolished CHK1^{serine345} phosphorylation following etoposide-induced DNA damage. The authors do not comment if they examined if MCL-1 knockdown led to abrogation of G_2 arrest.

Peasland et al demonstrated, using cells with an inducible kinase dead ATR (ATR^{KD}), that both CHK1 serine^{345} and serine^{317} were phosphorylated after hydroxyurea and camptothecin and that the ATR^{KD} inhibited both after hydroxyurea, but only serine^{345} after camptothecin (Peasland et al., 2011). They concluded that serine^{345} was ATR-specific, but that serine^{317} could be phosphorylated by other kinases after camptothecin, but not hydroxyurea.

The importance of ATR in the activation of CHK1 and the downstream elements of the G_2 checkpoint has been confirmed by other investigators. Numerous studies have demonstrated that caffeine and pentoxyphylline can abrogate the G_2/M checkpoint (Wang et al., 1999, Kawabe, 2004). Liu et al showed abrogation of the G_2 checkpoint if ATR function was impaired by ATR siRNA

(Liu et al., 2008) in ML-1 (myeloid leukaemia) cell lines. Liu et al also showed that loss of ATM did not impair the function of the G_2 checkpoint; but that the checkpoint function did depend on DNA-PKcs. In glioma (M059) cell lines the G_2 checkpoint was stronger in cells with wild type DNA-PKcs (M059-K) compared with mutant DNA-PKcs (M059-J) in response to DNA damage caused by a novel DNA damaging agent 2'-C -Cyano-2'-deoxy-1-B-D-arabino pentofuranosylcyto-sine (CNDAC). The results were replicated by depleting DNA-PKcs with siRNA in wild type DNA-PKcs (M059-K) glioma cells.

1.6.5 CHK1 is activated by ATM

ATM is a protein kinase deficient in ataxia-telangectasia (AT). AT is a recessive neurodegenerative disorder characterized by cerebellar ataxia, progressive neural cell death, retinal telangectasia, immunodeficiency and a predisposition to developing de novo cancers. In the clinical condition, AT, there is an inactivating mutation in the AT gene leading to a deficiency in ATM. ATM is a key protein in the response to double-strand breaks (DSBs) in DNA (Shiloh, 2003).

In the absence of DNA damage, ATM is present in cells as an inactive dimer. It is recruited and activated by the Mre11-Rad50-NBS1 (MRN) complex, leading to its autophosphorylation at serine^{1981}. The phosphorylation of ATM breaks up the inactive dimer into the active monomer. ATM goes on to phosphorylate downstream effector substrates, including CHK1 (serine^{317}) and CHK2 (serine^{68}) leading to G_1, S and G_2 cell cycle checkpoint activation. Loss of ATM function leads to the failure of cell cycle checkpoint arrest, repair of DNA and subsequent apoptosis. ATM activates p53 via phosphorylation of CHK2; which

in turn phosphorylates p53 at serine^{20}. This initiates G_1 cell cycle arrest, pausing the cell cycle to allow for DNA repair (Kastan et al., 1992).

ATM is also important in the control of G_2/M cell cycle checkpoint arrest. The function of the ATM pathway has been demonstrated in an immortalized human neural stem cell line (Khanna and Jackson, 2001). If the DDR is induced by exposing cells to a single fraction of ionising radiation (0.25 Gy) the ATM pathway has been shown to be activated. The level of activation can be measured by the formation of γ-H2AX foci, autophosphorylation of ATM^{serine1981} and phosphorylation of substrates including Smc1$^{-serine966}$, Chk2$^{-threonin68}$ and p53$^{-serine15}$, which were inhibited by the ATM inhibitor KU55933 (Kudos) (Carlessi et al., 2009). The role of ATM in the DDR can be shown by comparing the response to ionizing radiation in ATM shRNA silenced and control immortalised neural stem cells. ATM depleted cells show impaired repair of DSBs with reduced formation of γ-H2AX foci; there is an associated reduction in cell death.

Release from the G_2/M checkpoint following DNA damage by ionising radiation appears to be dependent on the level of residual DSBs (Krempler et al., 2007). Krempler et al showed that cell cycle arrest is maintained if more than 10-20 DSBs persist but cells are released from arrest if there are fewer DSBs. The persistent arrest of cells with DSBs was shown in AT cells following exposure to a single fraction of ionising radiation.

1.6.6 CHK1 activates downstream cyclin-dependent kinases and leads to cell cycle arrest

Cyclin-dependent kinases (CDKs) are proteins that regulate the cell cycle and can mediate the effect of checkpoint signalling. The Cdc25 family of phosphatases allow cells to proceed through the cell cycle. There are 3 members of the family Cdc25A, Cdc25B and Cdc25C. The Cdc phosphatases remove inhibitory phosphorylations on Cdk/Cyclin complexes allowing progression through the cell cycle (Reinhardt and Yaffe, 2009). Cdc25A appears to play a role at both the S-phase checkpoint and the G_2/M transition checkpoint (Ferguson et al., 2005, Jin et al., 2003). The activating dephosphorylation of cdc2 (also known as CDK1) by Cdc25A that allows G_2/M transition. Phosphorylation of Cdc25A by CHK1 targets it for proteosomal degradation, by the 26S proteasome, preventing its interaction with its cyclin/cyclin-dependent kinase substrates (Chen and Sanchez, 2004).

A number of studies have looked at the relationship between the checkpoint proteins, ATM, ATR, CHK1 and CHK2, and the Cdc25 family of proteins. In one of these studies, U2OS (human osteosarcoma – wild type p53) cells and IMR-90 (immortalised human fibroblasts) cells were exposed to UV light. UV light triggers a DNA damage response via ATR. The cell lines demonstrated a decline in Cdc25A phosphatase activity and the amount of protein present. However, there was no reduction in Cdc25B and Cdc25C activity or amount of either protein present (Mailand et al., 2000).

In another experiment, Mailand et al compared the response to UV radiation exposure of U2OS wild type cells and U2OS cells with a conditional negative-p53 allele and showed a similar decease in activity and amount of Cdc25A in

both cell lines (Mailand et al., 2000). Further experiments demonstrated that CHK1 was an effector of Cdc25A phosphorylation and subsequent activity. The CHK1-mediated response of cells to UV radiation could be abrogated by both caffeine (an ATM and ATR inhibitor) and the CHK1 inhibitor UCN-01. This suggests that Cdc25A activity in response to UV radiation is independent of the p53 pathway and the G_1 checkpoint, but dependent on CHK1.

Cdc25C is a protein phosphatase that controls passage from G_2 into mitosis. CHK1 phosphorylates Cdc25C at serine^{216}, phosphorylation leads to its activation and the formation of a complex with 14-3-3 proteins (regulatory proteins that bind to many signalling proteins). The complex is sequestered into the cytoplasm (Peng et al., 1997). This in turn prevents activation of the cyclin B/Cdc2 mitotic kinase complex due to Cdc25C functions dephosphorylating Cdc2; finally resulting in G_2 cell cycle arrest (Shapiro and Harper, 1999) and suppression of mitotic entry (Duensing et al., 2006). If Cdc25C is mutated so as to not allow phosphorylation on serine^{216} cells fail to arrest in G_2. Peng et al demonstrated in HeLa and Jurkat (T cell leukaemia, mutated p53) cells that the CHK1 protein phosphorylates Cdc25C at serine^{216} this leads to cell cycle arrest to allow for DNA repair (Peng et al., 1997). Sorensen et al sought to inhibit CHK1 in a U2OS cell line using UCN-01 (Sorensen et al., 2003). Inhibition of CHK1 (300 nM UCN-01 for 1 hour) led to increase in the expression of Cdc25A protein and an increase in the activity of Cdc25A as determined by an increase in Cyclin A and Cyclin E expression.

Wee1 is a kinase that phosphorylates cdc2 and Cdk2 (Lee et al., 2001). This has an inhibitory effect. Wee1 is directly phosphorylated on serine^{642} by CHK1; this phosphorylation promotes its association with 14-3-3 proteins. The

association of Wee1 with 14-3-3 proteins increases its catalytic activity and promotes its inhibitory phosphorylation of cdc2.

1.6.7 CHK1 activates HRR DNA repair via RAD51 and BRCA2

As described in section 1.3.4, HRR is critical for the error-free repair of DSB and stalled replication forks. BRCA2 and RAD51 are key proteins in this process. It has been shown that activated CHK1 promotes the association of RAD51 with chromatin (Sorensen et al., 2005). Activated CHK1 phosphorylates RAD51 on threonine^{309}. The experiments that support the interaction between CHK1 and RAD51 include co-immunoprecipitation of a CHK1/RAD51 complex, which can be abrogated by hydroxyurea treatment.

The importance of the threonine^{309} phosphorylation site has been confirmed by site-directed mutagenesis of RAD51^{threonine309A} in Hek 293 cells, which prevents its phosphorylation. Cells with a mutated threonine^{309A} RAD51 are more sensitive to hydroxyurea and have increased numbers of persistent DSBs, indicating that activation of RAD51 by CHK1 is required for HR following DSBs.

Sorensen et al also showed that knockdown of *CHK1* by CHK1 siRNA or chemical antagonists UCN-01 and CEP-3891 led to persistent un-repaired DSBs following replication-related damage by hydroxyurea or camptothecin (Sorensen et al., 2005) in SPD8 (Chinese hamster cells) and SW480SN.3 (human colorectal cancer). DSBs were quantified by pulsed-field gel electrophoresis of ^{14}C-thymidine labelled DNA. Depletion or inhibition of *CHK1* in both these cell lines led to the loss of RAD51 focus formation measured by

immunofluorescence microscopy. The same loss of RAD51 foci formation was seen if *CHK2* was depleted by CHK2 siRNA.

BRCA2 delivers RAD51 to the DNA and displaces RPA from the DNA replacing it with RAD51. BRCA2 is a tumour suppressor protein and mutations in BRCA2 were associated with cancer predisposition (breast, ovarian, prostate and pancreatic cancers). Both CHK1 and CHK2 phosphorylate the carboxyl-terminal domain of BRCA2 (Bahassi et al., 2008). Phosphorylation of BRCA2 facilitates its interaction with RAD51.

Cells which lack the phosphorylation domain of BRCA2 (MEF (mouse embryo fibroblasts) - lex1/lex2) show no localisation of RAD51 to DSBs. Cells with mutant BRCA2 are hypersensitive to DNA damaging agents. CHK2 depletion leads to loss of RAD51 localisation that is associated with DNA double-strand breaks.

1.6.8 CHK1 acts as a spindle checkpoint

The spindle checkpoint inhibits progression into anaphase if the chromosomes have failed to attach correctly to the mitotic spindle (Murray, 1995). CHK1 has also been shown to mediate spindle checkpoint activation by phosphorylating Aurora B kinase (Zachos et al., 2007). Aurora B kinase subsequently phosphorylates histone H3 at serine^{10}, resulting in anaphase delay to prevent cells acquiring defects associated with chromosome miss-segregation.

The importance of the CHK1 protein as a spindle checkpoint regulator has been shown using CHK1 knockdown (siRNA) in U2OS cell lines (Carrassa et al.,

2009), which led to an increase in giant polynucleated cells and G_1 arrested tetraploid cells. This suggests that U2OS cells with aberrant CHK1 have abnormal mitosis and do not activate the spindle cell checkpoint.

Zachos et al have shown that CHK1 is required to sustain this (Zachos et al., 2007). Cells that are deficient in Chk1 (using CHK1 siRNA) have up to 33% misaligned chromosomes and subsequent chromosomal instability.

1.7 Biomarkers for CHK1 inhibition

Potential biomarkers for CHK1 inhibition include cdc25A stability, Cdc25C serine^{216} and H3 at serine^{10}. An alternative downstream biomarker for CHK1 inhibition would be Wee1^{serine642} phosphorylation (Lee et al., 2001). All of these markers could be used as cellular proof-of-mechanism biomarkers of CHK1 activity, and its inhibition.

Phosphorylation of CHK1 itself is also a potential biomarker. Autophosphorylation of CHK1 at serine^{296} occurs in the presence of conventional cytotoxics and is abolished with CHK1 inhibition (Guzi et al., 2011). Guzi et al demonstrated that hydroxyurea increased CHK1^{serine296} phosphorylation in U2OS cells and that this was reduced in a concentration-dependent fashion by SCH 900776 (0.06 – 2 μM for 2 hours). Bryant et al showed in two triple-negative breast cancer cell lines, MDA-MB-468 and SKOV-3, that a 24 hour exposure to 31.25 to 1000 nM V158411 significantly reduced CHK1^{serine296} autophosphorylation (Bryant et al., 2014b).

Phosphorylation of CHK1^{serine345} has been used as a marker of ATR activity (Zhao and Piwnica-Worms, 2001). However, CHK1^{serine345} also appears to be phosphorylated in the presence of some CHK1 inhibitors used alone (Parsels et al., 2011). Bryant et al have shown that 31.25 to 1000 nM V158411 for 24 hours increases CHK1^{serine345} phosphorylation in a dose-dependent fashion in MDA-MB-468 and SKOV-3 triple-negative breast cancer cell lines (Bryant et al., 2014b). This raises the possibility that it could be used as a PD biomarker, demonstrating that the CHK1 inhibitor is present in a cell or tumour sample. The pre-clinical data pertaining to the CHK1 phosphorylation and its potential as a biomarker in pre-clinical studies is explored in more detail in Section 3.1.

H2AX has also been used extensively as a biomarker (Redon et al., 2010). Histone H2AX is phosphorylated on serine^{139} in response to DSBs in the chromatin that adjoins the damage (Rogakou et al., 1998). The disadvantage of H2AX as a biomarker for CHK1 activity is that it is not specific to CHK1. H2AX is part of the final common pathway to both homologous recombination and non-homologous end-joining. Therefore a number of potential control mechanisms for these DNA repair pathways may be implicated including ATR/CHK1, but also ATM/CHK2 and DNA-PK/JNK (Mukherjee et al., 2006, van Attikum and Gasser, 2005).

H2AX was used as a biomarker by Daud et al in the phase I clinical trial of SCH 900776 in combination with gemcitabine (Daud et al., 2010). They performed an *ex vivo* assay using patient plasma taken at the same time as PK samples. Plasma was diluted (1:4) and applied to K562 cells, following fixation H2AX levels were measured by flow cytometry. The authors concluded that there was prolonged bioactivity of SCH 900776 as quantified by H2AX levels. This correlated in H2AX levels seen in biopsies of normal skin taken at matched time points.

Geminin has been suggested as a potentially useful biomarker of cells arrested in S phase. Perez et al performed a pre-clinical validation study demonstrating that geminin, as quantified by both immunohistochemistry (IHC) and flow cytometry, increased in MDA-MB-231 breast cancer cells arrested in S phase by 0.1 ng/ml and 1 ng/ml SN-38 (Perez et al., 2006). Levels of staining by IHC correlated with those by flow cytometry. They used geminin staining as a biomarker in a phase I study of UCN-01 in combination with cisplatin. Tumour biopsies from cutaneous skin metastases were performed in 3 out of 7 patients.

Geminin staining (by IHC) was seen in 2-8% of tumour cells prior to treatment, geminin staining significantly increased following the administration of 30 mg/m^2 cisplatin suggesting cells were arresting in S, but this increase was abrogated by 33.75 mg/m^2/day UCN-01 (as 72 hour continuous infusion) suggesting that the S phase checkpoint was abrogated leading to cells progressing into G_1.

Neither the phase I trial of LY2603618 in combination with pemetrexed or pemetrexed and cisplatin published any biomarker data (Weiss et al., 2013, Calvo et al., 2014). The three phase I studies of PF-0477736 in combination with gemcitabine (2010) and AZD7762 in combination with gemcitabine (2011) or AZD7762 in combination with irinotecan (2011) presented in abstract form at ASCO have not presented any biomarker or pharmacodynamic data (Brega et al., 2010, Ho et al., 2011, Sausville et al., 2011).

1.8 Chemistry of CHK1 inhibitors

This brief section seeks to explain the structures and chemistry of CHK1 inhibitors to date, where this has been published. The relative potency of the inhibitors and the type of assay that has been used to determine this is also discussed.

1.8.1 UCN-01

UCN-01 is a staurosporine analogue that initially was identified as a protein kinase C inhibitor (Courage et al., 1995). The structure is shown in Figure 1-13. It was also shown to have activity against a range of other kinases including CHK1 and PDK1.

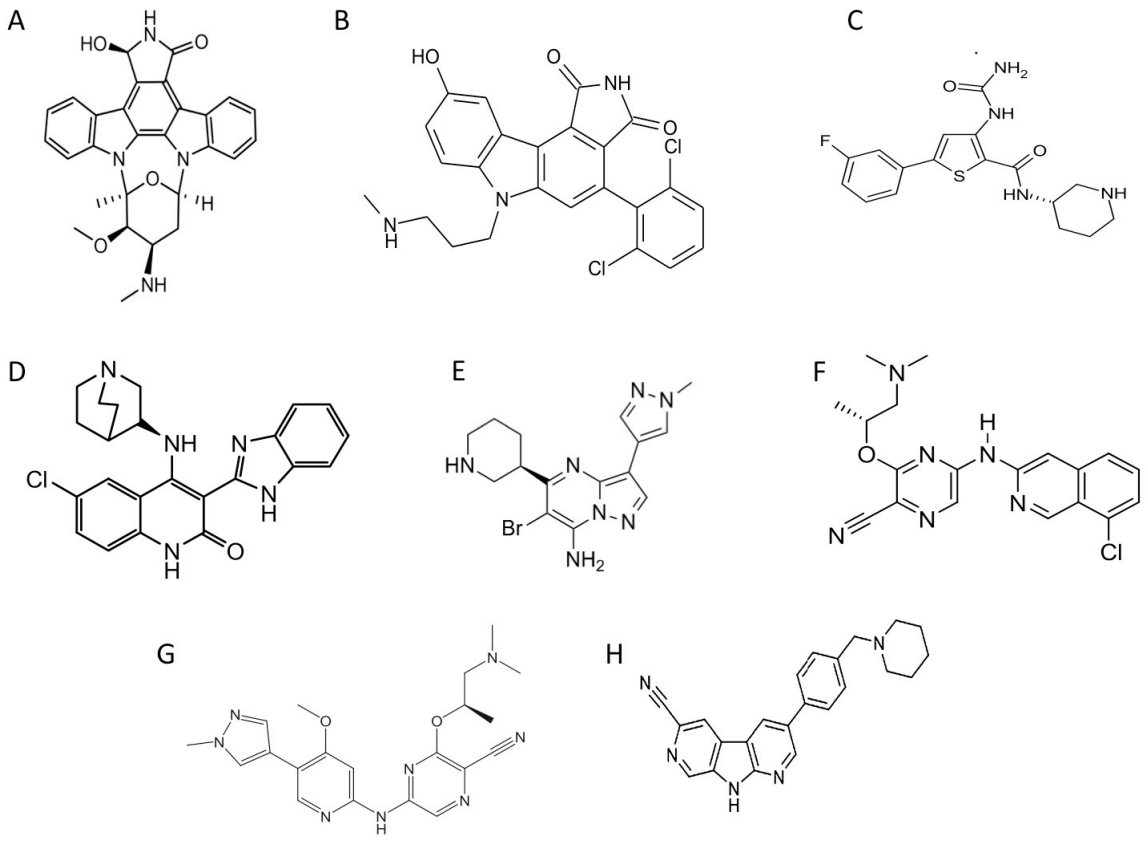

Figure 1-13 Structures of CHK1 inhibitors

A: UCN-01 (Courage et al., 1995), B: PD-321852 (adapted from patent application WO2008007113 A2), C: AZD7762 (Zabludoff et al., 2008), D: CHIR-124 (Tse et al., 2007b), E: SCH 900776 (Guzi et al., 2011), F: SAR-020106 (Walton et al., 2010), G: CCT244747 (Walton et al., 2012), H: GNE-900 (Blackwood et al., 2013)

1.8.2 PD-321852

PD-321852 is a phenyl-carbazole (4-(2,6-dichloro-phenyl)-9-hydroxy-6-(3-methylamino-propyl)-6H-pyrrolo[3,4-c]carbazole-1,3-dione) kinase inhibitor developed by Pfizer and University of Auckland (New Zealand) (Parsels et al., 2009). The structure is shown in Figure 1-13. It is a UCN-01 analogue with a greater specificity and potency for CHK1 than UCN-01. However, the authors indicate that it does have activity against other kinases (not specified) and these

may account for some of its effects. Its IC_{50} in a cell-free inhibition assay for CHK1 is 5 nM.

1.8.3 PF00477736

PF00477736 (Pfizer) is a novel diazepinoindolone, an ATP-competitive small molecular CHK1 inhibitor with a K_i for Chk1 of 0.49 nM (Blasina et al., 2008). The structure of PF00477736 has not been published. It has a 100-fold selectivity for CHK1 over CHK2. Other kinases that were inhibited by PF00477736 with a less than 100-fold selectivity included VEGF2R, Aurora-A, FGFR3, Flt3, Fms, Ret and Yes. However, despite the apparent ability of PF00477736 to inhibit Aurora-A in a kinase assay it did not appear to demonstrate this effect *in vitro* as it did not induce the blockade of cytokinesis or cell proliferation. In pre-clinical studies, the cellular potency of PF00477736 was measured by assessing cells entering mitosis (histone H3 phosphorylation by spectral dot-blot analysis) (Blasina et al., 2008). The cellular EC_{50} by this method was 45 nM.

1.8.4 AZD7762

AZD7762, a thiophene carboxamide urea [3-(carbamoylamino)-5-(3-fluorophenyl)-N-[(3S)-3-piperidyl]thiophene-2-carboxamide] (AstraZeneca). It is an ATP-competitive inhibitor of both Chk1 (K_i = 3.6 nM, IC_{50} = 5 nM in *in vitro assays*) and CHK2 (IC_{50} = <10 nM) with a similar potency (Zabludoff et al., 2008). The cellular IC_{50} was calculated by measuring the ability of AZD7762 to

inhibit the CHK1 mediated phosphorylation of cdc25C. AZD7762 has a less than 10 fold selectivity against other kinases including CAM kinases and Src-like kinases. The structure is shown in Figure 1-13.

1.8.5 CHIR-124

CHIR-124 (Chiron) [(S)-3-(1H-benzo[d]imidazol-2-yl)-6-chloro-4-(quinuclidin-3-ylamino) quinolin-2(1H)-one] (Figure 1-13) is a novel quinolone-based small molecular inhibitor of CHK1 with an IC_{50} = 0.3 nM (Tse et al., 2007b). This was determined in a cell-free kinase assay examining the ability of CHK1 to inhibit cdc25C phosphorylation. CHIR-124 also has some limited activity against PDGFR, FLT3 and GSK3, but with 10 to 100-fold higher IC_{50} values.

1.8.6 CEP-3891

CEP-3891 (Cephalon) was developed as a more specific small molecular inhibitor of CHK1 (Sorensen et al., 2003). The cellular IC_{50} (determined by the reduction in Cdc25A phosphorylation) of CEP-3891 is 4 nM. Other kinases inhibited by CEP-3891 included TrkA (9 nM), MLK1 (42 nM) and VEGFR2 (164 nM). No structure of CEP-3891 has been published.

1.8.7 XL9844

XL9844 (EXEL-9844 – Exelixis Inc) is a very potent oral aminopyrazine inhibitor of both CHK1 and CHK2 (K_i 2.2 nM and 0.07 nM, respectively) (Matthews et al.,

2007). No structure has been published. These K_i results were determined in a cell-free radiolabelled-ATP competitive assay. The inhibition of both CHK1 and CHK2 was shown to be reversible with competition with increasing concentrations of ATP. XL9844 also inhibited VEGFR2 (IC_{50} = 12 nM) and Flt-4 (IC_{50} = 6 nM).

1.8.8 SCH 900776

SCH 900776 (MK-8776) (Schering Plough/Merck) is a pyrazolo[1,5-a]pyrimidine-based compound (Figure 1-13) that acts a potent inhibitor of CHK1 (K_d = 2 nM, IC_{50} = 60 nM in a cell-free kinase assay). SCH 900776 does not inhibit CHK2 (IC_{50} = 1.5 μmol/L) and is a weak CDK2 (IC_{50} = 160 nM) inhibitor (Guzi et al., 2011).

1.8.9 SAR-020106

SAR-020106 (Sareum) is a pyrazolo[1,5-a]pyrimidine (Figure 1-13) inhibitor of CHK1 with an IC_{50} of 13.3 nM when tested against the isolated recombinant CHK1 enzyme in a cell-free assay (Matthews et al., 2009). The compound is available when delivered intravenously. It has an IC_{50} for CHK2 and CDK1 of > 10 μM. Other kinases that were modestly inhibited included FLT3, IRAK4, Met, MST2, p70S6K, Ret, RSK1 and TrkA.

1.8.10 CCT244747

CCT244747 (Figure 1-13) is a novel oral CHK1 inhibitor developed by the Institute for Cancer Research in London and Sareum Pharmaceuticals (Walton et al., 2012). It has been developed from the compound SAR-020106. Its IC_{50} against recombinant CHK1 is 8 nM. It shows >75 times selectivity against FLT3 and >1000 fold selectivity against CHK2 and CDK1. It has been shown to have a cellular IC_{50} for CHK1 of 29-170 nM when looking at the cellular abrogation of the G_2 checkpoint in a mitosis induction assay. Mouse xenograft models of human tumours have confirmed that clinically relevant concentrations of CCT244747 are detectable following oral administration with an oral bioavailability of 62%.

1.8.11 LY2603618

LY2603618 is an intravenous selective CHK1 inhibitor developed by Eli-Lilly (King et al., 2014). It has an *in vitro* kinase activity against Chk1 of 7 nM in a cell-free assay. The structure has not been published.

1.8.12 GNE-900

GNE-900 (9H-Pyrrole[2,3-b:5,4-c']dipyridine-6-carbonitrile,3-[4-(1-piperidinyl methyl)phenyl]) (Figure 1-13) is a potent and selective orally bioavailable inhibitor of CHK1 developed by Genentech by high-throughput screening of their small molecule library (Blackwood et al., 2013). It is an orally bioavailable ATP-competitive small molecular inhibitor of CHK1 with an IC_{50} for CHK1 in a

cell free kinase assay of 1.1 nM. It has a 300-fold selectivity compared to kinases that regulate other parts of the cell cycle; Aurora, PLK and CDK 1/2.

1.8.13 V158411

V158411 is a novel inhibitor of both CHK1 and CHK2. The structure of V158411 has not been published. Its molecular weight is 538 kDa. Its IC_{50} in an *in vitro* kinase assay was 3.5 nM (CHK1) and 2.5 nM (CHK2) (Bryant et al., 2014a). In a cellular assay in HT29 (colorectal cancer, p53 mutated) cells, V158411 inhibited the phosphorylation of $CHK1^{serine296}$ with an IC_{50} of 48 nM and $CHK2^{serine516}$ with an IC_{50} of 904 nM. There is no information in the public domain about the activity of V158411 against a wider kinase panel including other kinases such as FLT3.

1.8.14 Other CHK1 inhibitors

There is no published information on the structure or chemistry of a number of CHK1 inhibitors including LY2606368, GDC-0425 or ARRY575.

1.9 CHK1 inhibitors

The pre-clinical evidence for the use of Chk1 inhibitors as single agents in clinical trials is less developed and less numerous than the data for their use in conjunction with conventional cytotoxic therapy (see Section 1-11). Only a few CHK1 inhibitors appear to be cytotoxic as single agents in cell line and animal studies. It is unclear whether those inhibitors that are cytotoxic as single agents mediate this cytotoxicity through their direct effect on CHK1 or by other mechanisms. Further work needs to be done to look at tumour and patient characteristics that may make tumours and patients suitable for treatment with a CHK1 inhibitor as a monoagent and this is explored further in Chapter 6.

The first pre-clinical data on a CHK1 inhibitor to be published was with UCN-01 which entered Phase 1 clinical trials in 1995. Subsequently, 10 CHK1 inhibitors have been developed with greater potency and a higher specificity for CHK1. Most of these ‘second generation’ inhibitors are ATP-competitive. The majority of these compounds are administered i.v., though a number of oral compounds are under development. Table 1-2 outlines those CHK1 inhibitors being developed and their stage of development.

Name of compound and Company	Pre-clinical data published	Development phase	Route and trial Combination	Dose-limiting toxicity	Future Development
Multiple kinases including CDKs and Chk1					
UCN-01	Yes (Courage et al., 1995, Dai et al., 2002, Mack et al., 2003)	Phase 1 – 2 trials (short and long infusions) (Sausville et al., 2001, Dees et al., 2005)	IV single agent in AST	Hypotension and hyperglycaemia	Stopped – no further development planned
		Phase 1 (Lara et al., 2005, Perez et al., 2006)	IV in combination with cisplatin in AST	Neutropenic sepsis and SVT	Stopped – no further development planned
		Phase 1 (Hotte et al., 2006)	IV in combination with topotecan in AST	Neutropenia, thrombocytopenia and hyperglycaemia	Stopped – no further development planned
		Phase 2	IV in combination with topotecan in ovarian cancer	Hyperglycaemia	Stopped – no further development planned
Chk1 and Chk2 inhibitor					
AZD7762 - Astra Zeneca	Yes (Zabludoff et al., 2008, Morgan et al., 2010, Mitchell et al., 2010b, McNeely et al., 2010)	2 Phase 1 trials (Sausville et al., 2011, Sausville et al., 2014, Seto et al., 2013)	IV in combination with gem in AST	Myocardial ischaemia and neutropenia	2 Phase 1 studies published – development stopped due to toxicity
		Phase 1 (Ho et al., 2011)	IV in combination with irinotecan in AST	Myocardial ischaemia	ASCO 2011 abstract
Selective Chk1 inhibitors					
PF00477736 - Pfizer	Yes (Blasina et al., 2008)	Phase 1 (Brega et al., 2010)	IV in combination with gem in AST	Thrombocytopenia and neutropenia	ASCO 2010 abstract Stopped – no further development planned
PD-321852 - Pfizer	Yes (Parsels et al., 2009)	Pre-clinical	IV compound. No clinical trials		Stopped – no further development planned
SCH900776 (MK-8776)	Yes (Montano et al., 2012,	Phase 1 (Daud et al., 2010)	IV in combination with gem in AST	SVT and thrombocytopenia	Closed - ASCO 2010 abstract

- Schering Plough	Guzi et al., 2011)	Phase 1	IV in combination with cytarabine in leukaemia		Closed - awaiting publication
LY2603618 - Eli-Lily	Yes (Wang et al., 2014)	Phase 1 (Weiss et al., 2013, Calvo et al., 2014) Phase II active	IV in combination with pemetrexed or gemcitabine in NSCLC IV in combination with pemetrexed and cisplatin in NSCLC		Phase I closed and 1 study published Phase II – in follow up
LY2606368 - Eli-Lily	No	Phase 1	IV single agent in AST		Phase 1 – finishing Feb 2012
CHIR-124 (Chiron/Novartis)	Yes (Tse et al., 2007b, Tao et al., 2009)	Pre-clinical	IV		
XL844 (Exelixis)	Yes (Matthews et al., 2007)	Phase 1	Oral in combination with gem in AST and lymphoma		Phase 1 - terminated
SAR020106 (Sareum)	Yes (Walton et al., 2010)	Pre-clinical	IV		
GDC-0425 (Roche/Genentech)	No	Phase 1	IV in combination with gem in AST		Phase 1 recruiting
CEP3891 (Cephalon)	Yes (Syljuasen et al., 2004)	Pre-clinical	IV		
CCT244747 (ICR/Sareum)	Yes (Walton et al., 2012)	Pre-clinical	Oral		
ARRY575 (GDC-0575) (Array Pharma/Genentech)	No	Pre-clinical	Oral		
V158411 - Vernalis	Yes (Bryant et al., 2014a and Bryant et al., 2014b)	Pre-clinical	IV		

Table 1-2 CHK1 inhibitors under development.

IV – intravenous; AST – advanced solid tumours; Gem – gemcitabine. Additional data from http://clinicaltrials.gov

1.10 Assay methods used in pre-clinical research

The effects of CHK1 inhibitors, alone and in combination with cytotoxic agents has been evaluated by different methods and each method has advantages and disadvantages and measures subtly different outcomes.

Several 96-well plate assays can be employed, these are quick, simple and relatively high throughput, but don't distinguish between growth arrest and cell kill. That is, a GI_{50} value could reflect 50% cell kill followed by growth of the remaining treated cells at the same rate as untreated control or a slowing of the growth rate such that the treated cells underwent one less cell doubling than the controls or a mixture of these 2 outcomes. Quantification of cell number and or viability in these assays can be via quantitative protein stain e.g. sulphurhodamine B (SRB) (Skehan et al., 1990). However, cells treated with a cytotoxic agent may continue to grow in size if not number (unbalanced cell growth due to nuclei containing multiple copies of DNA, but with the cell failing to divide) leading to an over-estimate of cell number in the treated cells (Keepers et al., 1991, Martin and Clynes, 1993)

Alternative methods are measurement of cellular (mitochondrial) dehydrogenase activity by following the reduction of tetrazolium salts to coloured formazan products, this is the principle of MTT, MTS, XTT, Alamar blue assays and is said to reflect viable cells only but may also be influenced by unbalanced cell growth. Cellular ATP has also been coupled to chemi-luminescence detection (Cell Titerglo) as a means to quantify viable cells as an endpoint in 96-well plate assays. Although the ATP and dehydrogenase assays would be predicted to produce similar results, recent comparison of the literature on drug sensitivity determined by these 2 methods in large

overlapping panels of cell lines revealed poor concordance of the data (Weinstein and Lorenzi, 2013).

Perhaps a more reliable method of quantitation is to measure DNA (Promega kit), but this is a relatively new method and has not been widely adopted. The most robust way of measuring growth inhibition is by direct cell counting but again this will not distinguish between a slowing of the growth rate and cell killing. The most reliable method of assessing cell kill is by measurement of the clonogenic potential, i.e., the ability of cells to form colonies after treatment compared to control. However, this is very time-consuming and requires larger volumes of reagents, making it costly and not all types of cells form countable colonies. Even though this method may offer some advantages over others, cells that have arrested, but are alive will fail to form colonies and so will falsely be assumed to have died. The methods that have been used to assess CHK1 inhibitor effects needs to be taken into account when interpreting the data.

1.11 Single agent activity of CHK1 inhibitors

There is relatively little published data on the single agent cytotoxicity of CHK1 inhibitors. Only 2 inhibitors, UCN-01 and LY2606368, have been taken into early phase clinical trials as single agents. In the early development of UCN-01 its main effects were thought to be mediated by its inhibition of protein kinase C (PKC) (Courage et al., 1995). Courage et al demonstrated that UCN-01 had growth inhibitory effects in A549 (NSCLC – wild type p53) and MCF7 (breast cancer – wild type p53) cell lines that were independent of PKC. Growth inhibition with UCN-01 was similar in PKC depleted and untreated control cells (GI_{50} 0.033 μM and 0.034 μM respectively in A549 cells, GI_{50} 0.0178 μM and 0.0175 μM respectively in MCF7 cells).

300 nM and 1 μM XL9844 did not have any significant single-agent activity in clonogenic assays in 4 cancer cell lines (PANC-1 (pancreatic cancer – p53 mutated), AsPC-1 (pancreatic cancer – p53 mutated), SKOV3 (ovarian cancer – wild type p53) and HeLa) (Matthews et al., 2007). The authors hypothesise that this may be due to insufficient constant exposure to the CHK1 inhibitor. Blackwood et al found that the orally bioavailable CHK1 inhibitor GNE-900 had little effect as single agent (GI_{50} in HT29 cells is 8.7 μM) (Blackwood et al., 2013). There is no published single agent data with PF00477736, CEP-3891 or SAR-020106.

1.11.1 AZD7762

AZD7762 (100 nM for 24 hours) did not affect the proliferation of HCT116 (colorectal cancer – wild type p53) in a 96 well plate assay (absorbance assay measuring DNA content) (McNeely et al., 2010). Zabludoff et al present a small amount of *in vivo* data with single agent AZD7762 in mouse xenografts studies (Zabludoff et al., 2008). They demonstrate that AZD7762 (25 mg/kg BD every 3 days) caused a modest reduction in the growth of SW620 (colorectal – mutated p53) xenografts compared to vehicle.

1.11.2 PD-321852

PD-321852 had modest single-agent activity in four pancreatic cell lines (MiaPaCa2, M-Panc96, BxPC3 and Panc1 (all p53 mutated)) using clonogenic assays (Parsels et al., 2009). Cells were treated for 24 hours in media containing PD-321852 prior to plating out into drug-free media for 12 to 14 days. They describe a 'threshold' toxic (the highest non-toxic) concentration of 100 nM and minimal toxicity at 300 nM in all 4 pancreatic cell lines.

1.11.3 CHIR-124

No single agent *in vitro* data has been published with CHIR-124. However, there is *in vivo* data (Tse et al., 2007b). In mouse models, CHIR-124 (10 or 20 mg/kg i.v. daily on days 2-7) alone had no effect on MDA-MB-435 (breast cancer cell line – p53 mutated) xenografts.

1.11.4 SCH 900776

Montano et al report a wide range of sensitivities to single-agent SCH 900776 (Montano et al., 2012). They demonstrate that a number of cell lines were sensitive to SCH 900776 in 96-well plate growth assays stained with Hoechst 33258 including HCC2998 (colonic cancer (p53 mutated) GI_{50} = 500 nM), U2OS (GI_{50} = 550 nM), A498 (GI_{50} = 500 nM) and TK-10 (renal cell cancer (p53 mutated) GI_{50} = 230 nM) cancer cell lines. However, a number of cell lines are resistant to a 24 hour exposure to SCH 900776 with a GI_{50} > 10 μM. These included MDA-MB-231 (breast cancer cell line – p53 mutated), MCF-10A (immortalised breast cell line), HCT116, HCT15 (colorectal cancer – p53 mutated) and SW620 cell lines. The authors do not comment on any potential factors that might contribute to the sensitivity to SCH 900776. In animal studies in mice bearing xenografts (A2780 (ovarian cancer – p53 wild type) and MiaPaca) SCH 900776 showed little single agent activity (Guzi et al., 2011).

1.11.5 V158411

The sensitivity of cell lines to single-agent V158411 has been explored by Vernalis (Bryant et al., 2014a, Bryant et al., 2014b). Work has demonstrated that triple-negative breast cancer cells (HCC1937 (BRCA1-mutated, p53 mutated), MDA-MB-157 (p53 mutated), MDA-MB-231, MDA-MB-453 (p53 mutated) and MDA-MB-468 (p53 mutated)), ovarian (SKOV-3 and A2780), leukaemia (MV4:11 (p53 wild type), HL60, and Jurkat) and lymphoma (U937

(p53 wild type) and Raji (p53 mutated)) cell lines are sensitive to single agent V158411.

HL60, Jurkat, MV4:11, Raji and U937 cell lines had GI_{50} of less than 1 μM following a 72 hour exposure to V158411 in a 96-well plate growth inhibition assay (Titer glo). (Bryant et al., 2014a, Bryant et al., 2014b). The sensitivity to V158411 appeared to show no correlation with their p53 status. It also did not appear to correlate with their known sensitivity to chemotherapy (gemcitabine and cisplatin).

A response to V158411 in sensitive cell lines appears to correlate with the degradation of CHK1 (Bryant et al., 2014a). There was also time-dependent phosphorylation of H2AX. Measurement of CHK1 and γ-H2AX in cells treated with V158411 for 24 hours revealed that cells that were not sensitive to V158411 showed degradation of CHK1, but no increase in γ-H2AX foci formation.

1.12 Synthetic lethality with CHK1 inhibitors

Synthetic lethality is used to describe a situation where the inactivation of two pathways independently is not cytotoxic, but when both pathways are targeted or one is constitutively inactive there is significant cytotoxicity. Combining CHK1 inhibitors with other inhibitors targeting DNA damage repair has been employed as a potential strategy to exploit synthetic lethality.

1.12.1 CHK1 and Myc

There are a number of publications that have focused on the potential utility of CHK1 inhibitors in Myc-amplified cancers. Myc is an oncogene amplified in a number of cancers including lymphomas (cMyc), neuroblastomas (MYCN) and a few breast and lung cancers. It has been noted that CHK1 is up-regulated in cMyc-overexpressing murine and human lymphomas (Hoglund et al., 2011a). The authors have also noted that CHK2 deficiency (or CHK2 inhibition with the dual CHK1/CHK2 inhibitor AZD7762) in cMyc-amplified lymphomas is synthetically lethal (Hoglund et al., 2011b). CHK1 inactivation, by either siRNA or by a novel experimental CHK1 inhibitor 'Chekin' (developed by Abbott laboratories, no further details of Chekin are available), resulted in cytotoxicity in cMyc-amplified cell lines. The mechanism is thought to be due replication stress induced by a myc amplification-associated hyperproliferative state, causing increased dependence on the S/G_2 checkpoints.

This work was supported by a second study by Ferrao et al which examined the effect of single agent PF00477736 on Eμ-myc lymphoma cell lines (Ferrao et al., 2011). The authors compared the effect of PF00477736 in colony forming

assays in soft agar on p53-wild type ARF null Eμ-myc lymphoma cell lines and p53-null ARF null Eμ-myc lymphoma cell lines. The p53-wild type cell lines were significantly more sensitive to 24 hour exposure to PF0047736 than the p53-null cell line (GI_{50} 0.31 μM and 2.46 μM respectively). This is contrary to the expectation that dysfunctional p53 will render a cell more sensitive to a CHK1 inhibitor.

CCT244747 has also been shown to have single agent activity against MYCN-associated neuroblastoma. In a hemi-zygotic transgenic mouse overexpressing MYCN (Walton et al., 2012). 7-day continuous oral administration of 100 mg/kg CCT244747 led to 79% tumour volume reduction (as assessed by MRI) compared to vehicle treated controls

1.12.2 CHK1 and PARP

Mitchell et al demonstrated that combining CHK1 inhibitors (UCN-01 and AZD7762) with the PARP inhibitor, PJ34, caused a synergistic impairment of cell viability in colony forming assays (Mitchell et al., 2010a). MCF7, 4T1 (p53 mutated), SKBR3 (p53 mutated) and BT474 (p53 mutated) breast cancer lines were exposed to vehicle, 3 μM PJ34, 50 nM UCN-01 or 25 nM AZD7762 or the combination of UCN-01 or AZD7762 + PJ34 for 48 hours. In 4T1, SKBR3 and BT474 cells, PJ34, 25 nM AZD7762 and 50 nM UCN-01 alone killed ~10% of cells. The combination of AZD7762 and PJ34 or UCN-01 was at least additive with between 20-25% cells killed. In Panc-1, MiaPaca2 (pancreatic cancer – p53 mutated) and MCF7 cells single agent PJ34, AZD7762 and UCN-01 killed

less than 10% of cells, but in combination showed synergism with 25-30% cell death.

The authors demonstrated that both UCN-01 and AZD7762 promoted H2AX and increased PARP 1 activity. If PARP function was inhibited with PJ34, there was loss of CHK1 inhibitor-mediated H2AX phosphorylation and activation of ERK 1/2. However, PJ34 is highly cytotoxic as a single agent at concentrations that do not significantly inhibit PARP so the cytotoxicity may have been due to off-target effects. There was synergism between CHK1 inhibitors and PARP inhibitors in cell lines with both low basal ERK 1/2 activity (MCF7) and high basal ERK 1 and 2 activity (MDA-MB-231 and Panc1 cell lines) suggesting that ERK1/2 activation is not the sole mediator of sensitivity to the combination of CHK1 and PARP inhibitors.

The use of a PARP inhibitor in combination with a CHK1 inhibitor and radiotherapy is considered in section 1-14.

1.12.3 CHK1 and MEK inhibitors

The MAPkinase pathway is frequently up-regulated in cancer promoting proliferation and inhibiting apoptosis. MEK and ERK are important components of this pathway Therefore, the combination of a CHK1 inhibitor (UCN-01) and MEK inhibitor (PD184352 - a MEK1/2 inhibitor developed by Pfizer) has been examined in 3 myeloma cell lines (8226 (mutated p53), H929 (wild type p53) and U266 (mutated p53)). Co-administration of 150 nM UCN-0 for 24 hours following 30 minutes with 10 μM PD184352 alone resulted in a marked increase

in cell death in myeloma cell lines (Dai et al., 2002). There appeared to be synergism with fewer than 25% apoptotic cells with either drug alone and between 50 and 75% apoptosis with the drugs in combination. The combination of UCN-01 and PD184352 was also effective at inducing apoptosis in cell lines resistant to doxorubicin (8226/Dox40), resistant to melphalan (8226/LR5) and dexamethasone (MM.1R)

1.13 CHK1 inhibitors in combination with chemotherapy

The majority of pre-clinical data that has been published with CHK1 inhibitors has been with conventional cytotoxic therapy and in particular with gemcitabine, topoisomerase inhibitors and platinum compounds.

1.13.1 CHK1 inhibitors and gemcitabine

The combination of gemcitabine and a CHK1 inhibitor has been examined by a number of investigators. Gemcitabine causes chain termination during DNA replication leading to S phase arrest. This arrest is dependent on CHK1 and allows cells a chance to repair gemcitabine-mediated DNA damage. Using a CHK1 inhibitor in combination with gemcitabine may potentiate cytotoxicity by overriding the checkpoint, causing the cell to try to progress through the cell cycle with damaged DNA.

Parsels et al demonstrated the sensitisation of a panel of pancreatic cancer cell lines (MiaPaCa2, BxPC3 and M-Panc-96) to gemcitabine by PD-321852 in clonogenic assays (Parsels et al., 2009). Pancreatic cell lines were chosen as gemcitabine is the first choice chemotherapy both in the adjuvant and metastatic context for pancreatic cancer. Cells were treated with gemcitabine and PD-321852 concomitantly for 24 hours before being seeded out in drug free media. There was a 13-fold (MiaPaCa2), 17-fold (M-Panc-96) and 6-fold (BxPC3) reduction in the gemcitabine IC_{50} by co-incubation with PD-321852.

The authors also showed that in pancreatic cells treated with PD-321852 and gemcitabine there was predictable stabilisation of Cdc25A. The degree of

stabilization varied between different cell lines. In addition there was loss of the CHK1 protein itself following treatment with 100 nM or 300 nM PD-321852 for 24 hours. The degree of loss of the CHK1 protein correlated with the relative degree of sensitisation of the pancreatic cell lines to PD-321852 in combination with gemcitabine. The reduction in CHK1 protein levels was also seen in cells treated with PD-321852 alone.

As with studies with other CHK1 inhibitors, PD-321852 inhibited the formation of gemcitabine-induced RAD51 foci. In some cells treated with PD-321852 γ-H2AX staining persisted for longer than in cells treated with gemcitabine alone. This correlated with an accumulation of cells in S-phase. However, there was variation in the γ-H2AX staining between different cell lines leading to concern that γ-H2AX may not be a reliable marker of CHK1 inhibition in all cell lines. The authors suggest that a more reliable marker of CHK1's downstream effects may be the measurement of γ-H2AX in combination with RAD51 foci accumulation. However, changes in γ-H2AX expression are not specific to activation of CHK1. γ-H2AX is a common downstream element of the ATM, ATR and DNA-PKcs pathways (Redon et al., 2010).

As a monoagent, the highly specific CHK1 inhibitor, PF00477736 did not change the cell cycle, but abrogated gemcitabine-induced S-phase arrest with an increase in the number of cells G_2-M and G_0-G_1 as S-phase measured by flow cytometry (Blasina et al., 2008). An increase in apoptosis (Tunnel assay) was observed with the combination of PF00477736 and gemcitabine compared to gemcitabine alone.

In further experiments, 30 nM gemcitabine was shown to cause S-phase arrest, but no appearance of γ-H2AX in a western blot, 360 nM PF00477736 alone did not increase γ-H2AX levels, but the combination of the two agents led to increased S-phase arrest and significant increase in γ-H2AX levels (Blasina et al., 2008).

100 nM AZD7762 for 24 hours, a dual CHK1 and CHK2 inhibitor, significantly potentiated (approximately 10-fold potentiation) the cytotoxicity of gemcitabine (2 hour exposure) in HCT116 cells in 96-well plate growth inhibition assays (absorbance assay measuring DNA content) (McNeely et al., 2010). In addition, the percentage of apoptotic cells (determined by cell morphology) increased from 6% with 2 μM gemcitabine for 2 hours alone to 26% with gemcitabine and 100 nM AZD7762. Confirmation that this was CHK1, rather than CHK2 came from knockdown experiments where *CHK1* siRNA, but not *CHK2* siRNA, produced similar effects to AZD7762.

Similar studies were conducted by Zabludoff et al, who confirmed that 300 nM AZD7762 sensitises SW620 cell lines to gemcitabine in 96-well plate assays (Zabludoff et al., 2008). There was a significant (20-fold sensitisation) shift in the GI_{50}; 24.1 nM with gemcitabine alone compared to 1.08 nM with gemcitabine and 300 nM AZD7762.

300 nM and 1 μM XL9844 have been shown to significantly potentiate (on average 2 to 4-fold with 300 nM XL9844 and 5 to 10-fold with 1 μM XL9844) gemcitabine-mediated cytotoxicity in PANC-1, AsPC-1, SKOV3 and HeLa cell lines in clonogenic assays (Matthews et al., 2007). In PANC-1 cells 0.3 – 3 μM XL9844 abrogated Cdc25A phosphorylation induced by 30 nM gemcitabine for

24 hours in western blot assays. In an ELISA, XL9844 in combination with 100 nM gemcitabine increased γH2AX expression in a concentration-dependent fashion in PANC1 cells treated either simultaneously or sequentially with both drugs for 24 hours.

XL9844 also enhanced the antitumour activity of gemcitabine in PANC-1 xenografts in athymic mice (Matthews et al., 2007). 400 mg/kg Gemcitabine was administered intravenously every 4 days (4 doses total) and 100 or 300 mg/kg XL9844 twice orally following each dose of gemcitabine to mice. Maximum tumour growth inhibition (TGI) was 74% with gemcitabine alone and 91% and >100% with 100 mg/kg and 300 mg/kg XL9844 respectively.

In animal studies in mice bearing xenografts (A2780 and MiaPaca) SCH 900776 showed little single agent activity (Guzi et al., 2011). However, in these xenograft models SCH 900776 potentiated gemcitabine cytotoxicity and caused a dose-dependent tumour regression with doses between 8 and 32 mg/Kg of SCH 900776. The tumours were 23% of their starting volume when treated with 150 mg/Kg gemcitabine in combination with 32 mg/Kg of SCH 900776. There was no potentiation of gemcitabine related myelotoxicity even with the highest dose of SCH 900776. Very limited PK data is presented in this paper.

CCT244747 was shown to enhance the cellular cytotoxicity (see Table 1-3) of SN38, gemcitabine, etoposide, carboplatin, 5FU and ionising radiation in SRB cytotoxicity assays in a panel of cell lines (HT29, SW620, MiaPaCa-2 and Calu6 (NSCLC, p53 mutated)) (Walton et al., 2012). The greatest sensitisation was observed with gemcitabine. Cell lines were continuously exposed in 96-well plates to the combination of a fixed concentration of cytotoxic agent (at the GI_{50}

of the agent) and variable concentration of CCT244747 for 96 hours prior to staining with SRB. CCT244747 also abrogated SN38 and gemcitabine-induced S phase arrest in HT29 and SW620 cell lines and etoposide-induced G_2 arrest in the HT29 cell line.

Drug	HT29	SW620	MiaPaCa-2	Calu6
SN38	1.9 +/- 0.14	2.6 +/- 0.6	5.0 +/- 0.82	1.4 +/- 0.24
Gemcitabine	8.5 +/- 1.6	12.2 +/- 2.7	16 +/- 6.3	5.6 +/- 0.96
Etoposide	1.9 +/- 0.63	4.9 +/- 2.2		
CDDP (carboplatin)	1.8 +/- 0.32	4.2 +/- 0.87		
5FU	2.2 +/- 0.2	4.9 +/- 0.8		
IR (1 hour prior)	3.9 +/- 0.32	4.5 +/- 1.2		
IR (1 hour delay)	3.0 +/- 0.67	4.9 +/- 1.6		

Table 1-3 Potentiation index of CCT244747 in combination with cytotoxic agents

Adapted from (Walton et al., 2012). The potentiation index is the ratio of SRB GI_{50}/combination GI_{50} where the combination GI_{50} is the concentration of CCT244747 that causes 50% cell growth inhibition with a fixed concentration (the GI_{50}) of the cytotoxic agent.

CCT244747 was also shown to significantly enhance the anti-tumour activity of gemcitabine *in vivo*. 100 mg/kg Gemcitabine (i.v. on days 0, 7 and 14) alone or in combination with 75 mg/kg CCT244747 (p.o. on days 0, 7 and 14) was administered to mice bearing HT29 tumour xenografts. Growth of the tumours was delayed by an additional 8.7 days in the combination treated mice compared to those treated with gemcitabine alone.

100 nM SAR-020106 potentiates gemcitabine cytotoxicity in the HT29, SW620 and Colo205 (colorectal cancer, p53 mutated) cells (Walton et al., 2010). Potentiation factors were 3.0, 12 and 29 respectively in 96-well SRB cell proliferation assays with a 24 hour simultaneous exposure to SAR-020106 and gemcitabine followed by 96 hours in drug-free media. Co-treatment with 0.01 to 5 μM SAR-020106 and 20 nM gemcitabine for 24 hours was also associated with increased expression of γ-H2AX and PARP cleavage indicative of DNA damage and apoptosis in western blot assays with concentrations of SAR-020106 greater than 1 μM.

Studies with GNE-900 in HT29 cells revealed a 93-fold sensitisation of gemcitabine following a continuous 72 hour exposure cell proliferation assays (Blackwood et al., 2013). Cell number was assessed by DNA content (Promega kit). In *in vivo* studies Sprague-Dawley rats the addition of 25 mg/kg GNE-900 (as a single dose on day 2) to 30 mg/kg gemcitabine (as a single dose on day 1) did not cause additional bone marrow toxicity compared to gemcitabine alone.

V158411 potentiates the cytotoxicity of gemcitabine in a triple-negative breast cancer cell line (MDA-MB-468) (Bryant et al., 2014b). Potentiation was observed in both p53 wild type and p53 mutated cell lines, but the effect was greatest in p53-mutant cell lines.

Gemcitabine potentiation is seen with both ATR inhibitors and WEE1 inhibitors. Prevo et al showed that the selective and potent ATR inhibitor VE-821 significantly potentiated the cytotoxicity of gemcitabine in a panel of pancreatic cell lines (MiaPaCa-2, PSN-1 and PancM (all with p53 mutations) under both

norm-oxic and hypoxic conditions (Prevo et al., 2014). Significant potentiation of gemcitabine has also been seen with WEE1 inhibitors in sarcomas (Kreahling et al., 2013). The authors demonstrated that the WEE1 inhibitor MK1775 had significant synergy with gemcitabine in a panel of sarcoma cell lines (U2OS (osteosarcoma, p53 wild type), MG63 (osteosarcoma, p53 null), A673 (Ewing's sarcoma, p53 null) and HT1080 (fibrosarcoma, p53 wild type) irrespective of p53 status. The results have been replicated in *in vivo* studies.

The variable potentiation of gemcitabine by CHK1 inhibitors in contrast to the apparent robust and reproducible potentiation by ATR inhibitors and WEE1 inhibitors has led to a suggestion that ATR and WEE1 maybe operating by a pathway that is independent of CHK1

1.13.2 CHK1 inhibitors and topoisomerase poisons

CHK1 inhibitors have been used in conjunction with topoisomerase poisons because the poisons lead to persistent SSB and DSB as described in section 1.4.2.

Zabludoff et al utilised AZD7762 in combination with camptothecin (Zabludoff et al., 2008). In HT29 cells the 70 mM camptothecin (for 2 hours) induced G_2 arrest (determined by staining for phospho-histone H3) was abrogated by AZD7762 (concentration range 6 nM to 12.5 μM). These authors also examined the sensitivity of MDA-MB-231 cells to the combination of topotecan and 300 nM AZD7762. Cells were treated in 96-well plates for 24 hours with both topotecan and AZD7762 and then a further 24 hours with AZD7762 alone then

drug free media for 72 hours before measuring DNA content (Promega kit). There was significant 15-fold enhancement of the cytotoxicity of topotecan with AZD7762 (GI_{50} 2.25 μM with topotecan and 150 nM with topotecan + 300 nM AZD7762).

In this study, Zabludoff et al also showed that the combination of 25 mg/kg AZD7762 (2 and 14 hours after irinotecan) with 25 or 50 mg/kg irinotecan (4 doses at 3 day intervals) produced a significant reduction in the growth of SW620 xenografts in athymic mice (Zabludoff et al., 2008). There were 13 complete tumour regressions in 18 mice, compared to irinotecan alone where there were no complete regressions. Sensitisation was independent of irinotecan dose.

In 96-well plate assays in which cells were incubated with drugs for 48 hours prior to staining for DNA content (Promega kit), CHIR-124 potentiated the cytotoxicity of camptothecin in a synergistic manner (isobologram analyses) in 4 cell lines with mutated p53: MDA-MB-231, MDA-MB-453, SW-620 and CoLo205 (Tse et al., 2007b). These authors also demonstrated that while UCN-01 and 100 nM CHIR-124 alone did not affect the cell cycle they abrogated 20 nM SN-38 induced S and G_2 arrest over a 24 hour period in MDA-MB-435 cells.

In combination with 5 mg/kg camptothecin (i.v. QDS on days 1-5) and 10 or 20 mg/kg CHIR-124 (i.v. daily on days 2-7) significantly reduced MDA-MB-435 tumour growth compared to mice treated with vehicle or camptothecin alone. This was accompanied by an increased level of apoptotic nuclear morphology observed by fluorescence microscopy in tumour sections (Tse et al., 2007b).

In contrast, UCN-01 and SCH 900776 did not potentiate SN38 (Montano et al., 2012) in MDA-MB-231 cells, MDA-MB-231 (with shRNA knockdown of *CHK1*) or MCF10A treated concomitantly for 24 hours in 96-well plates with SN38 alone or in combination with 50 nM UCN-01 or 1 μM SCH 900776 followed by drug-free media for 5 to 7 days.

SAR-020106 has been shown to abrogate etoposide-induced G_2 cell cycle arrest of HT29 cells with an IC_{50} of 55 nM (Walton et al., 2010). Maude et al demonstrated that treatment with 300 nM UCN-01 for 8 hours and 500 nM CEP-3891 for 8 hours following 24 hours exposure to 50 nM etoposide significantly increased the fraction of U2OS, HeLa and SaOS2 (osteosarcoma, p53 deleted) killed compared to etoposide alone (Maude and Enders, 2005). In U2OS cells there was 6-fold potentiation with UCN-01 and 8-fold potentiation with CEP-3891; in HeLa cells 7.6-fold and 7.5-fold respective potentiation and in SaOS2 cells 8-fold and 6 fold potentiation.

1.13.3 CHK1 inhibitors and platinum compounds

CHK1 inhibitors have been used in combination with platinum-based compounds because the formation of platinum-DNA adducts that cause intrastrand and interstrand cross-links prevent DNA replication and ultimately lead to apoptosis (see Section 1.3.4) (Raymond et al., 1998) (Siddik, 2003). .

10, 25, 50 and 100 nM UCN-01 enhanced the cytotoxicity (colony-forming assay) of cisplatin in AA8 (Chinese Hamster Ovary – (CHO)) cells exposed to cisplatin for 2 hours followed by 12 hours in combination with UCN-01 (Bunch

and Eastman, 1996). There was 3-fold enhancement with 25 nM UCN-01 and 10-fold enhancement with 100 nM. Bunch et al then showed in Chinese hamster ovary (CHO) cell lines that UCN-01 abrogated cisplatin-mediated G_2 cell cycle arrest (Bunch and Eastman, 1996) and potentiated cisplatin cytotoxicity (by at least 3-fold) at concentrations (50 and 300 nM for 1 or 6-day's continuous exposure) that were not cytotoxic as a single agent.

A 6 hour treatment with 50 and 300 nM UCN-01 abrogated G_2 arrest mediated by 5 μg/ml cisplatin treatment for 1 hour in AA8 cells. In AA8 cells 50 nM UCN-01 resulted in a 10-fold potentiation of the cytotoxicity of 2 μg/ml cisplatin and 60-fold potentiation of 10 μg/ml cisplatin.

Further work by this group (Eastman et al., 2002) demonstrated that 250 nM ICP-1 and 50 nM UCN-01 enhanced growth inhibitory effect of cisplatin in breast cancer cell lines with defective p53 (MDA-MB-231) compared to p53 wild type cells (MCF10A). They also confirmed earlier studies (Bunch and Eastman, 1996), that 50 nM UCN-01 for 22 hours after cisplatin and 250 nM ICP-1 22 hours after cisplatin abrogates G_2 cell cycle checkpoint arrest mediated by 20 μM cisplatin for 2 hours.

The sequence of chemotherapy administration and CHK1 inhibitors appears to be important. Mack et al treated NSCLC cell lines A549 and H596 (p53 mutated) with UCN-01 either before or after cisplatin treatment (Mack et al., 2003). Cells were treated for 3 hours with variable concentrations of cisplatin, UCN-01 was used for 24 hours at its single agent IC_{50} concentration (250 nM in A549 cells and 1000 nM in H596 cells); cells were then left in drug free media for 72 hours before proliferation was assessed using an MTT assay. Median

effect analysis revealed that if UCN-01 was administered after cisplatin, the effect was synergistic, compared with a less than additive effect when UCN-01 was administered before cisplatin. This was confirmed by analysis of cell cycle arrest by flow cytometry in A549 and Calu-1 (NSCLC - p53 null) cell lines (3 hour treatment with cisplatin, followed by 24 hours in drug-free media and then 24 hours with 100 nM UCN-01) and by assessment of apoptosis by nuclear morphology. There was a decrease in the proportion of cells in G_2 and an increase in apoptotic cells. The synergism of cisplatin and UCN-01 by median effect analysis was most marked in cell lines with mutated p53. However, these data from studies using UCN-01 should be treated with caution as UCN-01 also inhibits several CDKs as well as CHK1 so cell cycle arrest and cytotoxicity may be due to direct CDK inhibition rather than through CHK1 inhibition.

In contrast to studies with UCN-01 *CHK1* knockdown with siRNA in HeLa cells did not enhance the cytotoxicity of cisplatin, oxaliplatin or carboplatin in colony forming assays, although ATR and Rad9 knockdown did significantly enhance cisplatin cytotoxicity (Wagner and Karnitz, 2009). The authors then examined the ability of 20 or 80 nM AZD7762 to potentiate cisplatin (concomitantly with AZD7762 for 24 hours) cytotoxicity in clonogenic assays in the HeLa cells. Again, there was no significant potentiation of cisplatin cytotoxicity. These results were confirmed in other cell lines with a range of platinum compounds and *CHK1* depletion by siRNA; there was no potentiation of cisplatin in HCT116, U2OS and A549 and of oxaliplatin in HCT116 cells.

Similarly co-exposure to 50 nM UCN-01 or 1 μM SCH 900776 with cisplatin for 24 hours in a 96-well plate growth inhibition assay did not significantly potentiate cisplatin in 3 breast cell lines (MDA-MB-231, MDA-MB-231$^{Chk1-/-}$

(*CHK1* deleted to check for off-target effects) and MCF10A) by either (Montano et al., 2012). This raises the possibility that cell survival following platinum-related damage is independent of CHK1 and casts some doubt as to the potential use of CHK1 inhibitors in combination with platinum chemotherapy.

V158411 also potentiates the cytotoxicity of gemcitabine and cisplatin in a triple-negative breast cancer cell line (MDA-MB-468 p53-defective) (Bryant et al., 2014b). V158411 appears to potentiate carboplatin and cisplatin sensitivity in SKOV-3 ovarian cell lines, but has no effect on the sensitivity of SKOV-3 cells to oxaliplatin.

1.13.4 CHK1 inhibitors and taxanes

There is relatively little pre-clinical data with CHK1 inhibitors in combination with taxanes. PF00477736 enhanced the anti-tumour effect of docetaxel, another taxane, (Zhang et al., 2009). The authors examined the combination of 15 mg/kg or 30 mg/kg docetaxel (i.p. 3 doses at day 1, 8 and 15) and 7.5 mg/kg or 15 mg/kg PF00477736 (i.p. given as 2 doses, 1 with docetaxel and 12 hours later) in CoLo205 and MDA-MB-231 xenografts. 30 mg/kg docetaxel alone caused complete regression of MDA-MB-231 tumours in the xenograft model so only 15 mg/kg docetaxel was used in combination with PF00477736. In the MDA-MB-231 xenografts there was 14 days growth delay with 7.5 mg/kg PF00477736 and 36 days growth delay with15 mg/kg PF00477736 ($p < 0.05$ with both regimens). In the CoLo205 xenografts there were 3 complete responses with the combination of PF00477736 and docetaxel whereas when docetaxel was used alone all xenografts progressed after an initial response.

1.14 CHK1 inhibitors in combination with radiotherapy

CHK1 inhibitors have been postulated to be potential radiosensitisers. CHK1 was found to be up-regulated for up to 3 hours after radiation exposure in DU145 (p53 mutated prostate cancer) and HT29 (Mitchell et al., 2010b). When the cell lines were exposed to a CHK1 inhibitor, AZD7762, for 1 hour before and 24 hours after radiation exposure there was marked increased radiation cytotoxicity compared to irradiation alone. The effects were greatest in p53 mutated cell line but remained significant in p53 wild type cell lines (Dose Modifying Factor (DMF) of 1.58 and 1.11 respectively). Flow cytometry confirmed that AZD7762 abrogated G_2 cell cycle arrest following radiation exposure and caused IR-induced γ-H2AX foci to persist. However, this affect was only seen in certain cell lines (HT29 and H460 (NSCLC, wild type p53)) so may need to be interpreted with caution.

The use of a combination of a CHK1 inhibitor, chemotherapy and radiation has been explored in pancreatic cell lines. This is felt to be clinically relevant as the gold-standard treatment in locally advanced pancreatic cancer is chemo-radiation. AZD7762 in combination with radiation sensitised pancreatic cell lines (MiaPaCa-2, Mpanc96) in an additive fashion as shown in the table below (Table 1-4) (Morgan et al., 2010).

	Radiation alone	Gemcitabine and radiation	AZD7762 and radiation	AZD7762, Gemcitabine and radiation
Radiation enhancement ratio	1	1.2 +/- 0.07 ($p<0.05$)	1.5 +/- 0.08 ($p<0.05$)	1.9 +/- 0.16 ($p<0.05$)

Table 1-4 Radiation enhancement ratios with AZD7762

Adapted from Mitchell et al., 2010b. The radiation dose that led to 10% survival in the absence of AZD7762 divided by the radiation dose that led to 10% survival in AZD7762 treated cells.

The application of 300 nM UCN-01 for 1 hour to U2OS cells prior to exposure to ionising radiation (single 10 Gy fraction) reduced and delayed the expected radiation-induced degradation of Cdc25A (Sorensen et al., 2003). These results were replicated using CEP-3891 (a CHK1 inhibitor (Cephalon) with greater specificity for CHK1 than UCN-01); 500 nM CEP-3891 for 1 hour and using *CHK1* siRNA to silence CHK1 activity in the U2OS cancer cell line.

Using a U2OS model (Syljuasen et al., 2004) demonstrated that CEP-3891 abrogates IR-mediated S and G_2 cell cycle arrest and that this leads, after a delay of 24 hours, to an increase in the number of cells showing nuclear fragmentation. This nuclear fragmentation was distinct from apoptosis and occurred at an earlier time point in the presence of CEP-3891 compared with IR

alone. They also demonstrated potentiation of IR-mediated (0-6 Gy) cytotoxicity with 500 nM CEP-3891 in clonogenic assays.

A CHK1 inhibitor has been used in combination with a PARP inhibitor and radiotherapy. Vance et al examined the combination of a CHK1 inhibitor (AZD7762) and a PARP1 inhibitor (AZD2281 – olaparib) and the ability of the combination to radiosensitise pancreatic cell lines (Vance et al., 2011). In clonogenic assays they examined the ability of 100 nM AZD7762 +/- 1 μM AZD2281 to enhance the cytotoxicity of IR. In MiaPaCa-2 and MPanc-96 cell lines they demonstrated that AZD7762 alone had an enhancement ratio of 1.5 and 2.0 respectively, with AZD2281 alone the enhancement ratios were 1.5 in both cell lines and with AZD7762 and AZD2281 in combination 2.4 and 3.0. They also sought to determine if this radiosensitisation was dependent on p53 status in 2 isogenic cell line pairs (HCT116 (p53 +/+ and p53 -/-) and H460 (p53 wild type and p53 dominant negative). They demonstrated that the radiation enhancement ratio was significantly greater in the cell lines with a defective p53 phenotype with all 3 treatment combinations

1.15 Clinical trials with CHK1 inhibitors

1.15.1 UCN-01

The first CHK1 inhibitor to enter clinical trials was UCN-01 (7-hydroxystaurosporine). However, as explained in Sections 1-10-1 and 1-11-2, UCN-01 lacks specificity for CHK1, hampering the interpretation of the data. In the first single-agent phase I study, which recruited patients between April 1996 and March 1997, UCN-01 was administered to 47 patients as a 72 hour continuous infusion (Sausville et al., 2001). UCN-01 was shown to have an extremely long and variable half-life of 25.9 days (range 6 to 161 days) with avid protein-binding in the plasma.

An unexpected toxicity of UCN-01 was found to be profound hyperglycaemia due to increased peripheral insulin resistance characterized by an increase in immunoreactive C-peptide derived from pro-insulin (Sausville et al., 2001). Other side effects include hypotension, fatigue and nausea and vomiting. This first trial of a 72 hour infusion of UCN-01 was halted due to significant symptomatic dose-limiting toxicity (DLT) of hypotension and hyperglycaemia at 53 mg/m^2/day. A recent pre-clinical study by Sharma et al has shown that UCN-01 blocks insulin's action on endothelial cells via its blockade of phosphoinositide dependent kinase (Sharma et al., 2011). This may be the mechanism behind UCN-01's DLT of hyperglycaemia.

The long plasma half-life, when UCN-01 was given as a 72 hour infusion, led investigators to consider administration as a short infusion over 3 hours to reduce toxicity. When UCN-01 was given to 24 patients as a short infusion, hyperglycaemia was mild and easily managed (Dees et al., 2005). However

again the DLT in this short infusion trial was symptomatic hypotension at 95 mg/m^2, which stopped the trial.

Pre-clinical data suggested the potentiation of topoisomerase 1 inhibitors such as topotecan. A phase 1 study, in combination with topotecan, in patients with advanced solid malignancy combined a 3 hour infusion of UCN-01 on Day 1 and intravenous topotecan on days 1-5 of a 21-day cycle (Hotte et al., 2006). Toxicity attributed to UCN-01 by the investigators in this trial included hyperglycaemia, fatigue and nausea and vomiting. A phase II trial of UCN-01 in combination with topotecan in ovarian cancer unfortunately was halted due to a lack of efficacy. This terminated study has not been published.

Two phase 1 studies of UCN-01 in combination with cisplatin have also been performed. In the first the California Cancer Consortium delivered UCN-01 as a fixed dose of 45 mg/m^2/day as a 72-hour infusion with the intention of escalating cisplatin from 20 mg/m^2 to 75 mg/m^2 in 5 increments (Lara et al., 2005). Unfortunately when the cisplatin was increased to 60 mg/m^2 dose-limiting toxicities were seen with patient deaths due to sepsis and respiratory failure. The long half-life of UCN-01 was felt to be a contributory factor in the difficulties seen in this trial; and shorter infusions of UCN-01 at a lower dose were recommended for future trials. A dose of 60 mg/m^2 is the established therapeutic dose of cisplatin where activity is seen as a mono-agent. Three patients had tumour biopsies before and after combination chemotherapy. These showed a significant reduction in CHK1 and Cdc25C protein levels suggesting that UCN-01 was having its anticipated pharmacodynamic effect in tumours.

In the second phase I trial in combination with cisplatin, Perez et al administered UCN-01 as a 72-hour infusion starting 22 hours after the infusion of cisplatin in patients with advanced solid malignancy (Perez et al., 2006). Initially 45 mg/m^2/day UCN-01 was delivered, but this was decreased to 34 mg/m^2/day due to dose-limiting toxicity (hypoxia, subarachnoid haemorrhage, myocardial ischaemia, atrial fibrillation and hyperglycaemia). As well as conventional end-points of maximum tolerated dose and PK of UCN-01, this study looked for the pharmacodynamic end-point of S/G_2 cell cycle arrest by measuring geminin immunohistochemistry in tumour biopsies taken at baseline, 22 hours after cisplatin (prior to UCN-01), 24 and 72 hours after starting the UCN-01 infusion. Biopsy specimens showed abrogation of the S/G_2 checkpoint following UCN-01 compared to both baseline and post-cisplatin values.

Unfortunately this trial of UCN-01 only recruited 7 patients so assessment of the efficacy of UCN-01 in combination with cisplatin could not be made. The trial was ended as this point as it was felt impractical to administer a 72-hour infusion. Another factor was that data from the phase 1 single-agent trial delivering UCN-01 as a 3-hour infusion had become available and been shown to be equally efficacious as the 72 hour infusion.

1.15.2 PF00477736

No single agent studies of PF-00477736 have been performed. However, a phase I study of PF-00477736 in combination with gemcitabine was reported at ASCO 2010 (Brega et al., 2010). The study population was patients with gemcitabine-naïve advanced solid malignancy. 750 mg/m^2 gemcitabine was

given as a 1-hour infusion with PF-00477736 given 20 to 24 hours after the gemcitabine. Both PF-00477736 and gemcitabine were given on day 1 and day 8 of a 21-day cycle. PF-00477736 was delivered by 2 different schedules; early cohorts were given it over 3 hours (50 to 80 mg i.v. flat dose) whereas later cohorts were given PF-00477736 (80 to 340 mg i.v. flat dose) as a 24 hour infusion. It appears that pre-clinical data to support the longer infusion time came to light after the trial started (Blasina et al., 2008).

36 patients were treated the best response was a partial response in 3 patients (SCC of skin, NSCLC and mesothelioma). The MTD of PF-00477736 in combination with 750 mg/m^2 gemcitabine was 270 mg. No pharmacodynamic studies were performed. There was an intention to repeat the phase I study in combination with 1000 mg/m^{2}gemcitabine, and to perform biomarker analysis with the assessment of the effect on the S/G_2 checkpoint in serial tumour biopsies, but this has not been published.

1.15.3 AZD7762

AZD7762 has been used in combination with gemcitabine in two Phase 1 trials, one in American patients with advanced solid tumours and the second in Japanese patients (Sausville et al., 2014, Seto et al., 2013). In the study in American patients, first presented at ASCO 2011 (Sausville et al., 2011), 6 – 40 mg AZD7762 (i.v. flat dose) was administered in combination with gemcitabine to 42 patients. Patients received a single agent run-in phase of two doses of single agent AZD7762, and then AZD7762 was given concomitantly with 750 or 1000 mg/m^2 gemcitabine (i.v.) on days 1 and 8 of a 21-day cycle. Unfortunately

2 further patients had cardiac DLTs during the single agent phase (1 grade 3 symptomatic troponin rise and 1 grade 3 myocardial ischaemia). There was no evidence that gemcitabine affected the PK of AZD7762. There were 2 partial responses (6 mg AZD7762 with 750 mg/m^2 gemcitabine and 9 mg AZD7762 with 750 mg/m^{2}gemcitabine) to the combination treatment in NSCLC patients who were gemcitabine-naïve. The study concluded that the MTD of AZD7762 in combination with 1000 mg/m^2 gemcitabine was 30 mg.

The Japanese study followed a similar design with a single agent run-in phase followed by combination treatment with AZD7762 and 1000 mg/m^2 gemcitabine on days 1 and 8 of a 21 day cycle. 20 patients were treated. There were 2 DLTs in the 30 mg AZD7762 cohort. One patient developed a grade 3 rise in cardiac troponin and a second neutropenia and thrombocytopenia. The study concluded that the MTD of AZD7762 in combination with 1000 mg/m^2 gemcitabine in Japanese patients was 21 mg. There were no complete or partial responses. Five patients with NSCLC achieved disease stabilisation.

AZD772 has also been delivered in combination with irinotecan to patients with advanced solid tumours, though this Phase I clinical trial has only been published as an ASCO poster in 2011 (Ho et al., 2011) . After a single agent run-in phase of two doses (7 days apart) of single agent 6 – 144 mg AZD7762 (i.v. flat dose), AZD7762 was given concomitantly with 100 or 125 mg/m^2 irinotecan (i.v.) on days 1 and 8 of a 21-day cycle. 68 patients received the combination therapy in total. However, the trial was halted as cardiac DLT (1 myocardial infarction and 1 Grade 4 ventricular dysfunction) was seen during the single agent run-in phase in the trial. This was at the 96 mg AZD7762 with 100 mg/m^2 irinotecan dose level. There was 1 complete response to therapy in

a patient with a small cell carcinoma of the ureter and 1 partial response in a patient with colon cancer despite prior treatment with irinotecan.

With five cases of myocardial DLTs between the 3 early phase trials, the development programme of AZD7762 has been halted.

1.15.4 SCH 900776

A phase I study of SCH 900776 (CHK1 inhibitor – Schering Plough) in combination with gemcitabine was also reported at ASCO 2010 (Daud et al., 2010). 26 patients were treated with 800 mg/m^2 gemcitabine followed by 10 to 112 mg/m^2 SCH 900776 (i.v.) on Day 1 and Day 8 of a 21-day cycle. The time period between the administration of gemcitabine and SCH 900776 was not specified in the abstract or poster. 4 patients showed a response to the combination (melanoma, sarcoma, cholangiocarcinoma and pancreatic tumour). The trial determined an MTD of SCH 900776 in combination with 800 mg/m^{2}gemcitabine of 112 mg/m^2.

In the phase I trial, SCH 900776 was given as a 15 minute infusion, but SCH 900776 is reported to be orally bioavailable. The half-life of the IV preparation was between 6.24 and 9.33 hours. No pharmacodynamic data was published in the abstract, but the poster contained data related to γ-H2AX. Plasma samples from patients dosed with SCH 900776 were taken alongside pharmacokinetic samples, diluted with tissue medium 1:4 and administered to K562 cells grown in tissue culture. The cells were grown in this medium for either 2 or 24 hours and then fixed and stained for γ-H2AX. γ-H2AX intensity was measured by flow

cytometry. The clinical pharmacodynamic data correlated with the pre-clinical data. However, a decision has been made not to proceed with further clinical trials of SCH 900776 at present.

1.15.5 LY2603618

LY2603618 has been evaluated in a Phase I trial in combination with 500 mg/m^{2}pemetrexed in patients with advanced solid tumours (Weiss et al., 2013). 40-195 mg/m^2 LY2603618 (i.v. as a 4.5 hour infusion) was delivered as a single agent 7 days prior to pemetrexed and then 24 hours after pemetrexed every 21 days. 31 patients were treated in the study. There was one partial response by RECIST criteria (Therasse et al., 2000) in a patient with pancreatic adenocarcinoma (105 mg/m^2 cohort), nine other patients had stable disease following treatment. The MTD of LY2603618 in combination with 500 mg/m^2 pemetrexed was determined to be 150 mg/m^2. DLTs were diarrhoea, thrombocytopenia, fatigue and reversible-infusion reactions.

A second phase I study of LY2603618 (130-275 mg/m^2 on day 2 of a 21-day cycle) in combination with 75 mg/m^2 cisplatin (i.v. on day 1 of a 21-day cycle) and 500 mg/m^2 pemetrexed (i.v. on day 1 of a 21-day cycle) has treated 14 patients with advanced solid tumours (Calvo et al., 2014). No DLTs were reported. Two patients with NSCLC had a partial response. The recommended phase II dose of LY2603618 in combination with cisplatin and pemetrexed was 275 mg/m^2.

A further phase I study of LY2603618 (on day 2, 9, 16 of a 28 day cycle) has been performed in combination with 1000 mg/m^2 gemcitabine (i.v. on day 1, 8 and 15 of a 28-day cycle) in Japanese patients with advanced solid tumours, but has not been published. Phase Ib/II studies are ongoing or as yet unpublished in patients with pancreatic cancer in combination with gemcitabine, and in NSCLC in combination with pemetrexed.

1.15.6 LY2606368

The only 'second generation' CHK1 inhibitor to be taken into early phase clinical trials as a single agent is LY2606368. This trial has not been published but included expansion cohorts of patients with squamous head and neck cancer. A phase II clinical trial in this patient population is now being performed.

1.16 Aims of project

To evaluate novel CHK1 inhibitor, V158411, in terms of:

- Its effect on DNA damage-induced checkpoint function in parallel with chemo/radio-potentiation in a panel of cell lines characterised for their CHK1 expression and activity.

- To determine the single agent cytotoxicity in the panel of cell lines.

- To identify potential pharmacodynamic biomarkers of CHK1 activity suitable for measuring the activity of inhibitors in the clinic.

- To explore the role of p53 and identify other potential determinants of sensitivity to CHK1 inhibitors.

Chapter 2 Materials and Methods

2.1 Chemicals and Drugs

All chemicals, including tissue culture reagents, were supplied by Sigma (Poole, UK) unless otherwise stated. V158411 (kindly provided by Vernalis, Cambridge, UK). NU7441 (Newcastle University, UK), PF00477736 (Axon Medchem, Groningen, Netherlands), AZD7762 (Axon MedChem), Camptothecin, etoposide, hydroxyurea, (hydroxyurea 2 M) stock solution were dissolved in dry DMSO to form a 10 mM stock solution which was aliquoted and frozen. Gemcitabine and cisplatin were dissolved to form a 10 mM stock solution in PBS and frozen in aliquots. Ionising radiation was delivered using a medical irradiator (Xstrahl RS320 X-irradiator, 3.15 Gy/minute dose rate) with the dose of ionising radiation standardised for either adherent or suspension cell lines.

2.2 Cell lines and cell culture

Human cancer cell lines were obtained from ATCC (Manassas, Virginia, USA), (ECACC, Porton Down, UK) or from institute archives and authenticated by short-tandem repeat (STR) profiling, compared to the reference ATCC profiles, by LGC Standards (Teddington, Middlesex, UK). All media was supplemented with 10% foetal calf serum (FCS) and 2 mM penicillin-streptomycin. Cells were verified to be free from mycoplasma infection by PCR (Mycoalert™) every two months. All cell lines were cultured in humidified incubators at 37^{o}C with 5% CO_2.

Name	Species	Tissue of Origin	p53 status	Provenance	Media
MCF10A	Human	Breast	Wild Type	ATCC	RPMI-1640
MCF7	Human	Breast	Wild Type	ATCC	RPMI-1640
MDA-MB-231	Human	Breast	Mutated	ATCC	RPMI-1640
K562	Human	CML	Mutated	ATCC	RPMI-1640
HCT116 WT	Human	Colon	Wild Type	John Lunec[4]	RPMI-1640
HCT116$^{-/-p53}$	Human	Colon	Mutated	John Lunec[4]	RPMI-1640
M059J	Human	Glioblastoma	Mutated	NICR	DMEM
M059J-Fus1	Human	Glioblastoma	Mutated	NICR	DMEM + G418[1]
U2OS WT	Human	Osteosarcoma	Wild Type	John Lunec[4]	DMEM
U2OS DN p53	Human	Osteosarcoma	Dominant Negative[2]	John Lunec[4]	DMEM + G418[1]
Hep3B	Human	Liver	Null	ATCC	DMEM/F12[3]
Huh7	Human	Liver	Mutated	ECACC	DMEM/F12[3]
HepG2	Human	Liver	Wild type	ECACC	DMEM/F12[3]
PLC/PRF/5	Human	Liver	Mutated	ATCC	DMEM/F12[3]
SNU.182	Human	Liver	Not detected	ATCC	RPMI-1640
SNU.475	Human	Liver	Mutated	ATCC	RPMI-1640
AA8	Chinese Hamster	Ovary	Mutated	Keith Caldecott[5]	RPMI-1640
V3	Chinese Hamster	Ovary	Mutated	Keith Caldecott[5]	RPMI-1640
XRS-6	Chinese Hamster	Ovary	Mutated	Keith Caldecott[5]	RPMI-1640
EM9	Chinese Hamster	Ovary	Mutated	Keith Caldecott[5]	RPMI-1640
VC8	Chinese Hamster	Lung fibroblasts	Wild Type	Malgorzata Zdzienicka via Thomas Helleday[6]	DMEM
VC8-B2	Chinese Hamster	Lung fibroblasts	Wild Type	Thomas Helleday[6]	DMEM

Table 2-1 Cell lines

Details of species, tissue of origin, p53 status and provenance. DMEM (Dulbecco's modified Eagles medium), DMEM/F12 (Dulbecco's modified Eagles medium/nutrient F12 ham). [1]4 μg/ml G418 (Life Technologies, Paisley, UK); [2]The U20S p53DN express the p53-R248W dominant negative mutant p53 prepared by transfection of U20S: PG13-Luc cells (Moumen et al., 2005); [3]Supplemented with 2 mM L-glutamine (Sigma); [4]John Lunec, Northern Institute for Cancer Reasearch, Newcastle-upon-Tyne University, UK; [5]Keith Caldecott, Professor of Biochemistry, Sussex University, UK; [6]Thomas Helleday, Professor of Translational Medicine and Chemical Biology, Karolinska Institutet, Stockholm, Sweden.

2.3 Cytotoxicity assays

Cytotoxicity was assessed by clonogenic assays, which measure the ability of single cells to survive and proliferate into colonies after cytotoxic insult. Briefly, cells from exponentially growing monolayers in flasks were harvested by trypsinisation. A single cell suspension was ensured by syringing through a 22G needle. Cells were counted using an automated counter (Beckman Coulter, Brea, California, USA). A fixed numbers of cells (between 50 and 10000, with an aim to have between 20 and 100 colonies to count depending on the cytotoxicity of the drug) were seeded in 2 ml media into the wells of a six-well plate. After 24 hours the media was removed and replaced with media containing appropriate concentrations of the drug of interest. After incubation in drug-containing media for 24 hours the media was removed, each well washed with PBS and 2 mls of drug-free media was added. The plates were incubated for between 8 and 21 days for colonies to form. The media was then removed, the cells fixed with Carnoy's solution (25% glacial acetic acid (Fisher, Loughborough, UK) and 75% methanol (Fisher)), and stained with 1% crystal violet solution. Colonies were counted on the G-Box (Syngene, Cambridge, UK) with a minimum colony size of ~50 cells.

Cytotoxicity of drugs in K562 cells was assessed by performing clonogenic assays in a 3D matrix. Following counting a fixed number of cells were seeded using blunt needles into 2 mls of media (4:1 ratio of Methocult (Stemcell, Grenoble, France) and Isocove's media (Gibco, Paisley, UK) supplemented 0.6% L-glutamine). After 2 weeks colonies were stained with 0.5 mls per well MTT (0.5% in water) (MTT changes colour following reduction with mitochondrial dehydrogenase in viable cells) and counted on the G-Box.

2.4 Chk1 knockdown with siRNA

To confirm whether a drug of interest is affecting the intended target, the effect of drug can be compared to that of cells in which the target protein has been silenced by an alternative method. Knockdown with siRNA relies on the incorporation of the siRNA into the cellular genome this is facilitated by a transfection agent in a process that has to occur in the absence of antibiotics. siRNA binds to the target RNA promoting its degradation by the cellular apparatus.

MCF7 cells from exponentially growing monolayers in flasks were harvested by trypsinisation. A single cell suspension was ensured by syringing through a 22G needle. Cells were counted using an automated counter (Beckman Coulter). 1.5 μl of siRNA (target siRNA Chk1 (Qiagen) or scrambled siRNA (Sigma)) was mixed with 500 μl Opti-MEM (Life Technologies) and 5 μl Lipofectamine RNAmax (Invitrogen) and 7 x 10^5 cells in 2.5 mls antibiotic-free media for each well of a six-well plate. Wells were seeded with no siRNA, scrambled siRNA or

Chk1 siRNA both for western blotting after 48 hours, 5 days and 7 days and for to look for cloning efficiency at each time point.

2.5 Western blotting

Western blotting allows the immunological detection, and approximate quantitation of cellular proteins. The first step in western blotting is the preparation of a lysate. A lysate is prepared from cells by mechanical removal of the cells from the plate, the cellular material is placed into a lysis buffer which extracts the proteins from the other cellular components. The lysis buffer contains protease inhibitors, which prevent the breakdown of proteins. Subsequently cellular proteins are loaded onto a polyacrylamide matrix (gel) separated on the basis their size by an electrical current. The proteins are then transferred to a membrane and those of interest are detected by the binding of a specific primary antibody with signal amplification by a secondary antibody raised against the species of the primary antibody. The secondary antibody is conjugated to horseradish peroxidase which catalyses the production of light from a chemi-luminescent agent allowing detection of the protein. Relative quantities of protein can be quantified and compared to a housekeeping protein such as actin.

Cells from exponentially growing monolayers in flasks were harvested by trypsinisation. A single cell suspension was ensured by syringing through a 22G needle. Cells were counted using an automated counter (Beckman Coulter). Fixed numbers of cells were seeded in 10 mls media onto 10 cm plates. After

24 hours the media was removed and replaced with media containing appropriate concentrations of the drug of interest for 1 hour.

After the appropriate exposure to the drug-containing media (normally 1 hour), the media was removed and the cells washed with 2 mls ice cold PBS. Cells were scraped using a cell scraper and resuspended in 2 mls PBS. Samples were kept on ice. Cells were pelleted by centrifugation at 450 g for 5 minutes. The supernatant was removed and discarded. The pellet was resuspended in 75 μl of Phosphosafe buffer (Merck Chemicals, Nottingham, UK) containing additional protease inhibitor cocktail. Each sample was sonicated for 10 seconds and left at room temperature for 5 minutes to extract the protein. The samples were then spun again in a refrigerated centrifuge for 5 minutes at 16000 g. The supernatant was removed and kept on ice, the pellet discarded.

The protein content of the samples was quantified using a Pierce protein assay (ThermoScientific, Cramlington, UK) against an albumin standard curve (0.2-1.2 ug). Plates were read on FLUOstar Omega plate reader (BMG Labtech, Allmendgruen, Germany).

For Chk1 analysis 20 μg of the protein from the sample of interest was loaded into each well with sample buffer (4 x XT loading buffer (Bio-Rad, Hemel Hempstead, UK)), with water making the total volume up to 15 μl (12 and 15-well gels) or 20 μl (10-well gels) on 4-12% TGX gels (Bio-Rad) at 200 volts for 25 minutes (Mini-Protean Tetra Cell, Bio-Rad). For DNA-PK analysis 30 μg of the protein from the sample of interest was loaded into each well with sample buffer, with water making the total volume up to 30 μl (12 +2 well gels). on XT Criterion (3-8%) gels (Bio-Rad). Gels were run at 150 volts for 1 hour. All

samples were transferred onto HiBond C-Extra membrane (GE Healthcare, Little Chalfont, UK) at 100 volts (Mini-Protean Tetra Cell, Bio-Rad) on ice for 1 hour. Following washing in TBS-tween the membrane was blocked in 5% bovine serum albumin (BSA) for 1 hour. Phopho-antibodies were made up in 5% BSA and normal antibodies in 1% BSA. Antibodies used as follows: 1:1000 Chk1 (Santa Cruz Biotechnology, Dallas, TX, USA), 1:300 ATR (Santa Cruz Biotechnology), 1:1000 pChk1^{serine296} (Abcam, Cambridge, UK), 1:1000 pChk1^{serine345} (Cell Signalling Technology, Boston, MA, USA), 1:1000 DNAPK (Santa Cruz Biotechnology), 1:1000 pDNAPK^{serine2096} (Abcam), 1:100 cdc25c (Santa Cruz Biotechnology), 1:5000 Actin (Genscript, Piscataway, NJ, USA) The membrane was exposed to constantly agitated primary antibodies overnight at 4^0C. Following three 5-minute washes with TBS-tween the membrane was exposed to the appropriate secondary antibody (1:1000 mouse and 1:1000 rabbit polyclonal antibodies – DAKO, Glostrup, Denmark) in 1% BSA at room temperature for 1 hour. The membrane was washed a further 4 times for 5 minutes in TBS-tween. The membrane was treated with ECL-Prime (GE Healthcare) for 5 minutes prior to analysis in the G-Box (Syngene, Cambridge UK). Bands were quantified using the software GeneTools (Syngene).

2.6 Flow cytometry

Flow cytometry is used to determine the fraction of cells in each phase of the cell cycle on the basis of size and DNA content following staining with a DNA dye (propidium iodide or DAPI are two examples). Cells in G_2 and mitosis have twice the DNA content of cells in G_0 or G_1. Cells that display significant

aneuploidy cannot be analysed in this way. Many experiments to determine when cells are arresting, and which factors are playing a role at each stage of the cell cycle, require investigators to be able to trigger cell cycle arrest at specific points within the cell cycle. *In vitro* cell cycle arrest can be triggered using alpha-factor which arrests cells in G_1, nocodazole can be used to cause G_2 arrest (Aylon et al., 2004).

Cells from exponentially growing monolayers in flasks were harvested by trypsinisation. A single cell suspension was ensured by syringing through a 22G needle. Cells were counted using an automated counter (Beckman Coulter). Fixed numbers of cells were seeded in 10 mls media onto 10 cm plates. After 24 hours the media was removed and replaced with media containing appropriate concentrations of the drug of interest 1 hour

After the appropriate exposure to the drug-containing media (normally 1 hour), the media was removed and the cells washed with 2 mls PBS. Cells were harvested by trypsinisation (1 ml trypsin-EDTA) and resuspended in 5 mls normal media. Cells were pelleted by centrifugation at 450 g for 5 minutes. The pellet was washed in 2 mls PBS, vortexed and spun again at 450 g for 5 minutes. The pellet was resuspended in 1 ml of PBS and kept on ice.

Samples were analysed on a BD FacsCalibur (BD Biosciences, Franklin Lakes NJ, USA). 500 μl of well-mixed sample was mixed with 500 μl hypotonic propidium iodide solution (0.025% PI (Calbiochem)) around 30 seconds prior to analysis. Flow cytometry data was analysed using CellQuest software (BD Biosciences).

2.7 *In silico* analysis of microarray expression data

Microarrays allow the analysis of individual gene expression across the genome. The levels of mRNA from specific genes can be normalised to the mRNA levels from housekeeping genes so that the relative expression of one gene to another can be compared.

The Affymetrix Human Genome U133 Plus 2.0 Array hosts 57500 DNA probes covering the whole human genome. The probes hybridise to complementary sequences of biotin-labelled cDNA, which can be detected by a fluorochome. The level of mRNA expression corresponds to fluorescent intensity. The NCBI Gene Expression Omnibus (GEO) (http://www.ncbi.nlm.nih.gov/projects/geo/) contains publically available datasets from a range of tumour sites. Datasets from a range of tumours where both normal tissue and tumour were available were chosen. Data for individual genes of interest was analysed using the online GEO2R tool. Background signal intensity was subtracted and data normalised to the housekeeping gene *HPRT1*. Where more than one probe was associated with a single gene the average expression across the probes for the gene of interest was used.

2.8 Statistics

All data was analysed using GraphPad Prism 6 software. Statistical significance (* = $P < 0.05$; ** = $P < 0.01$, ***, $P < 0.001$) was determined using paired, two-

tailed t test or one-way ANOVA and either Tukey or Dunnett tests unless specified.

Chapter 3 Proof of target-drug interaction

The aim of this section of work is to measure inhibition of CHK1 in cells and the impact on DNA damage-induced cell cycle arrest. Total CHK1 expression, the phosphorylation of target proteins within the pathway, and the downstream consequences of activation or inhibition of proteins following a CHK1 inhibitor are considered.

3.1 Introduction to target-drug interaction with V158411

Cellular total CHK1 protein levels are unlikely to be responsive to DNA damage in the time-scale required for checkpoint activation. This has been confirmed by several studies that have shown that total CHK1 protein expression, in western blot assays, appears to be stable or increased following treatment with cytotoxic agents. For example, there was no change in total CHK1 protein levels in SW620 cells treated with 20 nM gemcitabine for 24 hours or 100 nM SN38 for 24 hours (Walton et al., 2010). Stable total CHK1 protein expression was also seen in MCF10A and MDA-MB-231 breast cell lines treated with 0.1 and 1 mM hydroxyurea for 24 hours (Montano et al., 2012). However, some studies demonstrated that total CHK1 protein levels in U87MG gliomas cell lines transiently increased (over 1-2 days) following exposure to 100 μM temozolomide for 3 hours, but then fell over a 10 day period in drug-free media (Hirose et al., 2001).

There is mixed data as to the effect of CHK1 inhibitors on total CHK1 expression. Exposure to 0.01 to 5 μM SAR-020106 for 24 hours appeared to

not affect total CHK1 protein expression in SW620 cells (Walton et al., 2010). However, exposure to 100 or 300 nM PD-321852 for 24 hours reduced total CHK1 protein expression compared to untreated controls in a panel of pancreatic cell lines (MiaPaCa2, BxPC3, PANC-1 and M-Panc-96) (Parsels et al., 2009).

As described in the introduction (section 1-5-1), most cancer cells have a defect in their G_1 checkpoint control, but there is relatively little data comparing total CHK1 protein expression between different cancer cell lines. Parsels et al demonstrated that baseline total CHK1 protein expression was similar in their panel of 4 pancreatic cancer cell lines (MiaPaCa2, BxPC3, PANC-1 and M-Panc-96) (Parsels et al., 2009). However, few other authors have presented data on a head to head comparison of total CHK1 expression between cell lines.

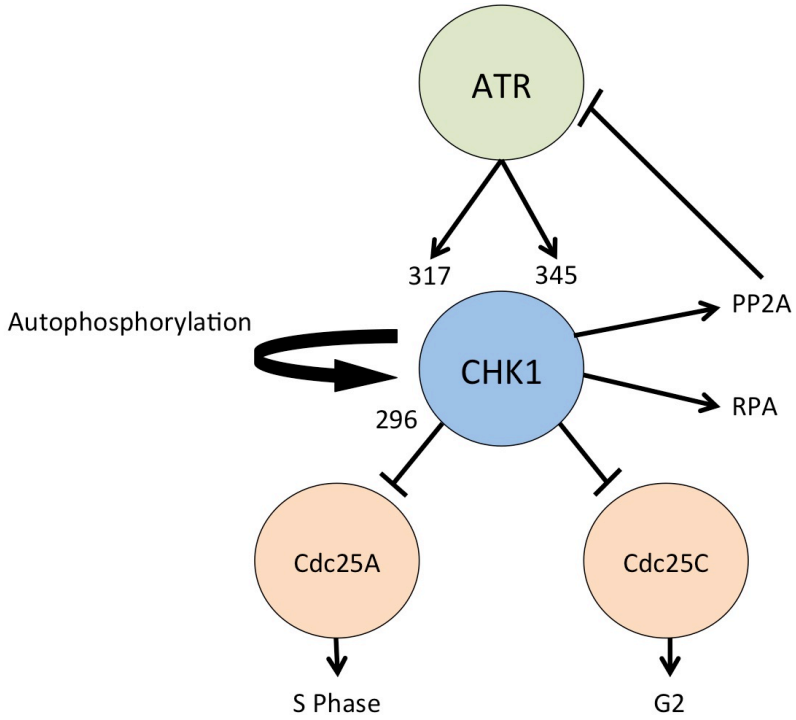

Figure 3-1 The ATR-CHK1 pathway and phosphorylation targets.

ATR phosphorylates CHK1 at serine^{317} and serine^{345}, activated CHK1 is autophosphorylated at serine^{296}. Arrows denote activation and T-bars denote inhibition.

As described in the Introduction (Section 1-6-6) Cdc25A stability, Cdc25C phosphorylation and phosphorylation of CHK1 itself have all been investigated as potential biomarkers of CHK1 activity. Downstream phosphorylation targets are more likely to be an indication of CHK1 function/activity and autophosphorylation at serine^{296} has been reported by several groups. CHK1^{serine296} has been demonstrated to be a site of autophosphorylation in response to CHK1 activation (Clarke and Clarke, 2005). CHK1 serine^{296} phosphorylation in untreated cell lines is very low (Walton et al., 2010). CHK1^{serine296} phosphorylation has been shown to be induced by some types of

cytotoxic therapy and reduced by the addition a CHK1 inhibitor. Guzi et al demonstrated that hydroxyurea (at an unspecified concentration overnight) increased CHK1^{serine296} phosphorylation in U2OS cells and that this was then reduced in a concentration-dependent fashion by 0.06 – 2 μM SCH 900776 for 2 hours (Guzi et al., 2011). This work was duplicated in breast cell lines (MCF10A and MDA-MB-231) (Montano et al., 2012). Hydroxyurea treatment for 24 hours increased CHK1^{serine296} phosphorylation in a concentration-dependent fashion and co-incubation with 1 μM SCH900776 abolished CHK1^{serine296} phosphorylation. Similarly, Walton et al showed that a 24 hour exposure to 100 nM SN38 significantly induced CHK1^{serine296} phosphorylation in SW620 cells (Walton et al., 2010, Walton et al., 2012). Walton et al demonstrated that a 24 hour exposure to CCT244747 at concentrations >50 nM abolishes SN-38 induced CHK1^{serine296} phosphorylation in HT29 cells (Walton et al., 2012).

Clarke and Clarke also demonstrated that CHK1 was phosphorylated by ATR at both serine^{317} and serine^{345} (Clarke and Clarke, 2005). Walton et al also observed that 24 hour exposure to SN38 increased CHK1^{serine317} and CHK1^{serine345} phosphorylation reflecting ATR activation. Curiously, this was reduced, but not abolished by concentrations >100 nM of the CHK1 inhibitor, CCT244747 (Walton et al., 2012). Similarly, 2 μM gemcitabine for 2 hours increased CHK1^{serine317} and CHK1^{serine345} phosphorylation, which was reduced by 100 nM AZD7762 for 24 hours following gemcitabine (McNeely et al., 2010). These curious results of a CHK1 inhibitor acting upstream on ATR phosphorylation events, was postulated by the report's authors to be secondary to a global reduction in CHK1 protein.

In studies using AZD7762 and gemcitabine in MiaPcCa-2 pancreatic cells (Parsels et al., 2011), 100 nM AZD7762 for 24 hours alone increased CHK1^{serine345} phosphorylation as did 50 nM gemcitabine for 2 hours and there was an additive effect when AZD7762 was combined with gemcitabine. It was suggested that this was due to loss of feedback inhibition of PP2A (that is normally activated by CHK1) to repress ATR activity. Subsequently, the authors looked at CHK1^{serine345} expression in biopsies (hair follicles and colonic biopsies) from mice treated with 30 – 60 mg/kg gemcitabine and 5 – 40 mg/kg AZD7762 alone and in combination (AZD7762 3 hours after gemcitabine and biopsies taken after a further 3 hours). There was no significant increase in CHK1^{serine345} phosphorylation with either drug on its own, but a significant increase when used in combination.

Other authors have also noted that CHK1 inhibitors increase CHK1^{serine345} phosphorylation significantly. For example, Montano et al showed in MDA-MB-231 cells that 24 hour exposure to 1 μM SCH 900776 significantly increased 31 - 500 mM hydroxyurea–induced CHK1^{serine345} phosphorylation (Montano et al., 2012).

Alternative downstream markers of CHK1 activity have been considered, such as phosphorylation of H2AX, but this is the target of many kinases in response to DNA damage and stalled replication forks and therefore not likely to be specific (Redon et al 2012). CHK1 inhibition (XL9844 – 18.5 to 4500 nM for 2 hours) in conjunction with 30 nM gemcitabine for 24 hours induces γ-H2AX in PANC-1 cells (Matthews et al., 2007). Simultaneous treatment with 30 nM gemcitabine and 1500 nM XL9844 increases γ-H2AX 4-fold. However, this is

not specific to the use of a CHK1 inhibitor as other cytotoxic therapy as a single agent induce γ-H2AX expression (Montano et al., 2012).

Guzi et al also looked at the phosphorylation of RPA at serine[33] as a marker of DNA damage and showed that phosphorylation was increased significantly when 0.06 – 2 μM SCH 900776 for 2 hours was used in conjunction with hydroxyurea (at an unspecified concentration overnight) (Guzi et al., 2011).

Other potential downstream markers of CHK1 activity include Cdc25A and Cdc25c. Activated CHK1 precipitates the degradation of Cdc25A and Cdc25A degradation induced by 30 nM gemcitabine for 24 hours was prevented by 300 to 3000 nM XL9844 for 2 hours. (Matthews et al., 2007).

Another measure of CHK1 activity is the impact on S and G_2 phase cell cycle arrest. As described in section 1.11.2 and 1.11.3. CHK1 inhibitors reduce topoisomerase I poison-induced S-phase arrest and topoisomerase II poison-induced and cisplatin-induced G_2 arrest. 50 nM UCN-01 and 300 nM SCH 900776 abrogated S phase arrest induced by 10 nM SN-38 in MDA-MB-231 cells (Montano et al., 2012).

In HT29 cells 500 nM CCT244747 for 24 hours (Walton et al., 2012). CCT244747 alone had minimal effects on the cell cycle distribution but reduced the 70% accumulation of cells in G_2 caused by exposure to 25 μM etoposide for 1 hour by 30% with a corresponding increase in cells in G_1 (9.6%) or S phase (67%, but not actively incorporating BrdUrd). Eastman et al demonstrated that exposure of MDA-MB-231 breast cancer cells and MCF10A breast epithelial cells to 20 μM cisplatin for 2 hours induced both S and G_2 arrest. This was

significant after 24 hours and maximal after 48 hours (Eastman et al., 2002). This arrest was abrogated in a concentration dependent fashion by both UCN-01 and ICP-1 in the MDA-MB-231 cell line.

The aims of this chapter are:

a) To characterise a panel of cell lines in terms of their CHK1 expression and activity after exposure to cytotoxic agents

b) To demonstrate CHK1 inhibition by V158411

c) To demonstrate cell cycle checkpoint abrogation by V158411.

3.2 Baseline cellular levels of CHK1

In view of the lack of specificity of H2AX phosphorylation for CHK1 and because Cdc25A stability/Cdc25c phosphorylation could be dependent on their expression in different cell lines it was decided to focus on phosphorylation of CHK1 itself. Prior to assessing the ability of V158411 to inhibit CHK1, the expression of total CHK1 protein and gemcitabine-induced CHK1^{serine296} phosphorylation in a panel of cell lines was assessed by western blot analysis. The panel consisted of human leukaemic (K562 p53 mutated), breast (MCF7 p53 wild type, MDA-MB-231 p53 mutated), colon (HCT116 p53 wild type and p53 -/-), glioblastoma (M059J p53 mutated, DNA-PKcs deficient and M059J-Fus1 p53 mutated, DNA-PKcs corrected) described in table 2-1. CHK1^{serine296} is autophosphorylated by CHK1 when it is in its activated state. Pilot experiments showed that a short 1 hour exposure to 1 μM gemcitabine induced a significant increase in pCHK1^{serine296} expression (data not shown). This short relatively high concentration exposure to gemcitabine was chosen over a longer lower concentration exposure as it was felt that a short exposure would be the easiest to use in the development of an *ex vivo* biomarker.

Figure 3-2 shows the baseline expression of total CHK1 protein in un-stimulated samples from a panel of cell lines. A seven-fold variation in cellular levels was observed; expression was highest in the K562 cells and lowest in MCF7 cells. Representative western blots from these experiments showing the expression of CHK1, pCHK1^{serine296} and actin are shown for 9 cell lines in the panel in Figure 3-3.

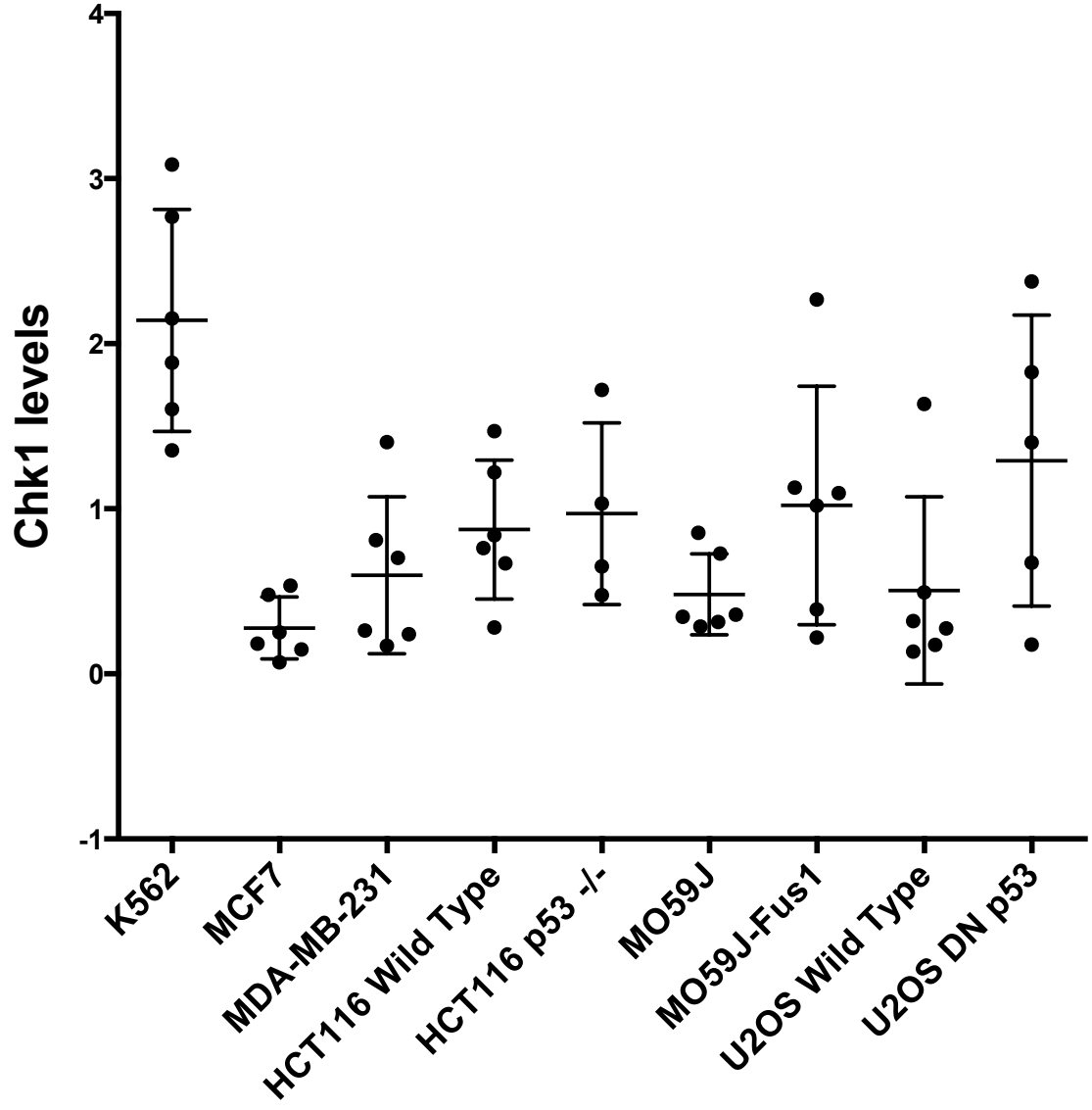

Figure 3-2 Expression of total CHK1 protein

Values are normalised to actin in a cell line panel comprising K562 (p53 mutated), MCF7 (p53 wild type), MDA-MB-231 (p53 mutated), HCT116 (p53 wild type), HCT116 (p53 -/-), M059J (p53 mutated), M059J-Fus1 (p53 mutated), U2OS (p53 mutated) and U2OS (dominant negative p53). Data are mean and standard deviation of at least 3 independent experiments

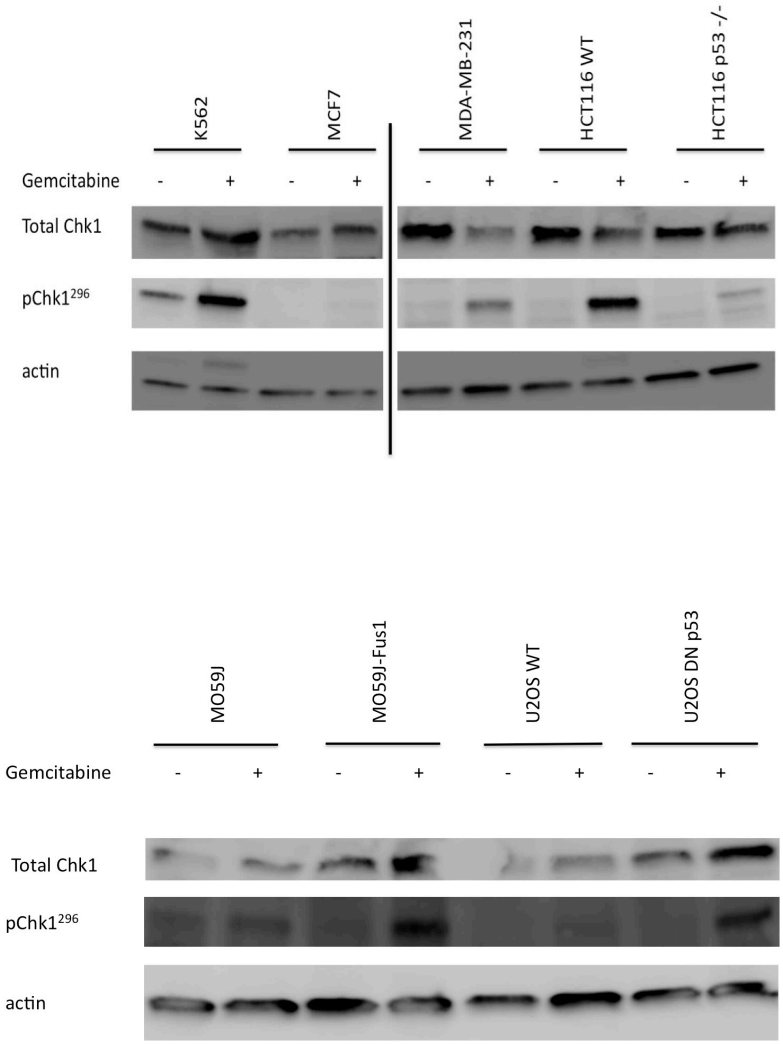

Figure 3-3 Expression of total CHK1 protein, pCHK1^{serine296} and actin by western blotting in a cell line panel.

Cell line panel comprises K562 (p53 mutated), MCF7 (p53 wild type), MDA-MB-231 (p53 mutated), HCT116 (p53 wild type), HCT116 (p53 -/-), M059J (p53 mutated), M059J-Fus1 (p53 mutated), U2OS (p53 wild type) and U2OS (dominant negative p53) with and without a 1 hour exposure to 1 μM gemcitabine.

The phosphorylation of CHK1 at serine^{296} in matched control samples and samples treated for 1 hour with 1 μM gemcitabine is shown in Figure 3-4. This demonstrates that gemcitabine reliably up-regulates the expression of pCHK1^{serine296} in all cell lines apart from the M059J and U2OS wild type cell

lines. Figure 3-5 shows the ratios by which pCHK1^{serine296} expression is up-regulated in treated samples compared to untreated controls. There is a wide range in the degree to which CHK1^{serine296} phosphorylation is induced (Figure 3-5), from 1.3-fold to 8-fold, and that this does not correlate with the baseline expression seen in Figure 3-2. Although, pCHK1^{serine296} levels were still higher in K562 cells, similar levels were seen in HCT116 wild type and M059J-Fus1 cell lines after gemcitabine exposure. Interestingly, both HCT116 p53 -/- and U2OS dominant negative p53 cells had lower baseline pCHK1^{serine296} levels than the wild type, but activation by gemcitabine did not appear to be p53-dependent.

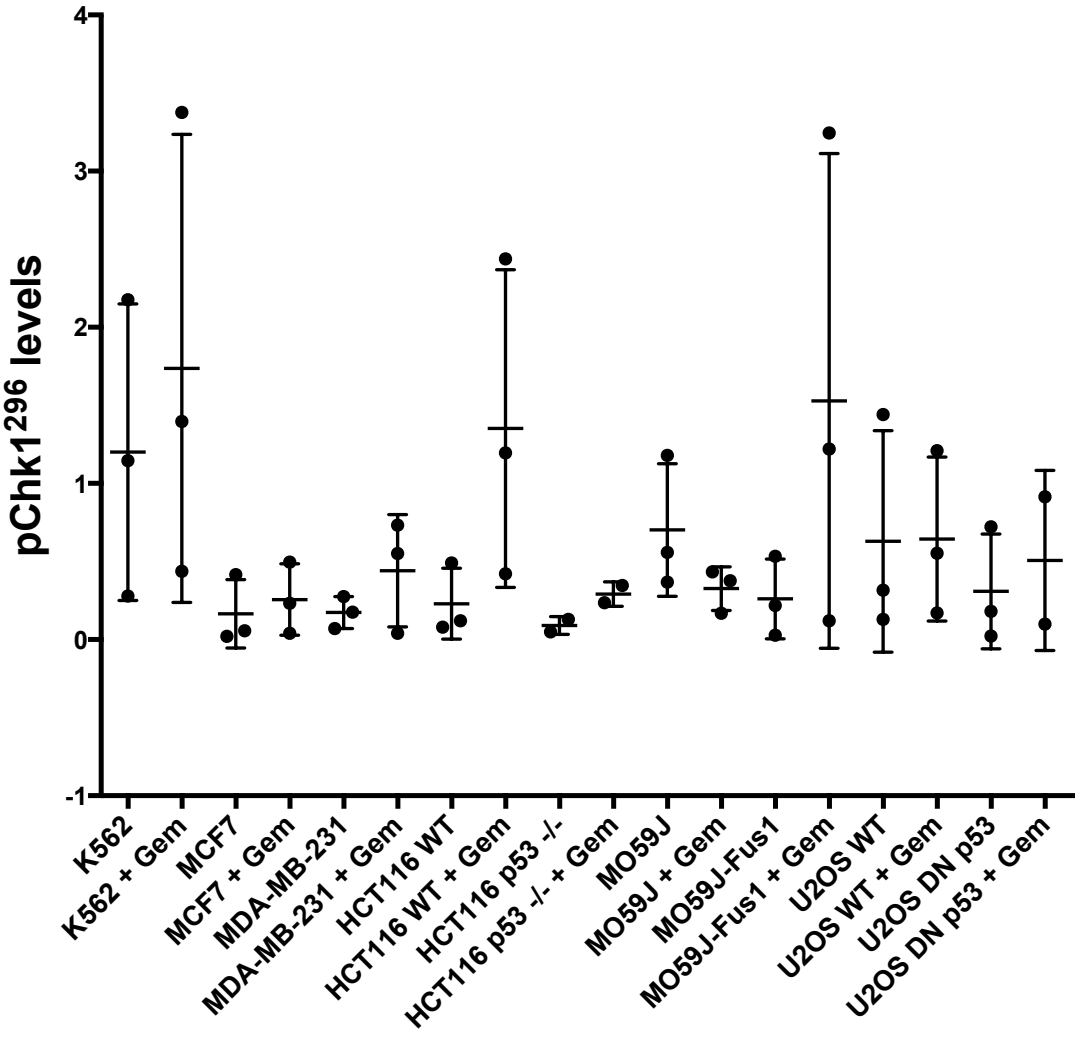

Figure 3-4 Expression of pCHK1^{serine296}

Values are normalised to actin in controls and paired samples 1 hour after 1 μM gemcitabine. Cell line panel comprising of K562 (p53 mutated), MCF7 (p53 wild type), MDA-MB-231 (p53 mutated), HCT116 (p53 wild type), HCT116 (p53 -/-), M059J (p53 mutated), M059J-Fus1 (p53 mutated), U2OS (p53 wild type) and U2OS (dominant negative p53). Data are mean and standard deviation of at least 3 independent experiments

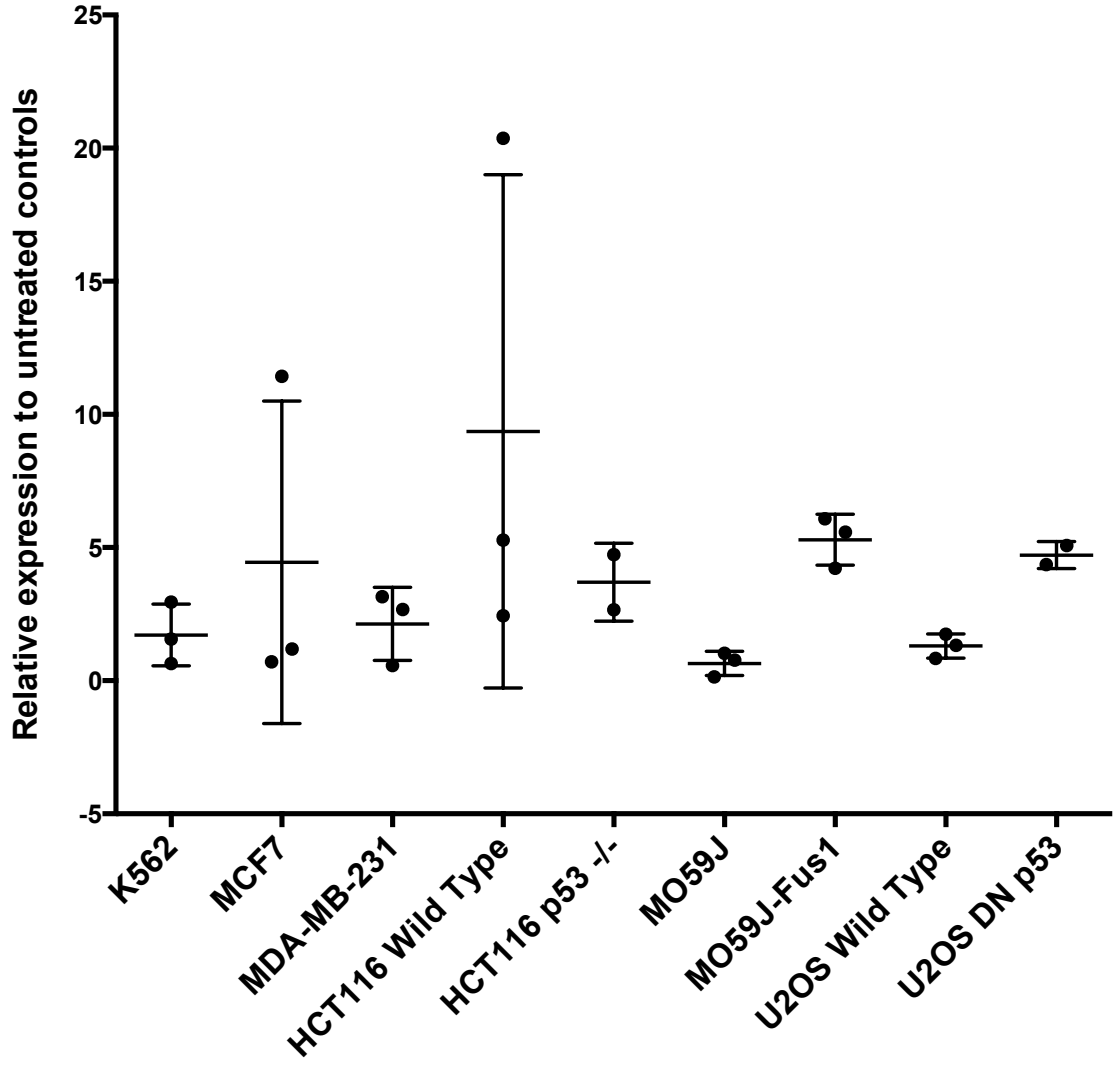

Figure 3-5 Relative expression of pCHK1^{serine296}

Data in cell line panel treated with 1 μM gemcitabine compared to untreated controls. Cell line panel comprising of K562 (p53 mutated), MCF7 (p53 wild type), MDA-MB-231 (p53 mutated), HCT116 (p53 wild type), HCT116 (p53 -/-), M059J (p53 mutated), M059J-Fus1 (p53 mutated), U2OS (p53 wild type) and U2OS (dominant negative p53). Data are mean and standard deviation of at least 3 independent experiments

3.3 Confirmation of specificity of V158411 for CHK1

A series of experiments were planned to attempt to confirm that V158411 was having its desired effects and single agent cytotoxicity (see section 4.1) via its action on CHK1 rather than on an unknown other target. It was hoped to be able to knock *CHK1* down with siRNA, confirm this knockdown and then to perform clonogenic assays with the combination of *CHK1* siRNA and V158411.

Figure 3-6 demonstrates the knockdown of *CHK1* in the MCF7 breast cancer cell line with siRNA at 48 and 120 hours after treatment. Unfortunately treatment with *CHK1* siRNA for 7 days led to the death of too many cells for there to be sufficient protein recoverable for western blot analysis.

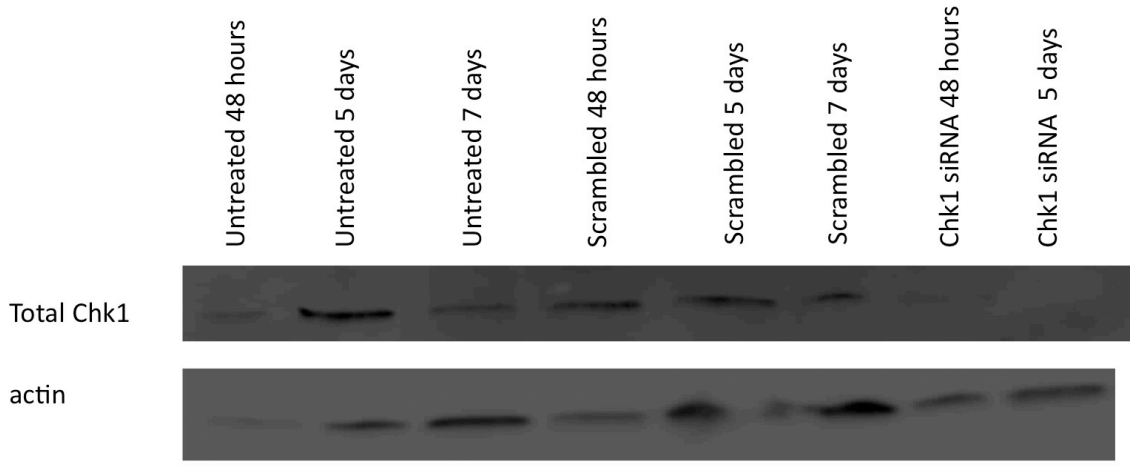

Figure 3-6 Representative western blot in MCF7 breast cancer cell line.

Expression in MCF7 (p53 wild type) cells of CHK1 and actin in untreated controls treated for 48 hours, 5 days and 7 days, cells treated with scrambled siRNA for 48 hours, 5 days and 7 days, and cells treated with *CHK1* siRNA for 48 hours, 5 days. Note no 7 day sample with *CHK1* siRNA as insufficient cells alive to extract protein for western blot analysis.

Figure 3-7 (A) quantifies this knockdown of *CHK1* by siRNA in comparison to cell line samples treated with control scrambled siRNA. There was 80% knockdown after 48 hours and more than 98% knockdown after 5 days.

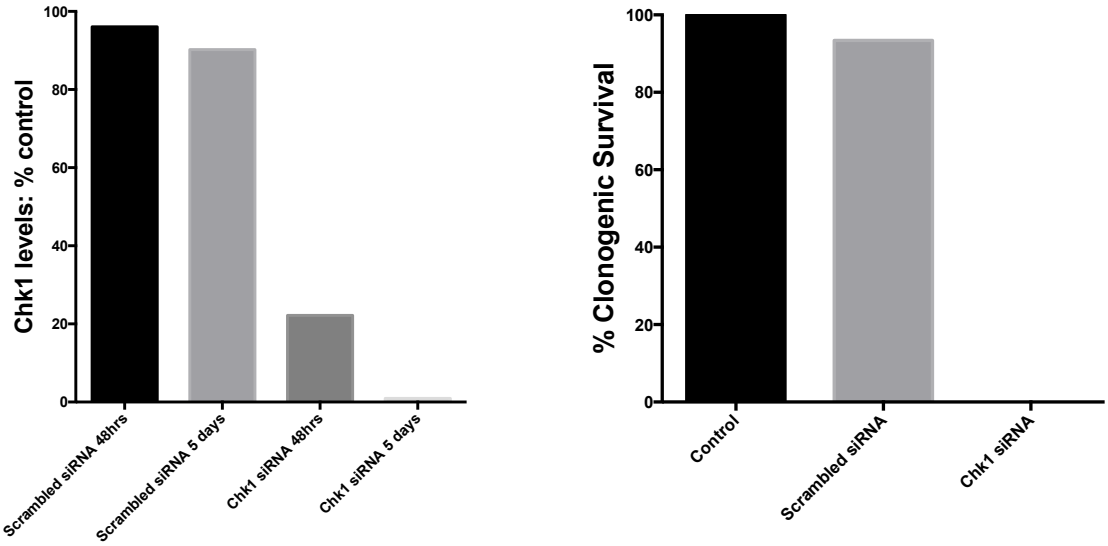

Figure 3-7 Data with siRNA knockdown and clonogenic survival

(A) siRNA knockdown of *CHK1* in MCF7 (p53 wild type) breast cancer cell line. A comparison of samples treated with scrambled and *CHK1* siRNA for 48 or 120 hours. (B) Clonogenic survival assay in MCF7 breast cancer cell line following treatment with scrambled siRNA and CHK1 siRNA.

In parallel with the samples prepared for western blotting a clonogenic assay was performed in control cells, those treated with scrambled siRNA and with *CHK1* siRNA for 48 hours. The results are shown in Figure 3-7 (B). This shows that there was no clonogenic survival after 2 weeks in cells treated for 48 hours with *CHK1* siRNA. Therefore it was not possible to test the specificity of V158411 *CHK1* knock-down cells.

3.4 Phosphorylation of CHK1 at serine^{345} and serine^{296}

The following series of experiments were performed to provide evidence that V158411 was inhibiting CHK1. The work was also aimed at investigating whether the phosphorylation of CHK1 at either serine^{296} or serine^{345} might be an appropriate biomarker that could be developed into a tool for use in early phase clinical trials. V158411 doses that were equimolar rather than equitoxic were used in these experiments. These equimolar concentrations were used in experiments examining protein expression, cell cycle and cytotoxicity. Hydroxyurea was used as a positive control for ATR activation and CHK1^{serine345} phosphorylation.

Representative western blots from these experiments are shown at the end of this section in Figures 3-12 (A and B) and 3-13 (A and B). All drug treatments were concomitant for 1 hour immediately prior to the preparation of lysates. The protein expression was normalised to the expression of actin.

3.4.1 Effect of single agent V158411 on pCHK1^{serine296} and pCHK1^{serine345} levels

Figure 3-8 demonstrates that V158411 reduces CHK1^{serine296} phosphorylation in a concentration dependent manner in MCF7, MDA-MB-231 and K562 cell lines. The representative blots for pCHK1^{serine296}, pCHK1^{serine345} and actin expression from these experiments are shown in Figure 3-13. 150 nM V158411 reduced the expression of pCHK1^{serine296} by 48% below baseline in MCF7 cells, 67% in MDA-MB-231 cells and 53% in K562 cell line. There was no significant inhibition of CHK1^{serine296} phosphorylation in HCT116 cells

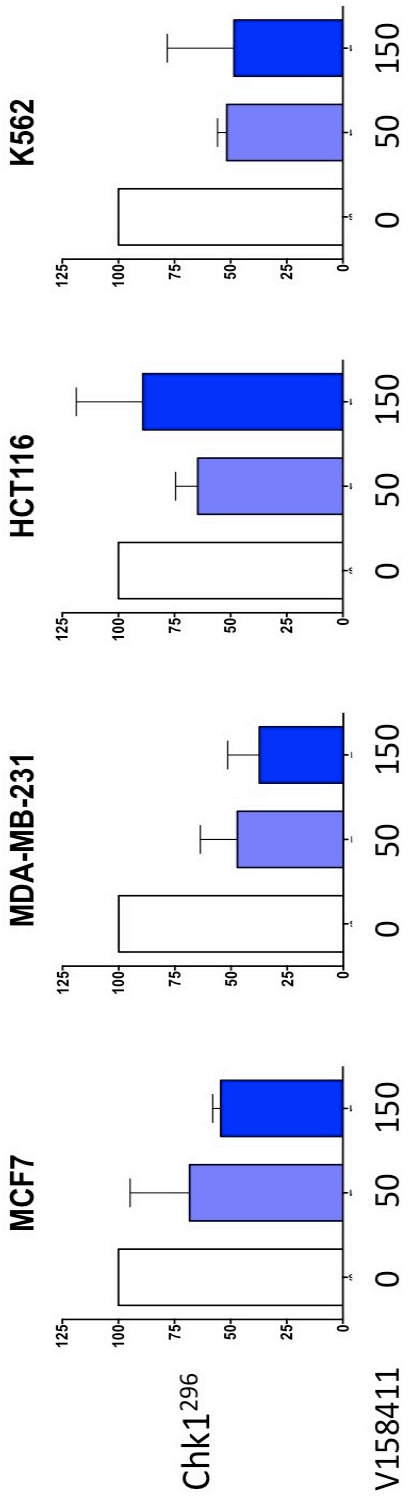

Figure 3-8 Phosphorylation of CHK1^{serine296} with V158411

Phosphorylation following treatment for 1 hour with 50 nM and 150 nM V158411 alone for 1 hour compared to untreated controls. Experiment performed in MCF7 (p53 wild type), MDA-MB-231 (p53 mutated), HCT116 (p53 wild type) and K562 (p53 mutated) cell lines. CHK1^{serine296} normalised to actin and then to untreated controls. Data are mean and standard deviation of at least 3 independent experiments.

CHK1^{serine345} phosphorylation is increased in all 4 cell lines by the presence of the CHK1 inhibitor V158411. This is shown in Figure 3-9. CHK1^{serine345} phosphorylation was increased in a concentration responsive manner. 150 nM V158411 increased the expression of pCHK1^{serine345} 11-fold in MCF7 cells, 8-fold in MDA-MB-231 cells, 10-fold in HCT116 cells and 6–fold in K562 cell lines.

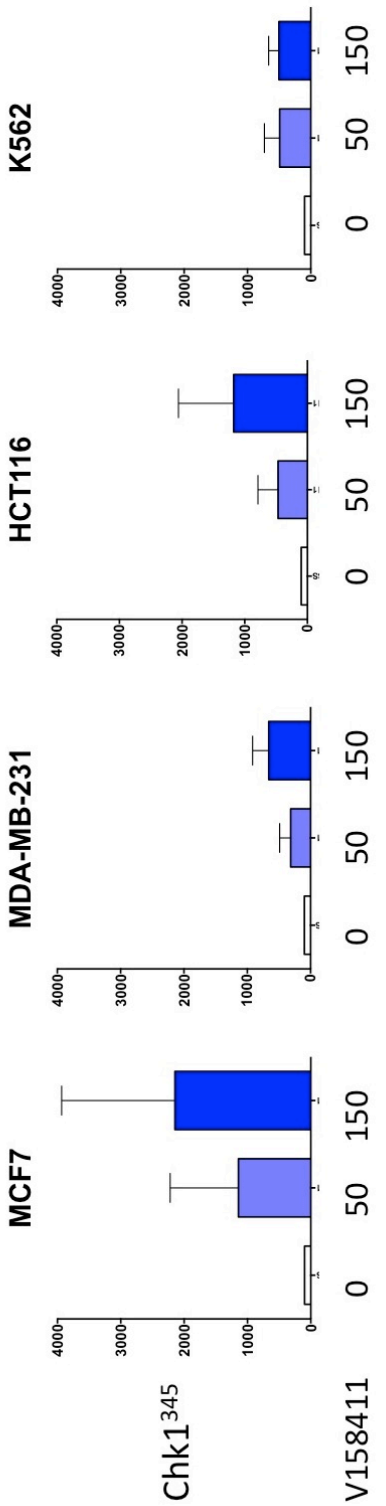

Figure 3-9 Phosphorylation of CHK1^{serine345} after exposure to V158411.

Phosphorylation following treatment for 1 hour with 50 nM and 150 nM V158411 alone for 1 hour compared to untreated controls. Experiment performed in MCF7 (p53 wild type), MDA-MB-231 (p53 mutated), HCT116 (p53 wild type) and K562 (p53 mutated) cell lines. CHK1^{serine345} normalised to actin and then to untreated controls. Data are mean and standard deviation of at least 3 independent experiments

3.4.2 Effect of V158411 on gemcitabine-induced changes in pCHK1^{serine345} and pCHK1^{serine296} phosphorylation levels

Figure 3-10 shows the CHK1^{serine296} phosphorylation following a 1 hour treatment with gemcitabine with and without 50 nM and 150 nM V158411. 1 μM gemcitabine consistently increased CHK1^{serine296} phosphorylation in all 4 cell lines. The increase was 8-fold in MCF7 cells, 7-fold in MDA-MB-231 cells, 4.5-fold in HCT116 cells and 9-fold in K562 cells.

V158411 reduced this increase in CHK1^{serine296} phosphorylation in a concentration-dependent fashion in all cell lines apart from MDA-MB-231. 50 nM V158411 reduced gemcitabine-induced CHK1^{serine296} phosphorylation from its stimulated level by 75% in MCF7 cells, 77% in MDA-MB-231 cells 78% in K562 cells and 66% in HCT116 cells. 150 nM V158411 reduced gemcitabine-induced CHK1^{serine296} phosphorylation from its stimulated level by 94% in MCF7 cells, 58% in MDA-MB-231 cells, 77% in HCT116 cells and 89% in K562 cells.

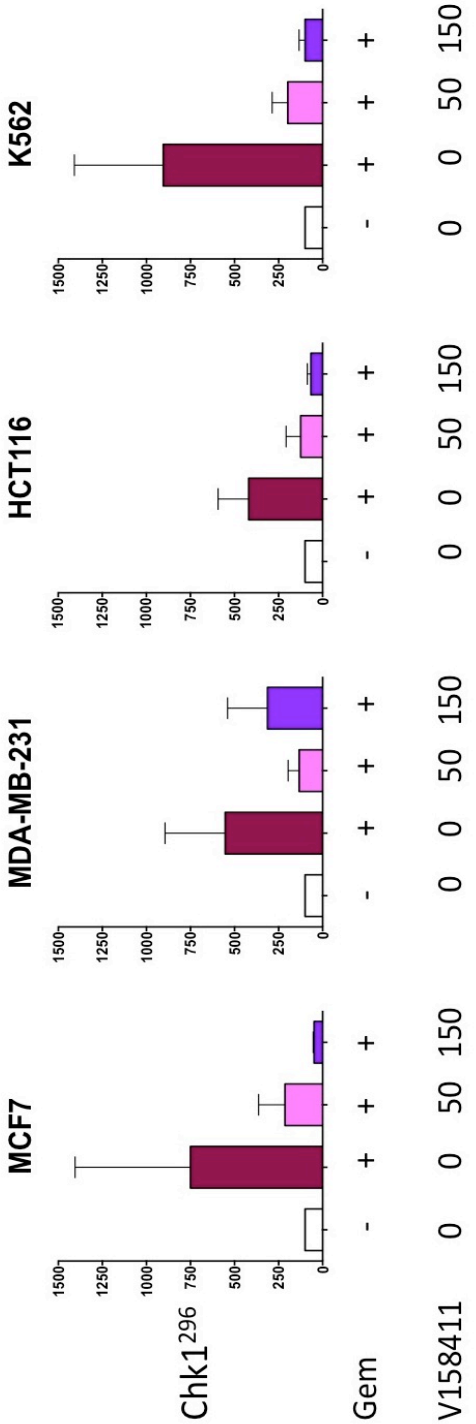

Figure 3-10 Phosphorylation of CHK1^{serine296} following exposure to V158411 and gemcitabine.

Phosphorylation following treatment for 1 hour with 1 μM gemcitabine ± 50 nM and 150 nM V158411 for 1 hour compared to untreated controls. Experiment performed in MCF7 (p53 wild type), MDA-MB-231 (p53 mutated), HCT116 (p53 wild type) and K562 (p53 mutated) cell lines. CHK1$^{serine\ 296}$ normalised to actin and then to untreated controls. Data are mean and standard deviation of at least 3 independent experiments

Both gemcitabine and V158411 individually increased the phosphorylation of CHK1^{serine345} and together the increase was additive in MCF7 and HCT116 cells but not MDA-MB-231 and K562 cells (Figure 3-11). 1 μM gemcitabine alone increased CHK1^{serine345} 3-fold and this was increased to 10-fold in combination with 150 nM V158411 in the MCF7 cells. In HCT116 cells there was a 10-fold increase in CHK1^{serine345} phosphorylation with 1 μM gemcitabine and this was increased to 16-fold with the addition of 150 nM V158411. However, in K562 cells there was no further increase in gemcitabine-induced with either V158411. In contrast, in MDA-MB-231 cells 50 nM or 150 nM V158411 did not increase CHK1^{serine345} phosphorylation induced by gemcitabine and in K562 there was a modest, and not significant, decrease in gemcitabine-induced CHK1^{serine345}.

The ratio between CHK1^{serine296} phosphorylation and CHK1^{serine345} phosphorylation following treatment with 1 μM gemcitabine and 1 μM gemcitabine in combination with 50 nM and 150 nM V158411 was explored in all 4 cell lines, but no consistent relationship could reliably be found (data not shown).

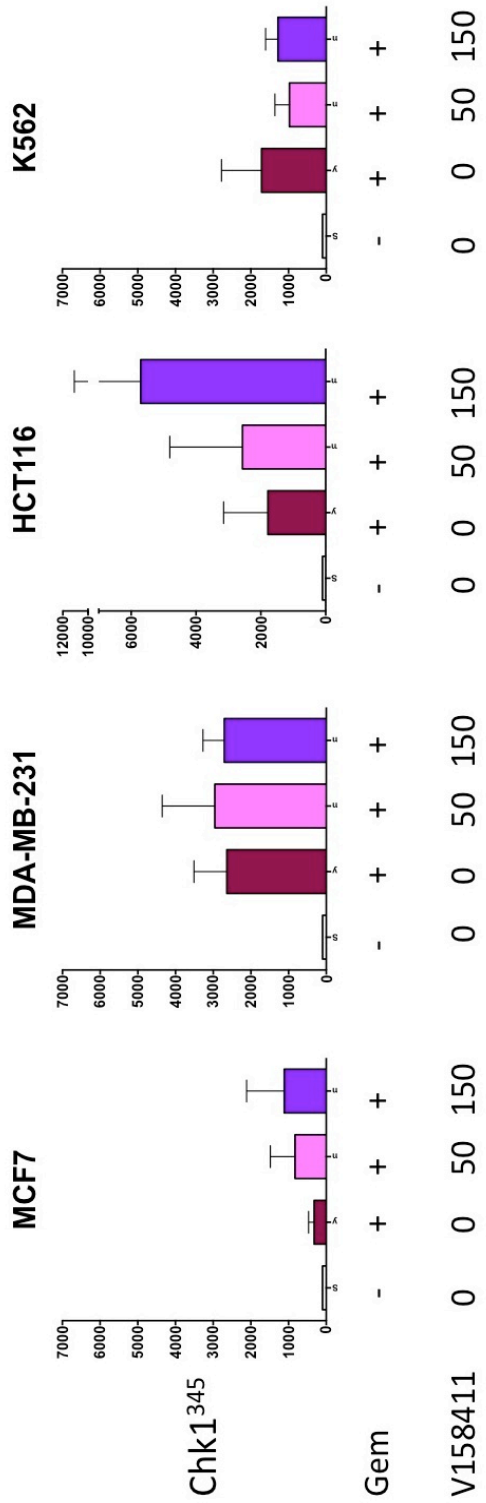

Figure 3-11 Phosphorylation of CHK1^{serine345} following exposure to V158411 and gemcitabine.

Phosphorylation following treatment for 1 hour with 1 μM gemcitabine +/- 50 nM and 150 nM V158411 for 1 hour compared to untreated controls. Experiment performed in MCF7 (p53 wild type), MDA-MB-231 (p53 mutated), HCT116 (p53 wild type) and K562 (p53 mutated) cell lines. CHK1^{serine345} normalised to actin and then to untreated controls. Data are mean and standard deviation of at least 3 independent experiments.

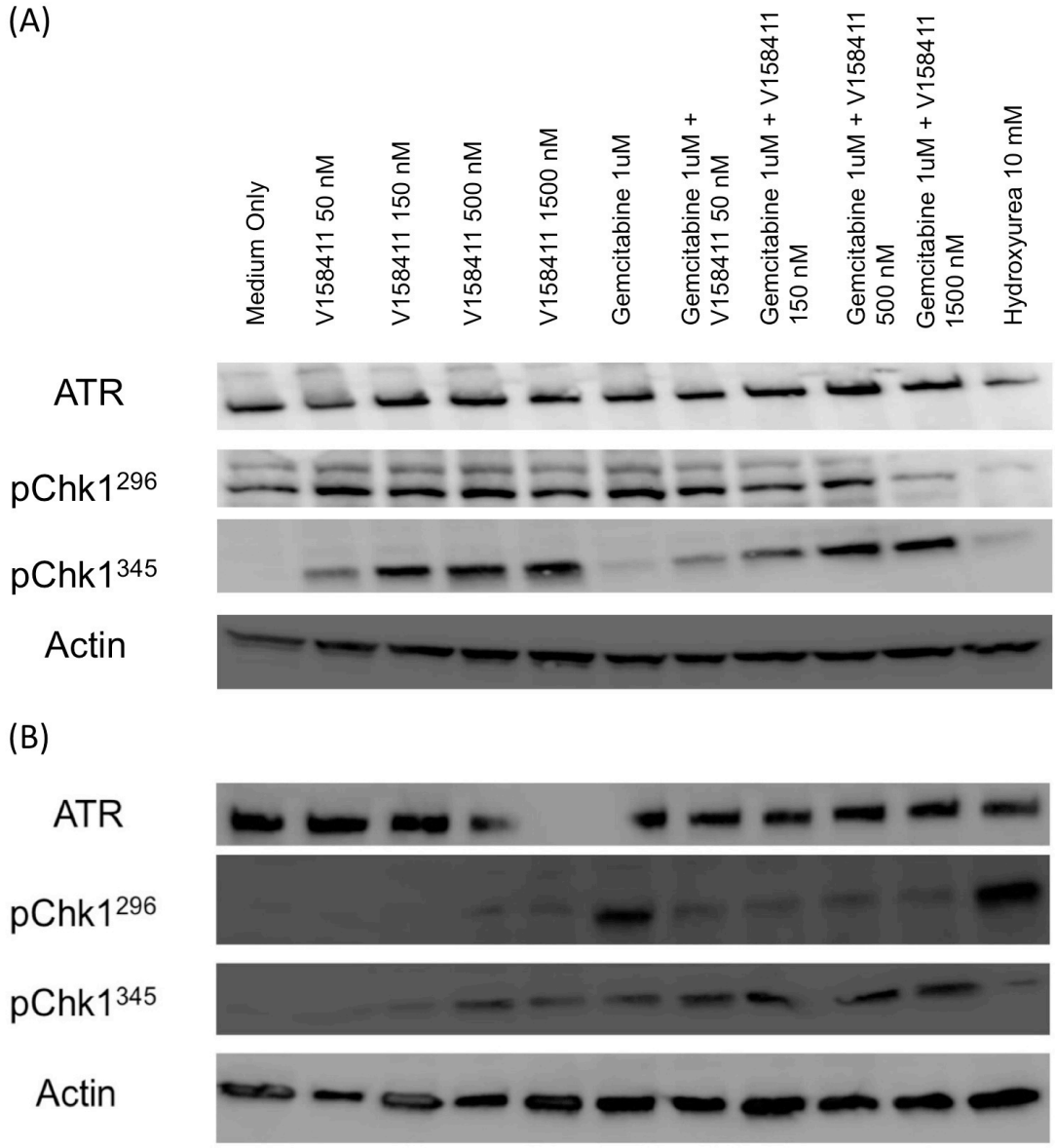

Figure 3-12 Example western blots in MCF7 and MDA-MB-231 cells.

Representative western blot in (A) MCF7 (p53 wild type) cells and (B) MDA-MB-231 (p53 mutated) cells. Expression of ATR, pCHK1^{serine296}, pCHK1^{serine345} and actin in untreated controls, and cells treated with 50 nM V158411, 150 nM V158411, 500 nM V158411, 1500 nM V158411, 1 μM gemcitabine, 1 μM gemcitabine + 50 nM V158411, 1 μM gemcitabine + 150 nM V158411, 1 μM gemcitabine + 500 nM V158411, 1 μM gemcitabine + 1500 nM V158411 and 10 mM. hydroxyurea All treatments for 1 hour prior to preparation of lysates.

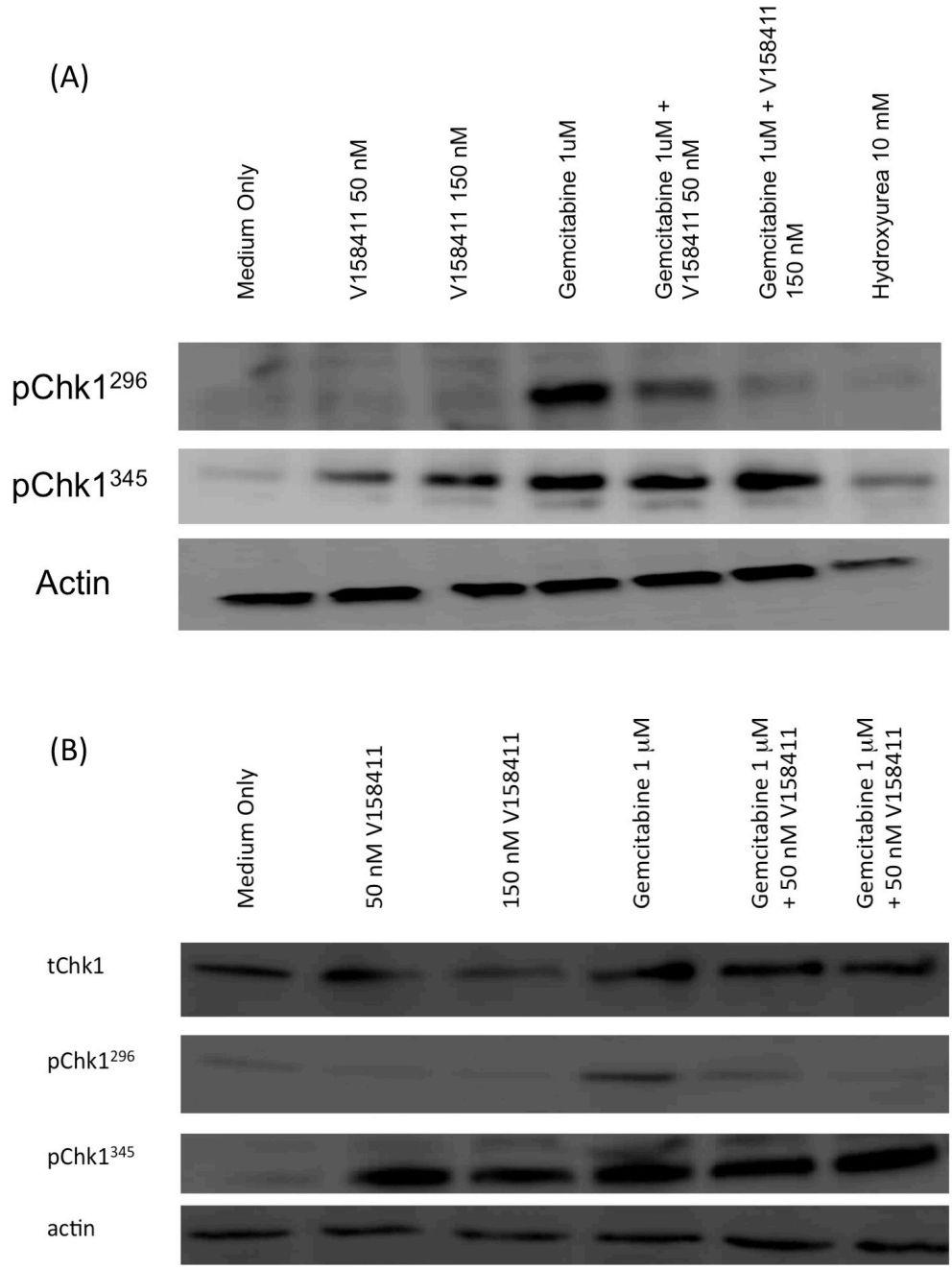

Figure 3-13 Example western blots in HCT116 and K562 cells.

Representative western blot in (A) HCT116 (p53 wild type) cells and (B) K562 (p53 mutated) cells. Expression of total CHK1, pCHK1^{serine296}, pCHK1^{serine345} and actin in untreated controls, and cells treated with 50 nM V158411, 150 nM V158411, 1 μM gemcitabine, 1 μM gemcitabine + 50 nM V158411, 1 μM gemcitabine + 150 nM V158411, and 10 mM hydroxyurea. All treatments for 1 hour prior to preparation of lysates.

3.5 Cell cycle perturbation by cytotoxic agents

Having demonstrated a clear effect of V158411 on phosphorylation targets indicative of CHK1 inhibition it was important to demonstrate that this translated into abrogation/attenuation of cell cycle arrest at the S and G_2 checkpoints. K562 cells were used in the initial experiments and then MDA-MB-231 breast cancer cells and HCT116 colorectal cancer cells were used in subsequent experiments. MCF7 breast cancer cells were not used as this cell line displays significant aneuploidy meaning that the quantification of flow cytometry data is unreliable. Although, S-phase data was collected, specific staining for cells in S-phase such as BrdU was not used. Therefore, the S-phase data is not included here as it is less reproducible than the data with regard to G_2 fraction.

3.5.1 The effect of conventional cytotoxics and IR on cell cycle distribution in K562 cells

Prior to looking at the abrogation of cell cycle arrest by V158411 it was important to determine which conventional cytotoxic agents (gemcitabine, cisplatin, hydroxyurea, camptothecin, etoposide and IR) caused a reliable increase in the G_2 fraction of cycling cells. These experiments were performed in K562 CML cell line.

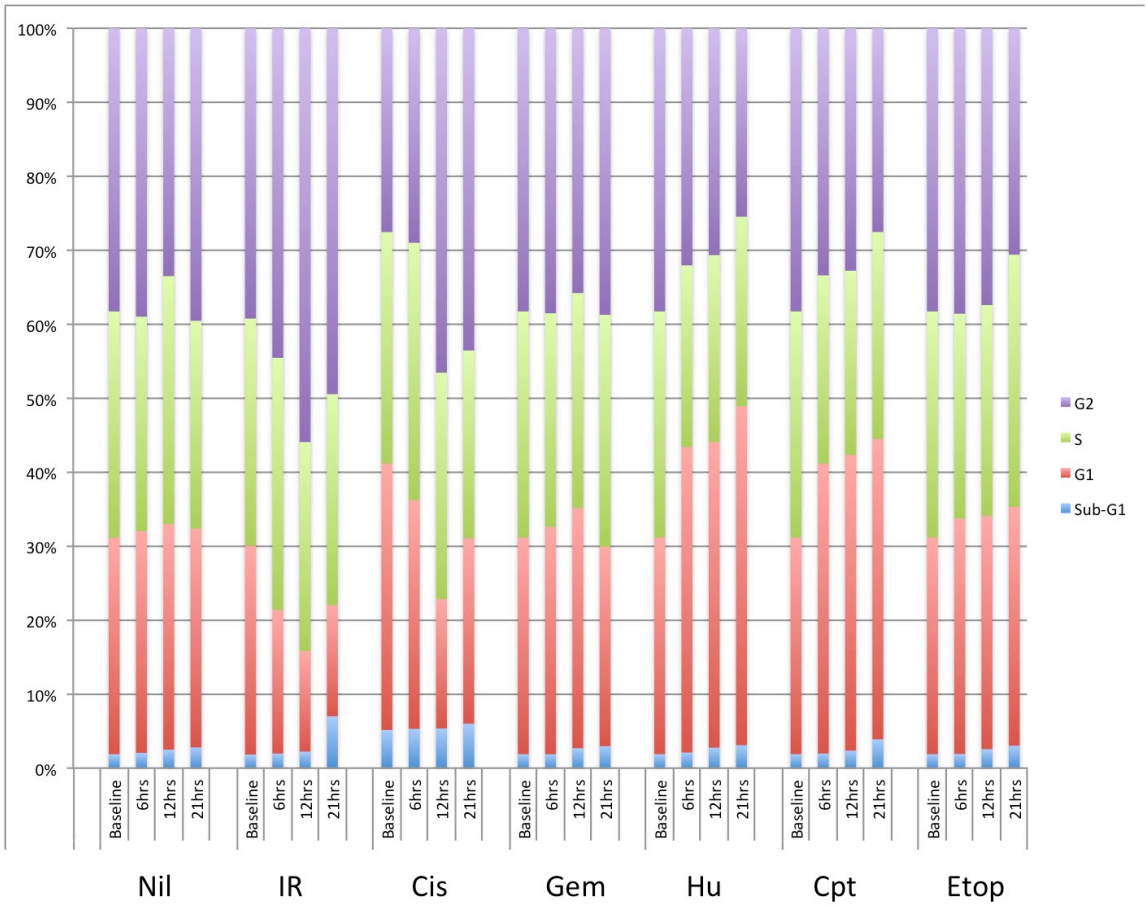

Figure 3-14 Analysis of cell cycle distribution by flow cytometry in K562 CML cells following cytotoxic therapy.

Untreated controls (Nil) and cells treated with 2 Gy IR (IR), 10 μM cisplatin (Cis), 1 μM gemcitabine (Gem), 500 μM hydroxyurea (Hu), 10 μM camptothecin (Cpt) and 5 μM etoposide (Etop) at baseline, 6 hours, 12 hours and 24 hours after cytotoxic exposure. K562 (p53 mutated) cell line doubling time approximately 12-14 hours.

Figure 3-14 demonstrates that 2 Gy IR and 10 μM cisplatin cause modest G_2 cell cycle arrest and were taken forward for future work both in K562 and other cell lines. None of the agents caused a significant S-phase arrest and gemcitabine, hydroxyurea, camptothecin and etoposide do not cause a significant increase in the G_2 fraction in K562 cells and so were not taken forward for future work.

3.5.2 Dose response of K562 cells to ionising radiation

Following the initial demonstration of G_2 arrest following exposure to 2 Gy IR a further experiment in K562 cells was performed to ascertain if higher doses of IR led to a greater proportion of cells arresting in G_2. Figure 3-15 shows the results of this experiment with 2, 4, 6, 8 and 10 Gy IR in comparison to un-irradiated control cells. Rather, than being dose-dependent, the G_2 arrest was time-dependent with maximum arrest observed at 12 and 24 hours. As 2 Gy is the standard dose in fractionated radiotherapy, 2 Gy of IR 24 hours prior to analysis was chosen as the dose to use in future work.

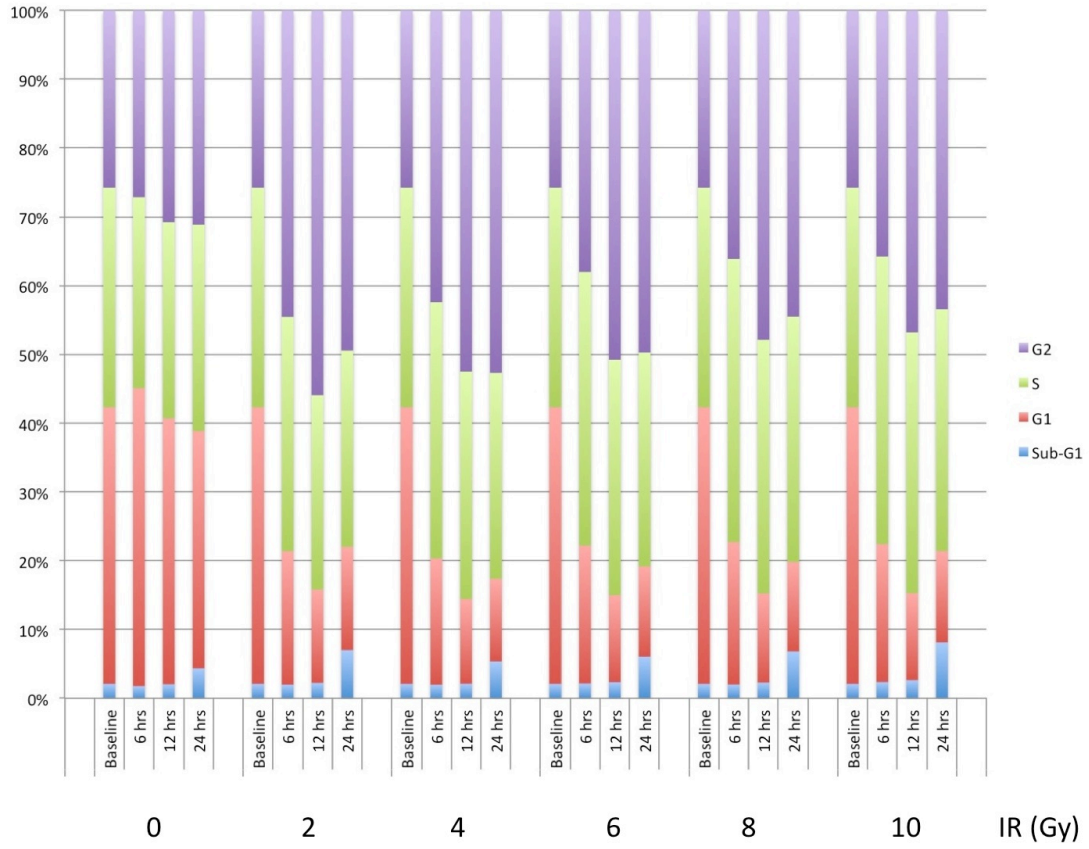

Figure 3-15 Analysis of cell cycle distribution by flow cytometry in K562 CML cells following IR.

Untreated controls and cells treated with 2 Gy, 4 Gy, 6 Gy, 8 Gy and 10 Gy IR at baseline, 6 hours, 12 hours and 24 hours after IR. K562 (p53 mutated) cell line doubling time approximately 12-14 hours.

3.6 Effect of V158411, ionising radiation and cisplatin on cell cycle distribution

A 24 hour exposure to 50nM, 150 nM and 500 nM V158411 has been shown in western blot experiments (see Section 3-5) to cause a concentration-dependent reduction in $CHK1^{serine296}$ phosphorylation justifying the duration of treatment used in these experiments. The following experiments were performed in K562, MDA-MB-231, HCT116 cell lines. Cells were treated with ionising radiation and then exposed to drug-free medium, 50 nM V158411, 150 nM V158411 or 500 nM V158411 for 24 hours hour prior to flow cytometry. In combination with cisplatin (based on the data presented in Figure 3-14), cells were co-treated with 1 μM cisplatin with plain medium, 50 nM V158411, 150 nM V158411 or 500 nM V158411 for 24 hours prior to flow cytometry.

Representative histograms from the experiments are shown in Figure 3-16 for K562 cells, Figure 3-17 for MDA-MB-231 and Figure 3-18 for HCT116 wild type cells. Analysis of this data is in the subsequent sections.

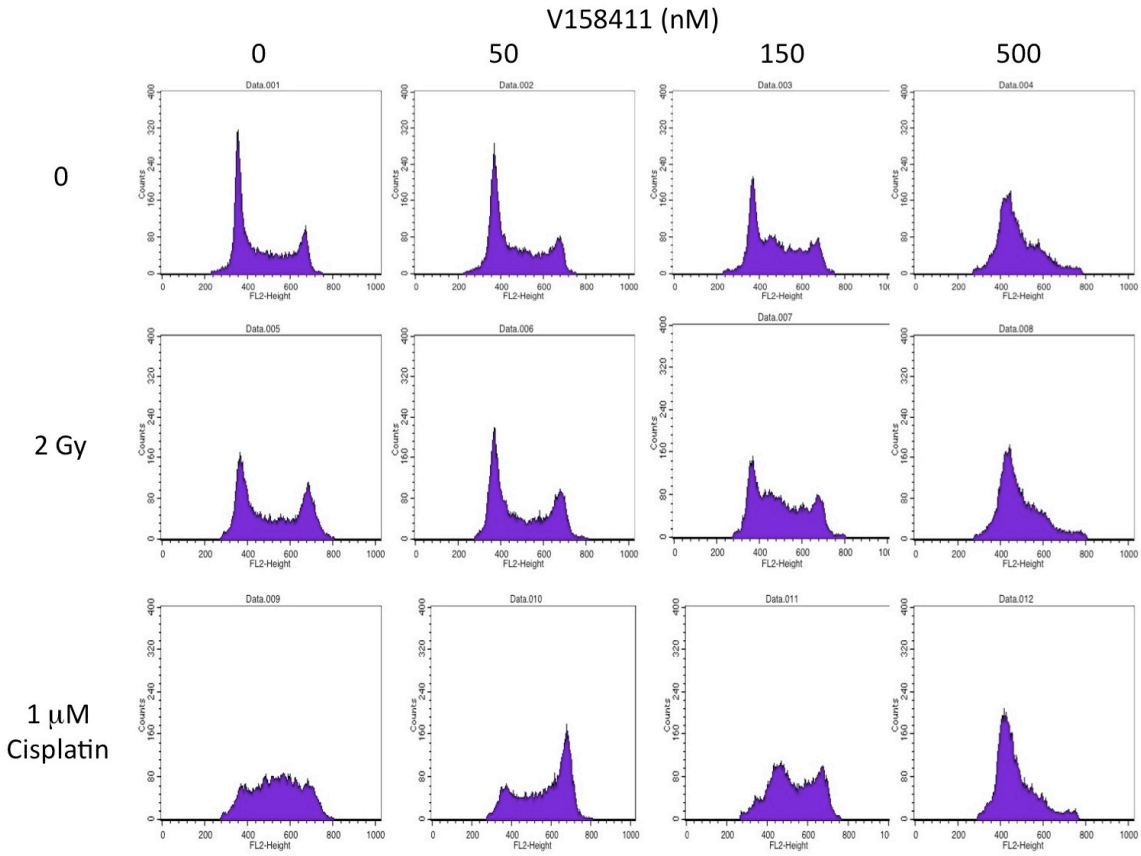

Figure 3-16 Representative example of flow cytometry in K562 cells.

Top row (L to R): untreated control, 50 nM V158411, 150 nM V158411 and 500 nM V158411. Middle row: 2 Gy IR, 2 Gy IR + 50 nM V158411, 2 Gy IR + 150 nM V158411 and 2 Gy IR + 500 nM V158411. Bottom row: 1 μM cisplatin, 1 μM cisplatin + 50 nM V158411, 1 μM cisplatin + 150 nM V158411 and 1 μM cisplatin + 500 nM V158411. K562 (p53 mutated) cell line doubling time approximately 12-14 hours. Minimum of 10000 events collected for each cytogram.

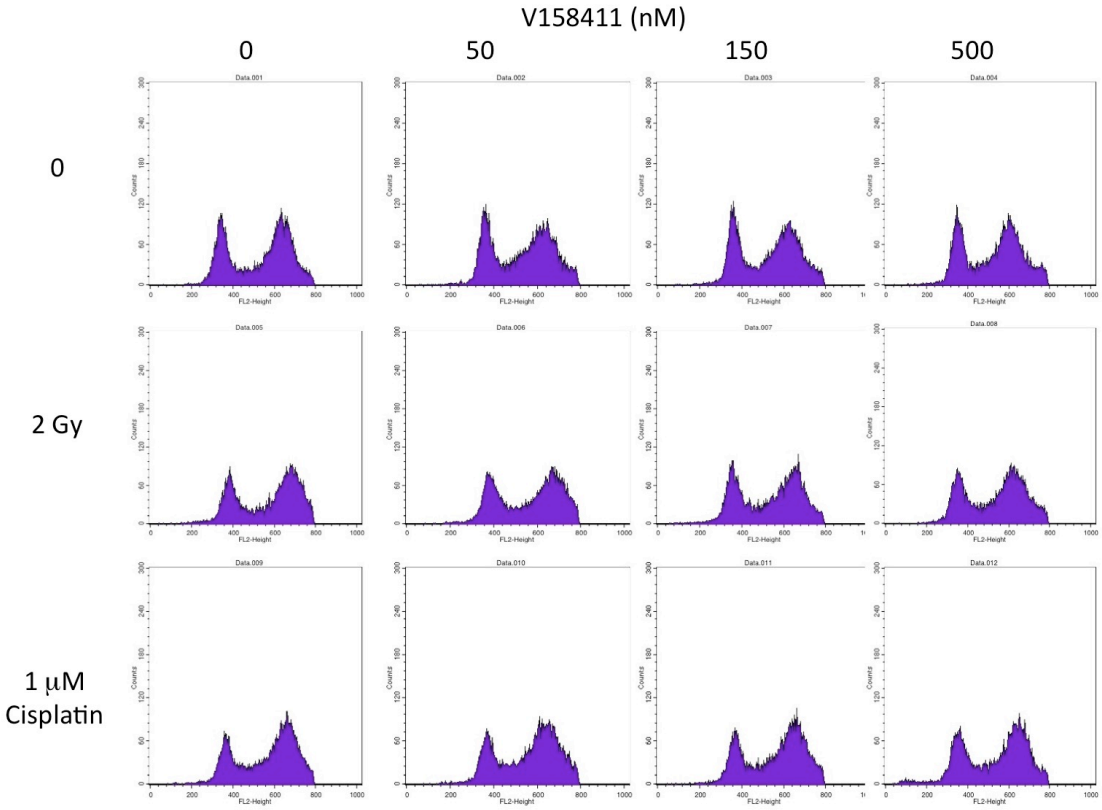

Figure 3-17 Representative example of flow cytometry in MDA-MB-231 cells.

Top row (L to R): untreated control, 50 nM V158411, 150 nM V158411 and 500 nM V158411. Middle row: 2 Gy IR, 2 Gy IR + 50 nM V158411, 2 Gy IR + 150 nM V158411 and 2 Gy IR + 500 nM V158411. Bottom row: 1 μM cisplatin, 1 μM cisplatin + 50 nM V158411, 1 μM cisplatin + 150 nM V158411 and 1 μM cisplatin + 500 nM V158411. MDA-MB-231 (p53 mutated) cell line doubling time approximately 40 hours. Minimum of 10000 events collected for each cytogram

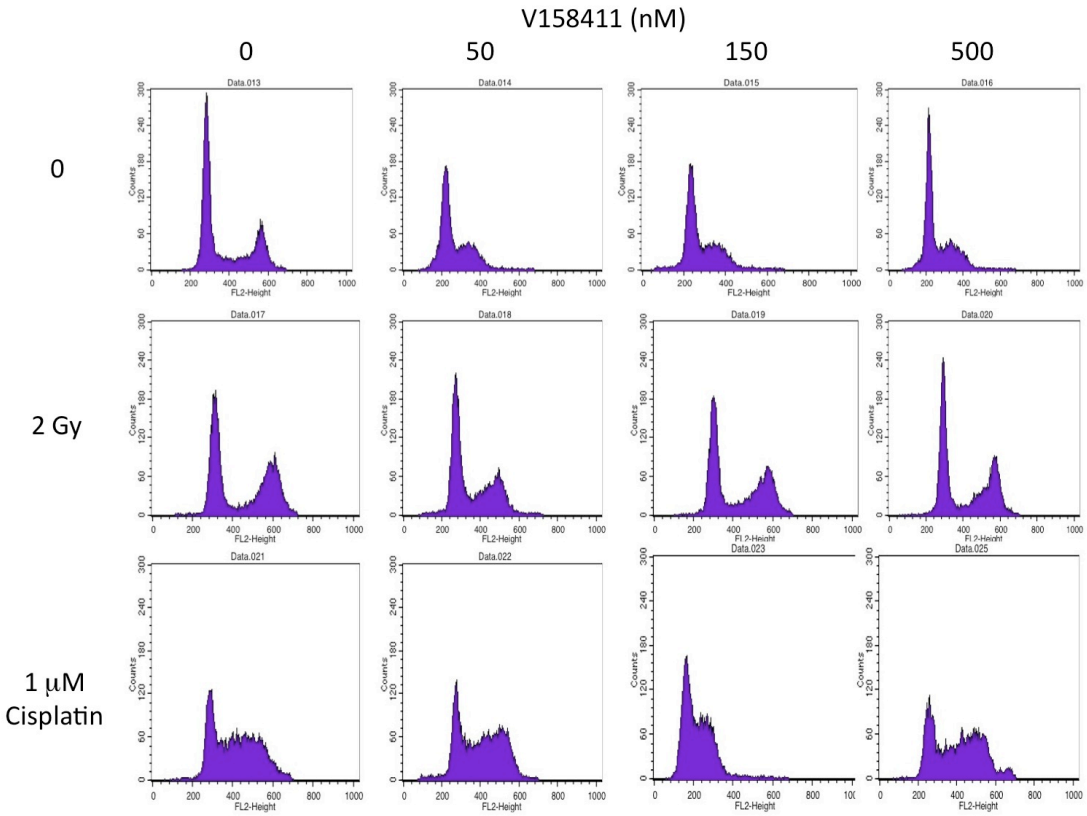

Figure 3-18 Representative example of flow cytometry in HCT116 wild type cells.

Top row (L to R): untreated control, 50 nM V158411, 150 nM V158411 and 500 nM V158411. Middle row: 2 Gy IR, 2 Gy IR + 50 nM V158411, 2 Gy IR + 150 nM V158411 and 2 Gy IR + 500 nM V158411. Bottom row: 1 μM cisplatin, 1 μM cisplatin + 50 nM V158411, 1 μM cisplatin + 150 nM V158411 and 1 μM cisplatin + 500 nM V158411. HCT116 (p53 wild type) cell line doubling time approximately 16-18 hours. Minimum of 10000 events collected for each cytogram

3.6.1 The effect of V158411 alone on G_2 cell cycle fraction in cell lines

The impact of a 24 hour exposure to 3 concentrations of V158411 (50 nM, 150 nM and 500 nM) was determined in K562, MDA-MB-231 and HCT116 by flow cytometry. The results are shown in Figure 3-19. V158411 caused a concentration-dependent depletion of the G_2 fraction of cells in all 3 cell lines that was significant at all 3 concentrations of V158411 ($p = 0.034$, $p = 0.041$,

and p = 0.0003 respectively (paired t-tests)) and in K562 cells with 150 nM and 500 nM V158411 (p = 0.003 and p = 0.0007 (paired t-test)) and 500 nM V158411 (paired t-test). There was a much smaller reduction in the G_2 fraction in MDA-MB-231 cells, which was only significant with 50 nM V158411 (p = 0.04 (paired t-test)). This reduced effect is likely to be because the cell cycle in MDA-MB-231 cells is much longer at around 40 hours than in K562 cells (12-14 hours) and in HCT116 cells (16-18 hours).

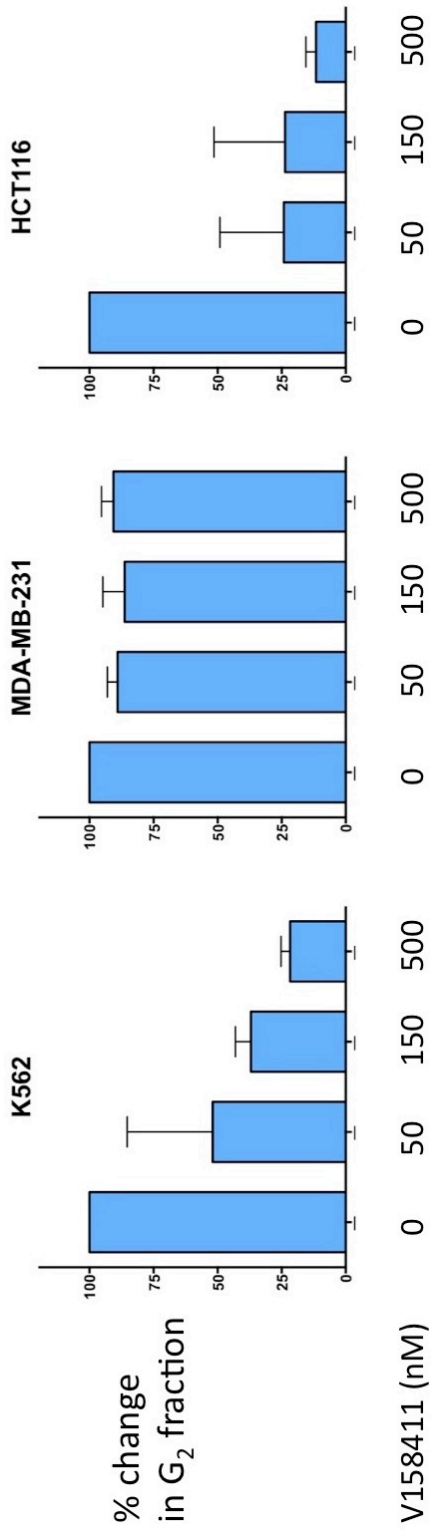

Figure 3-19 Flow cytometry in K562, MDA-MB-231 and HCT116 wild type cells

Untreated samples, 50 nM V158411, 150 nM V158411 and 500 nM V158411. % change in G_2 fraction is calculated as the change in G_2 fraction compared to time = 0 normalised to untreated controls. Cell line doubling time in K562 (p53 mutated) 12-14 hours, MDA-MB-231 (p53 mutated) 40 hours and HCT116 (p53 wild type) 16-18 hours. Data are mean and standard deviation of at least 3 independent experiments

3.6.2 The effect of ionising radiation +/- V158411 on G_2 cell cycle fraction in cell lines

In parallel with the flow cytometry experiment with V158411 alone, the effect of V158411 on the cell cycle perturbation by 2 Gy IR was determined in K562, MDA-MB-231 and HCT116 cells. Cells were treated with 2 Gy IR alone or in combination with 50 nM V158411, 150 nM V158411 and 500 nM V158411 for 24 hours prior to cell cycle analysis by flow cytometry. The results shown in Figure 3-20.

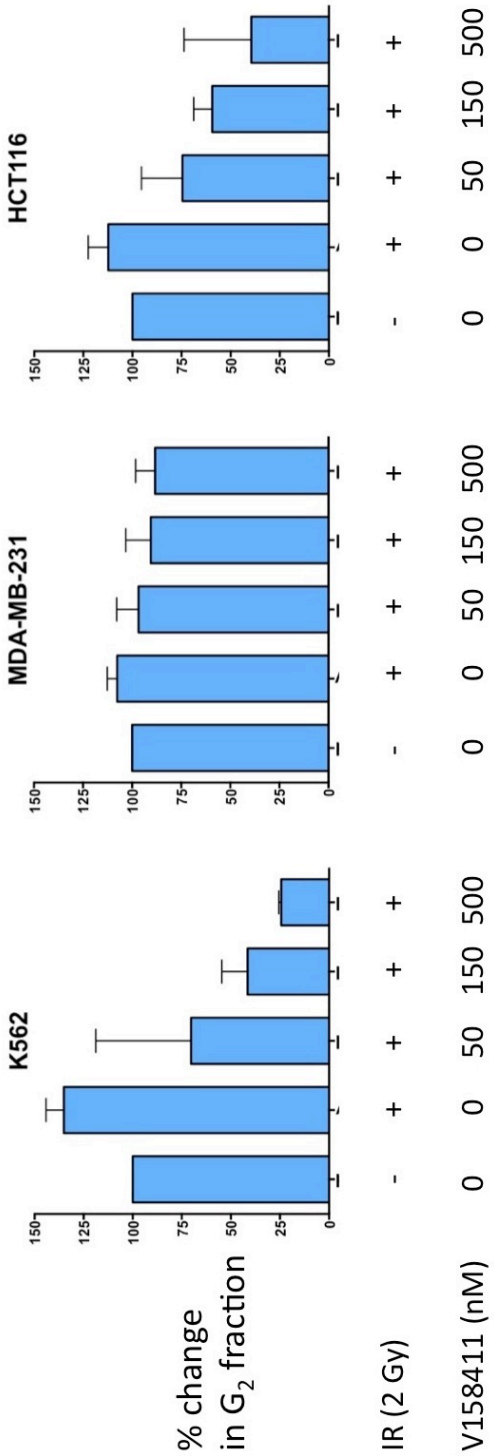

Figure 3-20 Flow cytometry in K562, MDA-MB-231 and HCT116 wild type cells

Untreated samples, 2 Gy IR, 2 Gy IR + 50 nM V158411, 2 Gy IR + 150 nM V158411 and 2 Gy IR + 500 nM V158411. % change in G_2 fraction is calculated as the change in G_2 fraction compared to time = 0 normalised to untreated controls. Cell line doubling time in K562 (p53 mutated) 12-14 hours, MDA-MB-231 (p53 mutated) 40 hours and HCT116 (p53 wild type) 16-18 hours. Data are mean and standard deviation of at least 3 independent experiments.

This demonstrates that 2 Gy IR does cause an increase in the G_2 fraction in all 3 cell lines, but this is only statistically significant in K562 ($p = 0.022$ (paired t-test)). Nevertheless V158411 abrogated what G_2 arrest there was in all 3 cell lines in a concentration-dependent manner in K562 and HCT116, but not MDA-MB-231 cells.

In K562 cells V158411 abrogated the IR-mediated increase in the G_2 fraction in a concentration dependent manner at concentrations ≥ 150 nM ($p = 0.004$ and $p = 0.003$ (paired t-test) at 150 and 500 nM, respectively). All 3 concentrations of V158411 (50 nM, 150 nM and 500 nM) cause significant abrogation of IR-mediated G_2 cell cycle arrest in HCT116 cells ($p = 0.030$, $p = 0.009$, and $p = 0.037$ respectively (paired t-tests)).

In the MDA-MB-231 cell line there was only a very small increase in the G_2 fraction with 2 Gy IR, which was not statistically significant but the G_2 fraction was significantly reduced by 500 nM V158411 ($p = 0.005$ (paired t-test)).

3.6.3 The effect of cisplatin +/- V158411 on G_2 cell cycle fraction in cell lines

As with IR, in parallel with the flow cytometry experiment with V158411 alone, cells from the 3 cell lines (K562, MDA-MB-231 and HCT116) were treated with 1 μM cisplatin on its own or in combination with 50 nM V158411, 150 nM V158411 and 500 nM V158411. The results are shown in Figure 3-21.

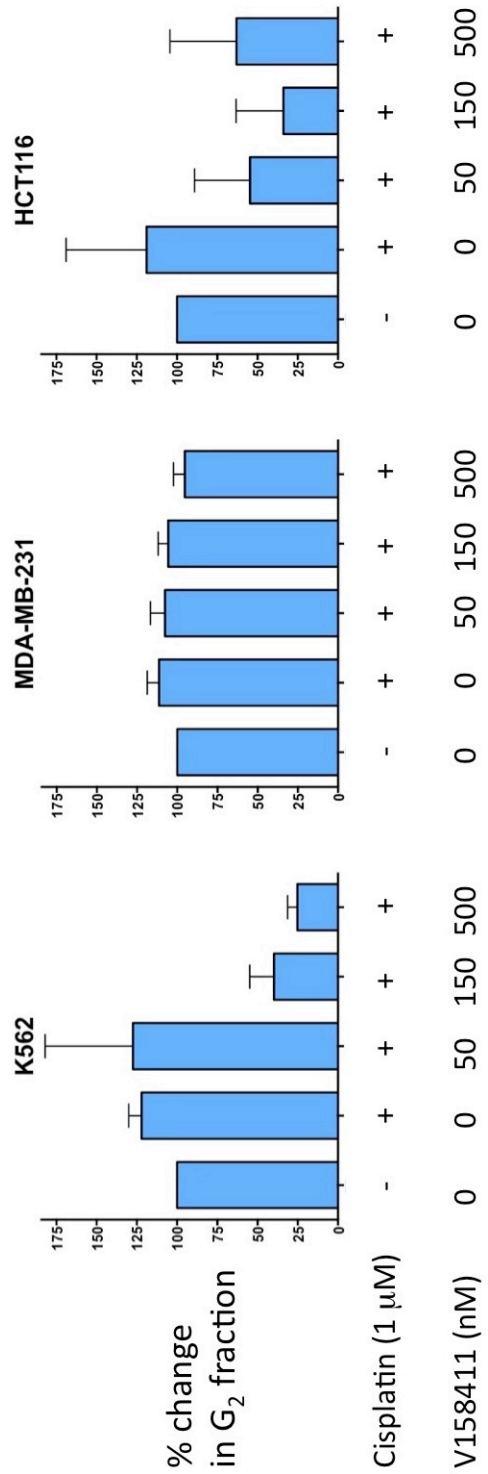

Figure 3-21 Flow cytometry in K562, MDA-MB-231 and HCT116 wild type cells

Untreated samples, 1 μM cisplatin, 1 μM cisplatin + 50 nM V158411, 1 μM cisplatin + 150 nM V158411 and 1 μM cisplatin + 500 nM V158411. % change in G_2 fraction is calculated as the change in G_2 fraction compared to time = 0 normalised to untreated controls. Cell line doubling time in K562 (p53 mutated) 12-14 hours, MDA-MB-231 (p53 mutated) 40 hours and HCT116 (p53 wild type) 16-18 hours. Data are mean and standard deviation of at least 3 independent experiments.

1 μM cisplatin increased the G_2 cell cycle fraction in all 3 cell lines, but this was only significant in K562 cell line ($p = 0.041$ (paired t-test)). 150 nM and 500 nM V158411 significantly abrogated this cisplatin-mediated arrest in K562 cells ($p = 0.009$ and $p = 0.003$ respectively (paired t-test)). There appeared to be a trend towards a reduction in the G_2 fraction following cisplatin treatment with increasing concentrations of V158411 in K562 cells, but this was not statistically significant. Likewise there was a trend in the HCT116 cell line, but none of the changes reached statistical significance. There was no change in MDA-MB-231 cells.

3.7 Discussion

Table 3-1 shows a summary of the data from 4 cell lines in which the investigations in this chapter were focussed and acts a summary of the expression of CHK1, phosphorylation of CHK1 in response to V158411 +/- IR and cisplatin and the effect of V158411 +/- IR and cisplatin on the cell cycle.

	MCF7	MDA-MB-231	HCT116	K562
CHK1 protein levels (untreated)	Low	Low-medium	Medium	High
$CHK1^{serine296}$ untreated	Low	Low	Low	High
% $CHK1^{serine296}$ reduction with V158411 (untreated cells)	30-90	65-80	25*	50
% $CHK1^{serine296}$ increase with 1 μM gemcitabine	400/800	200/700	800/500	200/900
% reduction by V158411 of gemcitabine induced $CHK1^{serine296}$ increase	50-100	60*	80-100	80-100
% $CHK1^{serine345}$ increase with V158411 (untreated cells)	1000-2000	300-700	500-1000	500*
% $CHK1^{serine345}$ increase with 1 μM gemcitabine	200	2500	1500	1500
%$CHK1^{serine345}$ increase with V158411 and 1 μM gemcitabine	200-800	2500	2000-3000	1000-1500*
% reduction in G_2 fraction with V158411 alone	-	10	70-90	50-80
% increase in G_2 fraction with 2 Gy IR)	-	135	120	110
% reduction by V158411 of IR-induced G_2 accumulation	-	0-100*	300-400*	200-400
% increase in G_2 fraction with 1 μM cisplatin	-	110	110	120
% reduction in G_2 fraction with V158411 and 1 μM cisplatin (%)	-	0-100*	300-400*	0-400

Table 3-1 Summary of baseline characteristics and changes in response to V158411 +/- IR and Cisplatin in MCF7, MDA-MB-231, HCT116 and K562 cancer cell lines.

% change in G_2 fraction: G_2 fraction (treated)/ G_2 fraction (untreated) x100

Values included in the table are mean. * no concentration response.

The data presented show a wide range of baseline total CHK1 protein expression between cell lines. Data in this chapter are largely generated using MCF7, MDA-MB-231, HCT116 and K562 cancer cell lines which had low, low-medium, medium and high levels of basal CHK1 protein expression, respectively.

There is relatively little published data comparing CHK1 levels between cell lines. In contrast to our data, Parsels et al showed that total CHK1 expression was similar in a panel of 4 pancreatic cancer (Parsels et al., 2009). The differences observed in the data reported here could reflect tissue specific differences as a wide panel of cell lines were used (CML, breast, colon, GBM and osteosarcoma). In the two breast cancer cell lines used, MCF7 and MDA-MB-231, the baseline CHK1 protein levels were quite similar. More research is required to examine the variability in a wider panel of cell lines within tumour types, between tumour types and in different normal tissues. Furthermore, work is required to examine the heterogeneity of expression of total CHK1 expression by immunohistochemistry (IHC) in normal tissue and tumour samples from patients.

The data presented shows that greater than 90% *CHK1* knockdown can be achieved with siRNA in MCF7 cancer cells, but this was not compatible with survival in clonogenic studies, precluding proposed studies to determine the specificity of V158411 for CHK1. In MCF7 cells 150 nM V158411 reduced CHK1^{serine296} phosphorylation by approximately 50% and led to around 30% clonogenic survival (see Section 4-2), suggesting that only partial *CHK1* knockdown may be required for a significant reduction in cell survival.

Other studies have not been published with respect to *CHK1* knockdown in MCF7 cells; however, Zenvirt et al knocked *CHK1* down in U2OS cells with siRNA with a significant reduction in cell survival in the absence of chemotherapy (Zenvirt et al., 2010). It would be interesting to explore whether lower concentrations of siRNA or alternative methods of siRNA transfection prevented this phenomenon. Work by other members of the group has explored the effect of ATR modulation in fibroblasts (GM847 cells) transduced via SV-40 with a doxycycline-inducible FLAG-tagged kinase-dead ATR (Peasland et al., 2011). The cells always express ATR and when induced by doxycycline ATR expression increases; the ATR is not active and acts as a dominant-negative. ATR kinase-dead cells did not grow in cell culture until ATR was re-expressed. Further data from the group has shown that MCF7 cells only grow when ATR was re-expressed by shRNA ATR.

To develop a pharmacodynamic assay for CHK1 inhibition the ideal situation would be to measure a downstream phosphorylation events in the absence of an additional activating agent. Autophosphorylation of CHK1 is likely to be most specific as it is largely independent of accessory proteins. A low level of endogenous CHK1 activity ($CHK1^{serine296}$ phosphorylation) was detected in all untreated solid tumour cell lines at consistently low levels. With only low levels of endogenous $CHK1^{serine296}$ phosphorylation there is only a small dynamic range to detect inhibition in an assay. This may explain why other authors have not presented data on how exposure to other CHK1 inhibitors as single agents modulate the phosphorylation of $CHK1^{serine296}$. However, in K562 CML cells endogenous levels were significantly higher and reductions in phosphorylation were more easily detected. Concentrations of 150 nM V158411 on its own for 1

hour reduced CHK1^{serine296} phosphorylation by 50% in MCF7 cells, 70% in MDA-MB-231 cells, 25% in HCT116 cells and 60% in K562 cells.

A more sensitive strategy is to examine the reduction in phosphorylation of CHK1^{serine296} following DNA damage. This increases the dynamic range for the detection of inhibition. The data presented here show that gemcitabine increased CHK1^{serine296} phosphorylation by 8-fold, 7-fold, 4.5-fold and 9-fold in MCF7, MDA-MB-231, HCT116 and K562 cells respectively and that 50 nM V158411 inhibited the gemcitabine-induced increase by ~80% and 150 nM V158411 completely abolished gemcitabine-induced phosphorylation, reducing it to significantly below baseline in all cell lines apart from MDA-MB-231 cells where there was a 2.3 fold reduction from the stimulated level. A short 1 hour treatment was chosen as this could be potentially used in the development a biomarker assay of *ex vivo* CHK1 activation for clinical use that required an *ex vivo* treatment. This confirmed that this is an appropriate concentration and duration to be used in the subsequent experiments and in the development of a potential *ex vivo* biomarker.

The data with V158411 is in line with published data showing exposure to cytotoxic agents increased CHK1^{serine296} phosphorylation. Montano and Guzi demonstrated that CHK1^{serine296} phosphorylation was increased in U2OS cells, MDA-MB-231 breast cancer cells and MCF10A breast cells by an overnight treatment with hydroxyurea (Guzi et al., 2011, Montano et al., 2012). Walton et al showed that 100 nM SN38 for 24 hours also increased CHK1^{serine296} phosphorylation in HT29 cancer cells (Walton et al., 2012).

The data presented here is also in keeping with that presented by Montano et al with SCH 900776 in U2OS, MDA-MB-231 and MCF10A cell lines where SCH 900776 abrogated the hydroxyurea-mediated increase in CHK1^{serine296} phosphorylation in a concentration-dependent fashion (Montano et al., 2012, Guzi et al., 2011). This is also supported by the data pertaining to CCT244747 which at concentrations > 100 nM abolished the SN-38-mediated increase in CHK1^{serine296} phosphorylation (Walton et al., 2012).

CHK1^{serine296} phosphorylation is a potential biomarker for CHK1 inhibitor activity especially after either co-treatment with a cytotoxic agent or following an *ex vivo* stimulation with gemcitabine. The antibody used in these experiments for the CHK1^{serine296} epitope is only suitable for use in western blotting. It could be used with western blots with PBMCs from *in vivo* animal experiments or from patients in early phase clinical trials.

However, new antibodies for CHK1^{serine296} are now available and it would be interesting to explore whether these could be used in other applications. CHK1^{serine345} phosphorylation is an alternative marker of interest. It is markedly elevated in the presence of V158411. There was a 11-fold, 8-fold, 10-fold and 6-fold increase of pCHK1^{serine345} in MCF7, MDA-MB-231, HCT116 and K562 cells respectively 1 hour after the administration of 150 nM V158411. This is in line with the data presented by Montano demonstrating that SCH 900776 increased CHK1^{serine345} phosphorylation (Montano et al., 2012).

Surprisingly, V158411 did not cause any further increase in CHK1^{serine345} phosphorylation compared to gemcitabine alone in MDA-MB-231 and K562 cancer cell lines. In MCF7 cancer cells the increase was less than that with

V158411 alone; however, in HCT116 there was a 3-fold increase in CHK1^{serine345} phosphorylation by gemcitabine and V158411 compared to V158411 alone which may have been merely additive.

The pattern of increase in CHK1^{serine345} phosphorylation was very different with V158411 alone compared to co-treatment with gemcitabine and V158411. With V158411 alone CHK1^{serine345} phosphorylation was greatest in MCF7 > HCT116 > K562 = MDA-MB-231. Whereas with co-treatment with gemcitabine and V158411 CHK1^{serine345} phosphorylation was greatest in MDA-MB-231 > HCT116 = K562 > MCF7. This presumably reflects cell-specific differences in the relative contribution to ATR activation via the stalling of replication forks with gemcitabine or via the inhibition of dephosphorylation events when CHK1 is inhibited.

CHK1^{serine345} phosphorylation may be useful as a demonstration of CHK1 inhibition in biopsy specimens in either *in vivo* experiments or from patients in early phase clinical trials, but it should be remembered that this reflects an effect on ATR activity that is not necessarily CHK1-specific.

The CHK1^{serine345} antibody used in our work and that of a number of other CHK1 inhibitors is also suitable for flow cytometry and IHC. Parsels et al demonstrated that induction of Chk1^{serine345} phosphorylation as measured by IHC (in skin biopsies and hair follicles from mice) can reliably be used as a biomarker of Chk1 activity in mice treated with a combination of AZD7762 and gemcitabine (Parsels et al., 2011). From my own experience I would favour work using skin biopsies as hair follicles are difficult to collect, vary widely between subjects and are require considerable dexterity to process.

Flow cytometry in K562 cells demonstrated that G_2 cell cycle arrest occurs after at least 6 hours (maximum at around 24 hours) consistently after treatment with cisplatin (10 μM until analysis at 6 hours, 12 hours and 24 hours) or 2 Gy IR (and increasing the IR dose caused no further cell cycle disturbance). Other cytotoxic therapy, camptothecin and gemcitabine, may have caused S phase arrest as documented by other authors (Tse et al., 2007b, Montano et al., 2012). However, quantifying S phase arrest without specific methods such as BrdU staining is unreliable.

Since only cisplatin and IR caused convincing S or G_2 cell cycle arrest in the K562 cells only these agents were investigated in the other cells. Only modest cell cycle effects were observed 24 hours after treatment with a DNA damaging agent in all cell lines.

Eastman and colleagues observed more marked G_2 arrest than reported here after 20 μM cisplatin for 2 hours in MDA-MB-231 cancer cells (Eastman et al., 2002). We used a lower concentration of cisplatin for a longer duration; 10 μM in initial experiments and then 1 μM in subsequent experiments for durations of up to 24 hours compared to 20 μM for 2 hours.

Of note, in contrast to experiments performed by Walton et al, we did not show a significant increase in the proportion of cells in G_2 24 hours after treatment with etoposide (Walton et al., 2012). Walton et al. used HT29 colorectal cells and treated them with 25 μM etoposide for 1 hour compared to our experiment where we used 5 μM etoposide for 6, 12 and 24 hours.

Single agent V158411 caused a significant concentration dependent reduction in the proportion of cells in G_2 in both K562 and HCT116 cells. There was a much more modest reduction in MDA-MB-231 breast cancer cells. This did not correlate with the extent of inhibition of CHK1^{serine296} phosphorylation seen with single agent V158411 in these cell lines. The greatest inhibition of CHK1^{serine296} phosphorylation by V158411 was seen in MDA-MB-231 cancer cell lines where there was the most modest reduction of cells in G_2 cell cycle arrest. This is in contrast to the effects seen on the cell cycle with other single agent Chk1 inhibitors, UCN-01, CHIR-124, SCH 900776 and CCT244747, where no significant changes in the cell cycle distribution were seen (Tse et al., 2007b, Montano et al., 2012, Walton et al., 2012).

Based on the data for both 296 and 345 phosphorylation where the effect was most pronounced in MCF7 and HCT116 cells and modest in MDA and K562 cells it was somewhat predictable that V158411 would have very little effect on cell cycle arrest in MDA-MB-231 cancer cells compared to HCT116 cells. However, the profound effect of V158411 on the cell cycle of K562 cells would not have been predicted by the CHK1 phosphorylation data.

V158411 abrogated DNA damage-induced G_2 cell cycle arrest in K562, and HCT116 in a concentration-dependent manner. This mimics the perturbation of etoposide-induced G_2 arrest seen in HT29 colorectal cancer seen by Walton et al with CCT244747 (Walton et al., 2012). Walton et al do not quantify the degree of G_2 cell cycle arrest seen with 25 μM etoposide for 1 hour or the extent of abrogation with the single concentration of 500 nM CCT244747 for 23 hours following etoposide that they use, but present the flow cytometry histograms.

In MDA-MB-231 G_2 arrest was very modest such that significant inhibition by V158411 was difficult to measure. Other studies have used MDA-MB-231 cells and have demonstrated cisplatin-induced G_2 arrest that was abrogated by both UCN-01 and ICP-1 (Eastman et al., 2002). In these studies the MDA-MB-231 cells were exposed to 20 μM cisplatin for 2 hours, left in drug-free media for 24 hours before a 30 or 48 hour exposure to UCN-01 and ICP-1. This longer exposure to UCN-01 and ICP-1 may have led to the more significant abrogation of G_2 cell cycle arrest; though the authors do not quantify this and simply give a visual representation of the data.

The absence of significant changes in the cell cycle distribution with single agent V158411 in MDA-MB-231 breast cancer cells in contrast to the other cell lines may be because the length of a cell cycle in K562 cells is 12-16 hours, in HCT116 cells 20-30 hours and in MDA-MB-231 cells 45-55 hours. So the K562 and HCT116 cells will all have gone through at least one cell cycle in 24 hours whereas only about half of the MDA-MB-231 cells will have been through one cell cycle. This is in line with the data presented by Eastman, albeit with a shorter, 2 hour exposure to a higher, 2 μM, concentration of cisplatin where significant increases in the G_2 fraction were not seen at 24 hours, but also after 30 and 48 hours (Eastman et al., 2002). Flow cytometry has not been performed at 48 hours as it was decided to keep to the same time points across cell lines to ensure the data was comparable rather than to tailor the time points to the duration of the cell cycle in each cell line. These data supports the mechanism that V158411 is acting via CHK1 to modulate the G_2 checkpoint.

CHK1 levels and phosphorylation and checkpoint activation after DNA damage vary across the cell lines and do not necessarily predict cell cycle effects after

DNA damage. Pilot experiments demonstrated that while gemcitabine induced CHK1 phosphorylation after just 1 hour there was no effect of cisplatin until at least 16 hours. However, gemcitabine failed to induce cell cycle arrest and therefore cell cycle perturbations was investigated after IR and cisplatin. The use of different agents in these 2 experiments was pragmatic, but could be seen as a weakness and does not allow direct comparison between the experiments. Because IR and cisplatin were the only agents to consistently cause G_2 arrest in the panel these were investigated alongside gemcitabine in cytotoxicity studies with V158411 in the next chapter.

Chapter 4 Cytotoxicity of V158411

Having determined that V158411 inhibits CHK1 autophosphorylation at serine^{296} almost completely at 150 and 500 nM and that this is associated with the abrogation of cell cycle arrest after DNA damage (IR and cisplatin). The impact of V158411, alone and in combination with DNA damaging agents (gemcitabine, cisplatin and IR), on cell survival was examined.

4.1 CHK1 inhibitors and cell viability

The majority of pre-clinical studies with CHK1 inhibitors have explored their potential to be used as chemosensitisers in combination with conventional cytotoxics. The rationale for these studies as described in section 1-5-1 is that cell cycle arrest is needed to allow repair of DNA damage before it becomes cytotoxic. In cancer cells that have lost G_1 cell cycle control there is greater dependence on the CHK1-mediated S and G_2 checkpoint control.

The rationale for single agent therapy with CHK1 inhibitors is less strong. Not surprisingly therefore, there is relatively little published data regarding the single-agent activity of 'second generation' CHK1 inhibitors. Some investigators have demonstrated that certain cell lines are sensitive to single agent CHK1 inhibitors, but currently it is not clear what determines sensitivity. This will be explored in greater depth in chapters 5 and 6.

The dual CHK1/CHK2 inhibitor 100 nM AZD7762 for 25 hours alone showed minimal cytotoxicity in a panel of cell lines clonogenic assays (Mitchell et al., 2010b). The most sensitive cell lines in this panel were SF-295 (glioblastoma -

57% survival), and MiaPaca2 (65% survival). There was greater than 70% survival with all the remaining cell lines (HT29, DU145, A549, H460, PC-Sw and 1522 (normal skin fibroblasts)).

In contrast Montano et al demonstrated that SCH 900776 was significantly cytotoxic as a single agent in 4 cell lines within a wider panel (Montano et al., 2012). Cell lines were exposed to SCH 900776 for 24 hours in 96 well plates followed by a 5 to 7 day incubation in drug-free media. A fluorescent DNA stain, Hoechst 33258, was used to assess cell proliferation. Most cell lines tolerated concentrations of up to 10 μM SCH 900776 for 24 hours, however 4 (A549, U2OS, TK-10 and HCC2998) showed significant cytotoxicity following exposure to 500 nM SCH 900776.

In studies with the dual CHK1/CHK2 inhibitor XL9844, Matthews et al demonstrated a modest effect of the drug on clonogenic survival. The effect was greatest in HeLa cells where a 24 hour exposure to 300 nM XL844 reduced survival by 32% (Matthews et al., 2007).

As described in the Introduction (section 1-13); in most pre-clinical studies CHK1 inhibitors have been used in conjunction with gemcitabine or topoisomerase I poisons. Varying degrees of chemosensitisation have ben observed and often related to p53 status. In a panel of human cancer cell lines (p53 mutant SW620 and MDA-MB231 cells and paired HCT116 cells with and without p53) AZD7762 increased the growth inhibitory effects (MTT assay) and cytotoxicity of both gemcitabine and topotecan, with more pronounced potentiation in cells with mutated p53. (Zabludoff et al., 2008). At a concentration of 300 nM AZD7762 potentiated the effect of gemcitabine more

than 20-fold in p53 mutated SW620 cells and the effect of topotecan 15-fold in p53 mutant MDA-MB-231 cells. The potentiation of gemcitabine was confirmed using clonogenic survival assays in p53 wild type and mutated HCT116 cells exposed for 2 hours to gemcitabine, then 24 hours with or without 100 nM AZD7762 followed by drug-free media for 10-14 days prior to colony counting. In these studies AZD7762 increased the cytotoxicity of 1 μM gemcitabine 40-fold in the p53 mutant HCT116 cells compared to 10-fold in the p53 wild type HCT116 cells.

Data were confirmed in SW620 xenograft models where 60 mg/kg gemcitabine (i.v.) was administered every 3 days and 12.5 or 25 mg/kg AZD7762 (i.v.) 4 and 16 hours after each gemcitabine dose increased the inhibition of tumour growth by gemcitabine by >70% by AZD7762. However, the most remarkable data was obtained with the combination of AZD7762 with irinotecan in the SW620 model, with complete tumour regressions being observed in all mice treated with 50 mg/kg irinotecan and 25 mg/kg AZD7762 (two doses 2 and 14 hours after the irinotecan).

There is also some mixed cytotoxicity data with CHK1 inhibitors in conjunction with platinum compounds (that cause DNA cross-links) and a single study in conjunction with taxanes (spindle poisons). Eastman and Bunch demonstrated that the prototype CHK1 inhibitor 50 nM UCN-01 significantly potentiated cisplatin-induced growth inhibition in AA8 CHO cells and in MDA-MB-231 (Bunch and Eastman, 1996, Eastman et al., 2002). Cells were treated for 2 hours with cisplatin, then had 22 hours in drug-free media prior to 24 hours in UCN-01 prior to estimating growth by DNA content 6 days later. However, in other studies the clonogenic survival of HeLa cells treated with cisplatin was not

impaired by 24 hour co-exposure with 20 and 80 nM AZD7762 (Wagner and Karnitz, 2009). In similar studies there was no potentiation of cisplatin-induced growth inhibition in human breast cancer MDA-MB-231, MDA-MB-231$^{CHK1-/-}$ or immortalised human breast fibroblasts MCF10A cells by either 50 nM UCN-01 or 1 μM SCH 900776 co-exposure for 24 hours followed by 5-7 days in drug-free medium (Montano et al., 2012). However, in this study there was substantial sensitisation to hydroxurea by both CHK1 inhibitors in all 3 cell lines, even those lacking CHK1.

Somewhat curiously, PF00477736 has been shown to sensitise xenografts to the taxane docetaxel (Zhang et al., 2009). In the xenograft model of CoLo205 and MDA-MB-231, mice were administered 15 or 30 mg/kg docetaxel intra-peritoneal (i.p.) once on day 1, 8 and 15 with or without 7.5 or 15 mg/kg PF00477736 (i.p.) concomitantly with the docetaxel and a second dose after a delay of 6 hours. There was significant tumour growth delay in both xenografts with the combination compared to single agent docetaxel or PF00477736.

There is far less published pre-clinical data concerning radio-potentiation with CHK1 inhibitors than there is with combination therapy with other chemotherapeutic agents. As described in section 1.14 promising levels of radiosensitisation have been observed with UCN-01, AZD7762 and CEP-3891 both *in vitro* and *in vivo* but so far this has not translated into clinical studies of CHK1 inhibitors in combination with IR.

There is data supporting the notion that radiosensitisation by CHK1 inhibitors will be greater in p53 null/mutant cells. 100 nM AZD7762 for 1 hour prior to IR and 24 hours after a single fraction of IR (range 0-14 Gy), significantly

radiosensitised DU145 1.6-fold, HT29 and H460 with a dominant negative p53 1.58-fold in colony forming assays (Mitchell et al., 2010b). Significantly in matched H460 cells with wild type p53 radiosensitisation was only 1.11-fold (not significant) and there was no significant radiosensitisation in 1522 (normal human fibroblasts) sensitisation is 1.05 fold, in A549 NSCLC cells sensitisation is 1.2-fold.

In a separate paper, Yang et al demonstrated that AZD7762 was an effective radiosensitiser in H23 (p53 mutated radio-sensitive) and PC14PE6 (p53 wild type radio-resistant) NSCLC cell lines (Yang et al., 2011). Cells were treated with 100 nM AZD7762 for 1 hour before and 24 hours after exposure to a range of doses of IR (0 – 7 Gy). They also developed a mouse xenografts model of PC14PE6 NSCLC with brain metastases and showed that 25 mg/kg AZD7762 (i.v.) prolonged the median survival time following whole brain irradiation (15 Gy) delivered 1 hour after AZD7762. Median survival was 30 days with no treatment, 40 days with IR alone and 51 days with IR + AZD7762 ($p = 0.05$ compared to IR alone).

There is mixed evidence as to whether a CHK1 inhibitor should be administered concomitantly with cytotoxic therapy or after a delay. Zabludoff compared the effect of AZD7762 on the cytotoxicity of gemcitabine in isogenic p53 +/+ and p53 -/- HCT116 cells in a colony-forming assay (Zabludoff et al., 2008). Cells were treated with variable gemcitabine concentrations for 2 hours followed by either immediate 24 hour treatment with 100 nM AZD7762 for 24 hours immediately or after a 24 hour incubation in drug-free media. The chemosensitisation was greatest in this assay if 100 nM AZD7762 was delivered immediately after the 2 hour exposure to gemcitabine. Further work

was performed using 100 nM AZD7762 for 24 hours in combination with 50 nM gemcitabine for 2 hours in 3 different scheduling regimens in a panel of pancreatic cell lines (MiaPaCa-2, M-Panc96, BxPC3 and Panc-1) (Parsels et al., 2011). The authors demonstrated that the best schedule depended on the concentration of gemcitabine used. 50 nM gemcitabine for 2 hours is relatively non-toxic to the pancreatic cell lines and in this scenario there was greatest chemo-potentiation (4.5-6 fold) if AZD7762 was given immediately after gemcitabine. However, if higher concentrations of gemcitabine were used a delay of 24 hours led to greater potentiation. These authors had observed similar effects with PD-321852 in MiaPaCa-2 and Panc-1 cells (Parsels et al., 2009). The authors suggest that at higher concentrations of gemcitabine the cells have arrested in early-S phase and time needs to have elapsed for the cells to have escaped the S phase arrest for cytotoxicity to be potentiated by the agent targeting the G_2 checkpoint.

Walton et al showed *in vitro* studies with SW620 cells that co-exposure to gemcitabine (fixed concentration of IC_{50}) and the CHK1 inhibitor SAR-020106 (variable concentrations – not specified) for less than 24 hours did not enhance gemcitabine cytotoxicity but enhancement was observed if the co-exposure was for at least 48 hours (Walton et al., 2012). Studies in mice revealed that concomitant administration of the CHK1 inhibitor SAR-020106 with gemcitabine or irinotecan was more effective at delaying the growth of SW620 mouse xenografts (Walton et al., 2010). 4 doses of 60 mg/kg gemcitabine (i.v.) or 3 doses of 12.5 mg/kg irinotecan (i.p.) were delivered every 3 or 7 days respectively. 40 mg/kg SAR-020106 (i.p.) was delivered either 1 hour before (concomitant schedule) or 24 hours after (delayed schedule) the cytotoxic therapy. The growth delay with concomitant administration of gemcitabine and

SAR-020106 was 8.5 days compared to 6.3 days when SAR-020106 was delivered on the delayed schedule.

In contrast, pre-clinical studies by Montano with SCH 900776 led the early phase clinical trial team to deliver SCH 900776 24 hours after gemcitabine (Montano et al., 2012, Daud et al., 2010). Montano et al compared the sensitivity of MDA-MB-231 cells to either simultaneous treatment with hydroxyurea and 2 μM SCH 900776 for 24 hours or 2 μM SCH 900776 was only added for the last 6 hours of the 24 hour incubation period. The authors showed that there was a 50-fold decrease in the IC_{50} of hydroxyurea with both regimens. However if the same concentrations of both drugs were used concurrently for only 6 hours there was no cytotoxicity. It is unclear how this pre-clinical evidence led the early phase investigators to use a schedule where there was a 24 hour delay between the delivery of gemcitabine and SCH 900776. This may be based on unpublished data.

The approach of delaying the administration of the CHK1 inhibitor for a defined period after the cytotoxic agent is supported by data with GNE-900 (Blackwood et al., 2013). The authors administered 20 mg/kg GNE-900 orally concomitantly with 60 mg/kg gemcitabine (i.p.) or after 8, 16, 24, 36 or 48 hours to mice bearing HT-29 xenografts. Maximal chemosensitisation was seen with a 24 hour gap between gemcitabine and the CHK1 inhibitor with what the authors describe as a therapeutic window between 16 and 36 hours. There was no effect when GNE-900 was given concomitantly with gemcitabine or with a delay of 8 or 48 hours.

With respect to the scheduling of a CHK1 inhibitor in conjunction with IR, Mitchell and colleagues comment in their discussion that, in pilot *in vitro* studies that they do not include in detail in their publication, treatment with 100 NM AZD7762 after IR was more effective at enhancing the effect of IR than treatment with AZD7762 for 24 hours prior to IR (Mitchell et al., 2010b).

The aims of this chapter are:

a) To determine the cytotoxicity of single agent V158411 in a panel of cell lines.

b) To determine the chemosensitisation by V158411 of cell lines to gemcitabine and cisplatin.

c) To determine the radiosensitisation of cell lines by V158411

d) To establish the schedule dependency of radiosensitisation using the same cell lines in which the effects of V158411 on CHK1 phosphorylation and cell cycle kinetics had been determined.

4.2 Single agent cytotoxicity of V158411

CHK1 inhibitors may be useful as single agent therapies as well as in combination with traditional cytotoxics or radiotherapy. To determine if V158411 had single agent activity in the 4 cancer cell lines (MCF7, MDA-MB-231, HCT116 and K562 cells) investigated in Chapter 3, the clonogenic survival following a 24 hour exposure to increasing concentrations of V158411 was assessed (Figure 4-1). The LC_{50} values ranged from 114 nM in MCF7 cells to 511 nM in MDA-MB-231 cells (Table 4-1).

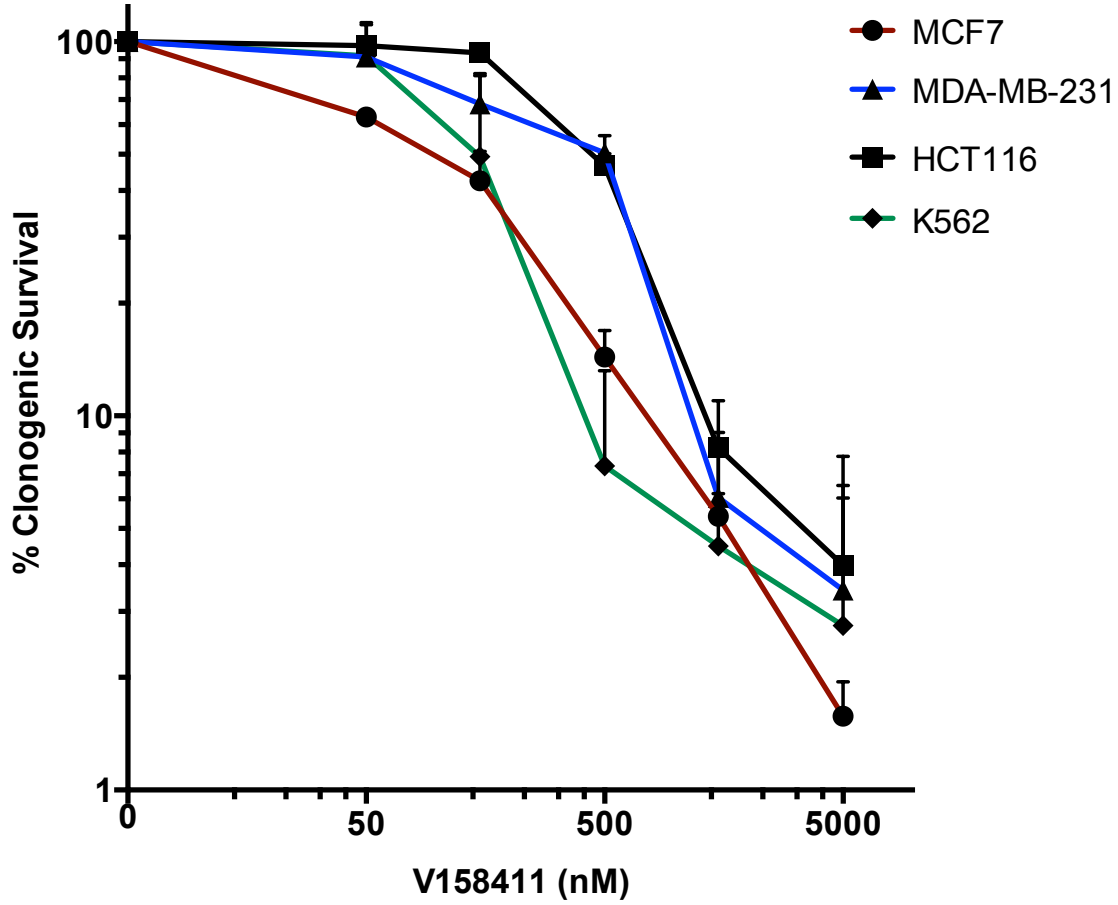

Figure 4-1 Cytotoxicity of single agent V158411

Cytotoxicity assays (clonogenic) in MCF7 (p53 wild type), MDA-MB-231 (p53 mutated), HCT116 (p53 wild type) and K562 (p53 mutated) cancer cell lines. Data are mean +/- SEM of 3 independent experiments. Within each experiment there were at least 2 replicates.

Cell Line and p53 status	V158411 LC_{50} (nM): mean and (SD)	V158411 LC_{90} (nM): mean and (SD)
MCF7 (p53 wild type)	113.8 (40.3)	986.9 (152.3)
MDA-MB-231 (p53 mutant)	511.3 (64.5)	1411.2 (56.7)
K562 (p53 mutant)	152.5 (87.2)	482.1 (524.5)
HCT116 (p53 wild type)	476.4 (41.2)	1453 (99.9)

Table 4-1 LC_{50} and LC_{90} values of V158411

Data from cytotoxicity assays (clonogenic) in MCF7 (p53 wild type) and MDA-MB-231 (p53 mutated) breast cancer, HCT116 (p53 wild type) colorectal and K562 (p53 mutated) CML cancer cell lines. Mean and standard deviation from at least 3 experiments.

4.3 The effect of V158411 concentration and exposure duration on cytotoxicity

To assess whether a shorter duration exposure to a higher concentration of V158411 or a longer exposure to a lower concentration would result in higher cytotoxicity, MCF7 and HCT116 cells were treated for 24, 72 or 120 hours with V158411 in clonogenic assays. The concentrations of V158411 were chosen so that the total exposure/AUC (area under the curve) given over the varying time periods would be constant; that is 50 nM x 24 hours, 16 nM x 72 hours, 10 nM x 120 hours; 150 nM x 24 hours, 50 nM x 72 hours, 30 nM x 120 hours and finally 500 nM x 24 hours, 166 nM x 72 hours and 100 x 120 hours (Figure 4-2).

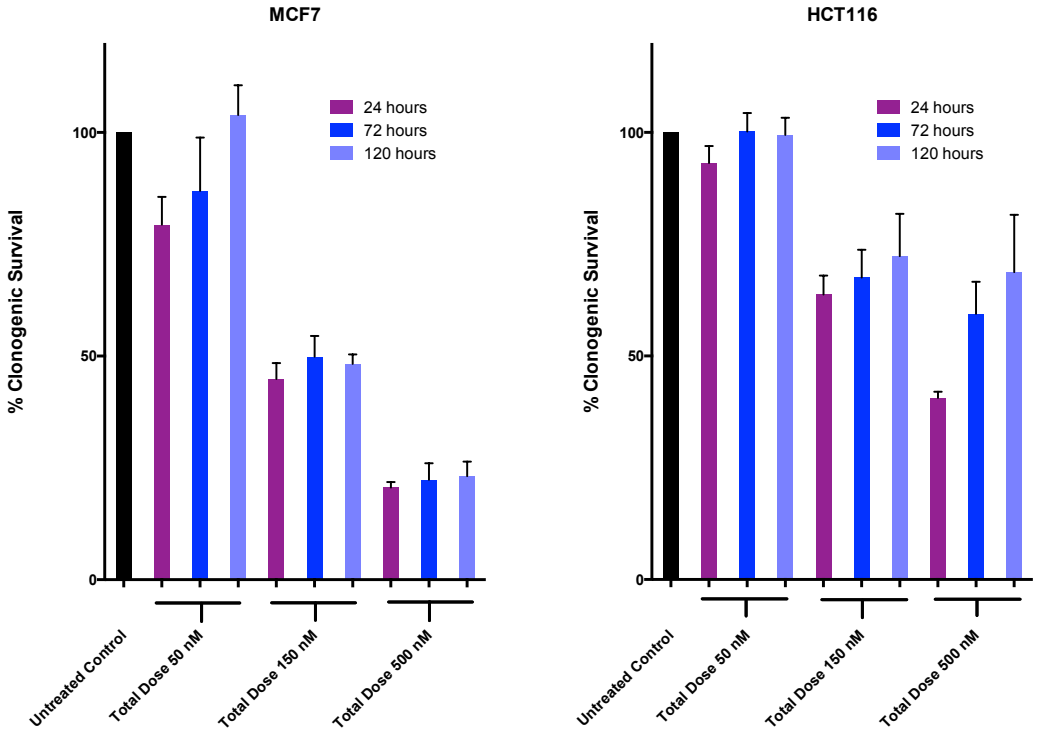

Figure 4-2 Cytotoxicity assay (clonogenic) exploring dose duration/intensity.

Clonogenic survival of MCF7 (p53 wild type) and HCT116 (p53 wild type) cells following treatment with V158411: 50 nM x 24 hours, 16 nM x 72 hours, 10 nM x 120 hours; 150 nM x 24 hours, 50 nM x 72 hours, 30 nM x 120 hours; 500 nM x 24 hours, 166 nM x 72 hours, 100 nM x 120 hours. Summary of 3 independent experiments Data are mean +/- SEM of 3 independent experiments. Within each experiment there were at least 2 replicates.

Greatest cytotoxicity is seen with a shorter (24 hours versus 72 hours versus 120 hours) exposure to a higher concentration of V158411 in both MCF7 and HCT116 cell lines. A 24 hour exposure is significantly more cytotoxic than a 72 hour exposure in both MCF7 and HCT116 cells ($p = 0.019$ and $p = 0.006$ respectively (paired t-test)). However, there is no statistically significant difference between a 72 hour exposure and 120 hour exposure in both MCF7 and HCT116 cell lines ($p = 0.124$ and $p = 0.084$ respectively (paired t-test)).

As expected cytotoxicity was both concentration and time-dependent. Within each group of equivalent AUC the highest concentration for the shortest time was more cytotoxic than lower concentrations for longer exposure period. This was true for MCF7 at a total AUC of 50 nM for 24 hours and for HCT116 cells at all AUCs. Time dependency was more apparent in MCF7 cells where 50 nM for 24 hours was less cytotoxic than when the exposure was extended to 50 nM for 72 hours and 150 nM for 24 hours was less cytotoxic than 166 nM for 72 hours. In HCT116 although 50 nM for 24 hours was less cytotoxic than 50 nM for 72 hours, there was less difference between 150 nM for 24 hours and 166 nM for 72 hours.

4.4 Chemo-potentiation

The majority of the pre-clinical literature with CHK1 inhibitors has focused on its use in combination with gemcitabine, topoisomerase I poisons and platinum compounds. For the purposes of this project V158411 was used in combination with either gemcitabine or cisplatin in the MCF7 (p53 wild type) and MDA-MB-231 (p53 mutated) breast cancer cell lines.

4.4.1 Single agent cytotoxicity of gemcitabine and cisplatin

Prior to performing combination cytotoxicity studies with V158411 the single agent cytotoxicity of gemcitabine and cisplatin in MCF7 and MDA-MB-231 cell lines was assessed in clonogenic assays after 24 hour drug exposure (Figure 4-3). The drugs had similar cytotoxicities in both cell lines with MDA-MB-231 cancer cells being marginally more sensitive (Table 4-2).

Cell Line	MCF7: mean and (SD)	MDA-MB-231: mean and (SD)
Gemcitabine LC_{50} (nM)	21 (15.0)	17 (8.3)
Gemcitabine LC_{90} (nM)	205 (127.9)	100 (140.7)
Cisplatin LC_{50} (μM)	2 (n/a)	1.3 (0.52)
Cisplatin LC_{90} (μM)	23 (n/a)	18 (n/a)

Table 4-2 LC_{50} and LC_{90} values of gemcitabine and cisplatin.

Data from MCF7 (p53 wild type) and MDA-MB-231 (p53 mutated) breast cancer cell lines. Mean and standard deviation from at least 3 experiments where data is available.

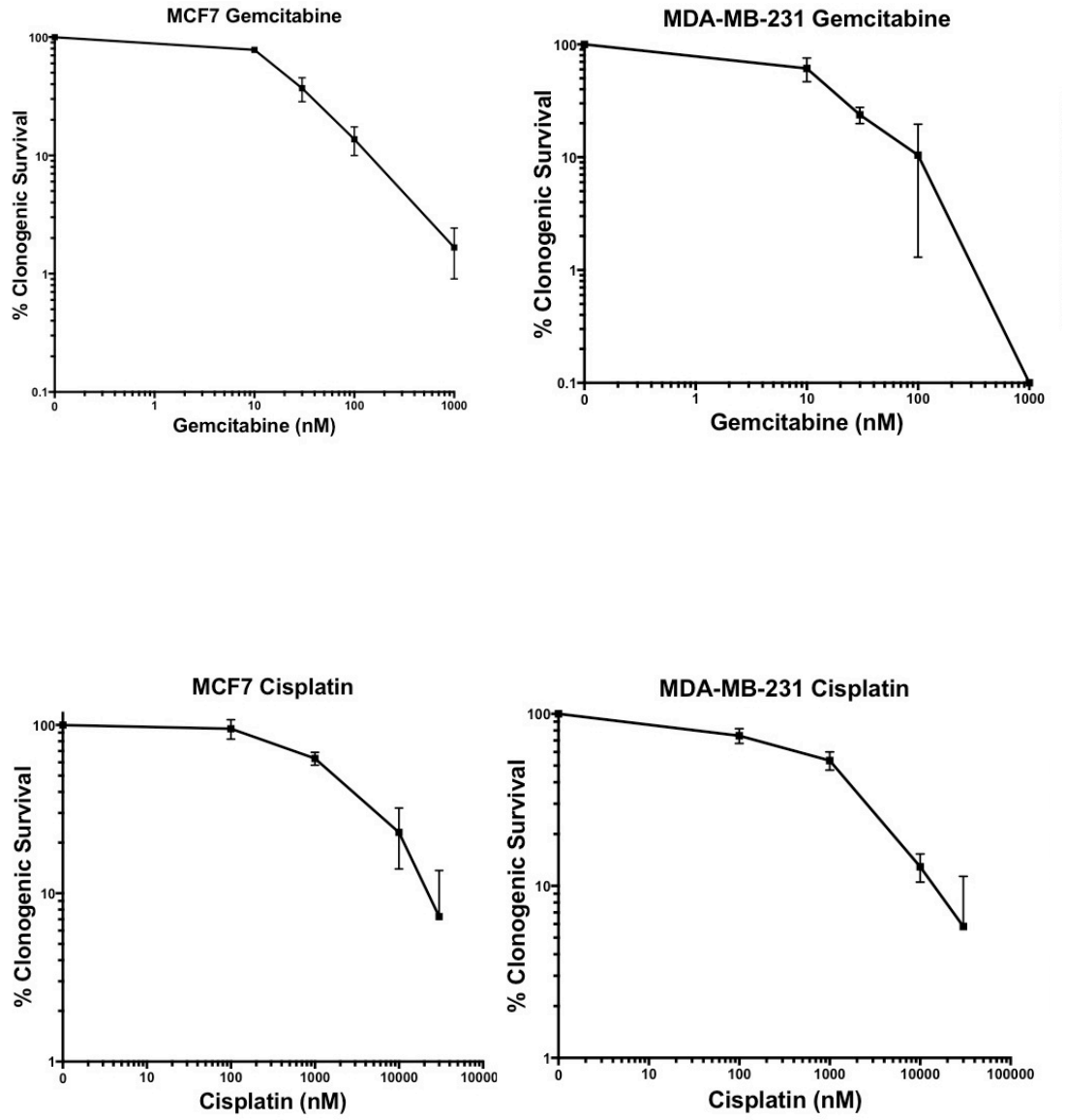

Figure 4-3 Cytotoxicity of single agent gemcitabine and cisplatin in MCF7 and MDA-MB-231 breast cancer cell lines.

Cytotoxicity assays (clonogenic) in MCF7 (p53 wild type), MDA-MB-231 (p53 mutated). Data are mean +/- SEM of 3 independent experiments. Within each experiment there were at least 2 replicates.

4.4.2 Combination of gemcitabine with 50 nM and 150 nM V158411

The ability for V158411 to potentiate the cytotoxicity of gemcitabine in MCF7 and MDA-MB-231 breast cancer cell lines was assessed in clonogenic assays. Cells were co-exposed to increasing concentrations of gemcitabine and 2 concentrations of V158411, 50 nM and 150 nM (representing the approximate LC_{50} and a lower than LC_{50} concentration to explore synergism) for 24 hours and colonies allowed to form in fresh, drug-free medium 10 days later (Figure 4-4 and Figure 4-5).

Neither concentration of V158411 potentiated the cytotoxicity of gemcitabine in either cell line. There was no statistically significant difference in the LC_{50} values in either cell line when V158411 was used in addition to gemcitabine.

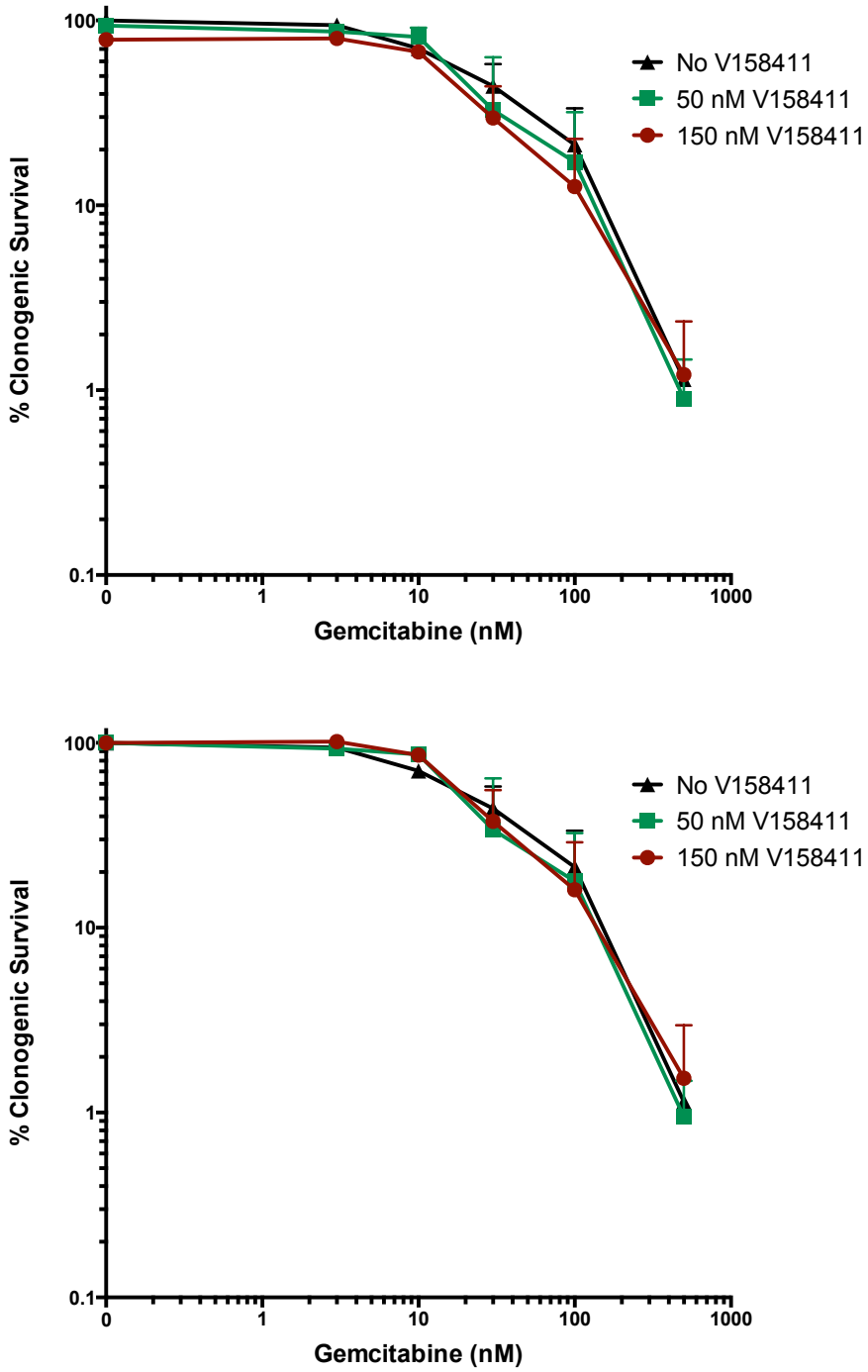

Figure 4-4 Cytotoxicity of gemcitabine +/- V158411 in MCF7 cells.

MCF7 (p53 wild type) breast cancer cell line treated with gemcitabine alone or in combination with 50 nM V158411 or 150 nM V158411 for 24 hours. Upper graph: Absolute survival; lower graph: survival normalised to DMSO or 50 nM or 150 nM V158411 alone control. Data are mean +/- SEM of 3 independent experiments. Within each experiment there were at least 2 replicates.

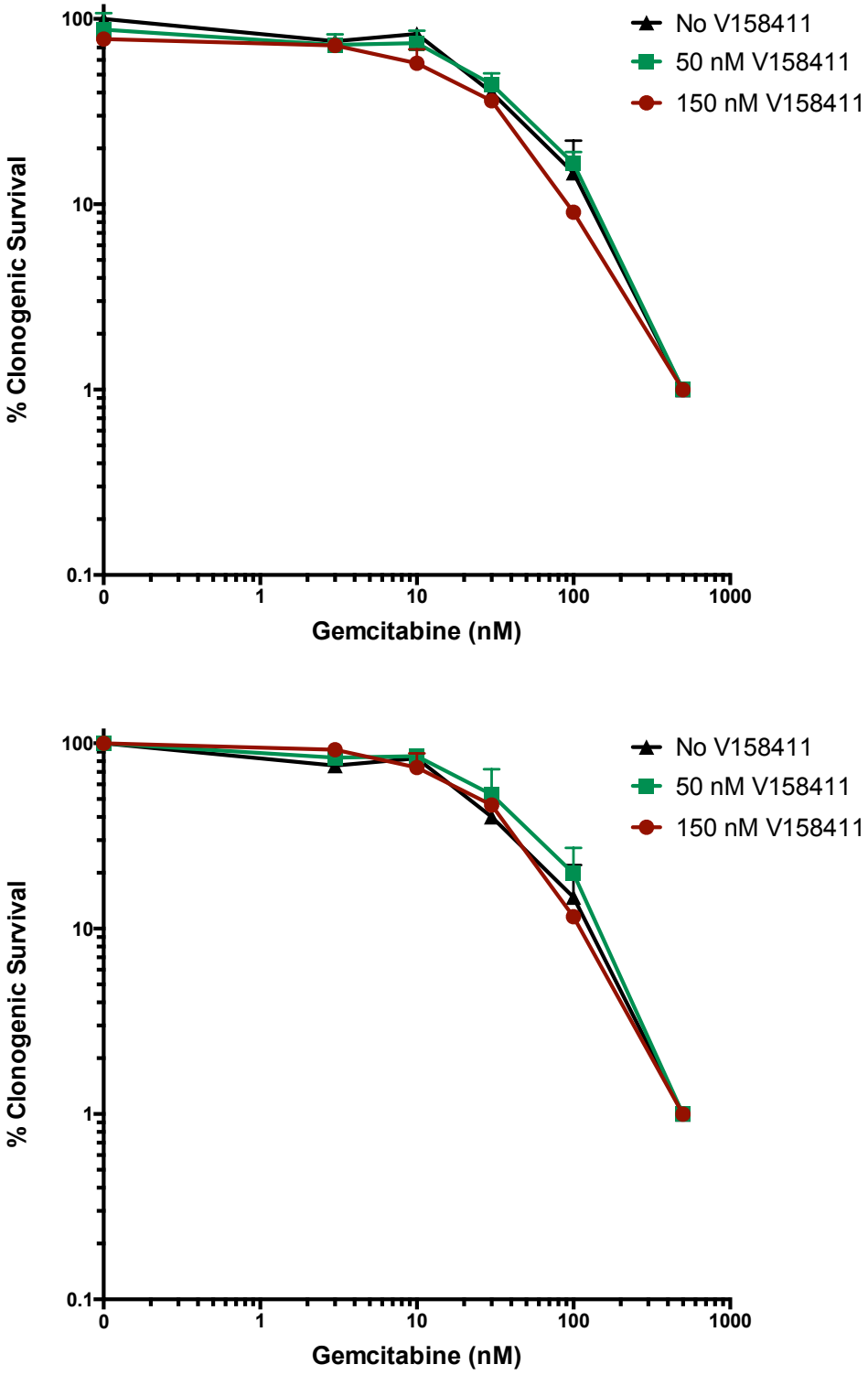

Figure 4-5 Cytotoxicity of gemcitabine +/- V158411 in MDA-MB-231 cells.

MDA-MB-231 (p53 mutated) breast cancer cell line treated with gemcitabine alone or in combination with 50 nM V158411 or 150 nM V158411 for 24 hours. Upper graph: Absolute survival; lower graph: survival normalised to DMSO or 50 nM or 150 nM V158411 alone control. Data are mean +/- SEM of 3 independent experiments. Within each experiment there were at least 2 replicates.

4.4.3 Combination of cisplatin with 50 nM and 150 nM V158411

The ability for V158411 to potentiate the cytotoxicity of cisplatin in MCF7 and MDA-MB-231 breast cancer cell lines was assessed in clonogenic assays. Cells were co-exposed to increasing concentrations of cisplatin and 2 concentrations of V158411, 50 nM and 150 nM for 24 hours (Figure 4-6 and Figure 4-7).

As can be seen in both figures (Figure 4-6 and Figure 4-7) neither concentration of V158411 potentiated the cytotoxicity of cisplatin in either cell lines. There was no statistically significant difference in the LC_{50} values in either cell line when V158411 was used in addition to cisplatin.

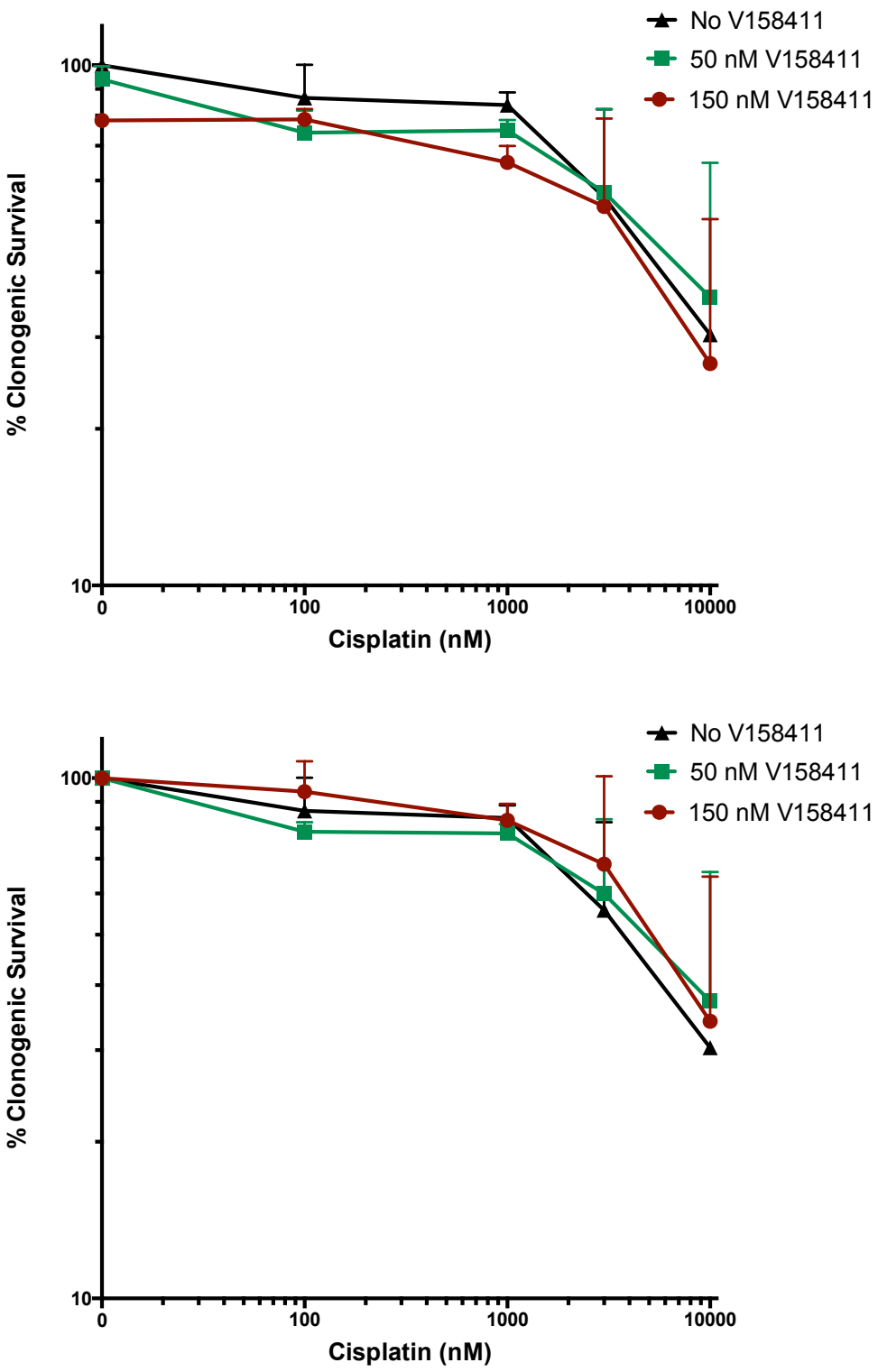

Figure 4-6 Cytotoxicity of cisplatin +/- V158411 in MCF7 cells.

MCF7 (p53 wild type) breast cancer cell line treated with cisplatin alone or in combination with 50 nM V158411 or 150 nM V158411 for 24 hours. Upper graph: Absolute survival; lower graph: survival normalised to DMSO or 50 nM or 150 nM V158411 alone control. Data are mean +/- SEM of 3 independent experiments. Within each experiment there were at least 2 replicates.

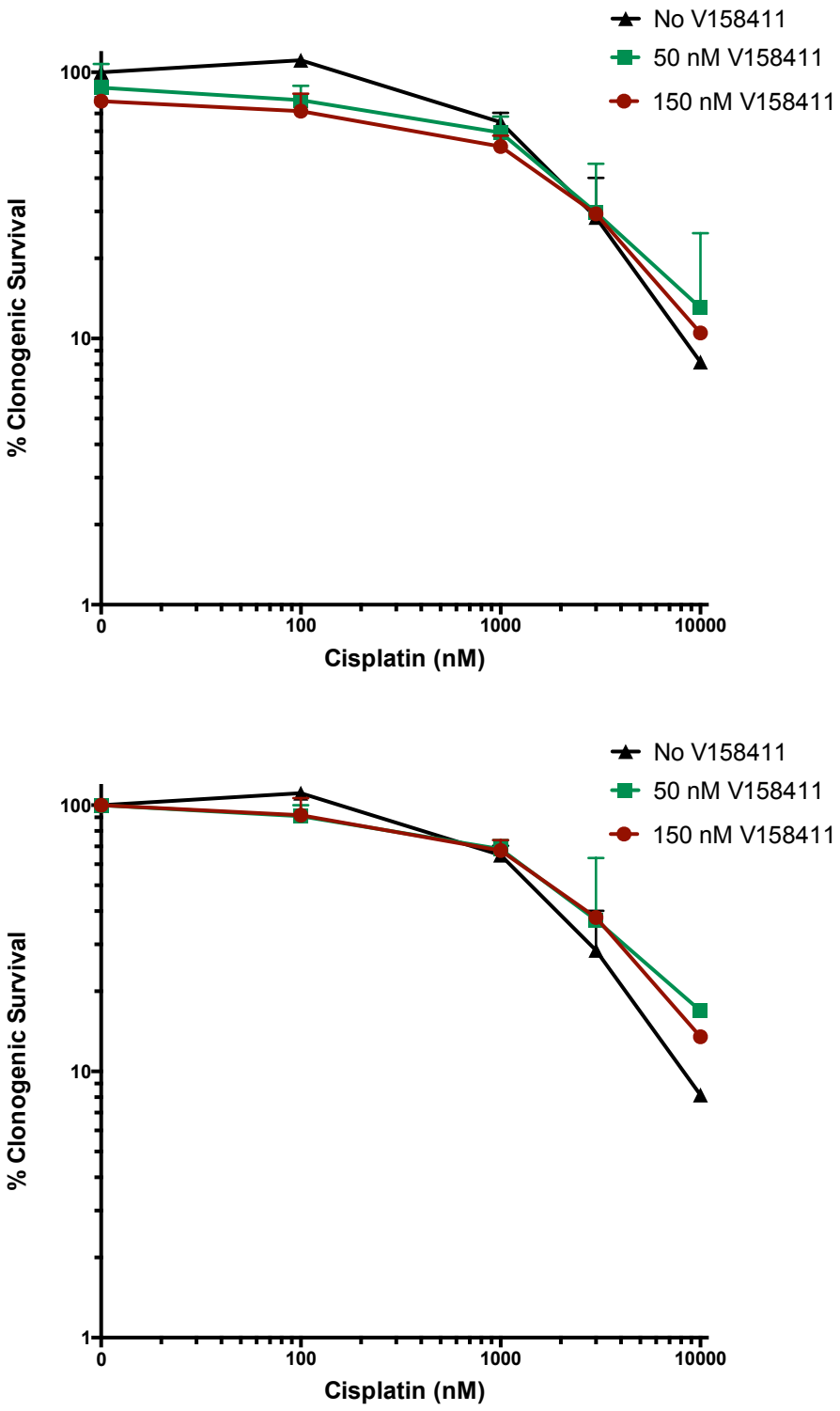

Figure 4-7 Cytotoxicity of cisplatin +/- V158411 in MDA-MB-231 cells.

MDA-MB-231 (p53 mutated) breast cancer cell line treated with cisplatin alone or in combination with 50 nM V158411 or 150 nM V158411 for 24 hours. Upper graph: Absolute survival; lower graph: survival normalised to DMSO or 50 nM or 150 nM V158411 alone control. Data are mean +/- SEM of 3 independent experiments. Within each experiment there were at least 2 replicates.

4.5 Radio-potentiation

The ability of V158411 to potentiate the cytotoxicity of ionising radiation (IR) in MCF7 and MDA-MB-231 cell lines was assessed. Cells were treated with V158411 or control DMSO for 2 hours prior to exposure to IR and for a further 22 hours after exposure.

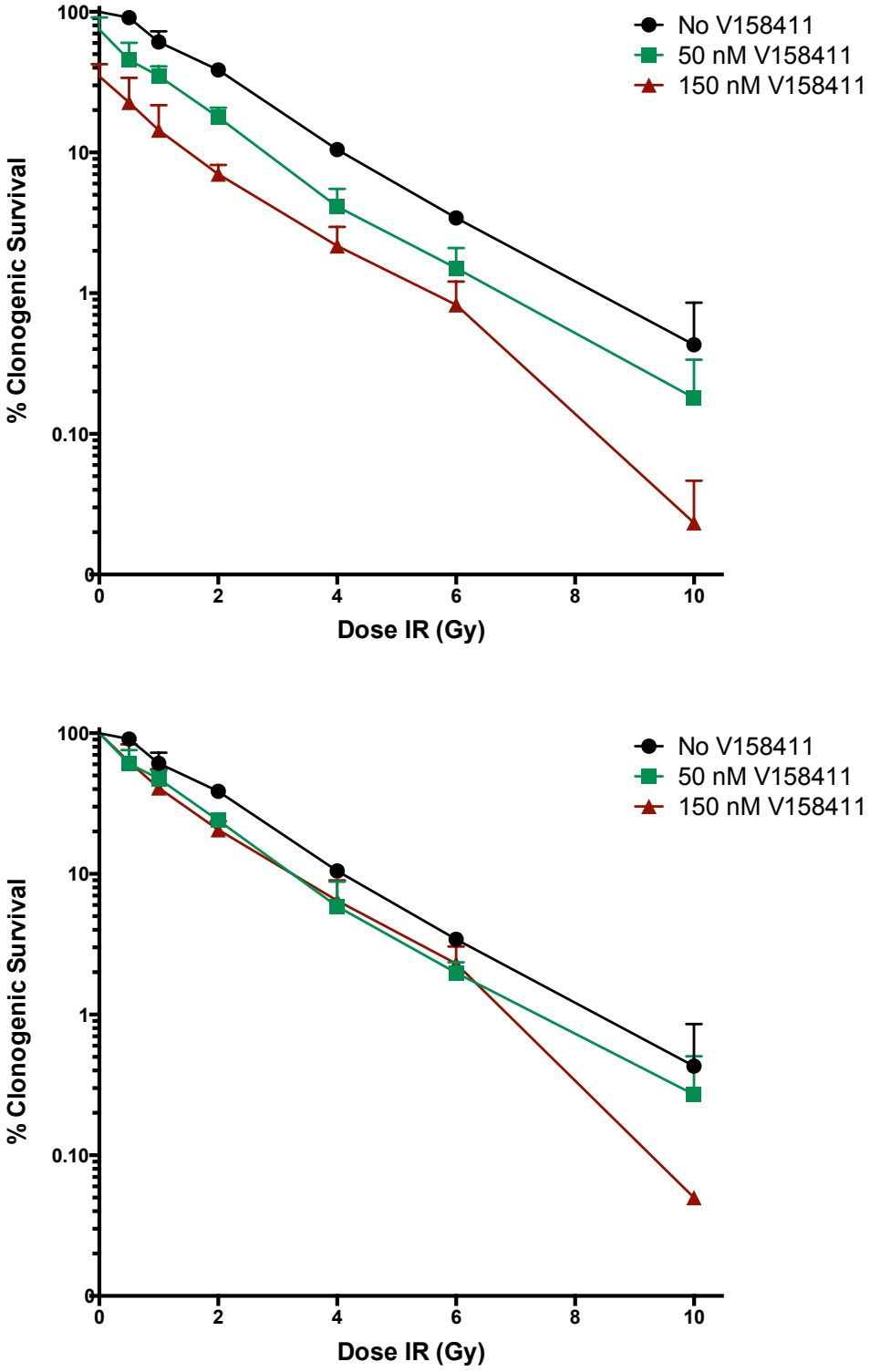

Figure 4-8 Cytotoxicity of IR +/- V158411 in MCF7 cells.

MCF7 (p53 wild type) breast cancer cell line treated with 0-10 Gy IR alone or in combination with 50 nM V158411 or 150 nM V158411 for 24 hours. Upper graph: Absolute survival; lower graph: survival normalised to DMSO or 50 nM or 150 nM V158411 alone control. Data are mean +/- SEM of 3 independent experiments. Within each experiment there were at least 2 replicates.

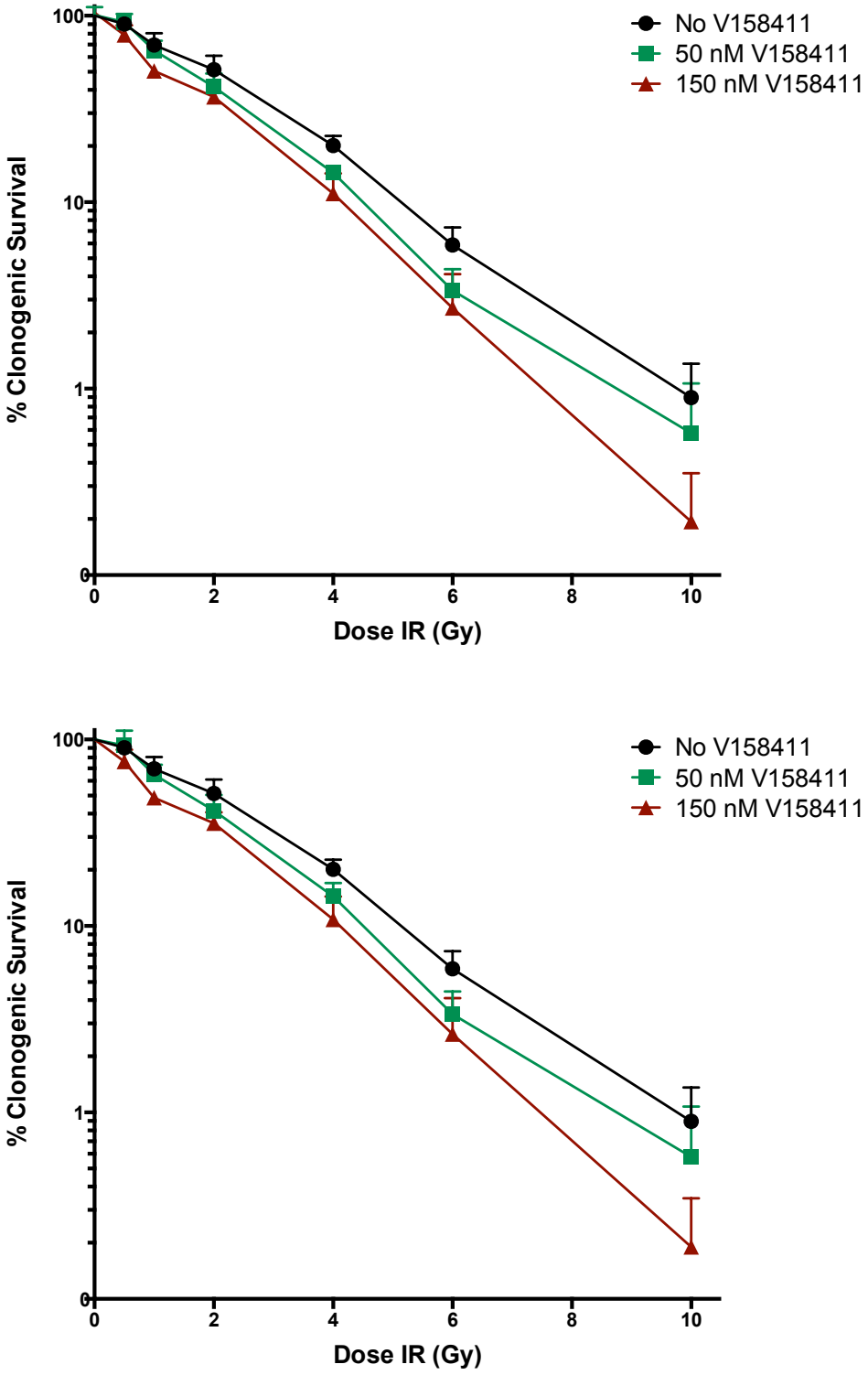

Figure 4-9 Cytotoxicity of IR +/- V158411 in MDA-MB-231 cells.

MDA-MB-231 (p53 mutated) breast cancer cell line treated with 0-10 Gy IR alone or in combination with 50 nM V158411 or 150 nM V158411 for 24 hours. Upper graph: Absolute survival; lower graph: survival normalised to DMSO or 50 nM or 150 nM V158411 alone control. Data are mean +/- SEM of 3 independent experiments. Within each experiment there were at least 2 replicates.

V158411 enhanced IR-induced cytotoxicity in both cell lines (Figure 4-8 and Figure 4-9) at both 50 nM and 150 nM, but this was only significant in the MDA-MB-231 cancer cell line (MCF7 p = 0.059, MDA-MB-231 p = 0.023 (ANOVA)). Radiotherapy is most commonly administered in 2 Gy fractions, so radiation enhancement ratios (RER) at 2 Gy IR were calculated for both cell lines (Table 4-3). There was no statistically significant difference between 50 nM and 150 nM V158411 in the enhancement of IR in either cell line.

	MCF7		MDA-MB-231	
	RER: mean and (SD)	p-value	RER: mean and (SD)	p-value
No V158411 versus 50 nM V158411	1.70 (0.147)	0.05	1.242 (0.039)	0.006
No V158411 versus 150 nM V158411	1.91 (0.247)	0.038	1.46 (0.219)	ns

Table 4-3 RER (mean and SD) with V158411.

RER in MCF7 (p53 wild type) and MDA-MB-231 (p53 mutated) cancer cell lines. ns – not significant. p values calculated by paired t-tests. Summary of data from at least 3 independent experiments.

4.6 The effect of dose schedule on the cytotoxicity of V158411 in combination with ionising radiation

In the previous experiments when V158411 was used in combination with IR; it was delivered for 2 hours prior to, and 22 hours immediately after IR. It is unclear whether this is the best strategy for enhancing the cytotoxicity of IR. In early phase clinical trials some CHK1 inhibitors (as a 1 to 3 hour infusion) have been used concomitantly with conventional chemotherapy and others following a 24 hour delay.

An experiment was designed to assess whether there was any difference in the ability of V158411 to enhance the cytotoxicity of IR depending on the dosing schedule. Since MDA-MB-231 and MCF7 cells behaved similarly in previous experiments, for the scheduling experiments a different cell line, HCT116 was introduced to replace the MDA-MB-231 cell line. MCF7 and HCT116 cells were exposed to V158411 for 24 hours prior to 2 Gy IR or for 24 hours immediately after 2 Gy IR, or for 24 hours following a 24 hour delay after IR (Figure 4-10).

In both cell lines 2 Gy IR caused an approximately 50% reduction in survival. In MCF7 cells, pre-treatment with V158411 prior to IR was less effective than treatment either immediately after IR, but nevertheless caused a concentration-dependent significant increase in cytotoxicity compared to IR alone (1.4 fold at 50 nM, 2.7 fold at 150 nM).

In HCT116 cells, pre-treatment with V158411 appeared to protect cells from IR, with survival being significantly greater than with IR alone (50 nM V158411 (32% increase in survival) $p = 0.0004$ and 150 nM V158411 (12% increase in survival) $p = 0.014$ respectively (paired t-test)). In MCF7 cells co-treatment and

delayed post IR exposure to V158411 caused similar radiosensitisation that was approximately 2 fold at 50 nM and 3 fold at 150 nM ($p = 0.0085$ and $p = 0.0153$ respectively (paired t-test)). Radiosensitisation by V158411 in HCT116 cells was modest and not statistically significant, being around 1.2-fold at 150 nM and negligible at 50 nM ($p = 0.16$ and $p = 0.13$ respectively (paired t-test)).

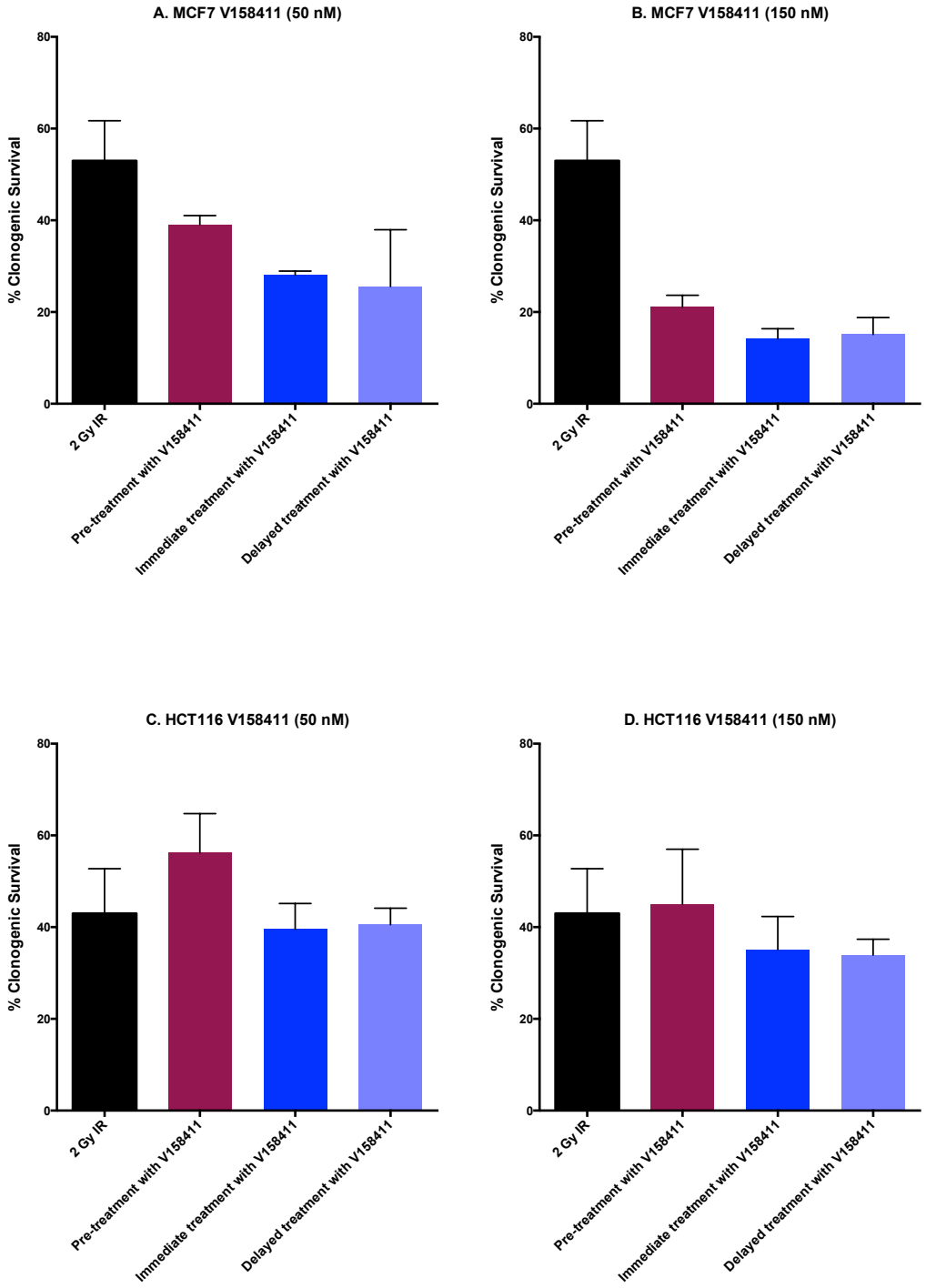

Figure 4-10 Cytotoxicity of IR +/- V158411 in different dose schedules.

The effect of dose schedule of V158411 and ionising radiation. A and B in MCF7 (p53 wild type) breast cancer cell line and C and D in HCT116 (p53 wild type) colorectal cancer cell line. Black bars - cells treated with 2 Gy IR alone, purple bars – cells treated for 24 hours with V158411 prior to 2 Gy IR, dark blue bars – cells treated with V158411 for 24 hours immediately after 2 Gy IR, light blue bars – cells treated with V158411 for 24 hours after a 24 hour delay following the delivery of 2 Gy IR. Data are mean +/- SEM of 3 independent experiments. Within each experiment there were at least 2 replicates.

4.7 Discussion

The sensitivity (LC_{50}) of the four cell lines examined to single agent V158411 ranged from 114 nM (MCF7 – breast cancer) to 511 nM (MDA-MB-231 - breast cancer). There seems to be a threshold concentration (50 nM) below which very little cytotoxicity is seen in any of the four cell lines; this is despite the fact that there is greater than 50% inhibition of $CHK1^{serine296}$ phosphorylation in 3 of 4 (MDA-MB-231, HCT116 and K562) of the cell lines with 50 nM V158411 (see Table 4-4). There is discordance between the inhibition of $CHK1^{serine296}$ phosphorylation and cytotoxicity; the cell lines with the greatest inhibition of $CHK1^{serine296}$ phosphorylation at the lowest concentration of V158411 (MDA-MB-231) are the cell line in which V158411 is the least cytotoxic. Interestingly, MCF7 cells were the cells in which endogenous CHK1 activity was most resistant to inhibition by V158411, but were the most sensitive cell line in cytotoxicity assays.

Cell Line	V158411	CHK1 inhibition	Cell death
MCF7	50 nM	32%	34%
	150 nM	53%	60%
MDA-MB-231	50 nM	52%	6%
	150 nM	67%	30%
K562	50 nM	53%	10%
	150 nM	55%	54%
HCT116	50 nM	40%	2%
	150 nM	17%	9%

Table 4-4 CHK1 inhibition with V158411 and relationship to single agent cytotoxicity.

CHK1 inhibition data (% reduction in CHK1^{serine296} following 1 hour treatment with 50 and 150 nM V158411) from section 3.4. Cytotoxicity in single agent assay with 50 and 150 nM V58411.

There are a limited number of studies published with CHK1 inhibitors used as single agents so comparisons between this data with V158411 and the literature are restricted. However, in studies with the dual CHK1/2 inhibitors AZD7762 and XL9844 only modest cytotoxicity was observed and this is restricted to a few cell lines. Mitchell et al demonstrated minimal cytotoxicity with the dual CHK1/CHK2 inhibitor AZD7762 in a panel of cancer cell lines (Mitchell et al., 2010b). A lack of significant single agent activity was also seen with another dual CHK1/CHK2 inhibitor, XL9844, where in clonogenic assays the most significant reduction in survival following a 24 hour exposure to 300 nM XL844 was a 32% reduction in survival in HeLa cells (Matthews et al., 2007). Similarly, Montano et al showed that a 24 hour exposure to 500 nM SCH 900776 was

cytotoxic to 4 (A549, U2OS, TK-10 and HCC2998) out of wider panel of cancer cell lines (Montano et al., 2012). The cytotoxicity of V158411 as a single agent in U2OS cells is considered in section 5-2.

This over 3-fold factor range in sensitivity (single-agent CHK1 cytotoxicity) within tumours from a common tissue of origin suggests that factors other than the tissue of origin play a role in determining sensitivity to V158411. It has been hypothesised that cancers with a defective G_1 cell cycle checkpoint will be more sensitive to CHK1 inhibitors. However, MCF7 breast cancer cells have a normal p53 phenotype and MDA-MB-231 breast cancer cells have a mutated p53 so in this case p53 status does not appear to be the main determinant of sensitivity to single-agent V158411. This is not an isogenic cell line pair so comparing the two different cell lines has to be approached with caution; experiments using isogenic-paired cell lines are considered in Chapter 5. p53 is a commonly mutated in cancer, but is only one part of the complex apparatus that is involved in the control of the G_1 checkpoint. Other components of the G_1 checkpoint control pathway may play a role in determining the sensitivity of cells to CHK1 inhibitors. Other potential determinants of sensitivity to CHK1 inhibitors that have been considered by other authors include Myc, Ras, ERK 1/2, MEK, JNK-p38 MAP kinase and these will be considered in more detail in Chapter 6 (Hoglund et al., 2011b, Mitchell et al., 2010a, Xia et al., 1995).

The experiment looking at the duration for which V158411 should be administered as a single agent demonstrates that the peak concentration of V158411 is the important determinant of cytotoxicity in both MCF7 and HCT116 cancer cell lines. In both cell lines, a shorter exposure to V158411 (24 hours) resulted in greater cytotoxicity than the same AUC spread over 3 or 5 days.

Most other studies with CHK1 inhibitors have not explored exposures to CHK1 inhibitors that are longer than 24 hours in clonogenic assays or considered whether the concentration of a CHK1 inhibitor or duration of exposure are the most important determinant of cytotoxicity, particularly as a single agent.

Blasina et al examined a variable length exposure to PF00477736 and gemcitabine (continuous co-exposure followed by drug-free media for a total of 96 hours) in growth inhibition (MTT) assays in HT29 cells (Blasina et al., 2008). They showed that cytotoxicity was seen with as short as an 8 hour exposure (~25% cell death) to the drugs and this increased in a linear fashion with longer exposures (12, 24 and 48 hours). In SW620 cells SAR-020106 (concentration not specified) enhanced gemcitabine (at the IC_{50}) cytotoxicity to the greatest extent if the co-exposure was for at least 48 hours (Walton et al., 2012).

Information regarding the relative importance of concentration versus duration or AUC may be relevant to the design of *in vivo* pre-clinical experiments and clinical trials. The data presented in this chapter suggests that less frequent administration of V158411 to achieve higher peak plasma concentrations may be more efficacious than frequent administration that achieves lower peak plasma concentrations. This would have to be modulated based on the toxicity seen in normal tissues with different regimens and would need to be tailored to allow normal tissues to adequately recover. All other experiments examining the cytotoxicity of V158411 either alone or in combination with cytotoxic therapy or IR have used a 24 hour exposure to V158411 rather than any longer treatments.

Disappointingly, there was no significant chemo-potentiation with either gemcitabine or cisplatin in either MCF7 or MDA-MB-231 breast cancer cell lines. In combination with cisplatin, there was a suggestion of antagonism between V158411 and cisplatin with a non-significant resistance to cisplatin in combination with V158411.

This was unexpected as the majority of studies with alternative CHK1 inhibitors have shown significant chemo-potentiation of both gemcitabine and cisplatin (as described in sections 1.11.1 and 1.11.2). Possible explanations for some of these differences perhaps lie in the type of assay (clonogenic, apoptosis or growth inhibitory), longer co-exposures in growth inhibition assays, and the type of inhibitor that was used (CHK1 or CHK1/CHK2). In all the combination studies with V158411 the data was normalised to the cytotoxicity seen with V158411 alone. It is not clear from all the studies in the literature whether the combination cytotoxicity data has been normalised to that seen with the CHK1 inhibitor alone. It is possible that some of the effects may have been the measurement of additive effects.

Blasina et al demonstrated potentiation of gemcitabine cytotoxicity in human cancer cell lines (20-fold in SW620 cells and 10-fold in HCT116$^{\text{wild type p53}}$) and CoLo205 xenografts (43% potentiated tumour growth inhibition (TGI) with 20 mg/Kg PF00477736 OD and 75% TGI with 20 mg/Kg PF00477736 BD) with the selective CHK1 inhibitor PF00477736 (Blasina et al., 2008). Studies examining the dual CHK1/CHK2 inhibitor 300 nM AZD7762 in conjunction with gemcitabine used a 24 hour co-treatment followed by a further 24 hour exposure to AZD7762 alone (Zabludoff et al., 2008). Growth was assessed using a colorimetric assay based on tetrazolium salt reduction (MTT). Recently

it has been shown that, data regarding drug sensitivity using this type of assay are different from other 96-well plate assays based on ATP content (Weinstein and Lorenzi, 2013). Neither assay truly represents cytotoxicity, and the data presented in this chapter based on clonogenic assays may more faithfully represent cell killing. Alternatively, it could be that longer exposure periods are needed to enhance the cytotoxicity of gemcitabine and cisplatin, or that an inappropriate schedule of cytotoxic and V158411 were used.

Most scheduling data with CHK1 is based on chemotherapy combinations, in particular with gemcitabine. In colony forming assays in HCT116 cells 100 nM AZD7762 caused the greatest sensitisation if given immediately after a 2 hour exposure rather than following 24 hours in drug free media (Zabludoff et al., 2008). In further studies using AZD7762 and PD-32152 the best dosing schedule was dependent on the concentration of gemcitabine used. With low concentrations of 50 nM gemcitabine greatest sensitisation (4.5 to 6-fold) was seen if 100 nM AZD7762 was delivered immediately after a 2 hour treatment with gemcitabine. However, if higher concentrations of gemcitabine were used, delayed treatment with gemcitabine gave greater (8 to 10-fold) enhancement of gemcitabine cytotoxicity (Parsels et al., 2011, Parsels et al., 2009).

Matthews et al, like ourselves, measured colony formation following a 24 hour co-exposure to a CHK1 inhibitor (100 and 300 nM XL9844) with 0 to 80 nM gemcitabine followed by 7-10 days in drug-free media, and showed chemosensitisation in all 4 cancer cell lines PANC-1 (3-fold with 300 nM XL9844), AsPC-1 (16 to 20-fold with 300 nM XL9844), SKOV-3 (6-fold with 300 nM XL9844) and HeLa (8-fold with 300 nM XL9844) tested (Matthews et al.,

2007). However, none of the cell lines used the Matthews study were the same as the ones used here, so a direct comparison cannot be made

One potential reason for the lack of gemcitabine potentiation by 50 nM or 150 nM V158411 is that in the cell lines investigated here, gemcitabine did not cause measurable cell cycle perturbation and hence inhibition of cell cycle checkpoints by V158411 would be predicted to have an insignificant effect. However, cisplatin did cause a G_2 arrest and therefore the effect of V158411 on cisplatin cytotoxicity was evaluated. Unfortunately no chemosensitisation was seen. There is mixed data in the literature regarding cisplatin potentiation by CHK1 inhibitors.

With the prototype non-specific inhibitor, UCN-01 there was potentiation of cisplatin-mediated cytotoxicity in AA8 CHO cells (3-fold) and MDA-MB-231 breast cancer cells (2-fold) treated for 2 hours with cisplatin and after a 24 hour period in drug free media with 24 hours with 50 nM UCN-01 (Bunch and Eastman, 1996, Eastman et al., 2002). However, the more specific AZD7762 (20 and 80 nM 24 hour co-treatment) failed to potentiate cisplatin-mediated cytotoxicity (clonogenic assays) and 1 μM SCH 900776 (24 hour co-treatment) failed to potentiate cisplatin-induced growth inhibition (Hoechst fluorescent assay) in MDA-MB-231 and other cell lines (Wagner and Karnitz, 2009, Montano et al., 2012).

The studies in Chapter 3 showed that IR also cause cell cycle perturbation that was reduced by V158411 and in the studies presented in this chapter V158411 did enhance IR-induced cytotoxicity. There was significant radio-potentiation in both MCF7 and MDA-MB-231 breast cancer cell lines with radiation

enhancement ratios at 2 Gy following 50 nM V158411 of 1.93 and 1.30 respectively. This is similar to the level of radio-potentiation in multiple cancer cell lines DU145 (DMF = 1.6), HT29 (DMF = 1.7), and H460 with dominant negative p53 (DMF = 1.58) treated with 100 nM of the dual CHK1/CHK2 inhibitor AZD7762 (Mitchell et al., 2010b). Further work has been performed by Yang et al using AZD7762 as a radiosensitiser in a NSCLC cancer cell line (PC14PE6) and in a xenograft model (Yang et al., 2011). In the xenograft model of NSCLC brain metastases, they demonstrated significantly prolonged median survival following IR in combination with AZD7762. Unfortunately there is no other published data using any of the other selective CHK1 inhibitors as radiosensitisers

The data from the scheduling experiments in both MCF7 and HCT116 cell lines with V158411 and IR suggest that V158411 should be administered concomitantly with the IR or after a 24 hour delay rather than 24 hours prior to IR. This is similar to the finding that treatment with 100 nM AZD7762 after IR and showed greater enhancement of radiation toxicity than before IR (Mitchell et al., 2010b).

Chapter 5 Determinants of sensitivity to CHK1 inhibitors

Our understanding of the role of p53 in carcinogenesis has evolved; it was initially thought to be an oncogene because of high expression in tumours, more recently it has been shown that the high expression of a dominant negative mutant p53 and that p53 is actually a tumour suppressor gene (Massague, 2004). As shown in Figure 1.8 it plays a key role in the DDR – signalling to cell cycle control/programmed cell death (Bouwman and Jonkers, 2012). It is activated by CHK1 and CHK2 and by ATM both directly and via CHK2. As can be seen from Table 2-1 in Chapter 2 the majority of cancer cell lines used in pre-clinical cancer research do have a mutated p53. However, the functional implications of the p53 mutation are not always known.

5.1 p53 status as a determinant of sensitivity to single agent V158411

Despite the strong rationale for CHK1 inhibitors to have the greatest effect in p53 disrupted cells there is mixed data in the literature as to whether p53 status is an important determinant for sensitivity to CHK1 inhibitors, either as single agents or in combination with conventional cytotoxic therapy. UCN-01, ICP-1, PF00477736, and AZD7762 caused significantly greater sensitisation of cells with a mutated p53 (Blasina et al., 2008, Tse et al., 2007b, Zabludoff et al., 2008, Eastman et al., 2002). However, other studies have shown that CHK1-mediated cytotoxicity is independent of p53 (Guzi et al., 2011, Hirose et al., 2001).

In studies growth inhibition assays (in which DNA content was the endpoint) 250 nM ICP-1 or 50 nM UCN-01 caused a significant, 7-fold, enhancement of cisplatin-mediated growth inhibition in MDA-MB-231 cells with mutant p53 that was not observed in MCF10A (immortalised breast epithelial cells p53 wild type) cells (Eastman et al., 2002). Similarly, in cell counting assays Blasina et al demonstrated a greater degree of sensitisation by 180, 360 and 540 nM PF00477736 administered 24 hours after 1 nM gemcitabine continuously for 96 hours and 2.5 nM camptothecin continuously for 24 hours significantly enhanced (3-fold at 24 hours) in the p53 mutated HT29 cells compared to the p53 wild type HUVEC (human umbilical vein epithelial) (Blasina et al., 2008).

Similarly radiosensitisation by AZD7762 was greater in p53 mutant cells: HT29, du145 and Mia-Paca (DMFs 1.6 to 1.7-fold) compared to p53 wild type normal fibroblasts (DMF = 1.05) and A549 cells (DMF = 1.2) (Mitchell et al., 2010b) However, in these studies the phenotype of the compared cells was very different and factors other than p53 status most likely also contributed to the differential sensitisation. More reliable data can be generated using paired isogenic cell lines that differ only in their p53 status.

The potentiation of gemcitabine (2 hour exposure, varying concentration) by 100 nM AZD7762 for 24 hours was investigated in a HCT116 cell line pair (p53 +/+ and p53 -/-) by a colony-forming assay (Zabludoff et al., 2008). While both cell lines were equally sensitive to monoagent gemcitabine, 100 nM AZD7762 caused a greater sensitisation in the p53 -/- cells compared to the wild type cells. In growth inhibition (SRB) studies SAR-020106 caused a 2.3-fold greater sensitization of gemcitabine and 4.5-fold greater sensitization of SN38 an

A2780 cells with functionally inactivated (by HPV16E6) p53 than p53 wild type A270 cells (Walton et al., 2010).

Using the same pair of HCT116 cell lines radiosensitisation (0, 2, 3, 4 and 6 Gy) by 300 nM UCN-01 continuous exposure for 3 days was dependent on p53 status in clonogenic assays (Petersen et al., 2010). In the $p53^{-/-}$ the LC_{90} was 4.6 Gy which was reduced to 3.8 Gy with UCN-01, but in the wild type cells the LC_{90} was 3.9 Gy without 3.8 Gy with UCN-01. Similarly radiosensitisation in matched H460 cells was greater than in cells with a dominant negative p53 (DMF = 1.58) compared to the wild type (DMF = 1.11). However, in U2OS with a tetracyclin-inducible dominant negative cells p53-independent radiosensitisation was seen with both 100 nM UCN-01 for 24 hours and 500 nM CEP-3891 for 24 hours (Petersen et al., 2010).

In contrast, investigations in p53-deficient U87MG-E6 glioma cell lines, that were relatively resistant to temozolomide compared to wild type U87MG controls, revealed that 25-100 nM UCN-01 for 4 days enhanced temozolomide cytotoxicity 5-fold in clonogenic assays with both cell lines (Hirose et al., 2001).

The p53 status has also been investigated with respect to cell cycle checkpoint activation. For example, 250 nM ICP-1 failed to affect the modest cisplatin-induced (20 μg/ml for 2 hours) G_2 arrest in wild type MCF10A cells but significantly attenuated G_2 arrest in the p53 mutant MDA-MB-231 cells (Eastman et al., 2002). Similarly, sequential treatment with 20 nM SN38 for 24 hours followed by 100 nM CHIR124 for 24 hours resulted in 51% of HCT116 wild type cells remaining in G_2 arrest whereas only 15% of $HCT116^{p53-/-}$ cells remained in G_2. (Tse et al., 2007b).

In light of these data with other CHK1 inhibitors, the cytotoxicity of V158411 as a single agent and in combination with gemcitabine, cisplatin and IR was assessed using clonogenic assays in 2 pairs of isogenic cell lines differing in their p53 status: one that has been used extensively in other studies with CHK1 inhibitors (HCT116) and the other, U2OS cells transfected with the R248W dominant negative p53 mutant. Following on from the flow cytometry data in section 3.6; the ability of V158411 to reduce the G_2 cell cycle fraction was assessed in the HCT116 isogenic cell line pair. V158411's abrogation of IR and cisplatin mediated G_2 arrest was also examined. The aim was to determine if the novel CHK1 inhibitor, V158411, exerted differential effects on cell cycle distribution and cytotoxicity that was dependent on the p53 status of the cells.

The aims of this chapter are:

a) To determine the cytotoxicity of single agent V158411 in paired cell lines with different p53 status.

b) To determine the chemosensitisation by V158411 of cell lines to gemcitabine and cisplatin in HCT116$^{\text{wild type p53}}$ and HCT$^{-/-\text{p53}}$ cancer cell lines.

c) To determine the radiosensitisation of cell lines by V158411 in HCT116$^{\text{wild type p53}}$ and HCT$^{-/-\text{p53}}$ cancer cell lines.

d) To determine the role of p53 status as a determinant of V158411-induced cell cycle changes following radiotherapy and cisplatin in HCT116$^{\text{wild type p53}}$ and HCT$^{-/-\text{p53}}$ cancer cell lines

5.2 Confirmation of the p53 status of HCT116 and U2OS cells

To confirm that the HCT116$^{p53-/-}$ cells with a homozygous mutation in p53 (notated p53 -/-) lacked p53 expression and that the U2OS^{p53DN} over-expressed the dominant negative mutant p53; Western blotting experiments were conducted. As shown in Figure 5-1 wild type HCT116$^{p53+/+}$ cells expressed p53 but a 1 hour exposure to hydroxyurea was not sufficient to induce expression, in contrast no p53 could be detected in lysates from HCT116$^{p53-/-}$ cells. As expected the U2OS cells transfected with the dominant negative p53 mutant expressed abundant p53 protein (Figure 5.2). However, unlike the U2OS wild type cells that showed induction of p53 and downstream p21 following exposure to IR, in the U2OS^{p53DN} cells there was no induction of p21 indicating that the pathway was non-functional.

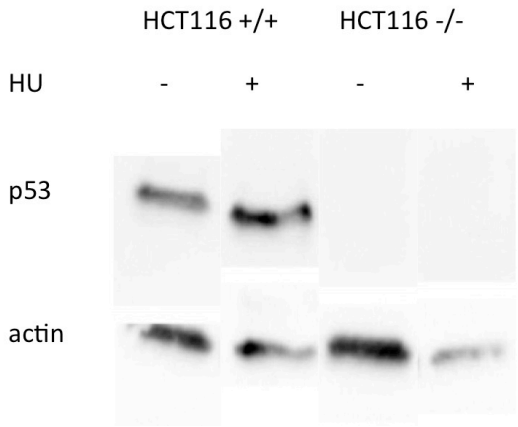

Figure 5-1 Western blot in HCT116$^{wild\ type\ p53}$ and HCT116$^{p53-/-}$ cells.

Control untreated and samples treated with 10 mM hydroxyurea for 1 hour. Expression of p53 and actin (p21 not performed). Figure courtesy of Fiona Middleton.

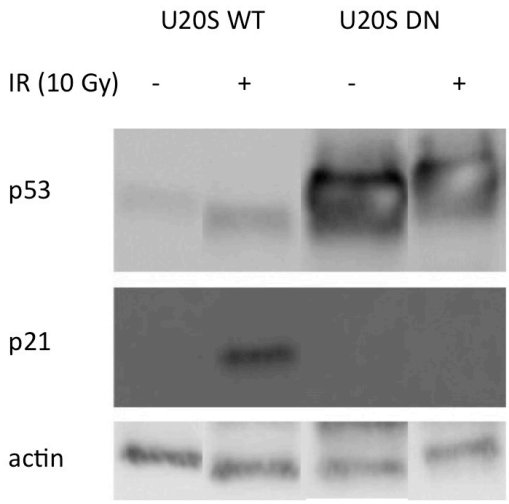

Figure 5-2 Western blot in U2OS isogenic cell line pair (wild type and p53 dominant negative).

Control untreated and samples treated with 10 Gy IR for 6 hours. Expression of p53, p21, and actin. Figure courtesy of Fiona Middleton

5.3 Single agent cytotoxicity of V158411 in the paired cell lines

Figure 5.3 shows the summary of the results of clonogenic assays with single agent V158411 in the wild type and p53-/- HCT116 cells and Figure 5.4 shows similar data obtained from the wild type and p53 dominant negative U2OS cells with a summary of the LC_{50} and the LC_{90} values given in Table 5-1. As can be seen from both the figures and the table there was no significant difference in the cytotoxicity between the wild type and p53 variant cells.

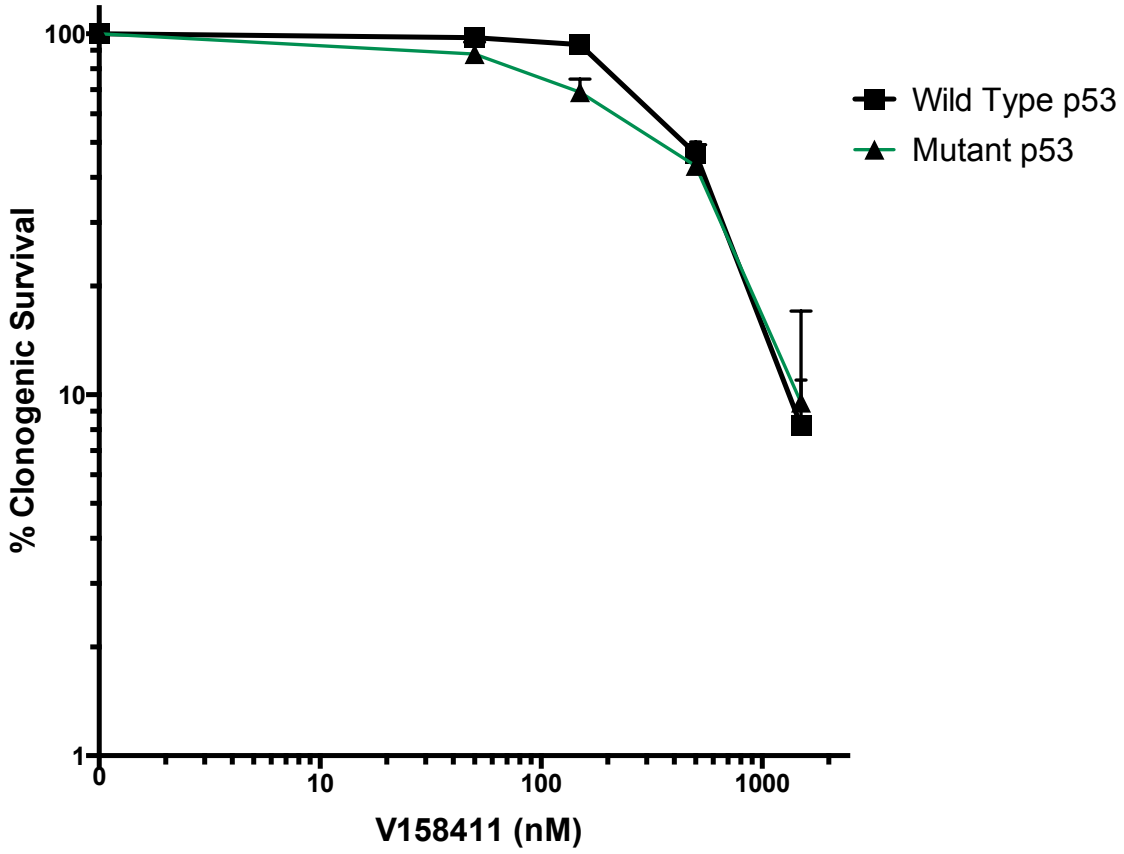

Figure 5-3 Cytotoxicity of single agent V158411 in HCT116$^{wild\ type\ p53}$ and HCT116$^{p53-/-}$ cells.

Data are mean +/- SEM of 3 independent experiments. Within each experiment there were at least 2 replicates.

Cell Line	V158411 LC_{50}: mean and (SD)	V158411 LC_{90}: mean and (SD)
HCT116 Wild Type	476.4 nM (46.2 nM)	1453 nM (n/a)
HCT116 p53 Mutant	406.0 nM (63.79 nM)	1486 nM (n/a)
U20S Wild Type	449.7 nM (1226 nM)	>1500 nM (n/a)
U2OS p53 DN	794.6 nM (n/a)	>1500 nM (n/a)

Table 5-1 LC_{50} and LC_{90} values for V158411

$HCT116^{wild\ type\ p53}$ and $HCT116^{p53-/-}$ cells and U2OS wild type and U2OS with dominant-negative p53. Mean and SD of at least 3 experiments where data is available.

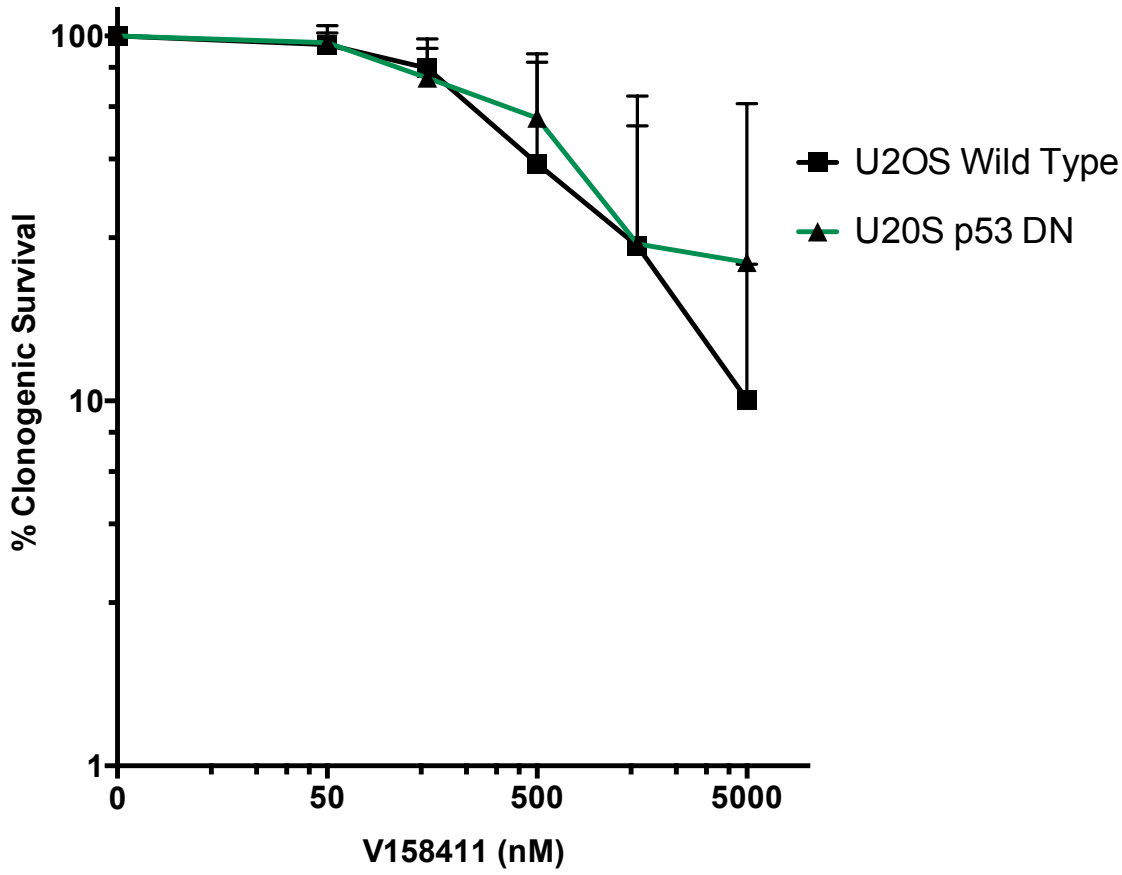

Figure 5-4 Cytotoxicity of single agent V158411 in U2OS wild type and U2OS with dominant-negative p53.

Data are mean +/- SEM of 3 independent experiments. Within each experiment there were at least 2 replicates.

5.4 p53 status as a determinant of sensitivity to gemcitabine and cisplatin

In section 4.3 there was no significant difference in the sensitivity of MCF7 (p53 wild type) or MDA-MB-231 (p53 mutated) cells to either gemcitabine or cisplatin and V158411 did not significantly potentiate the cytotoxicity of either gemcitabine or cisplatin in either cell line. However, as these cells differed in many phenotypic/genotypic respects besides their p53 status it is not possible to say if p53 status is a determinant of sensitivity or chemopotentiation

As a first step to investigating the potentiation by V158411 in the matched p53 wild type and dysfunctional HCT116 cells the cytotoxicity of gemcitabine and cisplatin was determined by clonogenic assay in these cells. In these studies the HCT116$^{p53-/-}$ cells were approximately 1.5 to 2-fold resistant to gemcitabine and cisplatin (see Table 5-2). These experiments were not replicated in the U2OS cell line pair due to time constraints.

Cell Line	HCT116$^{Wild\ Type\ p53}$: mean and (SD)	HCT116 p53 Mutant: mean and (SD)
Gemcitabine LC_{50} (nM)	4.7 (1.92)	9.2 (2.60)
Gemcitabine LC_{90} (nM)	19 (6.10)	33 (16.53)
Cisplatin LC_{50} (μM)	1.3 (3.47)	2.1 (8.04)
Cisplatin LC_{90} (μM)	16 (8.02)	28 (n/a)

Table 5-2 LC_{50} and LC_{90} values for gemcitabine and cisplatin in HCT116$^{wild\ type\ p53}$ and HCT116$^{p53-/-}$ cells.

Mean and SD values from 3 independent experiments where data available.

5.5 p53 status as a determinant of chemosensitisation by V158411

The effect of 50 nM and 150 nM V158411 on the cytotoxicity of gemcitabine and cisplatin was determined the HCT116$^{wild\ type\ p53}$ and HCT116$^{p53-/-}$ cells. V158411 did not potentiate gemcitabine or cisplatin in either cell line (Figure 5-5 and Figure 5.6).

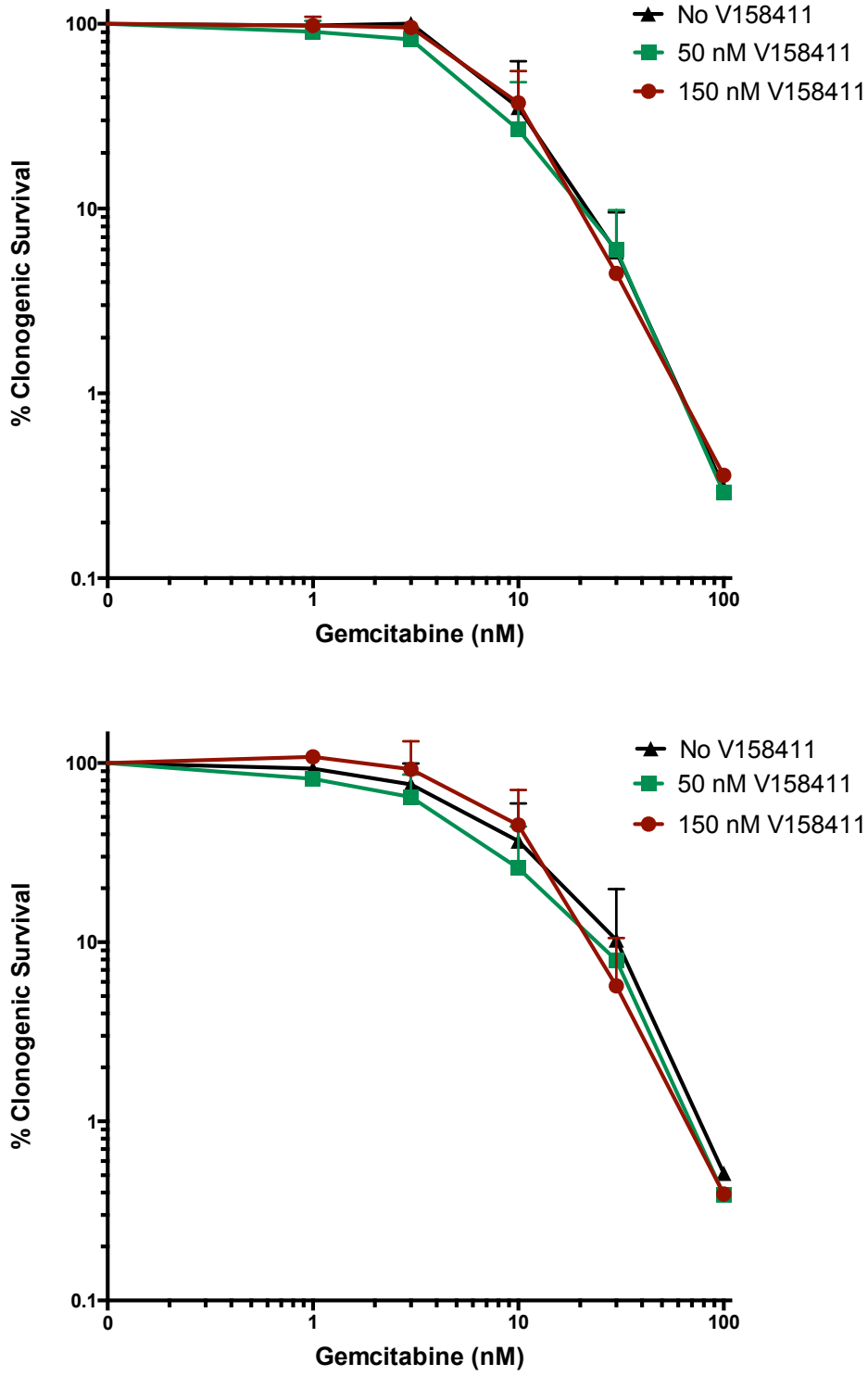

Figure 5-5 Cytotoxicity of gemcitabine +/- V158411 in HCT116$^{wild\ type\ p53}$ (upper graph) and HCT116$^{p53-/-}$ (lower graph)

Cells treated with gemcitabine alone or in combination with 50 nM V158411 or 150 nM V158411 for 24 hours. Survival normalised to DMSO or 50 nM or 150 nM V158411 alone control. Data are mean +/- SEM of 3 independent experiments. Within each experiment there were at least 2 replicates.

.

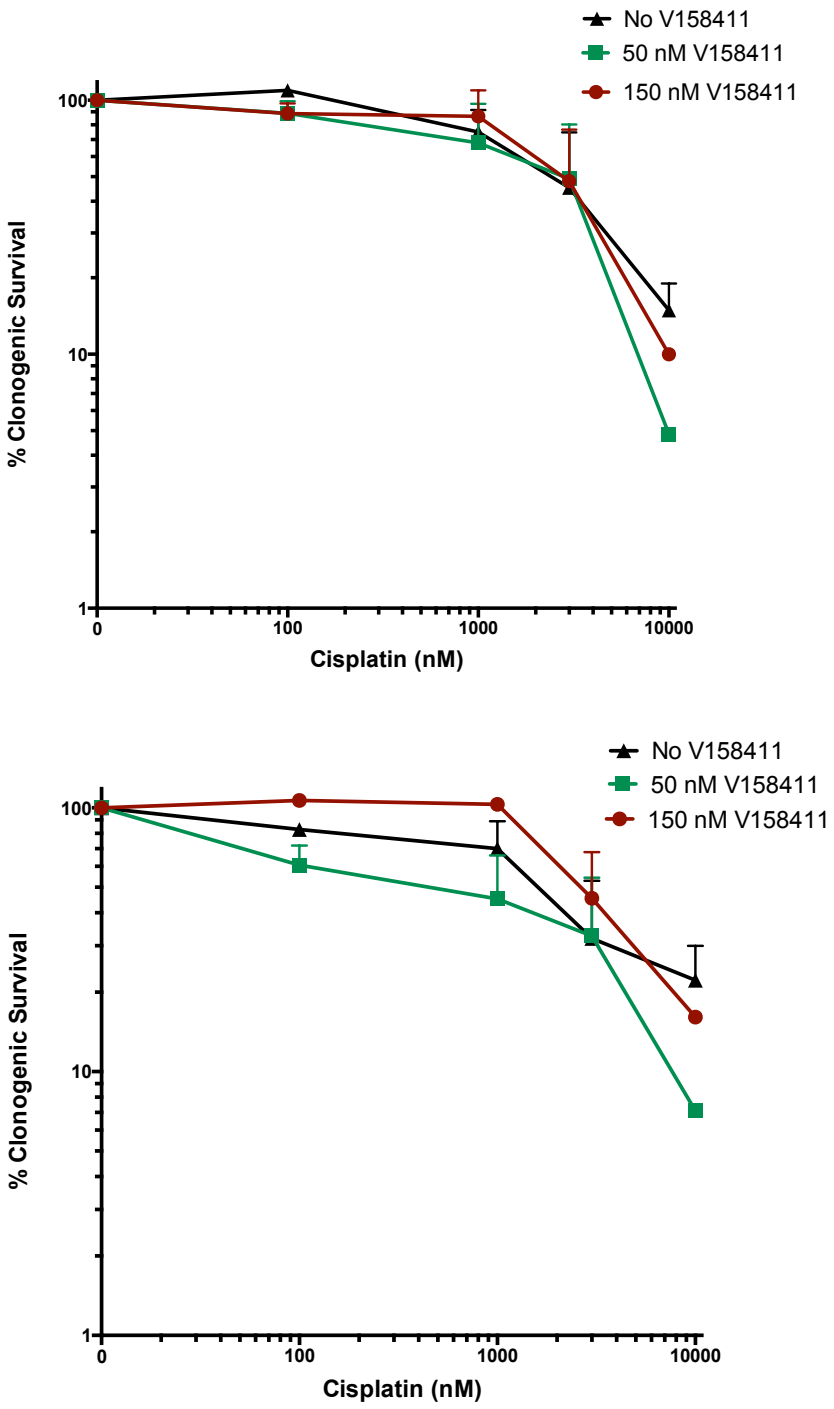

Figure 5-6 Cytotoxicity of cisplatin +/- V158411. HCT116$^{wild\ type\ p53}$ (upper graph) and HCT116$^{p53-/-}$ (lower graph)

Cells treated with gemcitabine alone or in combination with 50 nM V158411 or 150 nM V158411 for 24 hours. Survival normalised to DMSO or 50 nM or 150 nM V158411 alone control. Data are mean +/- SEM of 3 independent experiments. Within each experiment there were at least 2 replicates.

		HCT116$^{Wild\ Type\ p53}$		HCT116$^{-/-p53}$	
		LC_{50}	LC_{90}	LC_{50}	LC_{90}
Gemcitabine	No V158411	8.42 nM	27.17	7.63 nM	32.15 nM
	50 nM V158411	7.07 nM	26.14	5.65 nM	27.70 nM
	150 nM V158411	8.47 nM	26.63	9.66 nM	27.82 nM
Cisplatin	No V158411	2679 nM	n/a	2052 nM	n/a
	50 nM V158411	2905 nM	9184 nM	720.0 nM	9207 nM
	150 nM V158411	2918 nM	10000 nM	2840 nM	n/a

Table 5-3 LC_{50} and LC_{90} values of HCT116 cells

Cells treated with gemcitabine and cisplatin +/- 50 nM V158411 and 150 nM V158411. Data from at least 3 independent experiments.

5.6 p53 status as a determinant of radio-potentiation by V158411

Modest radiosensitisation with V158411 was seen in MCF7 and MDA-MB-231 cancer cell lines (see section 4-4). To determine if there was any impact of p53 status on radiosensitisation; the survival of HCT116$^{\text{wild type p53}}$ and HCT116$^{\text{p53-/-}}$ cells following irradiation with or without 50 nM or 150 nM V158411 was measured by clonogenic assay (Figure 5-7).

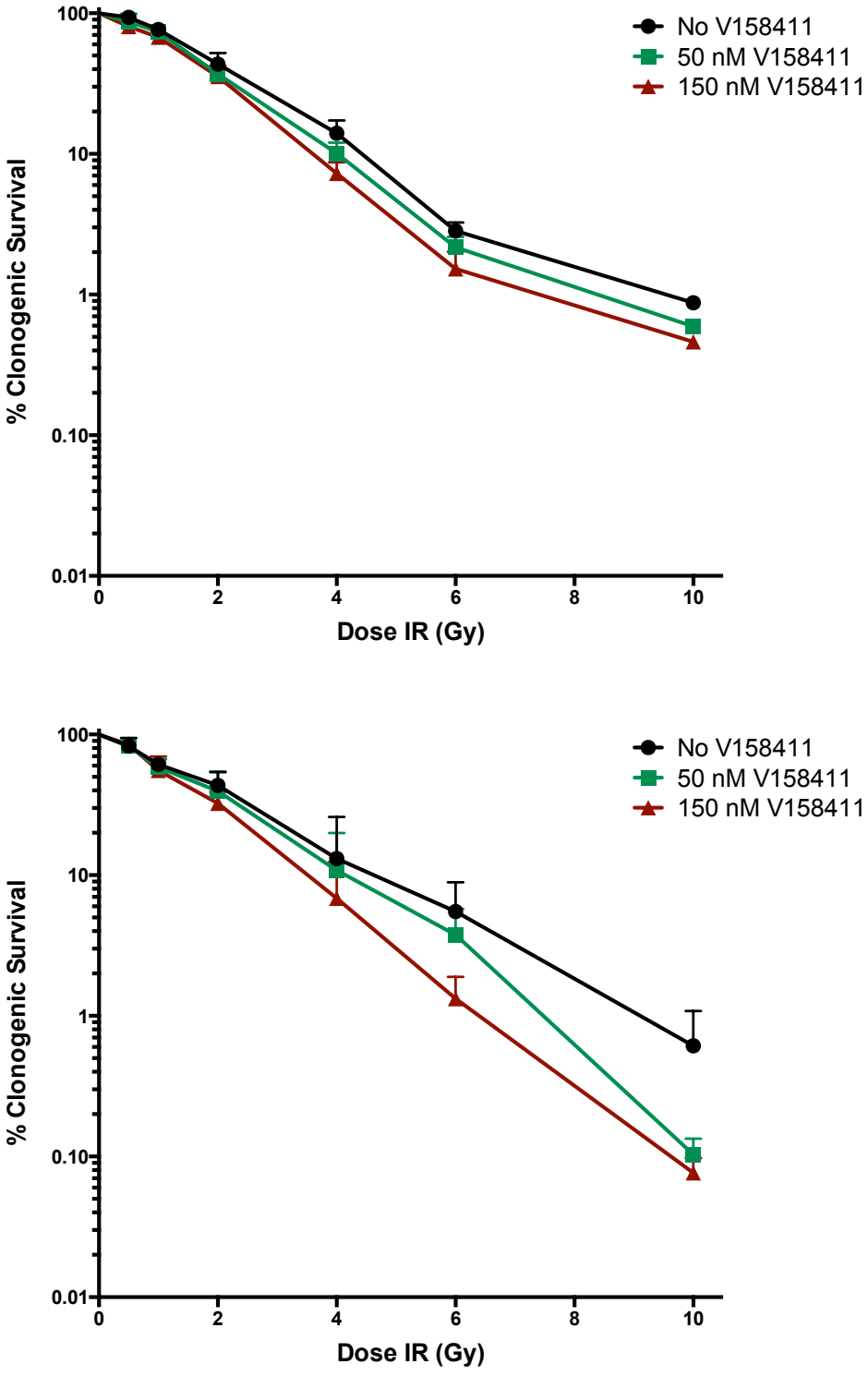

Figure 5-7 Cytotoxicity of IR +/- V158411 in HCT116$^{wild\ type\ p53}$ (upper graph) and HCT116$^{p53-/-}$ (lower graph)

Cells treated with 0-10 Gy IR alone or in combination with 50 nM V158411 or 150 nM V158411 for 24 hours. Survival normalised to DMSO or 50 nM or 150 nM V158411 alone control. Data are mean +/- SEM of 3 independent experiments. Within each experiment there were at least 2 replicates.

The HCT116$^{p53-/-}$ cells were not significantly more resistant than the HCT116$^{wild\ type\ p53}$ cells to IR alone at the LD_{50} (see Table 5-4). There was a modest sensitisation to IR by 50 nM and 150 nM V158411 in both the wild type and p53 -/- variants consistent with our previous data in unmatched cells. The extent of potentiation was similar in both wild type and p53 mutated cells.

	HCT116 Wild Type		HCT116$^{-/-p53}$	
	LD_{50}	LD_{90}	LD_{50}	LD_{90}
IR alone	1.80 Gy	4.72 Gy	1.64 Gy	4.82 Gy
IR + 50 nM V158411	1.64 Gy	4.07 Gy	1.45 Gy	4.23 Gy
IR + 150 nM V158411	1.54 Gy	3.81 Gy	1.24 Gy	3.75 Gy

Table 5-4 LD_{50} and LD_{90} values of HCT116 cells

Cells treated with IR +/- 50 nM V158411 and 150 nM V158411. Data from at least 3 independent experiments.

5.7 p53 status as a determinant of V158411-induced cell cycle changes

5.7.1 Cell cycle distribution following V158411 alone

The differences in cell cycle distribution following treatment with 150 nM V158411 alone for 24 hours was assessed in HCT116$^{\text{wild type p53}}$ and HCT116$^{\text{p53-/-}}$ cells (Figure 5-8). V158411 had no significant impact on the cell cycle distribution in either cell line (representative histograms are shown in Figure 5-9).

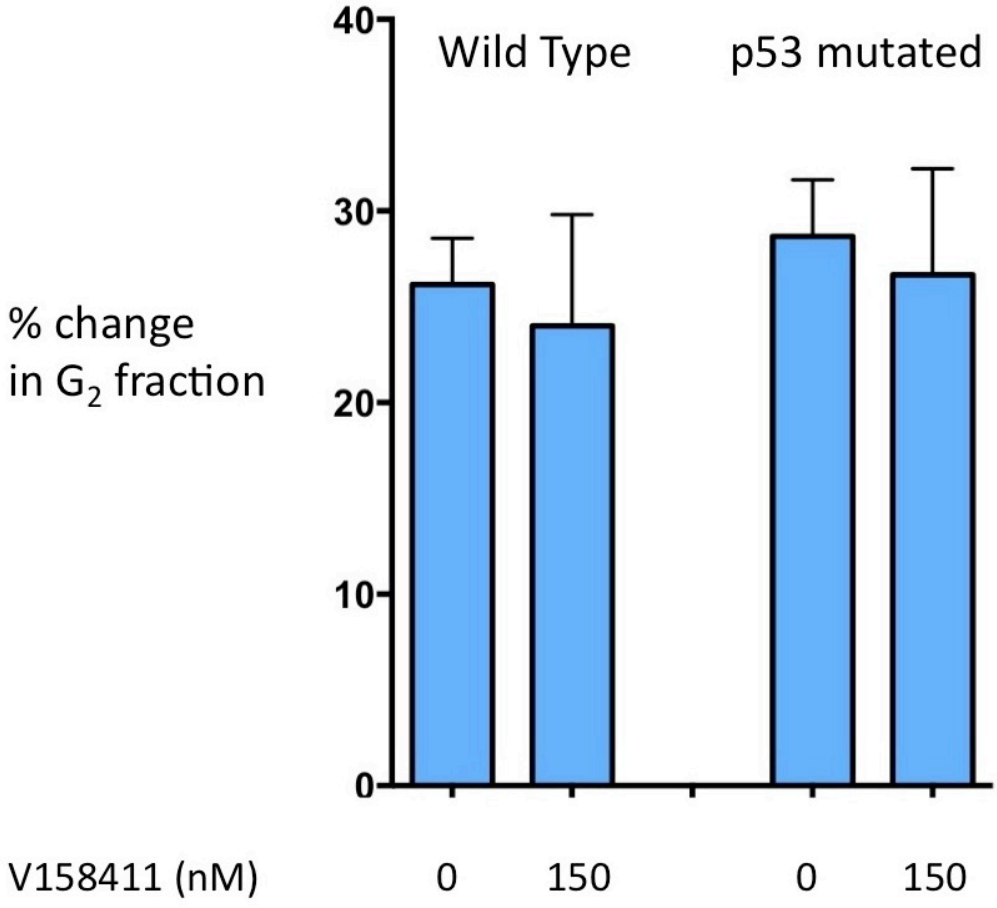

Figure 5-8 Flow cytometry in HCT116$^{\text{wild type p53}}$ and HCT116$^{\text{p53-/-}}$ cells

Untreated samples and 150 nM V158411. Data are mean +/- SEM of 3 independent experiments.

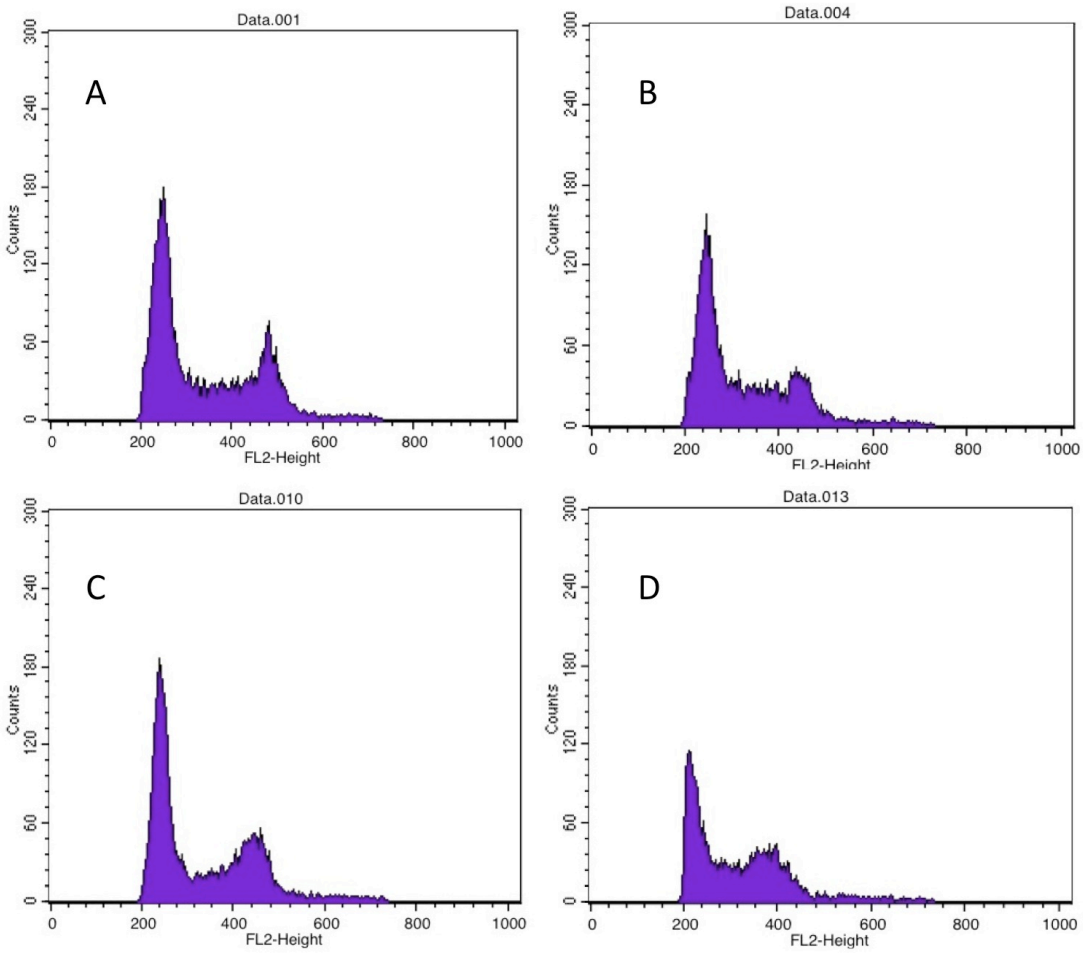

Figure 5-9 Representative example of flow cytometry in HCT116 wild type and p53 mutated cells

(A) HCT116 wild type untreated; (B) HCT116 wild type + 150 nM V158411 (24 hours); (C) HCT116 p53 mutated untreated; (D) HCT116 p53 mutated + 150 nM V158411 (24 hours). Cell line doubling time approximately 16-18 hours. Minimum of 10000 events collected for each cytogram

5.7.2 Cell cycle distribution following cisplatin or IR +/- V158411

The cell cycle distribution following treatment with 1 μM cisplatin for 24 hours or IR (24 hours after 2 Gy) with and without 150 nM V158411 co-treatment with for 24 hours was assessed in the HCT116$^{\text{wild type p53}}$ and HCT116$^{\text{p53-/-}}$ cells (Figure 5-11 and representative histograms are shown in Figure 5-10).

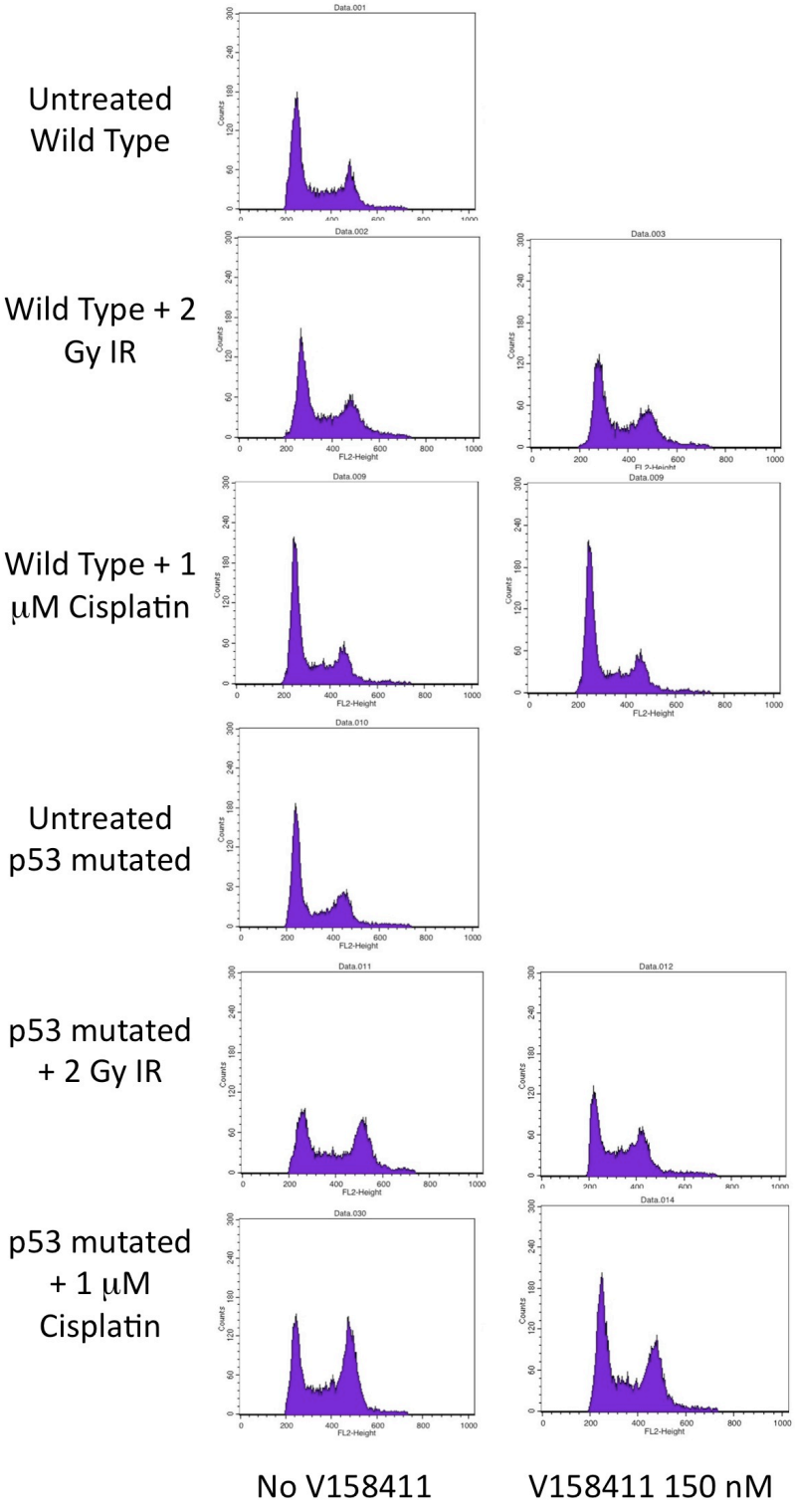

Figure 5-10 Representative example of flow cytometry in HCT116 cells

Comparison of HCT116 wild type and p53 mutated cells; untreated, and treated with 2 Gy IR (24 hours pre-analysis), 1 μM Cisplatin (24 hours) +/- 150 nM V158411 (24 hours). Cell line doubling time approximately 16-18 hours. Minimum of 10000 events collected for each cytogram

In the HCT116$^{wild\ type\ p53}$ cells, there was a small increase in the G_2 fraction following both cisplatin (significant, p = 0.029 (paired t-test)) and IR (non-significant, p = 0.129 (paired t-test)). V158411 did not change this significantly following either cisplatin or IR. However, in the HCT116$^{p53-/-}$ cells, there was a more substantial increase G_2 arrest with both cisplatin (non-significant, p = 0.08 (paired t-test)) and IR (statistically significant, p = 0.004 (paired t-test)). In these cells V158411 abrogated the cisplatin-induced G_2 accumulation (non-significant, p = 0.36 (paired t-test)) and attenuated the IR-induced G_2 arrest (non-significant, p = 0.156 (paired t-test)).

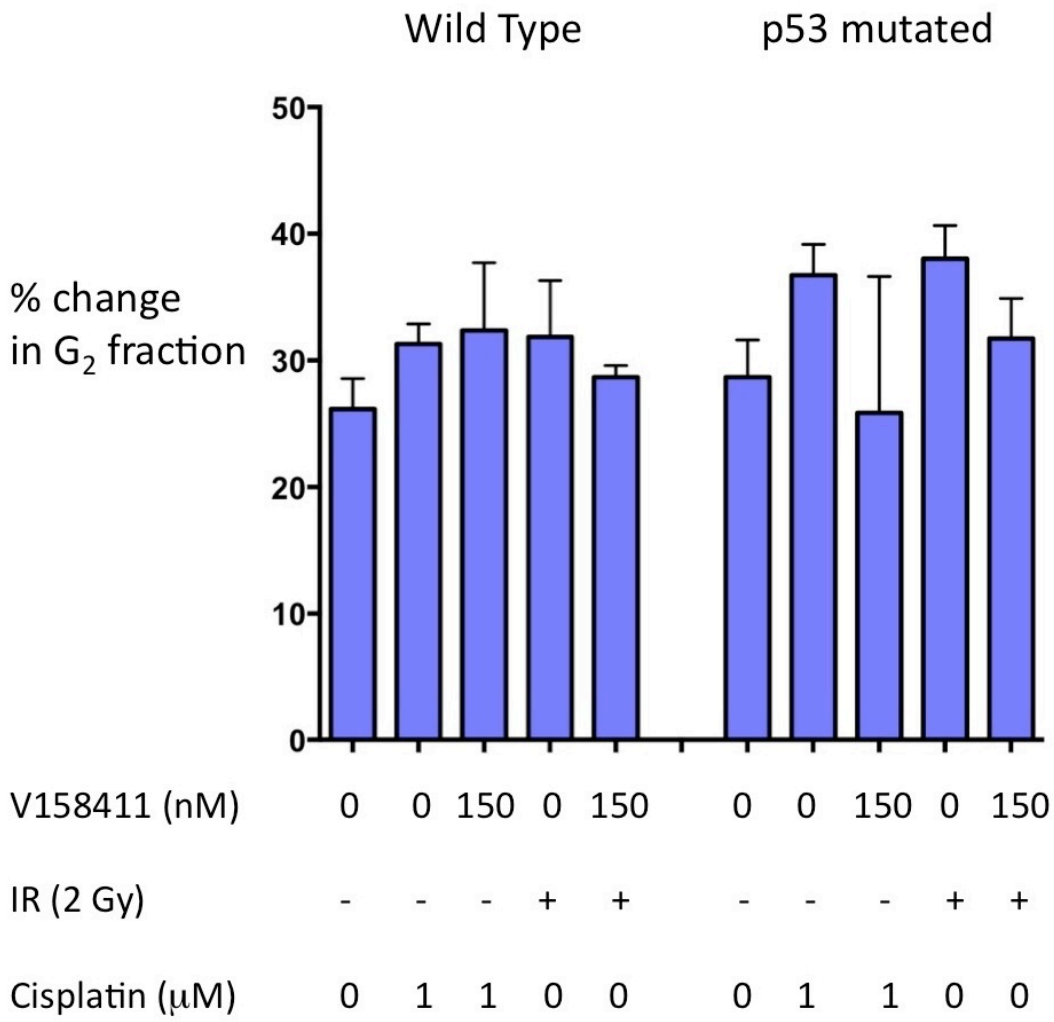

Figure 5-11 Flow cytometry in HCT116$^{wild\ type\ p53}$ and HCT116$^{p53-/-}$ cells

Untreated samples, 1 μM cisplatin and 1 μM cisplatin + 150 nM V158411; untreated samples, 2 Gy IR, and 2 Gy IR + 150 nM V158411. Data are mean +/- SEM of 3 independent experiments.

5.8 Discussion

Because of the high frequency of p53 mutations in cancer and the rationale for the selectivity of inhibitors of S/G_2 checkpoints in p53 dysregulated cancer it was important to determine if V158411 cytotoxicity and sensitisation was dependent on p53 status.

There was no difference in the cytotoxicity of single agent V158411 between $HCT116^{wild\ type\ p53}$ and $HCT116^{p53-/-}$ cells or between U2OS and $U2OS^{DNp53}$ cells, and V158411 did not impact on the cell cycle kinetics in the $HCT116^{wild\ type\ p53}$ and $HCT116^{p53-/-}$ cells. There is no published data on the impact of p53 status on the sensitivity to other CHK1 inhibitors used as single agents. It is possible that other CHK1 inhibitors have been investigated in this way, but similarly negative data have not been published.

As predicted from previously published data (El-Deiry, 2003, Ding et al., 2013), loss of p53 function conferred resistance to gemcitabine, cisplatin (and IR). In terms of chemo-resistance this was 1.5 to 2-fold, radio-resistance was not significant. As with the MCF7 and MDA-MB-231 breast cancer cell lines V158411 did not chemosensitise either $HCT116^{wild\ type\ p53}$ and $HCT116^{p53-/-}$ colorectal cancer cells to gemcitabine. Although cisplatin caused a more pronounced G_2 arrest in the $HCT116^{p53-/-}$ cells and V158411 had a greater impact on this arrest in the $HCT116^{p53-/-}$ cells it did not sensitise either cell line to cisplatin cytotoxicity. This lack of chemosensitisation is in contrast to observations with other CHK1 inhibitors (as described in the introduction). The closest study to ours was Zabludoff's demonstrating greater gemcitabine potentiation by 100 nM AZD7762 in $HCT116^{p53-/-}$ cells (15-fold potentiation) compared to $HCT116^{wild\ type\ p53}$ cells (10-fold potentiation) (Zabludoff et al.,

2008). However, in that study both cell lines were equally sensitive to single agent gemcitabine whereas we showed that the $p53^{-/-}$ cell line was less sensitive than the wild type parental cell line (LC_{50} 4.7 nM and 9.2 nM respectively) and AZD7762 is a dual CHK1/2 inhibitor.

Consistent with the data in the breast cancer cells IR caused a G_2 arrest that was attenuated by V158411, however this was only significant in the $HCT116^{p53-/-}$ cells. This was accompanied by a modest radio-potentiation with 50 nM and 150 nM V158411 in both the HCT116 wild type or HCT116 p53 mutated colorectal cancer cell lines.

Peterson et al looked at the ability in clonogenic assays (in 10 cm plate assays rather than the smaller 6 well plates used in our experiments) of UCN-01 to radio-sensitise the same $HCT116^{wild\ type\ p53}$ and $HCT116^{p53-/-}$ cells as used in our experiments (Petersen et al., 2010). They demonstrated that the $HCT116^{p53-/-}$ cells were relatively resistant to IR, but sensitised by 300 nM UCN-01 (3 day continuous exposure following IR), the LD_{90} fell from 4.6 to 3.8 Gy in the presence of UCN-01. There was no sensitisation in the $HCT116^{wild\ type\ p53}$ cells, the LD_{90} was 3.9 and 3.8 Gy in treated and untreated groups respectively.

This is in contrast to our data which showed no significant difference in the radiosensitivity of the $HCT116^{wild\ type\ p53}$ and $HCT116^{p53-/-}$ cells without a CHK1 inhibitor and similar sensitisation with both 50 and 150 nM V158411. Radiosensitisation by V158411 was not investigated by ourselves due to time constraints in the U2OS wild type and mutant p53 cells. However, in published work both 100 nM UCN-01 24 hours following IR and 500 nM CEP-3891 for 24 hours following IR caused significant radiosensitisation in both the p53 DN and

p53 wild type variants (Petersen et al., 2010). The LD_{90} was 5.2 Gy (no treatment), 4.0 Gy (UCN-01) and 3.5 Gy (CEP-3891) in the wild type cells and 5.1 Gy, 3.8 Gy and 3.4 Gy respectively in the U2OS-VP16 (p53 DN) cancer cells.

Guzi et al suggest a hypothesis in their discussion of the mechanism of action of SCH 900776 that when a CHK1 inhibitor is administered with gemcitabine the drug combination targets replication fork collapse and potentiates cytotoxicity independent of p53 status (Guzi et al., 2011). However, when a CHK1 inhibitor is administered after a delay there is potentiation of chemotherapy that in the presence of a p53 mutation, and an aberrant G_1 checkpoint, allows cells to accumulate in G_2-M with a resultant increase in cytotoxicity.

The data presented in this chapter suggests that p53 status is not an important determinant of sensitivity to single agent V158411 in either HCT116 or U2OS cells and that, as in previous chapter (with MCF7, MDA-MB-231 and HCT116 cancer cell lines), there was no chemosensitisation in either wild type or p53 mutated cell lines in combination with gemcitabine and cisplatin. This was despite the significantly greater effect of V158411 on cisplatin-induced G_2 arrest in the $HCT116^{p53-/-}$ cells compared to the $HCT116^{wild\ type\ p53}$ cells.

There was, similar radiosensitisation in both $HCT116^{wild\ type\ p53}$ and $HCT116^{p53-/-}$ cells despite the abrogation of IR mediated G_2 cell cycle arrest being greater in the mutated cell line.

The data presented in this chapter does not support the hypothesis that CHK1 inhibitors will potentiate DNA damaging agents to a greater extent in p53 dysfunctional cells. Nor does it agree with published literature that suggest p53

status is a factor. The data in this chapter suggests that other factors must play a role in determining the sensitivity of cancer cell lines to V158411 cytotoxicity. The data presented in Chapter 3 showed that a panel of cancer cell lines had a wide range of total CHK1 protein expression. The relationship between CHK1 protein expression, sensitivity to V158411 and other potential factors will be explored in Chapter 6.

Chapter 6 Dysregulation of DNA damage signalling and repair as a determinant of sensitivity to CHK1 inhibition

As has been explored in the previous chapter there is mixed evidence in both the literature and in our own data as to whether p53 plays a significant role in determining the sensitivity to CHK1 inhibitors. We wished to examine whether there were other important determinants of sensitivity to CHK1 inhibitors. It was postulated that there maybe other differences in tumour biology that could be exploited to stratify tumours for treatment with a CHK1 inhibitor either as a single agent or in combination with other small molecular inhibitors of DNA damage signalling and repair pathways.

6.1 DNA damage signalling and repair as a determinant of sensitivity to CHK1 inhibition

As described in section 1.12 both 50 nM UCN-01 and 25 nM AZD7762 were synergistically cytotoxic with the PARP inhibitor 3 μM PJ34 in a panel of breast cancer cell lines; MCF7, 4T1, SKBR3 and BT474 (Mitchell et al., 2010a). Similarly, in pancreatic cell lines (MiaPaCa-2 and MPanc-96) radiosensitisation by 100 nM AZD7762 and the PARP inhibitor (1 μM AZD2281) together was greater than either alone (Vance et al., 2011). However, a study of microarray data on 1846 breast cancer samples casts some doubt on to whether this effect is mediated by Chk1 (Daemen et al., 2012). Daeman et al initially examined the effect of AZD2281 in 22 breast cancer cell lines and identified 5 genes whose transcript levels were associated with resistance to AZD2281 and 2 genes which were associated with sensitivity. They validated these genes in with the

data from Affymetrix microarrays in the 1846 breast cancer patients. One of the genes identified as marker of sensitivity to a PARP inhibitor was *CHEK2*. AZD7762 is a dual CHK1 and CHK2 inhibitor so the synergy seen with a PARP inhibitor may be mediated by CHK2 rather than CHK1.

Mutations in the Ras-MEK-ERK pathway may affect the sensitivity of tumours to CHK1 inhibitors. Dai et al looked at the combination of a CHK1 inhibitor (150 nM UCN-01) and a MEK1/2 inhibitor (10 μM PD184352) in myeloma (8226, H929 and U266) cancer cell lines and showed a marked increase in cell death in combination compared to single agent UCN-01 (Dai et al., 2008). The authors measured using flow cytometry apoptotic cells by Annexin V staining and showed an increase in U266 cells from 11% with UCN-01 alone to 82% in combination with PD184352; in 8226 cells the increase was from 7% to 85% respectively. The combination also induced apoptosis in doxorubicin, melphalan and dexamethasone-resistant variants of the 8226 cells (8226/Dox40 8226/LR5 and MM.1R respectively).

In normal thyroid cells (quiescent WRT cells) the acute expression of activated Ras increased CHK1^{serine345} phosphorylation more than 5-fold (Abulaiti et al., 2006). Ras activation is common in thyroid malignancies suggesting that single agent CHK1 inhibitors may be of utility in thyroid tumours associated with Ras activation. Such a therapeutic strategy was taken forward by Gilad et al who demonstrated that ATR inhibition (by shRNA) was synthetically lethal in cell lines with oncogenic Ras expression (murine embryonic fibroblasts transformed with the introduction of oncogenic Ras by shRNA) (Gilad et al., 2010). The authors confirmed activation of the ATR pathway by oncogenic Ras as evidenced by increased CHK1^{serine345} phosphorylation. However, the authors do

sound a note of caution as they demonstrated that with only limited reduction in ATR activity (ATR haploinsufficiency) there was in fact tumour promotion in stark contrast to the synthetic lethality seen with more significant ATR inhibition.

There is evidence that CHK1 inhibitors may be of use as single agents in tumours with amplified Myc. CHK1 is up-regulated in myc-amplified (c-Myc) murine and human lymphomas (Hoglund et al., 2011a). A mouse model of the ATR-Seckel syndrome was noted to block the induction of c-Myc-induced lymphomas and pancreatic tumours (Murga et al., 2011). The authors went on to show that 5 mg/kg UCN-01 (i.p.) daily led to significant regression of murine myc-induced lymphomas and human Burkitt's lymphoma cell lines. The response to UCN-01 was proportional to the expression of the c-myc protein.

Both AZD7762 and PF00477736 have been shown to be cytotoxic in *in vitro* assays as single agents in c-Myc-amplified lymphomas (Hoglund et al., 2011b, Ferrao et al., 2011). However, this may potentially be due to CHK2 rather than CHK1. AZD7762 is a dual inhibitor of CHK1 and CHK2; Hoglund et al showed that CHK2 may be regulated by c-Myc though the mechanism is not fully understood (Hoglund et al., 2011b).

Similarly, CCT244747 had anticancer activity against N-myc-amplified neuroblastomas in transgenic mice (Walton et al., 2012). In TH-MYCN mice 7 days of continuous oral administration of 100 mg/kg CCT244747 showed a 79% reduction by volume in the growth of tumours compared to mice treated with vehicle alone ($p < 0.001$). The potential utility of CHK1 inhibitors in the treatment of neuroblastoma is supported by an alternative approach by Cole et al (Cole et al., 2011). They performed a loss-of-function screen of the protein

kinome in neuroblastoma and showed that out of 30 kinases that showed significant cytotoxicity that the loss of CHK1 function gave the greatest cytotoxicity (greater than 50% growth inhibition in all 4 neuroblastoma cell lines tested compared to no growth inhibition in immortalised neuronal cells (hTERT-RPE-1) even with more than 98% mRNA and protein depletion). They went on to show that compared to control cell lines neuroblastoma cells were sensitive to two novel CHK1 inhibitors SB21807 and TCS2312 (IC_{50} of 564 nM and 548 nM) respectively. The sensitivity of neuroblastoma cell lines to CHK1 inhibition correlated with MYC(N) protein levels and that CHK1 inhibition in neuroblastoma cells was associated with apoptosis in S phase.

In a search for alternative regulators of DNA damage response it has been noted that CHK2 is phosphorylated at threonine^{68} by DNA-PKcs and that CHK2 co-immunoprecipitates with Ku70 and Ku80 (Li and Stern, 2005). Using siRNA targeting DNA-PKcs Khanna and colleagues were able to demonstrate that DNA-PKcs is a direct activator of CHK1 via phosphorylation at serine^{345} (Khanna et al., 2013). There is also a link between CHK1 and Myc, and this too has been explored by Khanna and colleagues and reveals DNA-PKcs to be key here too (Khanna et al., 2013). The authors demonstrated that inhibiting CHK1 (using the small molecular inhibitors SB218078 or GO6796 or with siRNA) in cancer cell lines induced the tumour suppressor protein phosphatase protein phosphatase 2A (PP2A). PP2A dephosphorylates MYC at serine^{62} which downregulates MYC activity and leads the cancer cell down a pro-apoptotic route. CHK1 appears to regulate PP2A by decreasing the transcription of cancerous inhibitor of PP2A (CIP2A). A graphic of the proposed mechanism is shown in figure 6.1.

Inhibition of Claspin by siRNA also inhibited CIP2A expression (see Figure 3-1). The authors also showed that PF00477736 decreased the growth of neuroblastoma tumours and that this was associated with a 45% decrease in the expression of CIP2A. The authors showed that constitutive CHK1^{serine345} phosphorylation and CHK1-mediated transcriptional regulation of CIP2A was independent of the ATR/ATM pathway.

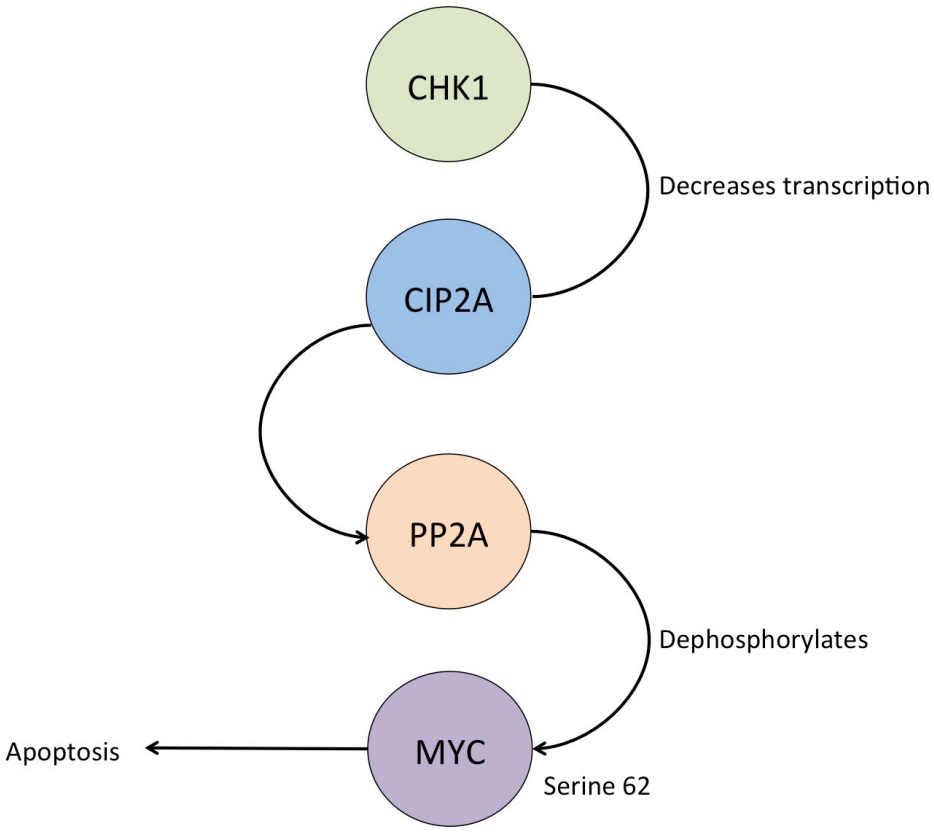

Figure 6-1 CHK1-CIP2A-PP2A-MYC pathway.

The relationship between CHK1 and MYC via CIP2A and PP2A. Pathway proposed by Khanna et al., 2013

DNA-PKcs (DNA-dependent protein kinase catalytic subunit) has an extensive role in DSB repair by NHEJ (Shrivastav et al., 2008, Serrano et al., 2013, Takata et al., 1998). DNA-PKcs deficient cells are hypersensitive to agents that

cause DNA DSBs including IR (Shao et al., 1999, Allalunis-Turner et al., 1995, Durocher and Jackson, 2001).

DNA-PKcs also appears to play a role in replication protein A (RPA) phosphorylation. RPA is a single strand binding protein that is involved in DNA repair and replication. It is critical to the recruitment and activation of ATR to single stranded DNA. There are a series of complex priming events that occur with phosphorylation of multiple sites on RPA, leading to activation of the downstream ATR-CHK1 pathway in response to replication stress (Serrano et al., 2013). Mutation or inhibition of DNA-PKcs (with 40 μM NU7026 for 2 hours) or mutation in RPA phosphorylation sites in UM-SCC-32 (human squamous cell carcinoma) cells led to a failure to arrest in G_2 and accumulation in mitosis following replication stress (stimulated by 100 μM etoposide for 2 hours) (Liu et al., 2012).

DNA-PKcs is also an important regulator of the DNA damage response to reactive oxygen species. DNA-PKcs has been implicated in the response to reactive oxygen species by regulating DNA repair via p53, HIF-1α and via AKT both NF-κB and HIF-1α (Chen et al., 2012). There is also cross-talk with ATM as described in Figure 6-2.

With this additional evidence for the key role of DNA-PK, we can adapt the pathway diagram (Fig 1-11) originally proposed in the introduction to include DNA-PKcs signalling to CHK1, CHK2, ATM and RPA (see Figure 6.2).

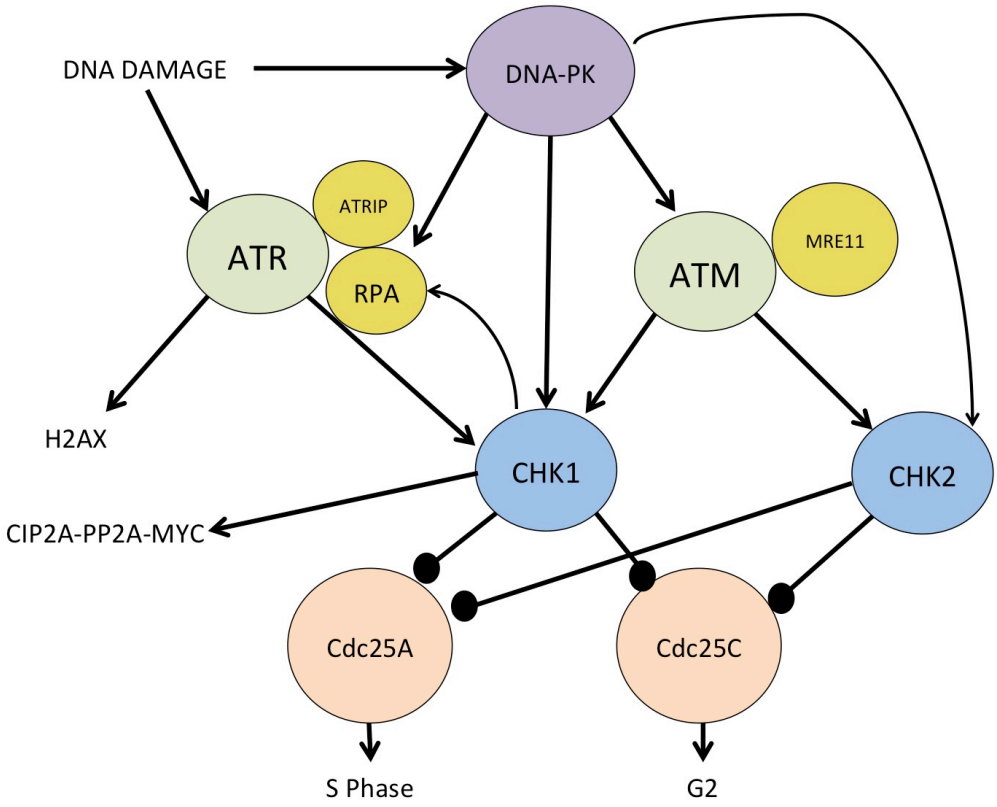

Figure 6-2 ATR/ATM-CHK1 pathway including the role of DNA-PKcs.

The role of DNA-PKcs and its postulated relationship with DNA damage, ATR, ATM, CHK1 and CHK2. Arrows denote activation and ball-ended-bars denote inhibition

There are a number of different approaches that could be deployed to identify determinants of sensitivity to CHK1 inhibitors as single agents. V158411 could be used in combination with small molecular inhibitors of potential pathways, V158411 could be evaluated in an siRNA synthetic lethality screen or V158411 could be used as a single agent in panels of cell lines with specific defects in DNA damage response pathways. We adopted the latter strategy and looked at V158411 in Chinese hamster ovary cells and Chinese lung fibroblasts and human cancer cell lines with known defects in DNA damage response pathways.

The aims of this chapter are:

a) To explore the sensitivity of a panel of Chinese hamster cells with known DDR defects to single agent V158411.

b) To explore the sensitivity of paired DNA-PKcs proficient and defective glioblastoma (M059J) cell lines to single agent V158411.

c) To explore differences in CHK1 and DNA-PKcs mRNA in publically available libraries of paired normal and tumour tissue samples.

d) To determine the sensitivity of a panel of liver cell cancers to V158411 +/- the DNA-PKcs inhibitor NU7441

e) To explore the expression of CHK1 and DNA-PKcs in a panel of liver cancer cells and the possible correlation with cytotoxicity to V158411.

6.2 Exploration of potential determinants of sensitivity in Chinese hamster ovary cells (CHO) and Chinese hamster lung fibroblasts (CHLF)

As a means of determining the potential for elements of the DNA damage response pathway to predict sensitivity to single agent V158411; its cytotoxicity in CHO cells and lung fibroblasts (CHLF) was examined. The parental CHO cell line are AA8 cells, V3 cells are deficient in NHEJ due to inactivation of DNA-PKcs, EM9 cells deficient in BER due to loss of XRCC1, and XRS-6 cells also lack NHEJ function due to Ku80 deficiency. VC8 CHLF cell line is defective in HRR due to a mutation in BRCA2 and the VC8-B2 cell line is proficient in HRR due to repair of this defect.

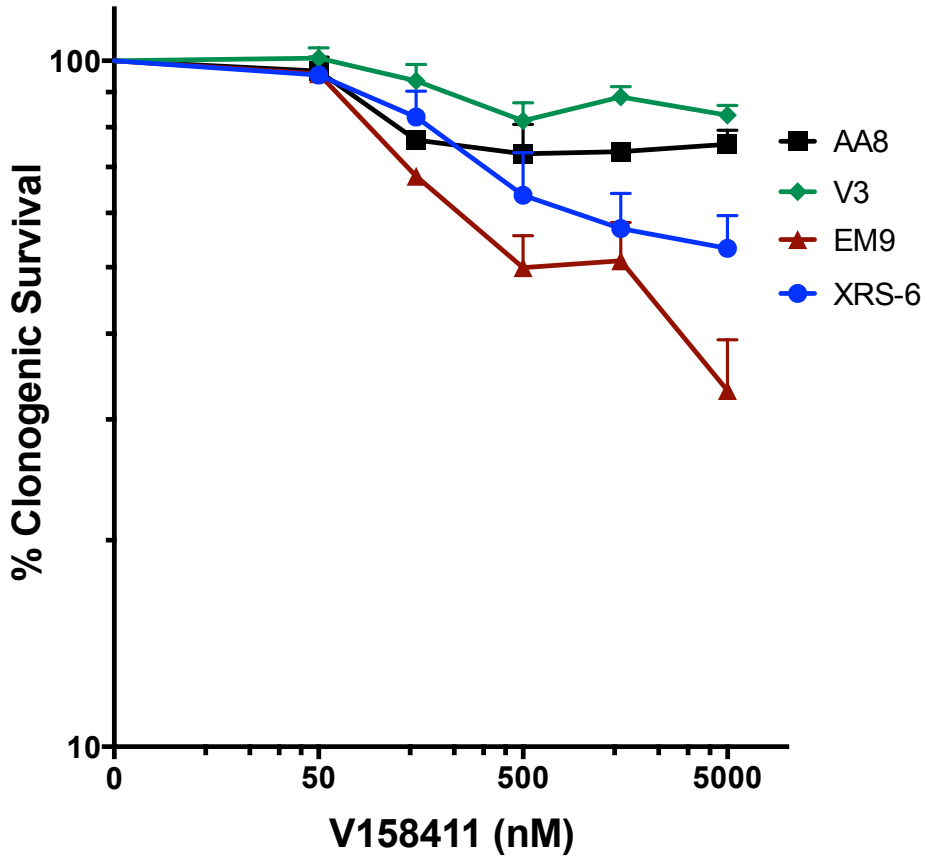

Figure 6-3 Clonogenic cytotoxicity assay in CHO cells.

V158411 in panel of CHO (p53 mutated) cells (AA8 (black), V3 (green), EM9 (red) and XRS-6 (blue)). Data are mean +/- SEM of 3 independent experiments. Within each experiment there were at least 2 replicates.

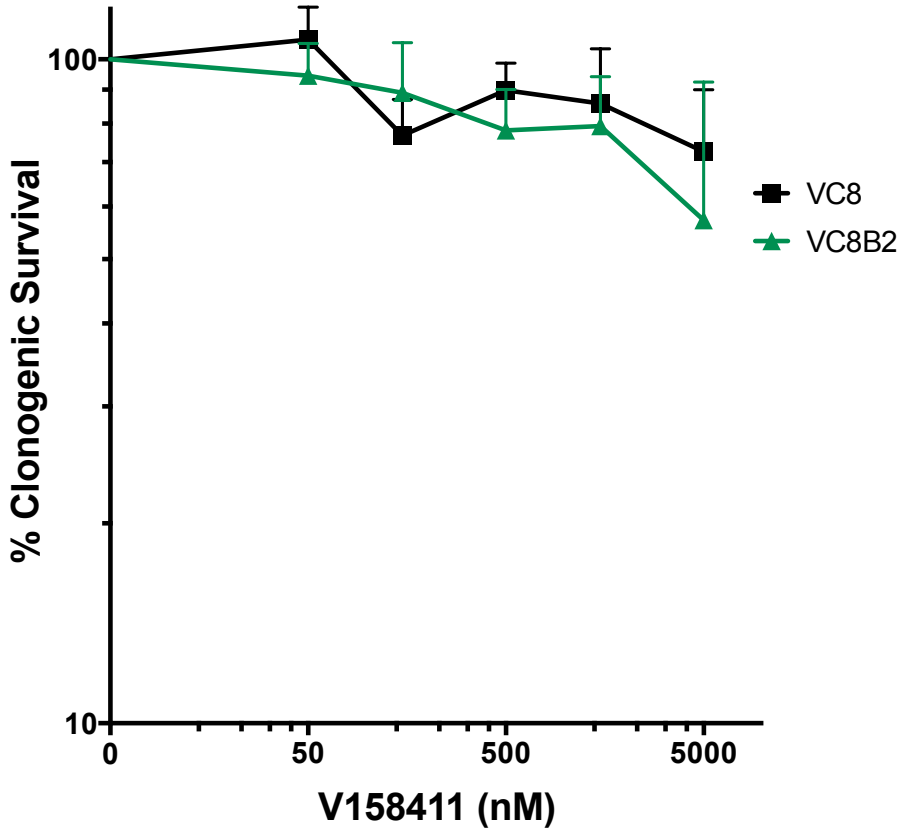

Figure 6-4 Clonogenic cytotoxicity assay CHLF cells.

V158411 in panel of Chinese lung fibroblast (p53 wild type) cells (VC8 (black) and VC8-B2 (green)). Data are mean +/- SEM of 3 independent experiments. Within each experiment there were at least 2 replicates.

Figure 6-3 shows the clonogenic survival of CHO cells exposed for 24 hours to single agent V158411 and Figure 6-4 the clonogenic survival in CHLF. In comparison to the human cell lines the Chinese hamster cells were resistant to V158411 with survival at 1 μM in the range 50.5% to 85.1%, compared to <10% in the human cancer cells (see figure 4-1 and table 4-1). BER-defective EM9 cells with an LC_{50} of 500 nM were significantly more sensitive than the parental AA8 cells ($p < 0.0001$, 2-way ANOVA). Surprisingly, although NHEJ defective, Ku80 mutant XRS-6 cells were more sensitive than the AA8 cells, this was not statistically significant (2-way ANOVA). The NHEJ defective, DNA-PKcs mutant

V3 cells were significantly resistant to V158411 ($p = 0.0027$, 2-way ANOVA). The only cell line with an LC_{50} of < 5 μM was the EM9 cell line, deficient in XRCC1, with an LC_{50} of 508 nM (Table 6-1). There was no statistically significant difference in the sensitivity of the HRR defective and HRR proficient CHLF cell lines VC8 and VC8-B2 to V158411.

Cell Line	V158411 LC_{50}	Survival at 1 μM V158411
AA8	>5 μM	73.5%
V3	>5 μM	85.1%
EM9	508 nM	50.5%
XRS-6	>5 μM	60.3%
VC8	>5 μM	87.8%
VC8-B2	>5 μM	78.8%

Table 6-1 LC_{50} values and estimated survival with 1 μM V158411 in CHO and CHLF cell lines.

LC_{50} not met within dose range of 50-5000 nM V158411 in 5 cell lines so stated as >5 μM.

6.3 V158411 in M059J glioblastoma cell line

In view of the curious resistance of the DNA-PKcs defective V3 cells, the cytotoxicity of V158411 was evaluated in another pair of DNA-PKcs proficient and deficient human cancer cells. The M059J cell line is a glioblastoma-derived cell line with a known defect in DNA-PKcs. The M059J-Fus1 cell line has had a functional DNA-PKcs restored by transfer of chromosome 8. This has been confirmed by western blotting for total DNA-PKcs and activated pDNAPK^{ser2096} following 10 Gy ionising radiation (Figure 6-5). In a clonogenic survival assay M059J cells with a LC_{50} of 823 nM were significantly more resistant to single-agent V158411 than M059J-Fus1 cells (LC_{50} = 89.5 nM; p = 0.03 (paired t-test)), (Figure 6-6). (Table 6-2). It should be noted that c-Myc is also on chromosome 8 and increased expression of cMyc could have contributed to the sensitivity, so these experiments were repeated using co-incubation with a DNA-PKcs inhibitor.

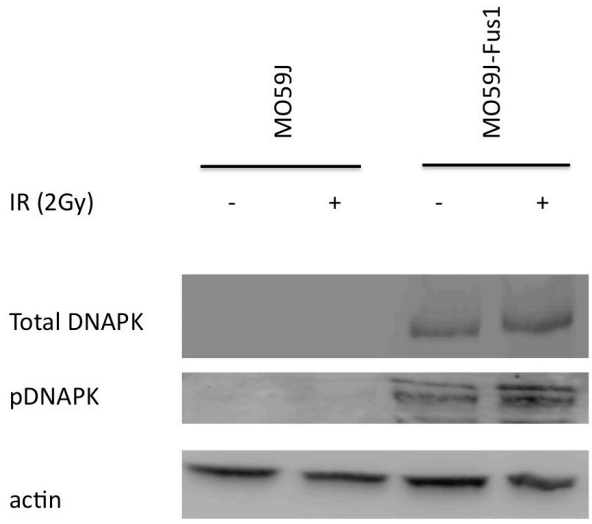

Figure 6-5 Western blot in M059J and M059J-Fus1 cell line +/- 10 Gy ionising radiation.

M059J (p53 mutated, DNA-PKcs deficient) and M059J-Fus-1 (p53 mutated, DNA-PKcs corrected).

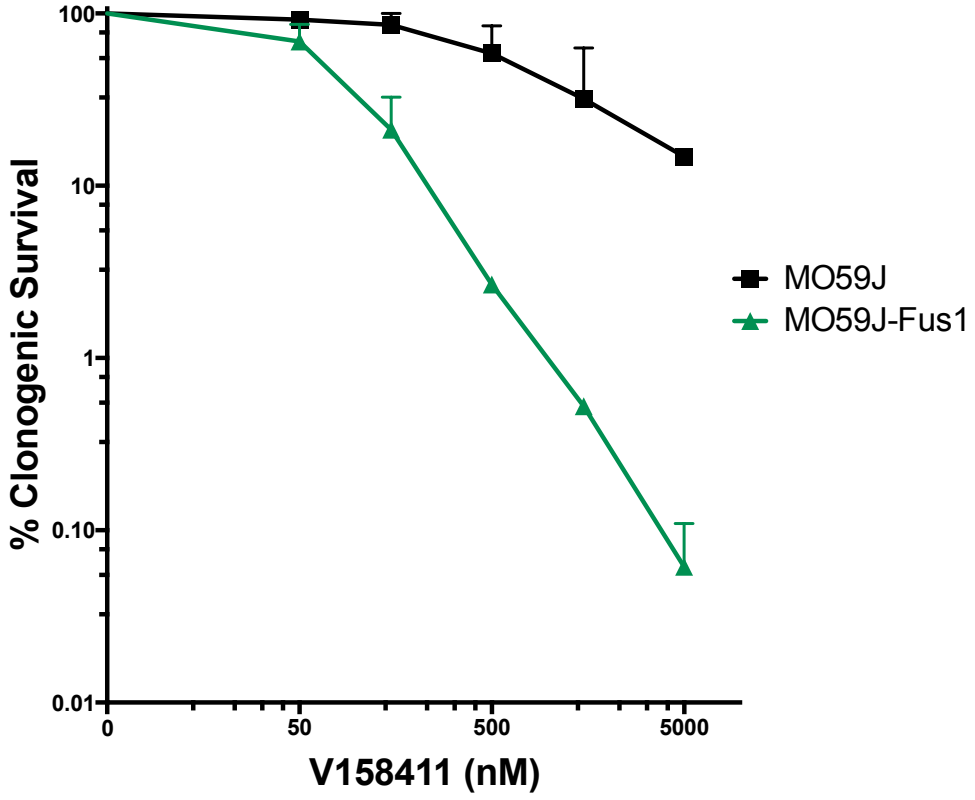

Figure 6-6 Clonogenic cytotoxicity assay in M059J cells.

V158411 in M059J (black) and M059J-Fus1 (green) cell line. M059J (p53 mutated, DNA-PKcs deficient) and M059J-Fus-1 (p53 mutated, DNA-PKcs corrected).Data are mean +/- SEM of 3 independent experiments. Within each experiment there were at least 2 replicates.

6.3.1 V158411 with the DNA-PKcs inhibitor NU7441

To further explore the role of DNA-PKcs in determining the sensitivity of M059J cells to V158411. V158411 was used in combination with the DNA-PK inhibitor NU7441 (1 μM) in clonogenic assays. Figure 6-7 summarises the results of these experiments. NU7441 had no effect on the sensitivity of M059J cells lacking DNA-PKcs to V158411. However, in the M059J-Fus1 cells with functional DNA-PKcs NU7441 significantly increased resistance to V158411 (p

= 0.0002 2 way ANOVA) and caused an approximate 2-fold increase in the LC_{50} and LC_{90} of V158411 (Table 6-2).

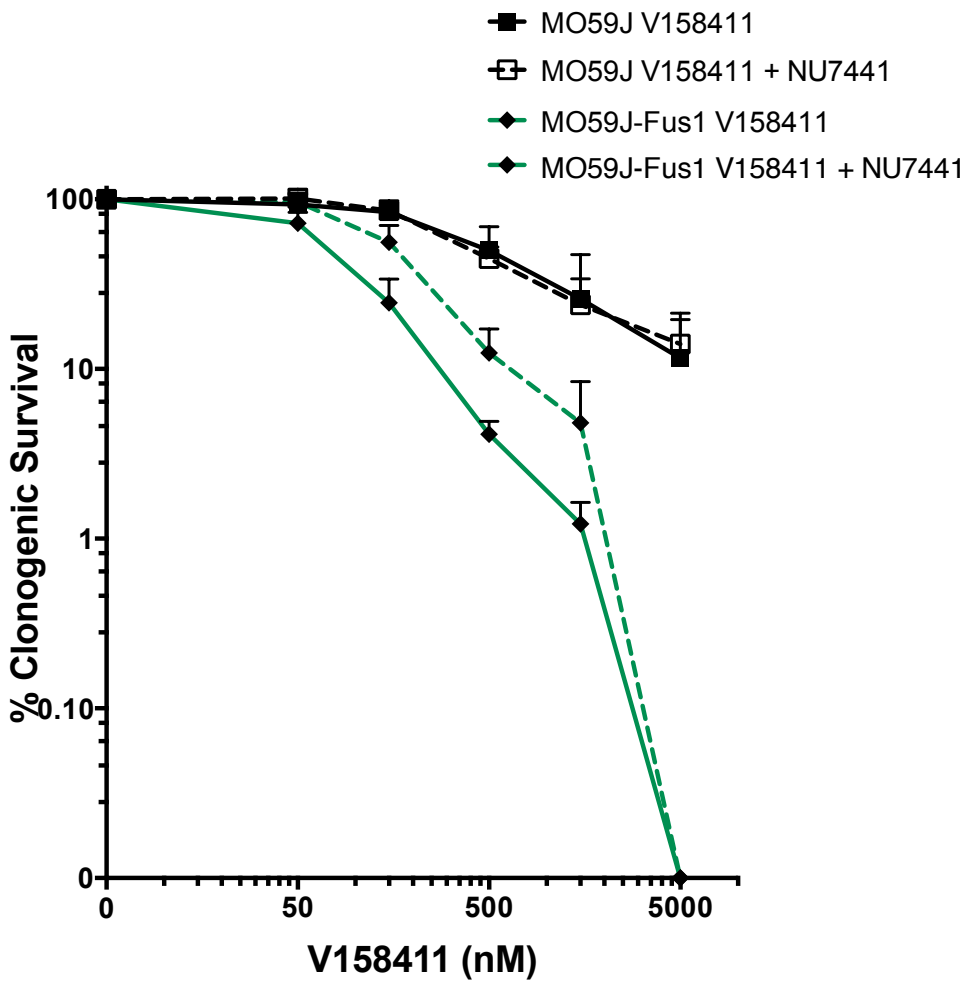

Figure 6-7 Clonogenic cytotoxicity assay with V158411 +/- NU7441.

V158411 +/- NU7441 1 mM in M059J (black) and M059J-Fus1 (green) cell line. M059J (p53 mutated, DNA-PKcs deficient) and M059J-Fus-1 (p53 mutated, DNA-PKcs corrected). Data are mean +/- SEM of 3 independent experiments. Within each experiment there were at least 2 replicates.

Drug	M059J LC_{50}	M059J LC_{90}	M059J-Fus1 LC_{50}	M059J-Fus1 LC_{90}
V158411	823.0 nM	1498 nM	89.5 nM	417.5 nM
V158411 + NU7441	455.0 nM	>5000 nM	196.5 nM	817.1 nM

Table 6-2 LC_{50} and LC_{90} values of V158411 +/- 1 μM NU7441 in M059J and M059J-Fus1 glioblastoma cancer cell lines

M059J (p53 mutated, DNA-PKcs deficient) and M059J-Fus-1 (p53 mutated, DNA-PKcs corrected).

6.3.2 A comparison of V158411, PF00477736 and AZD7762 in M059J cells

To determine whether the effect seen in the M059J and M059J-Fus1 cells was unique to V158411 or a class effect of CHK1 inhibitors, the clonogenic survival of the cells V158411 was compared to two commercially available CHK1 inhibitors, the selective CHK1 inhibitor PF00477736 and the CHK1/CHK2 inhibitor, AZD7762 (Figure 6-8 and

Table 6-3).

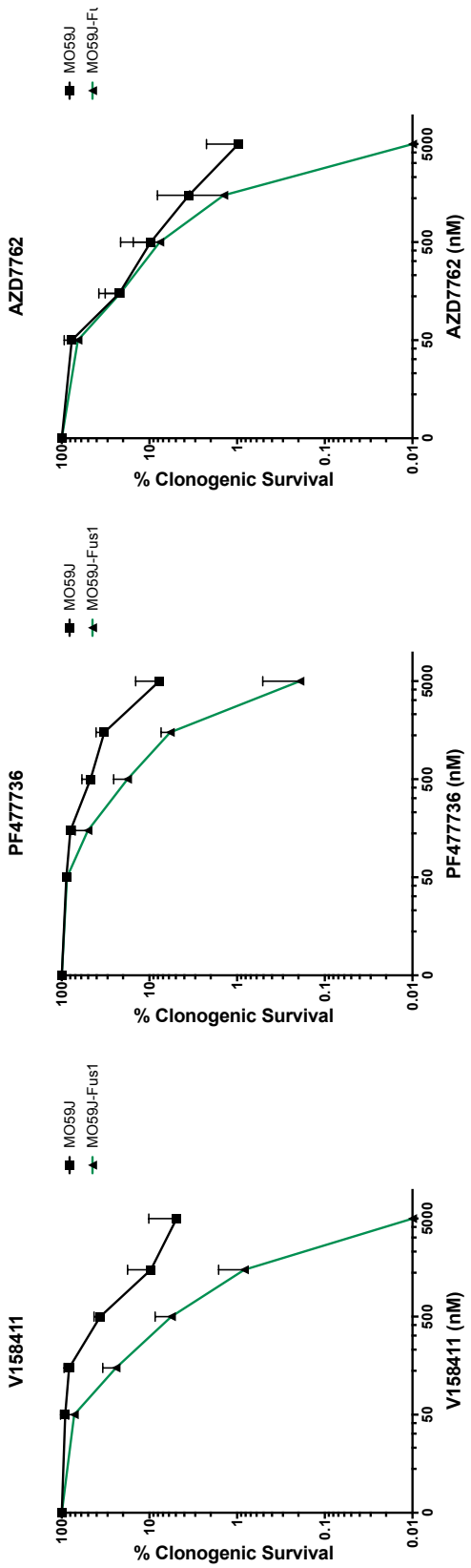

Figure 6-8 Clonogenic cytotoxicity assay with panel of CHK1 inhibitors.

V158411 in M059J (black) and M059J-Fus1 (green) cell line. PF477736 in M059J and M059J-Fus1 cell line. AZD7762 in M059J and M059J-Fus1 cell line. M059J (p53 mutated, DNA-PKcs deficient) and M059J-Fus-1 (p53 mutated, DNA-PKcs corrected). Data are mean +/- SEM of 3 independent experiments. Within each experiment there were at least 2 replicates.

Drug	M059J LC_{50}	M059J LC_{90}	M059J-Fus1 LC_{50}	M059J-Fus1 LC_{90}
V158411	396.9 nM	1498 nM	96.37 nM	417.5 nM
PF00477736	471.5 nM	4684 nM	155.9 nM	1153 nM
AZD7762	99.18 nM	497.5 nM	85.45 nM	441.3 nM

Table 6-3 LC_{50} and LC_{90} values with panel of CHK1 inhibitors.

V158411, PF00477736 and AZD7762 in M059J and M059J-Fus1 glioblastoma cancer cell lines. M059J (p53 mutated, DNA-PKcs deficient) and M059J-Fus-1 (p53 mutated, DNA-PKcs corrected).

There was a similar difference in cytotoxicity seen between the M059J and M059J-Fus1 cell lines with both selective CHK1 inhibitors, V158411 and PF00477736, but no significant difference with the dual CHK1/CHK2 inhibitor AZD7762. AZD7762 was 4-fold more potent in the M059J cell line than V158411 but had a similar LC_{50} in the M059J-Fus1 cell line.

6.4 mRNA expression data from archival libraries of paired normal and tumour tissue

Publically available microarray data can be analysed to examine which DNA damage response genes are up-regulated in tumour tissue compared to normal tissue. Of particular interest to the current project is the mRNA expression of CHK1 and DNA-PKcs in paired datasets of normal and tumour tissues. Datasets from studies in breast cancer, pancreatic cancer, NSCLC, hepatocellular carcinoma and CLL have been analysed.

6.4.1 Breast cancer

GEO dataset GSE29431 is derived from a study of breast cancers by Lopez et al (Lopez et al., 2012). It contains 54 samples from breast carcinomas and 12 unmatched normal breast tissue samples. Figure 6-9 (A) shows that CHK1 mRNA expression is significantly elevated in the breast cancer tissue samples compared to the normal breast tissue ($p = 0.0044$ (unpaired t-test)). Figure 6-9 (B) demonstrates that DNA-PKcs mRNA expression is significantly downregulated is breast cancer tissue samples compared to unmatched breast tissue controls ($p = 0.0027$ (unpaired t-test)). There is no correlation between CHK1 and DNA-PKcs mRNA expression in this breast cancer dataset.

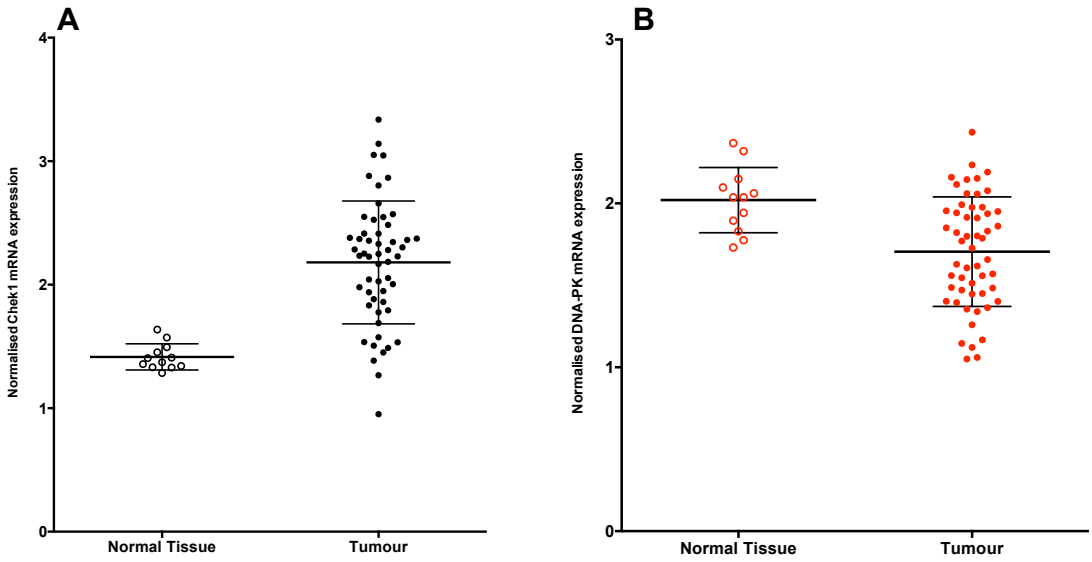

Figure 6-9 Analysis of mRNA data in breast cancer.

Analysis of array GSE29431 of paired normal and tumour tissue from patients with breast cancer. (A) CHK1 (black) mRNA expression normalised to HPRT in normal (open circles) and tumour tissue (filled circles). (B) DNA-PKcs (red) mRNA expression normalised to HPRT in normal (open circles) and tumour (filled circles) tissue

6.4.2 Pancreatic cancer

GEO data series GSE15471 is an array of 36 paired normal and tumour tissue samples from patients with pancreatic cancer from a study by Badea et al (Badea et al., 2008). Figure 6-10 shows the expression of 30 DNA damage response genes in tumour tissue compared to paired normal tissue. Figure 6-10 shows that CHK1 mRNA expression in tumour tissue compared to normal tissue had the second highest expression in the panel and that DNA-PKcs mRNA is also over-expressed. Figure 6-11 (A) demonstrates that CHK1 mRNA expression was significantly up-regulated in tumour tissue compared to paired normal tissue samples ($p = 0.0003$ (paired t-test)). Its upstream activator ATR was also up-regulated. DNA-PKcs mRNA expression (Figure 6-11 (B)) was also

significantly up-regulated in tumour tissue compared to paired normal tissue samples ($p < 0.0001$ (paired t-test)). Other genes involved in NHEJ, XRCC4 and ligase 4, were also among those very highly expressed. However, there was poor correlation between the up-regulation of these two parameters with $r^2 = 0.19$ (data not shown).

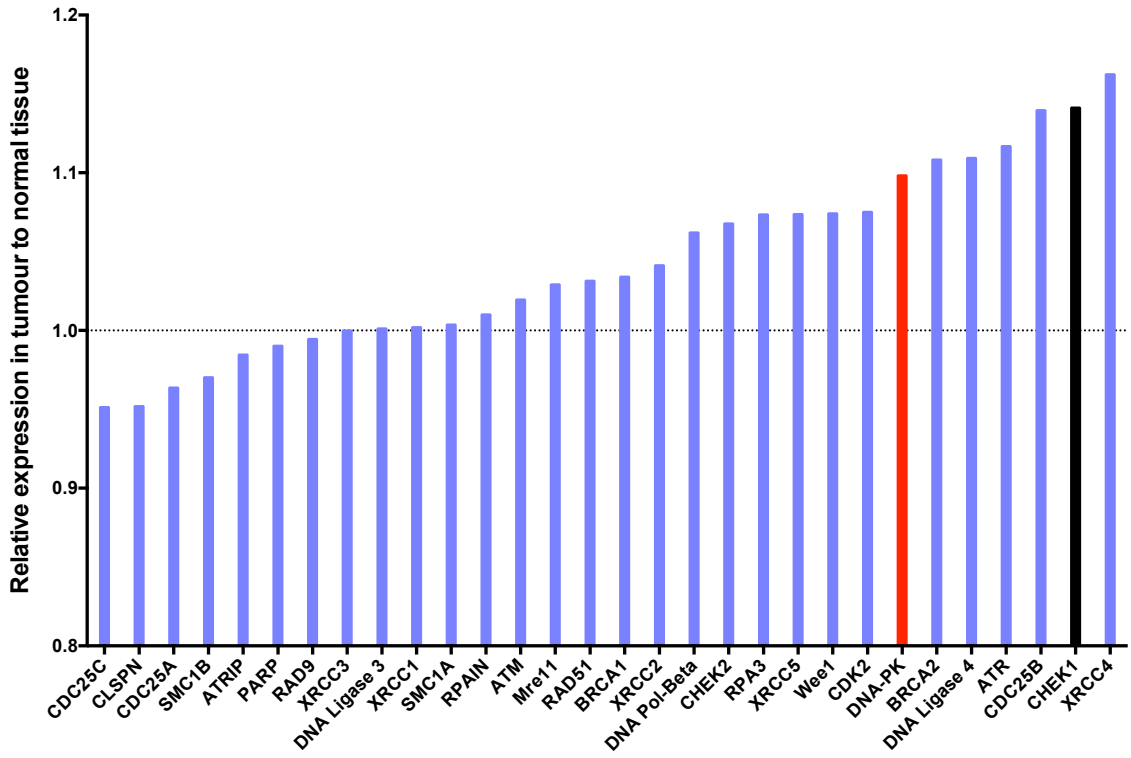

Figure 6-10 Analysis of mRNA data in pancreatic cancer

Analysis of array GSE15471 of paired normal and tumour tissue from patients with pancreatic cancer. All mRNA expression normalised to HPRT expression. DNA-PKcs highlighted in red and CHK1 in black.

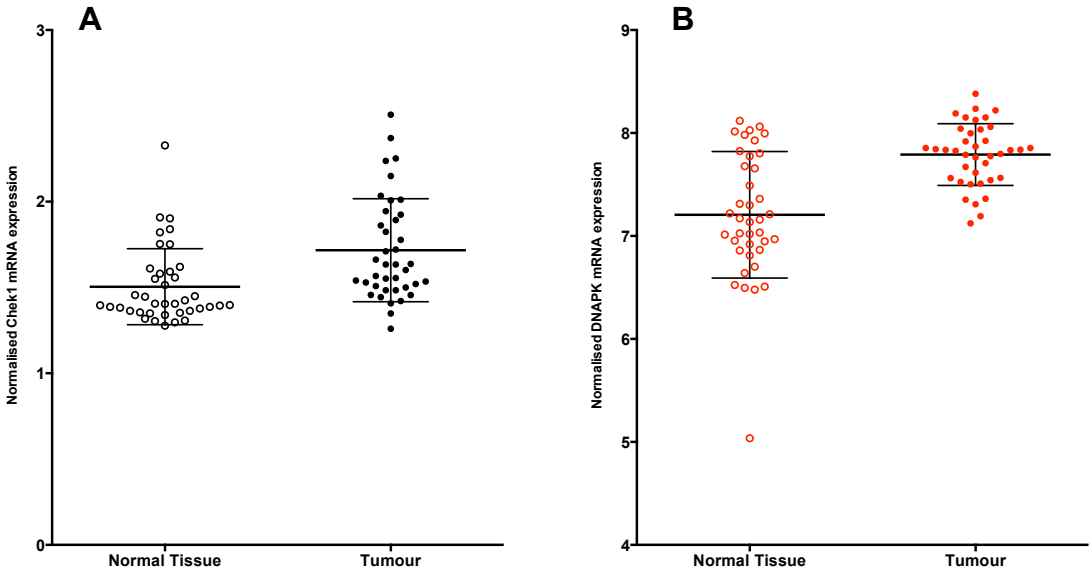

Figure 6-11 Analysis of mRNA data in pancreatic cancer

Analysis of array GSE15471 of paired normal and tumour tissue from patients with pancreatic cancer. (A) CHK1 (black) mRNA expression normalised to HPRT in normal (open circles) and tumour tissue (filled circles). (B) DNA-PKcs (red) mRNA expression normalised to HPRT in normal (open circles) and tumour (filled circles) tissue

6.4.3 Non-small cell lung cancer (NSCLC)

GEO data series GSE18842, from a study originally performed by Sanchez-Palencia et al (Sanchez-Palencia et al., 2011), contains samples from 46 NSCLC tumours with 42 paired and 3 un-paired controls. Figure 6-12 (A) shows that CHK1 mRNA expression was significantly increased in NSCLC tumour samples compared to matched controls ($p < 0.0001$ (paired t-test)) in this data set. Figure 6-12 (B) shows that, like CHK1 expression, DNA-PKcs mRNA expression was also significantly up-regulated in tumour tissue ($p < 0.0001$ (paired t-test)). There was moderate correlation between CHK1 mRNA and DNA-PKcs mRNA expression in matched samples; Figure 6-13 shows this

correlation which has an r^2 value of 0.729 (linear regression analysis; 95% confidence interval 0.6233 – 0.8111, $p < 0.0001$).

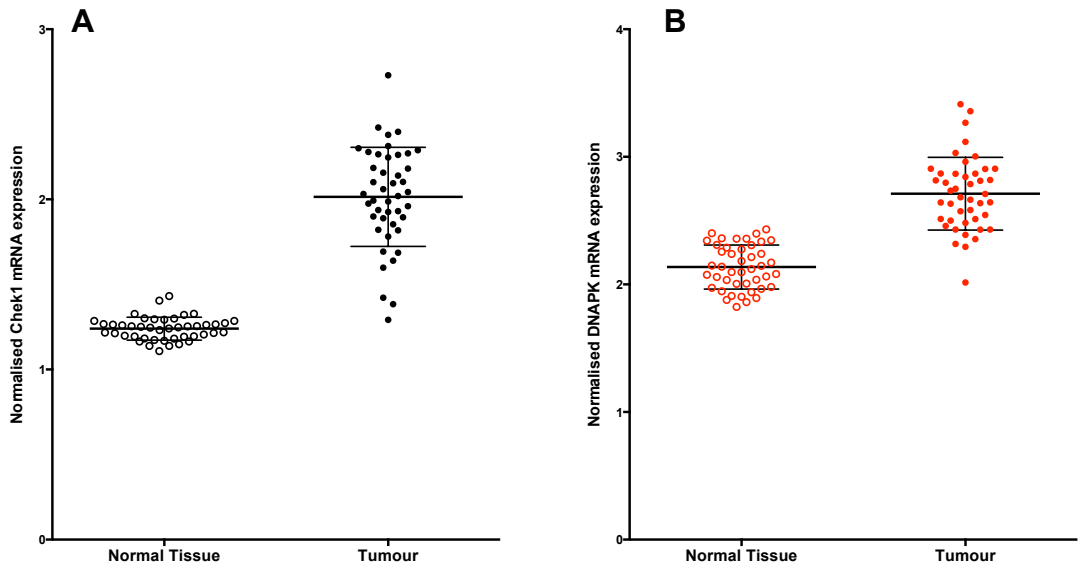

Figure 6-12 Analysis of mRNA data in NSCLC cancer

Analysis of array GSE18842 of paired normal and tumour tissue from patients with NSCLC. (A) CHK1 (black) mRNA expression normalised to HPRT in normal (open circles) and tumour tissue (filled circles). (B) DNA-PKcs (red) mRNA expression normalised to HPRT in normal (open circles) and tumour (filled circles) tissue

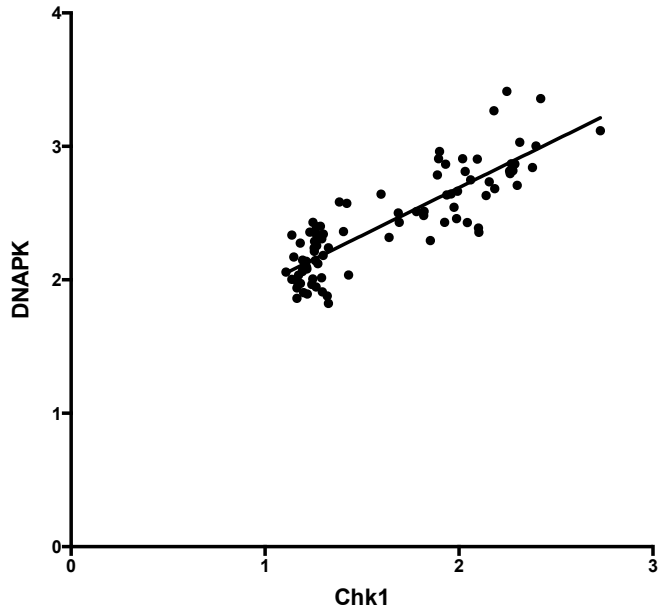

Figure 6-13 Analysis of mRNA data in NSCLC cancer: DNA-PKcs versus CHK1.

Analysis of array GSE18842 of NSCLC. DNA-PKcs and CHK1 mRNA expression normalised to HPRT expression plotted against each other.

6.4.4 Hepatocellular carcinoma (HCC)

GSE6764 is a GEO data series from Wurmbach et al (Wurmbach et al., 2007) that contains unpaired samples from patients with a spectrum of liver disease. It contains samples of normal liver tissue through the spectrum of cirrhotic liver disease to dysplastic liver disease into HCC (very early, early, advanced and very advanced HCC). There were samples from 75 patients in total. The tumour samples came from patients with HCC associated with hepatitis C virus infection (HCV). Figure 6-14 and Fig 6-15 show that both CHK1 and DNA-PKcs mRNA expression became increasingly dysregulated with advancing HCC; Figure 6-15. Figure 6-16 shows the relatively weak correlation between DNA-PKcs and CHK1 mRNA expression; the r^2 value for this correlation is 0.344 (linear regression analysis, $p < 0.0001$)

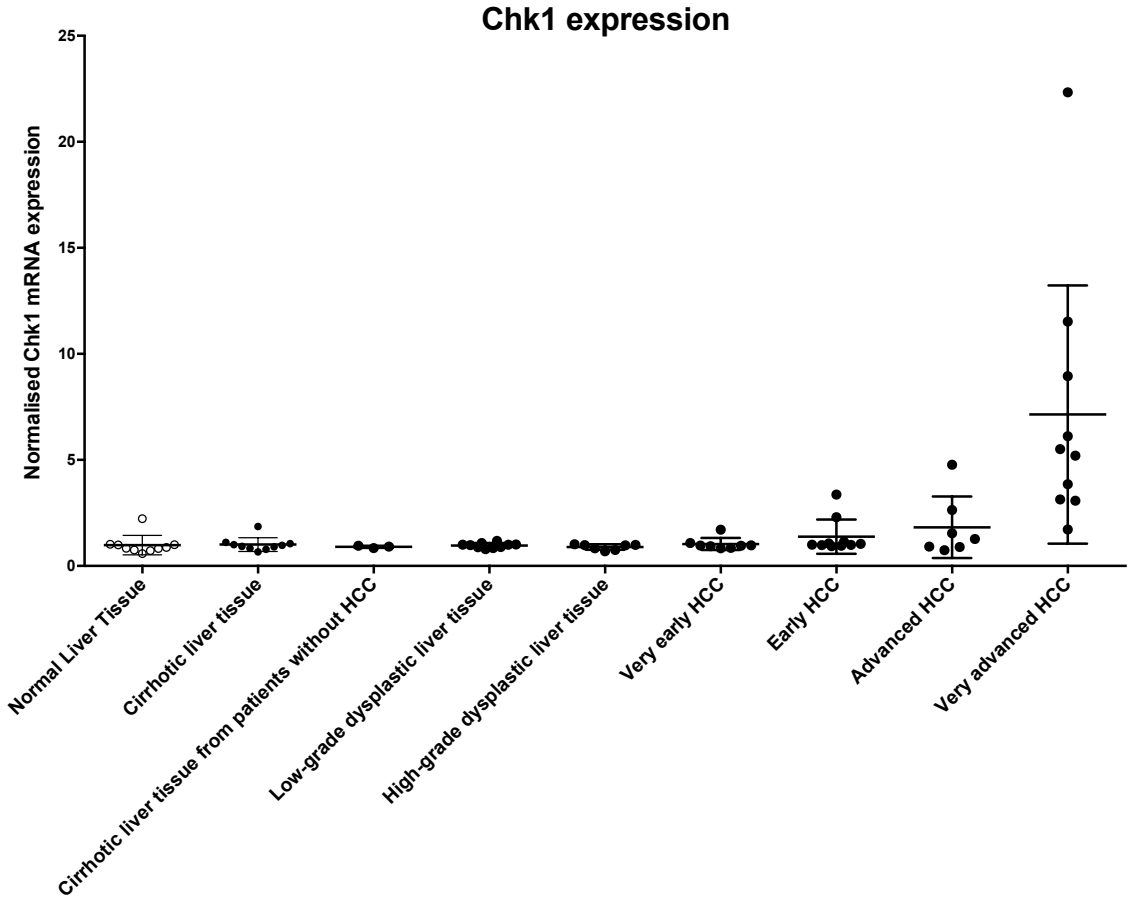

Figure 6-14 Analysis of mRNA data in HCC.

Analysis of array GSE6764 of spectrum of liver disease, normal tissue (open circle) and abnormal tissue (filled circle). CHK1 (black) mRNA expression normalised to HPRT expression.

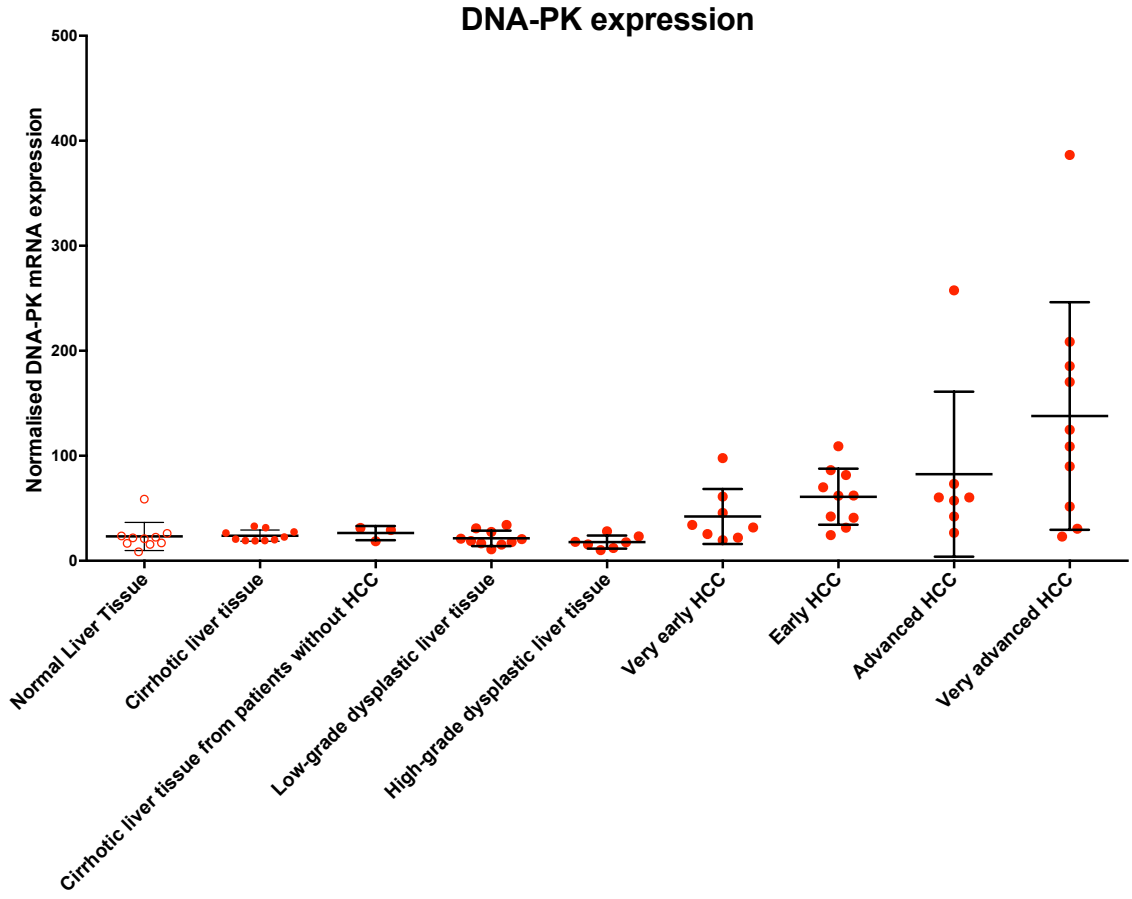

Figure 6-15 Analysis of mRNA data in HCC.

Analysis of array GSE6764 of spectrum of liver disease, normal tissue (open circle) and abnormal tissue (filled circle). DNA-PKcs (red) mRNA expression normalised to HPRT expression

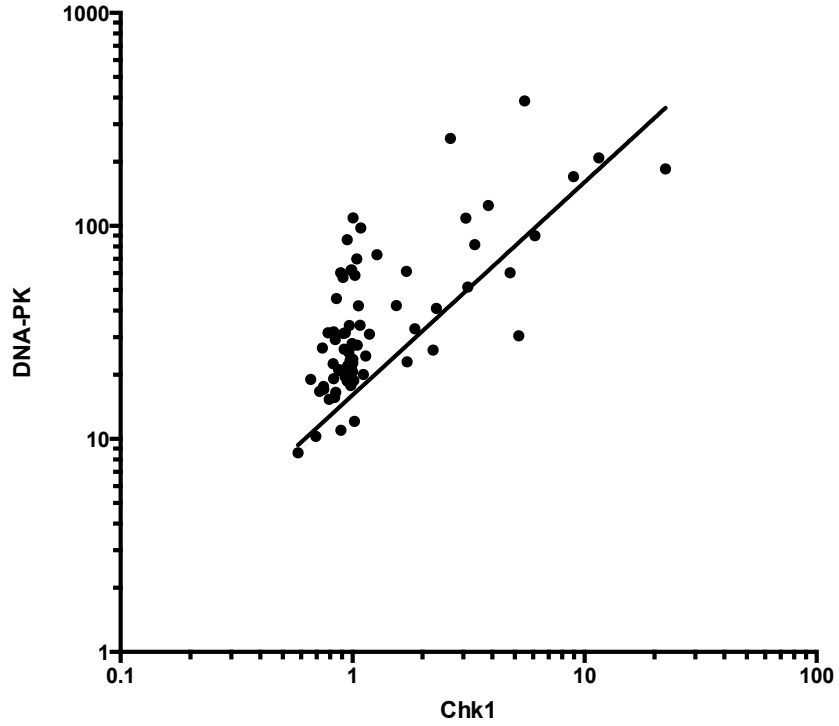

Figure 6-16 Analysis of mRNA data in HCC: DNA-PKcs versus CHK1.

Analysis of array GSE6764 of hepatocellular carcinoma. DNA-PKcs and CHK1 mRNA expression normalised to HPRT expression plotted against each other.

6.4.5 Chronic lymphocytic leukaemia (CLL)

A CLL GEO data series GSE22529 contains samples from 41 patients with CLL and 11 age-matched controls (Gutierrez et al., 2010). Figure 6-17 (A) shows the comparison of CHK1 mRNA expression between normal B cell controls and B cell samples from patients with CLL. There was a small increase in CHK1 mRNA expression in the samples from patients with CLL, but this was not significant. Figure 6-17 (B) shows the DNA-PKcs mRNA expression in the same populations. There was no difference between the two groups.

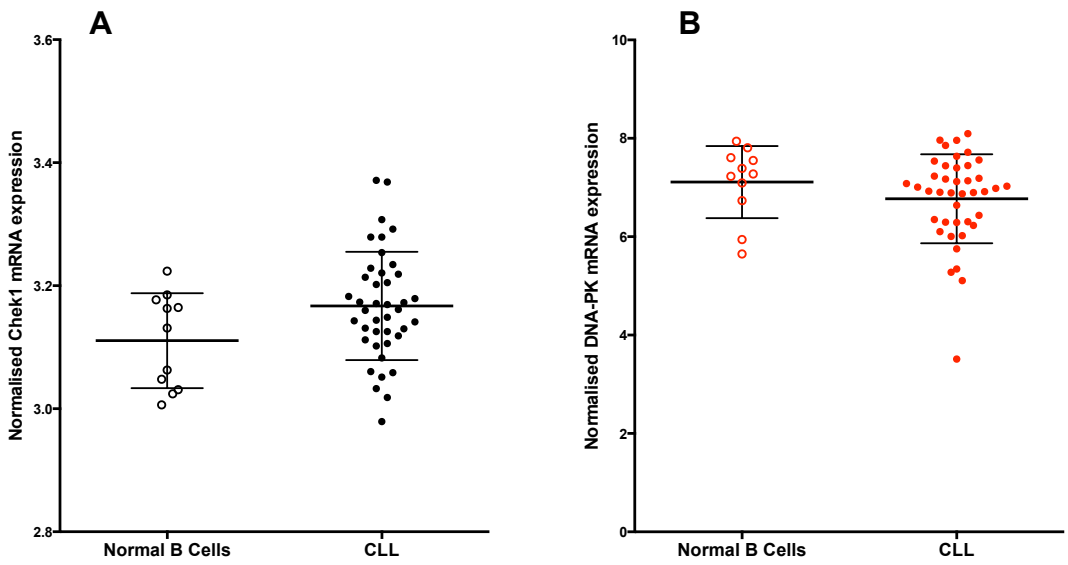

Figure 6-17 Analysis of mRNA data in CLL.

Analysis of array GSE22529 of CLL. (A) CHK1 (black) mRNA expression normalised to HPRT in normal (open circles) and CLL (filled circles). (B) DNA-PKcs (red) mRNA expression normalised to HPRT in normal (open circles) and CLL (filled circles) tissue

6.5 Cytotoxicity of V158411 in a panel of HCC cancer cell lines.

Following the results seen in the M059J/M059J-Fus1 DNA-PKcs proficient and deficient paired glioblastoma cells and the correlation of CHK1 and DNA-PKcs expression in the archived HCC datasets, the sensitivity of a panel of liver cancer cell lines was assessed. These cell lines were already known to have differences in their DNA-PKcs expression. The sensitivity of these cell lines to V158411 with and without 1 μM NU7411 was assessed in clonogenic assays. Figure 6-18 and Figure 6-19 show the results of these experiments and Table 6-4 the LC_{50} and LC_{90} values these experiments. There was a wide range of sensitivity to single agent V158411 with LC_{50} values ranging from 153 nM in SNU.182 cell line to 4613 nM in the resistant PLC/PRF/5 cell line.

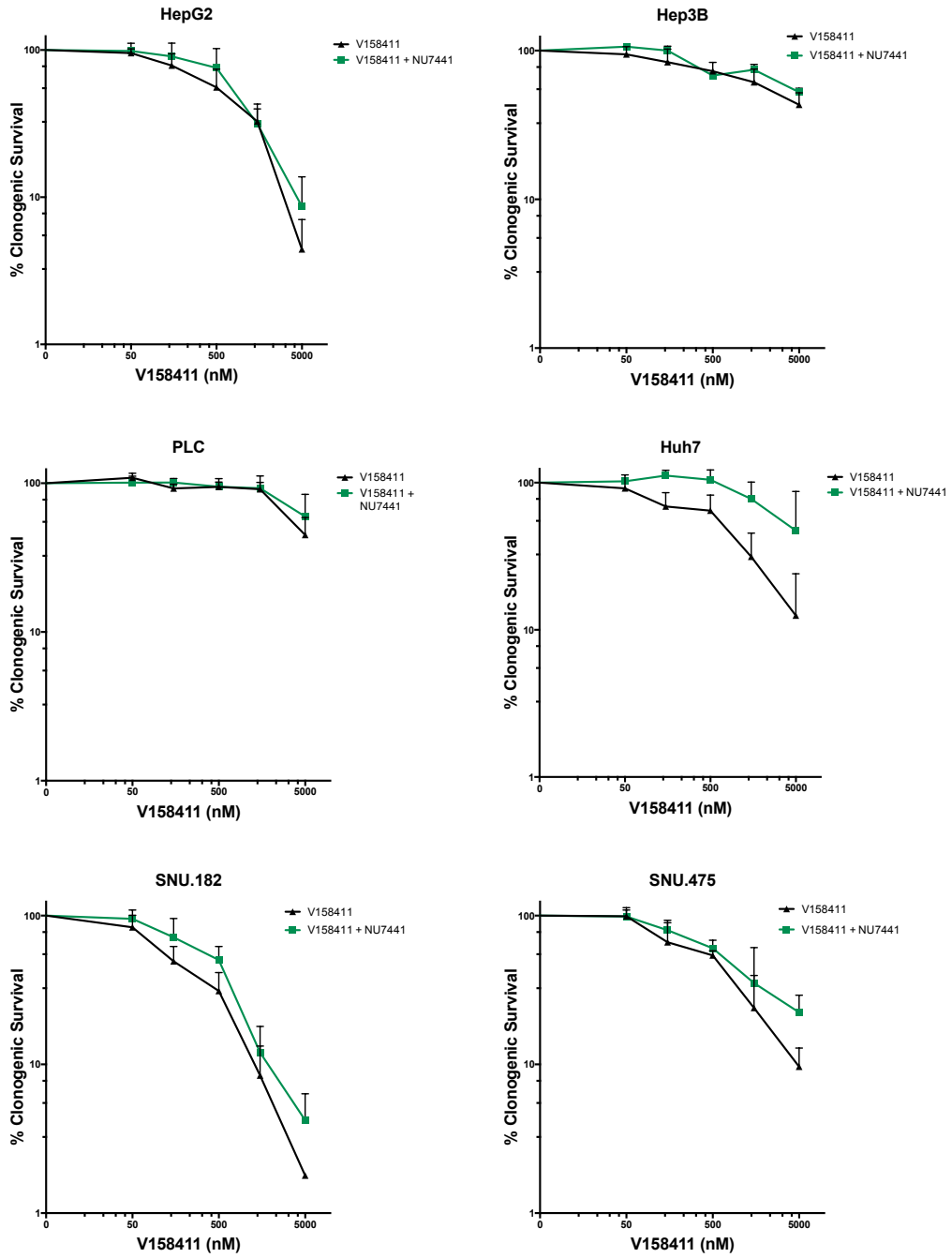

Figure 6-18 Cytotoxicity of V158411 in liver cell line panel.

Clonogenic cytotoxicity assay in liver cancer cell lines. Individual cell lines (PLC/PRF/5 (p53 mutated), HepG2 (p53 wild type), Hep3B (p53 null), Huh7 (p53 mutated), SNU.182 (no p53 mutation detected) and SNU.475 (p53 mutated)) with V158411 (black) +/- 1 μM NU7441 (green). Data are mean +/- SEM of 3 independent experiments. Within each experiment there were at least 2 replicates.

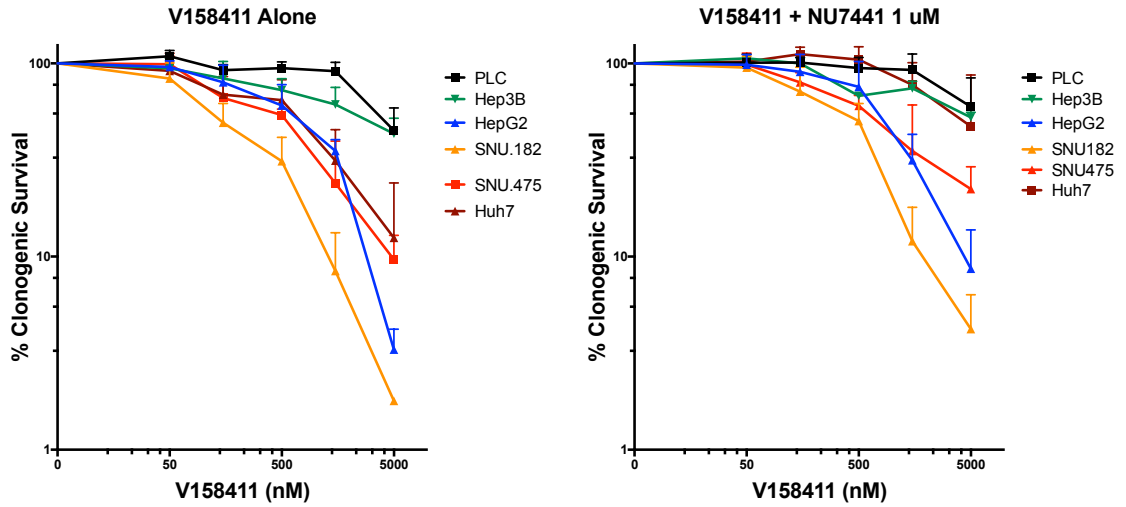

Figure 6-19 Cytotoxicity of V158411 in liver cell line panel.

Clonogenic cytotoxicity assay. Summary of panel of HCC cell lines (PLC/PRF/5 (black, p53 mutated), HepG2 (blue, p53 wild type), Hep3B (green, p53 null), Huh7 (rust, p53 mutated), SNU.182 (yellow, no p53 mutation detected) and SNU.475 (red, p53 mutated)) with V158411 or V158411 + 1 μM NU7441. Data are mean +/- SEM of 3 independent experiments. Within each experiment there were at least 2 replicates.

	LC_{50}		LC_{90}	
Cell Line	V158411	V158411 + NU7441	V158411	V158411 + NU7441
PLC/PRF/5	4613 nM	>5000 nM	>5000 nM	>5000 nM
Hep3B	3692 nM	>5000 nM	>5000 nM	>5000 nM
HepG2	748.5 nM	1081 nM	4309 nM	4795 nM
Huh7	937.4 nM	4682 nM	>5000 nM	>5000 nM
SNU.182	153.2 nM	509 nM	1430 nM	2404 nM
SNU.475	634.1 nM	911 nM	4914 nM	>5000 nM

Table 6-4 LC_{50} and LC_{90} values of V158411 +/- 1 μM NU7441 in liver cancer cell lines.

Data are mean of at least 3 independent experiments.

The impact of the DNA-PKcs inhibitor NU7441 on the cytotoxicity of V158411 was assessed in all cell lines by ANOVA analysis. The only cell line in which 1 μM NU7441 caused a statistically significantly protection from V158411 was in Huh7 cells ($p = 0.02$ (ANOVA)), in the remaining 5 liver cancer cell lines the protection afforded by NU7441 was not significant. Nevertheless a consistent pattern was seen in that less sensitivity to V158411 was observed in the presence of NU7441 and in every cell line the LC_{90} and/or LC_{50} of V158411 was higher in the presence of NU7441

6.6 DNA-PKcs status as a determinant of sensitivity to CHK1 inhibitors in a panel of cell lines

To extend the investigation of the potential correlation identified between CHK1 and DNA-PKcs mRNA expression, and the cytotoxicity data in V3 compared to AA8 cells and the M059J/M059J-Fus1 glioblastoma cell line pair further experiments were planned to look for a correlation between the expression of CHK1 and DNA-PKcs protein in the panel of cell lines used in the current study. Furthermore, it was wished to explore whether the expression of either CHK1 or DNA-PKcs protein correlated with the sensitivity to V158411 seen in clonogenic assays.

6.6.1 DNA-PKcs expression main cell line panel

DNA-PKcs expression and autophosphorylation, as an indication of activity, was measured in untreated cells and in cells one hour after 10 Gy ionising radiation in all the cell lines previously used (K562, MCF7, MDA-MB-231, HCT116 (wild type and p53 -/-), M059J/M059J-Fus1 and U2OS (wild type and dominant negative p53). Figure 6-20 shows representative western blots from these experiments.

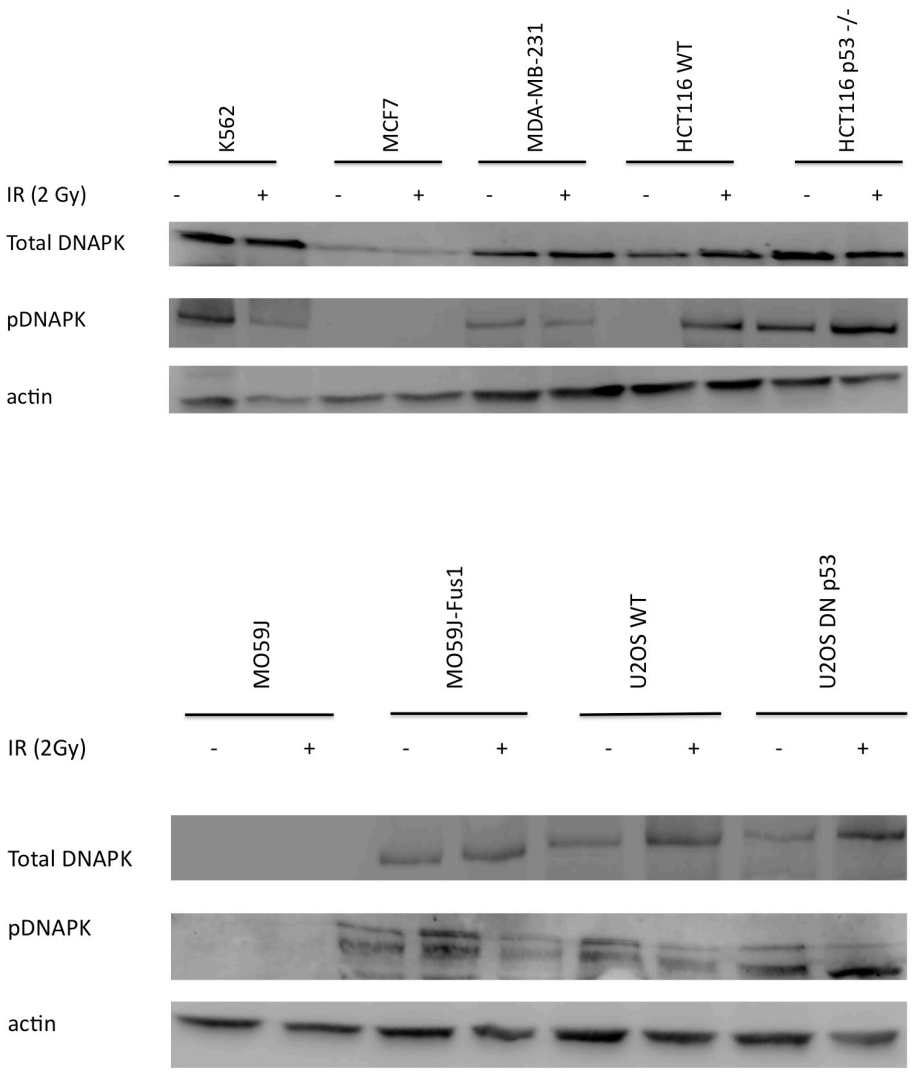

Figure 6-20 Example western blots in cell line panel.

Representative western blots of DNA-PKcs, pDNA-PKcs^{serine2096} and actin in cell lines treated with 10 Gy ionising radiation.

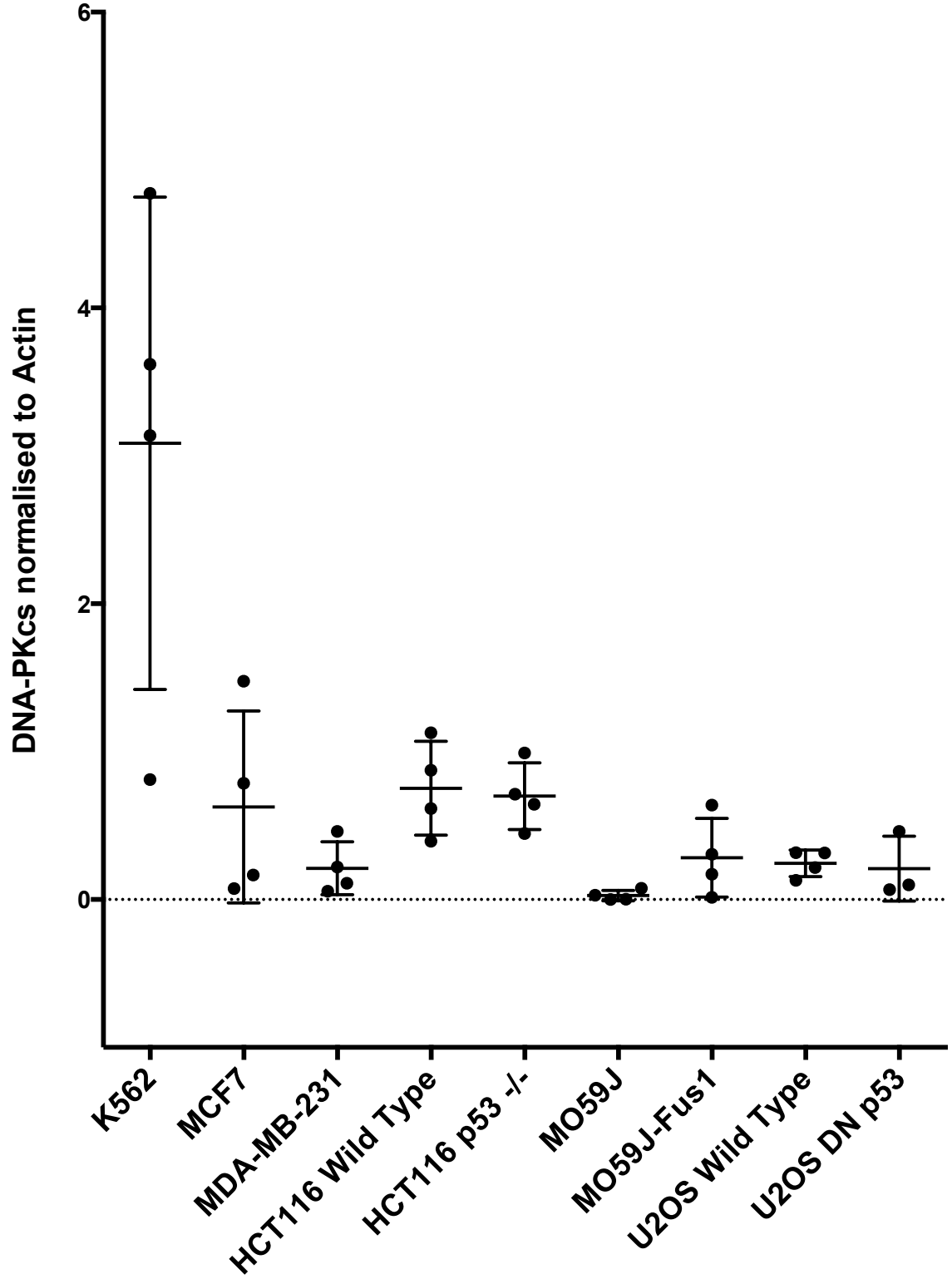

Figure 6-21 Expression of DNA-PKcs in cell line panel.

Expression of DNA-PKcs normalised to actin in a cell line panel. Data are mean +/- SEM of at least 3 independent experiments.

The mean expression of total DNA-PKcs normalised to actin is shown in Figure 6-21. There is a wide variation in total DNA-PKcs expression with the highest expression in K562 cell line. The mean level of pDNA-PKcs^{serine2096} (the autophosphorylation form) normalised to actin both in untreated cell lines and samples treated with 10 Gy IR is shown in

Figure 6-22. There was considerable interassay variability in these results suggesting that the results should be interpreted with caution. The ratio between untreated and treated samples is shown in Figure 6-23. 10 Gy IR induces the expression of pDNA-PKcs^{serine2096} in the majority of cell lines. Some cell lines (MCF7, MDA-MB-231) with a low baseline expression of pDNA-PKcs^{serine2096} did not have any detectable increase in expression following treatment with 10 Gy IR.

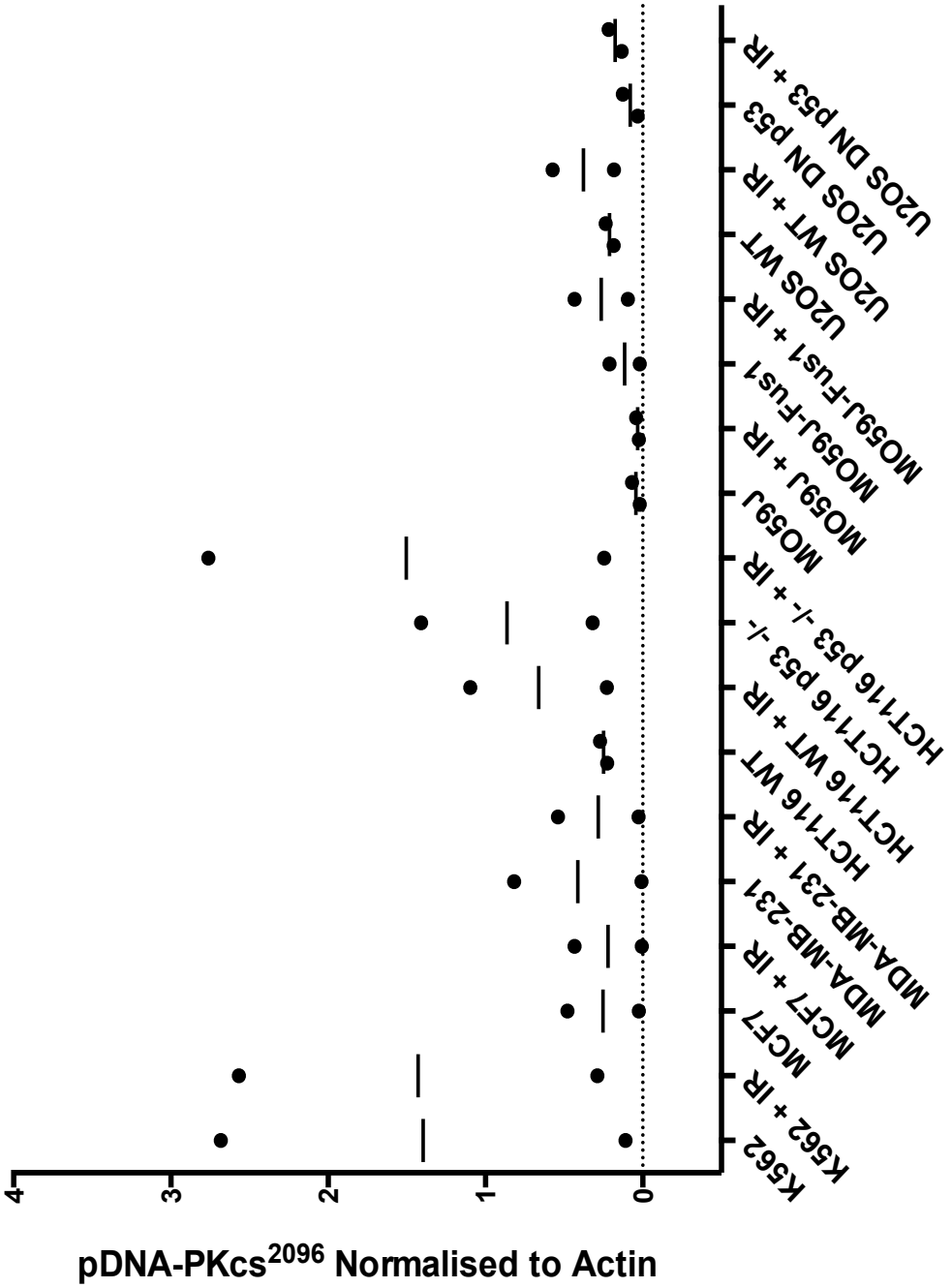

Figure 6-22 Expression of pDNA-PKcs^{serine2096} in cell line panel.

Expression of pDNA-PKcs^{serine2096} normalised to actin in controls and paired samples 1 hour after 10 Gy ionising radiation. Note significant interassay variability. Data from 2 independent experiments.

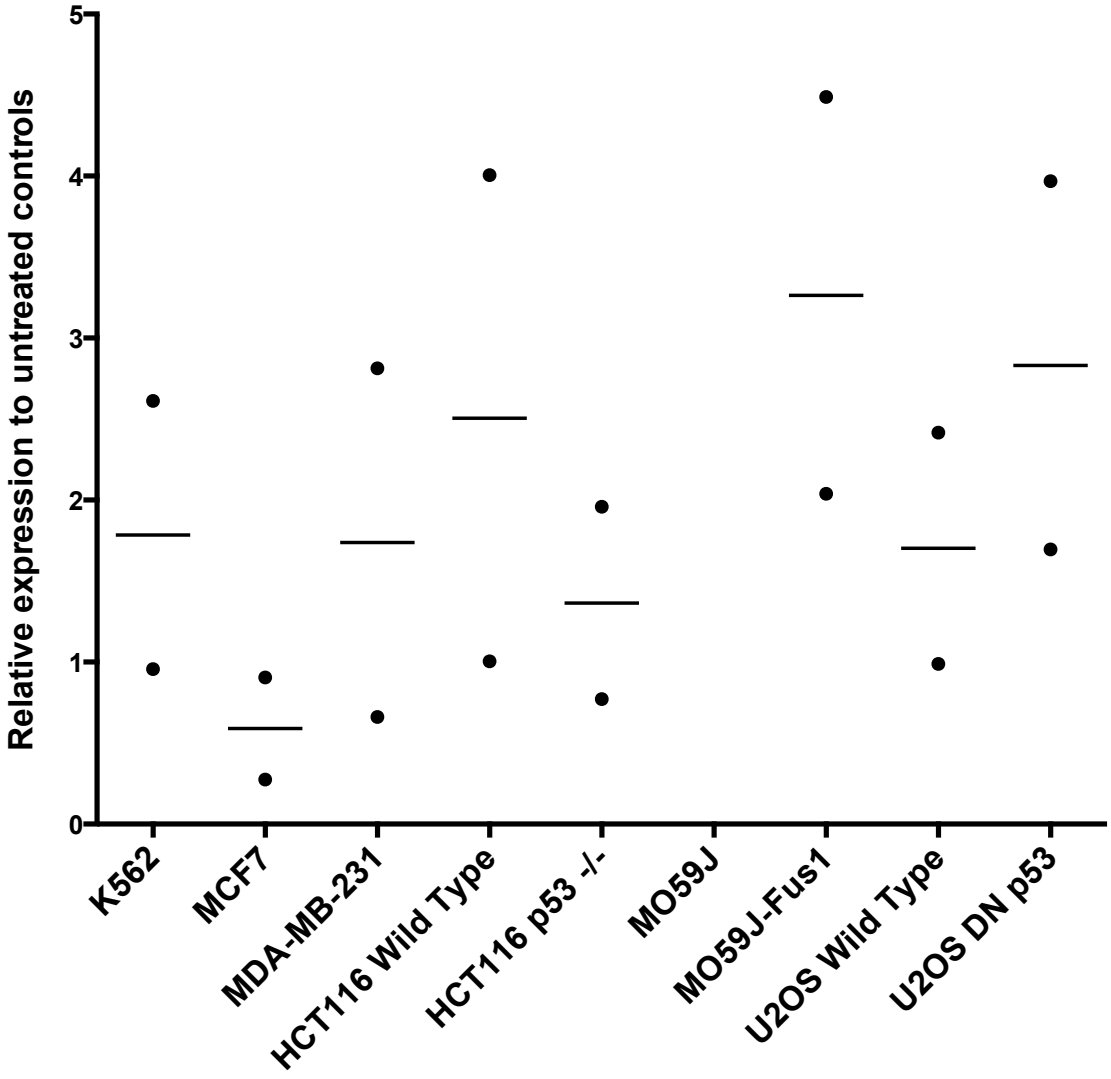

Figure 6-23 Relative expression of pDNA-PKcs^{serine2096} in cell line panel.

Relative expression of pDNA-PKcs^{serine2096} in cell lines treated with 10 Gy ionising radiation compared to untreated controls. Note significant interassay variability. Data from 2 independent experiments.

6.6.2 DNA-PKcs expression in HCC cell lines

DNA-PKcs expression, total DNA-PKcs and pDNA-PKcs^{serine2096}, had previously been determined in the panel of liver cancer cell lines (PLC/PRF/5, Huh7, Hep3B, HepG2, SNU.182 and SNU.475) by Liam Cornell. DNA-PKcs

expression data is shown in Figure 6-24; pDNAPKcs^{serine2095} expression in untreated controls and cells treated with 10 Gy IR one hour before harvesting in Figure 6-25, and the ratio of pDNA-PKcs^{serine2096} expression between treated and untreated samples in Figure 6-26. There was significant inter-assay variation such that it was not possible to determine if there were differences in the expression of DNA-PKcs between cell lines (Figure 6-24). 10 Gy IR consistently increased DNA-PKcs autophosphorylation (pDNA-PKcs^{serine2096}) in all cell lines (Figure 6-25). There is wide variation in the extent of this upregulation between cell lines with the most significant increase being seen in the Hep3B cell line (Figure 6-26).

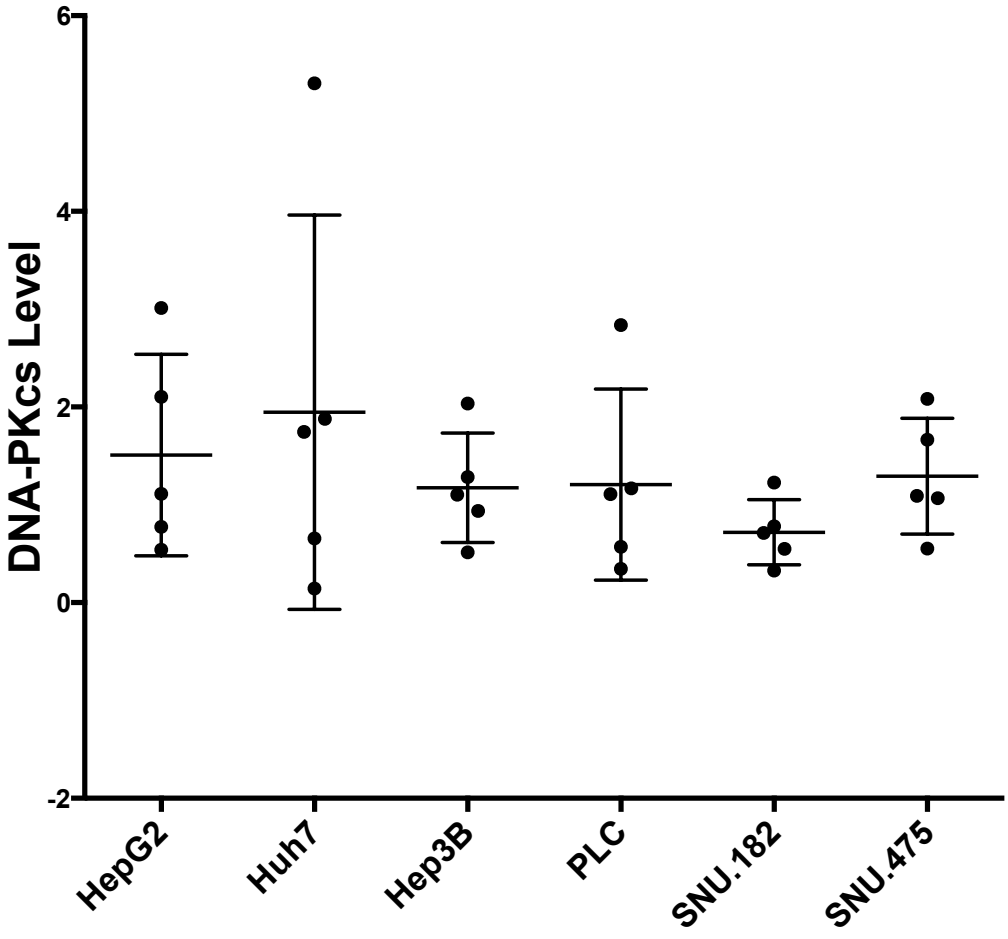

Figure 6-24 Expression of DNA-PKcs in liver cell line panel.

Expression normalised to actin in a panel of liver cancer cell lines. Data from at least 2 independent experiments. Note significant interassay variability. Data courtesy of Liam Cornell.

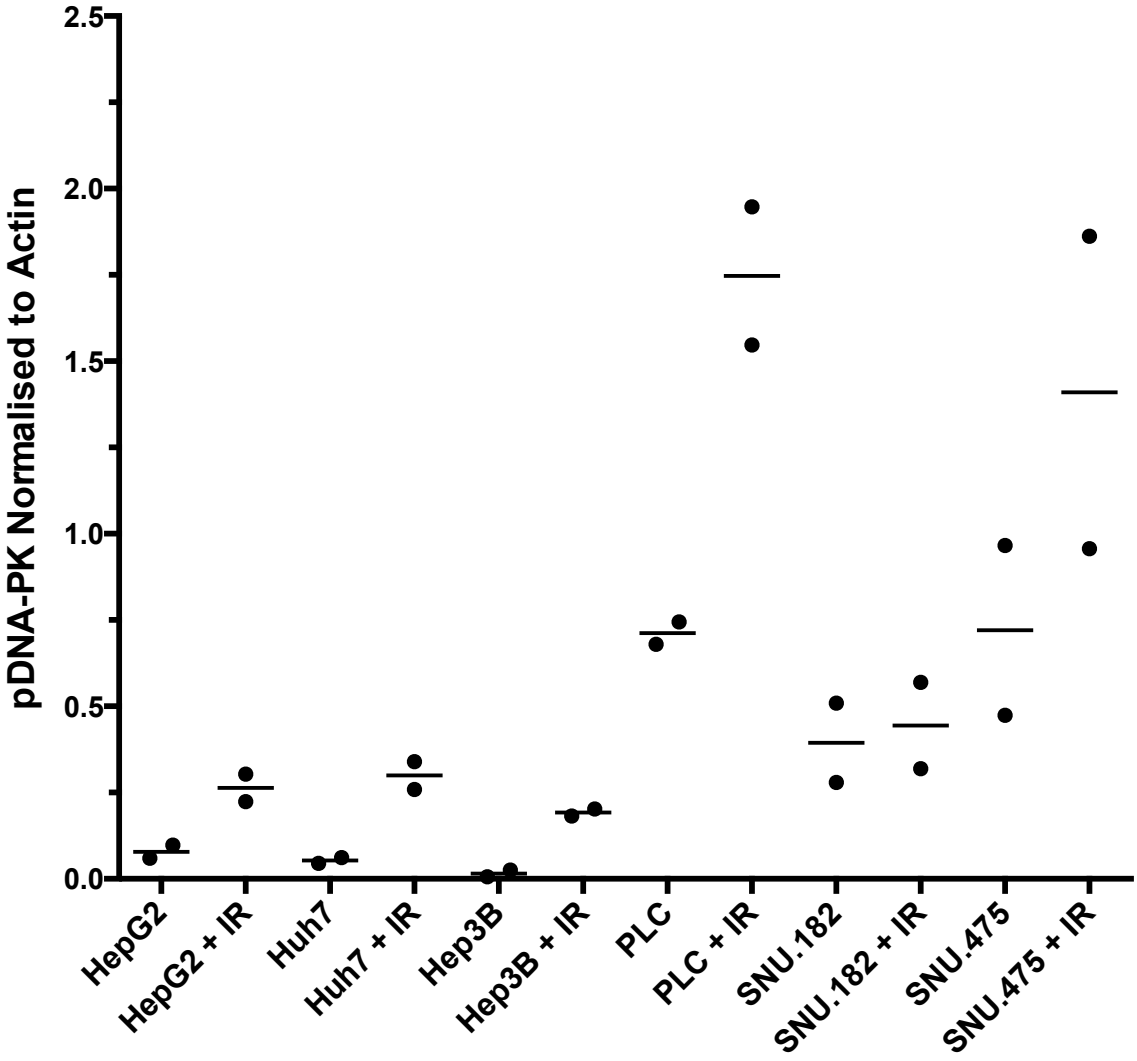

Figure 6-25 Expression of pDNA-PKcs^{serine2096} in liver cell line panel

Expression normalised to actin in controls and paired samples 1 hour after 10 Gy ionising radiation. Data from 2 independent experiments. Data courtesy of Liam Cornell

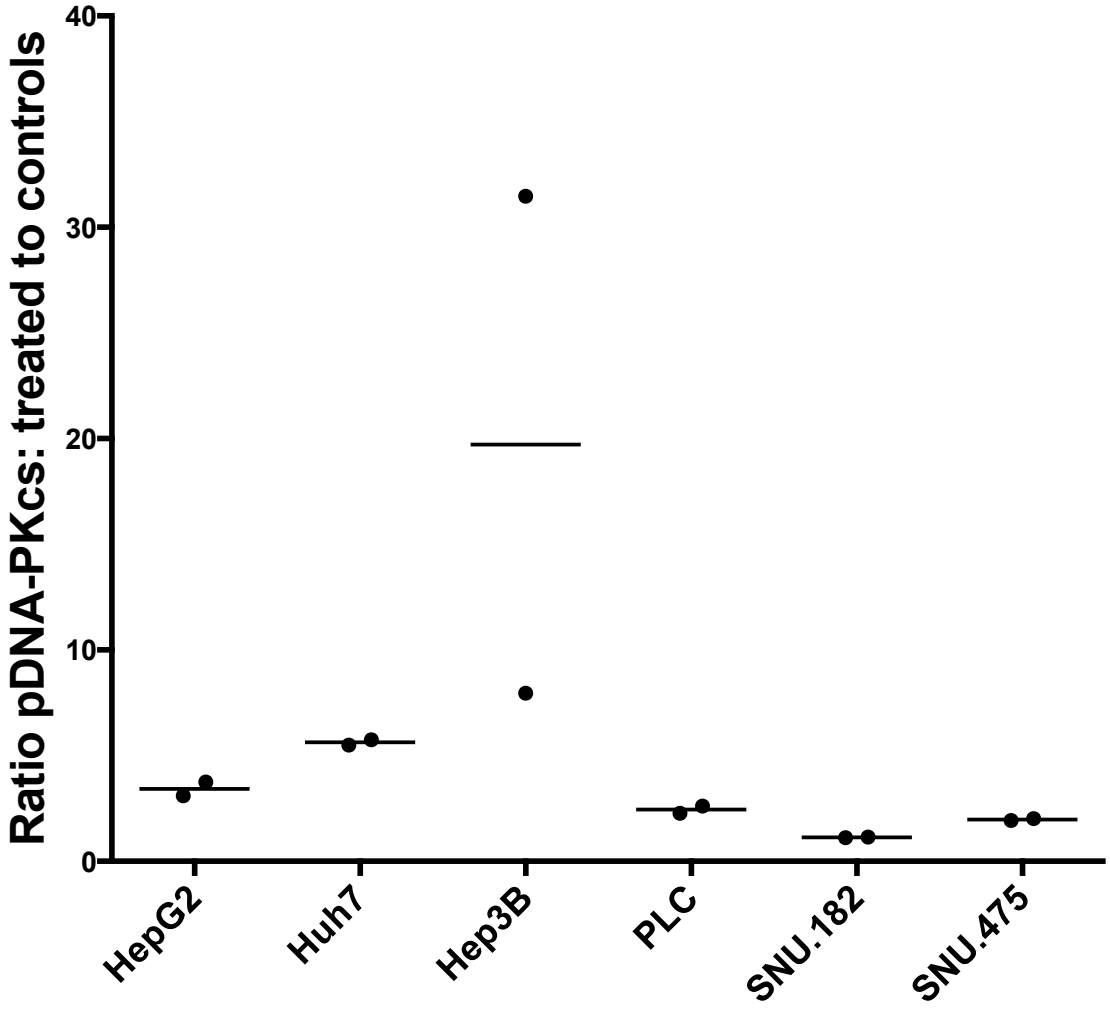

Figure 6-26 Relative expression of pDNA-PKcs^{serine2096} in liver cell line panel

Relative expression of pDNA-PKcs^{serine2096} in cell lines treated with 10 Gy ionising radiation compared to untreated controls. Data are mean 2 independent experiments. Data courtesy of Liam Cornell.

6.6.3 CHK1 expression in HCC cell lines

CHK1 expression in the liver cancer cell line panel was also examined by western blotting. A representative blot from these experiments is shown in Figure 6-27.

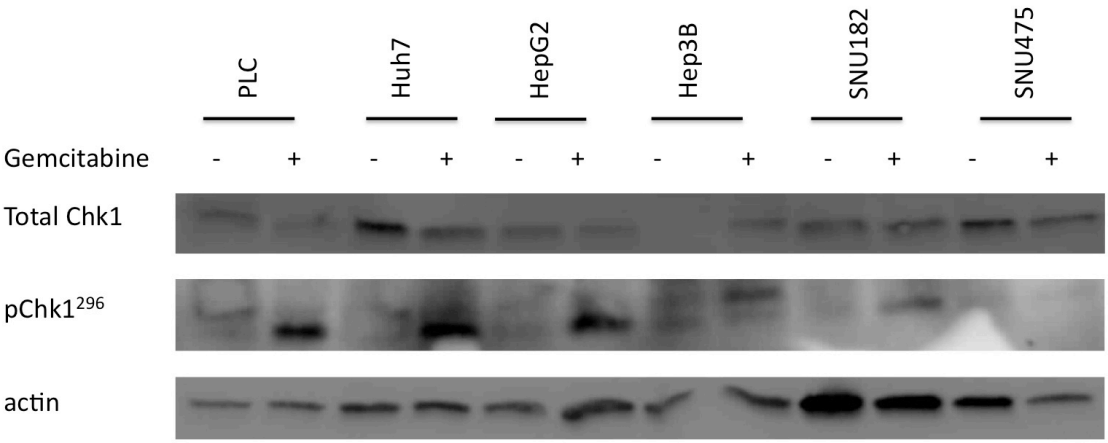

Figure 6-27 Representative western blot of CHK1 expression in liver cell line panel.

Expression of CHK1, pCHK1^{serine296} and actin in cell lines treated with 1 μM gemcitabine.

Total CHK1 expression normalised to actin expression is shown in Figure 6-28. There was only modest variation in CHK1 expression, it being highest, when normalised to actin expression, in HepG2 and Hep3B cell lines.

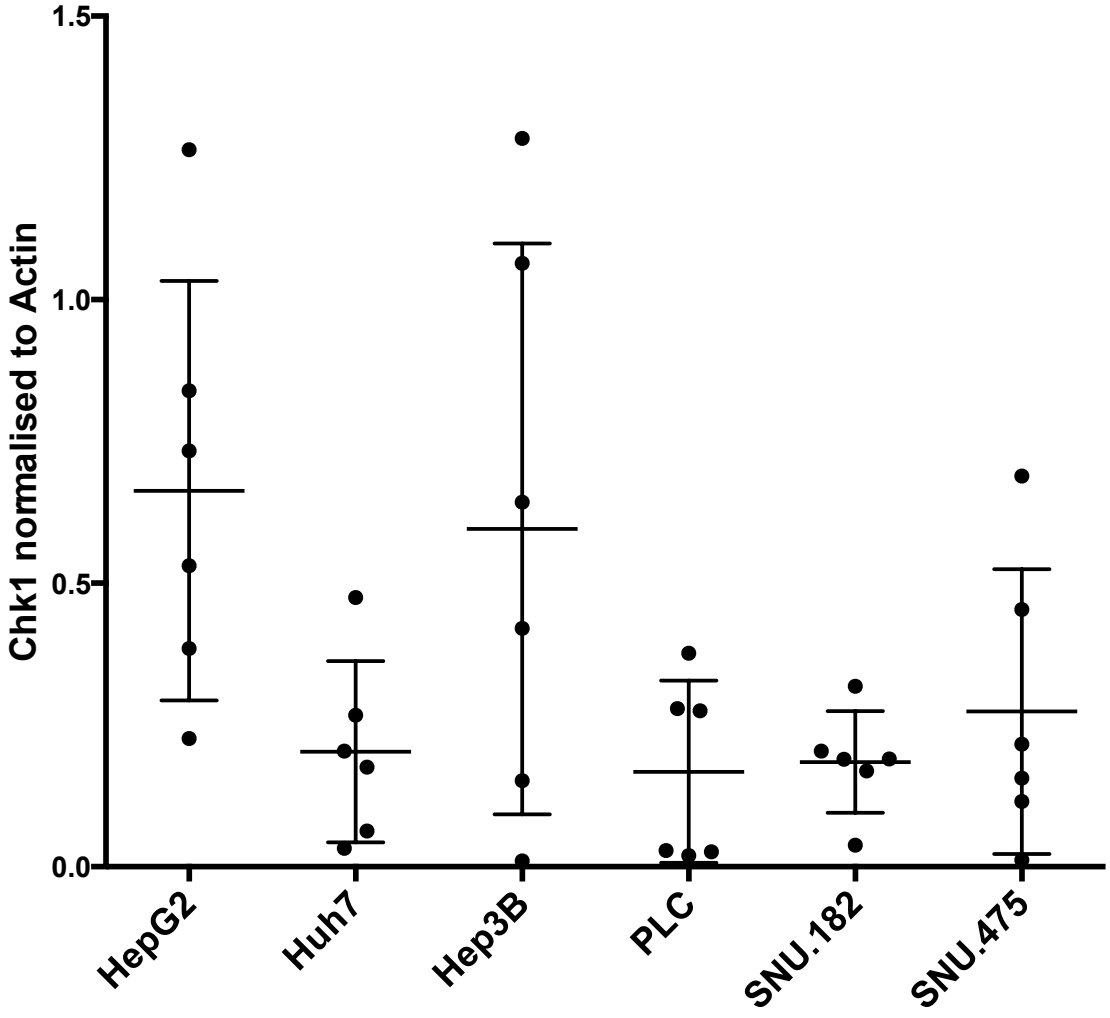

Figure 6-28 CHK1 expression in liver cell line panel.

Expression of CHK1 normalised to actin in a panel of liver cancer cell lines. Data are mean +/- SEM of 3 independent experiments.

The expression of pCHK1^{serine296} after a one hour exposure to 1 μM gemcitabine was also examined in the liver cancer cell line panel. A summary of this data is shown in Figure 6-29. Figure 6-30 shows that gemcitabine reliably increases the expression of the activated pCHK1^{serine296} across most of the cell line panel apart from SNU.475 cells where both the basal and induced pCHK1^{serine296} expression was very low. The greatest induction of pCHK1^{serine296} expression was seen in the Hep3B cell line.

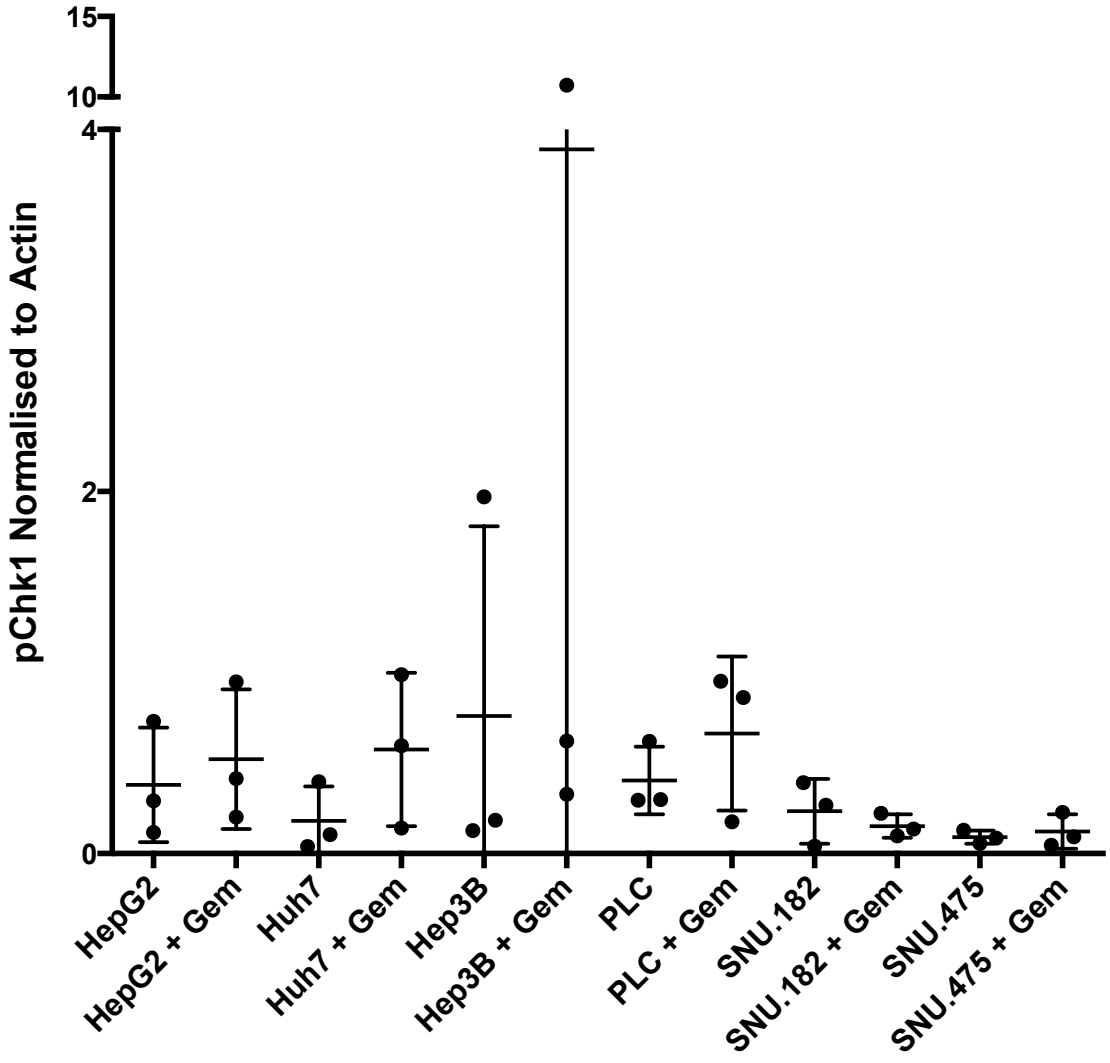

Figure 6-29 Expression of pCHK1^{serine296} in liver cell line panel.

Expression of pCHK1^{serine296} normalised to actin in controls and paired samples 1 hour after 1 μM gemcitabine. Data are mean +/- SEM of 3 independent experiments.

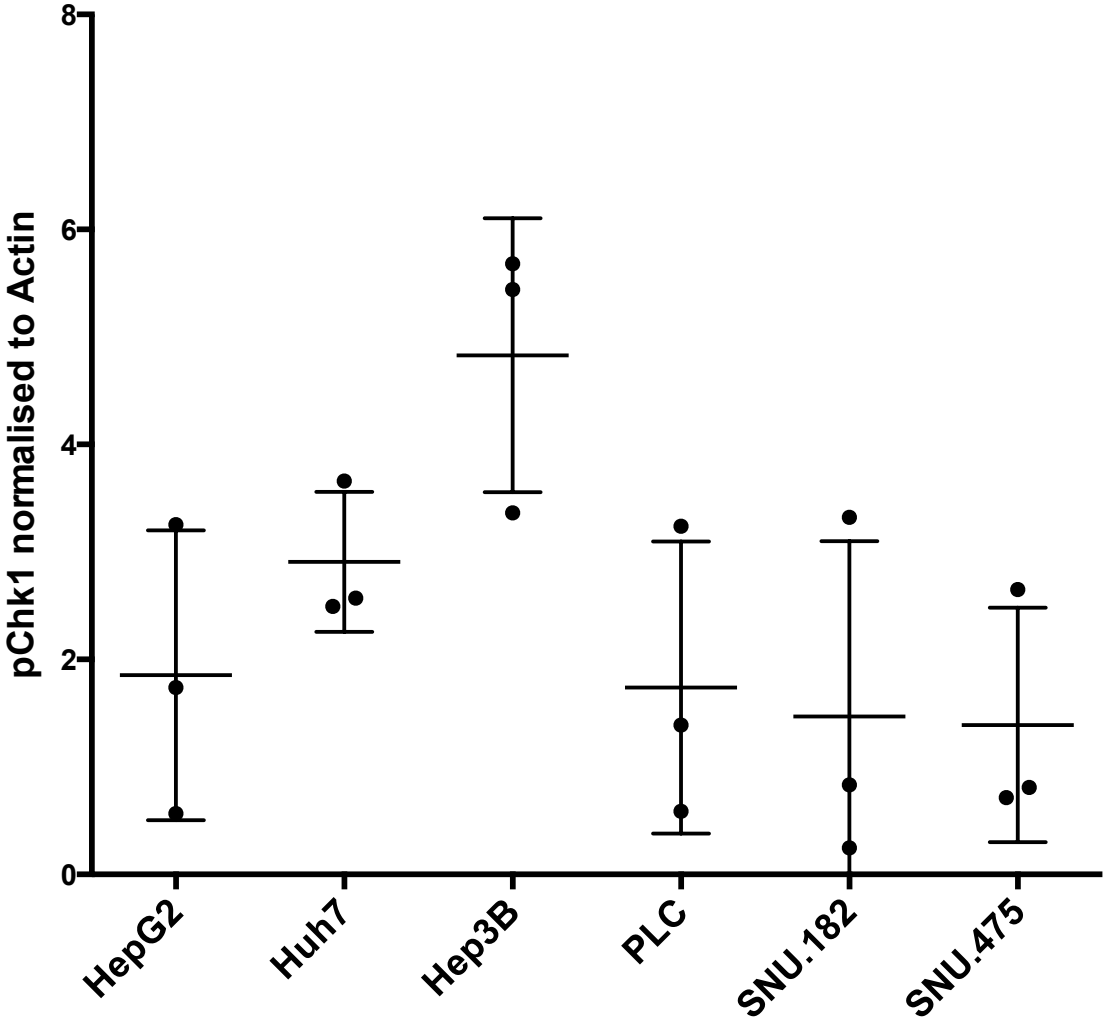

Figure 6-30 Relative expression of pChk1^{serine296} in liver cell line panel.

Relative expression of pChk1^{serine296} in cell lines treated with 1 μM gemcitabine compared to untreated controls. Data are mean +/- SEM of 3 independent experiments.

6.6.4 Correlation between CHK1 and DNA-PKcs expression in the cell line panel and with sensitivity to V158411.

To determine if CHK1 and DNA-PKcs were co-ordinately expressed in both the main cell line panel and liver cancer cell lines, as they are in some tumour types (see section 6.4); the correlation between CHK1 and DNA-PKcs expression and between induced pCHK1^{serine296} and pDNA-PKcs^{serine2096} expression was

analysed as shown in Figure 6-31. There was no correlation between total CHK1 and total DNA-PKcs expression (r^2 = 0.203, p = 0.09, linear regression analysis) or between induced pCHK1^{serine296} and pDNA-PKcs^{serine2096} expression (r^2 = 0.475, p = 0.130, linear regression analysis) in this cell line panel.

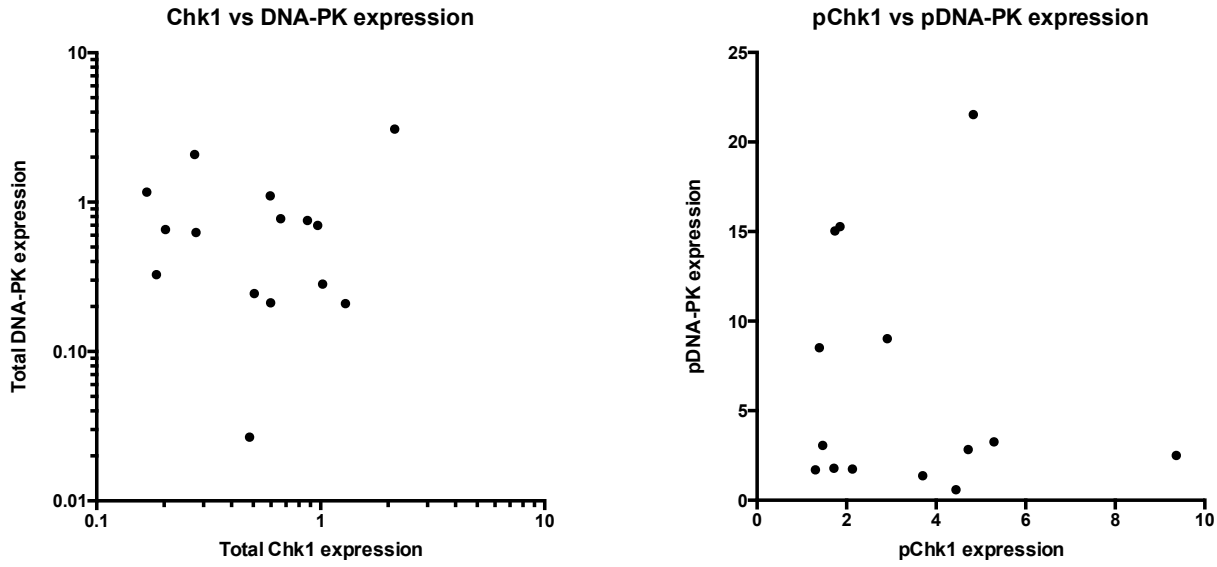

Figure 6-31 CHK1 and DNA-PKcs expression in all cell lines.

Correlation between (a) total CHK1 expression and total DNA-PKcs expression and (b) pCHK1^{serine296} and pDNA-PKcs^{serine2096} expression in a panel of cell lines including the liver cancer cell lines. Individual points constitute the mean expression levels from a summary of at least 3 experiments.

Further to this, the cytotoxicity of V158411 in clonogenic assays as summarised by their LC_{50} value in both the main cell line panel and the liver cancer cell line panel was correlated to the expression of total CHK1, total DNA-PKcs and the induced expression of pCHK1^{serine296} and pDNA-PKcs^{serine2096}. The results of this analysis are shown in Figure 6-32.

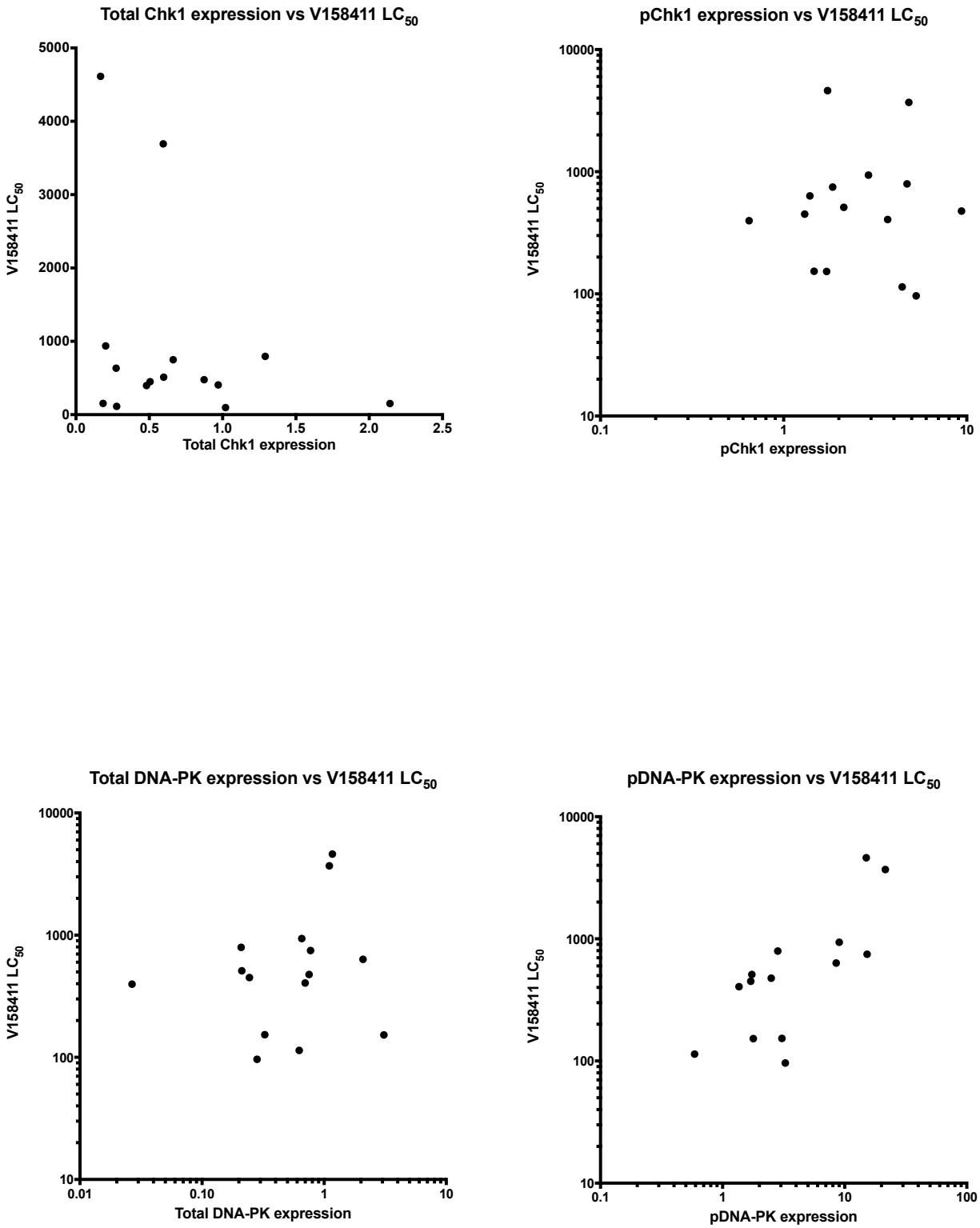

Figure 6-32 LC_{50} values and protein expression in all cell lines.

Correlation between V158411 LC_{50} values from a cell line panel including the liver cancer cell line panel and (a) total CHK1 expression, (b) $pCHK1^{serine296}$ expression 1 hour after 1 μM gemcitabine, (c) total DNA-PKcs expression and (d) $pDNA\text{-}PKcs^{serine2096}$ expression 1 hour after 2 Gy IR. Individual points constitute the mean expression levels from a summary of at least 3 experiments.

Using linear regression analysis, there was no correlation between V158411 LC_{50} and total CHK1 expression (r^2 = 0.08, p = 0.31), $pCHK1^{serine296}$ expression 1 hour after 1 μM gemcitabine (r^2 = 0.0004, p = 0.94), and total DNA-PKcs expression (r^2 = 0.018, p = 0.63). However, there was a correlation between V158411 LC_{50} and the expression of $pDNA\text{-}PK\text{-}cs^{serine2096}$ 1 hour after 10 Gy IR (r^2 = 0.63, p = 0.0007).

6.7 Discussion

The aim of this chapter was to explore the determinants of sensitivity to V158411 and in particular to identify factors that might make tumours and patients suitable for treatment with a CHK1 inhibitor as a single agent or in combination with another small molecular inhibitor of the DNA damage response system.

The starting point for this work was to examine the cytotoxicity of V158411 as a single agent in cells with specific DNA repair defects. For these studies we used the well characterised Chinese hamster ovary (CHO) and Chinese hamster lung fibroblast (CHLF) cells. There was no significant difference in sensitivity to single agent V158411 between the BRCA2 deficient VC8 and the BRCA2 corrected VC8-B2 CHLF cell lines indicating that HRR defects are not associated with CHK1 sensitivity. In contrast, CHO cell lines lacking XRCC1 (EM9) were more sensitive to V158411 than the parental AA8 cell line. XRCC1 is a scaffold protein in BER that is recruited to DNA SSB by PARP-1. Other authors have shown synergy between CHK1 inhibitors and PARP inhibitors (Mitchell et al., 2010a, Vance et al., 2011). Our data in CHLF cells suggests that the synergy between CHK1 and PARP inhibitors may be due to a BRCA2 independent mechanism. This suggests that BER defects may be synthetically lethal with CHK1 inhibitors.

Curiously the Ku-80- defective cells (XRS-6) were more sensitive but the V3 cell line that lacks DNA-PKcs was more resistant to V158411 than the parental AA8 cells. Since DNA-PKcs is recruited to DNA DSB by Ku80 and Ku70 to promote repair by NHEJ these observations may indicate that either (i) Ku80 has some

function, other than its role in NHEJ that protects cells from CHK1 inhibition or (ii) the role of DNA-PKcs in conferring sensitivity to V158411 would not appear to be linked to its role in NHEJ. There is growing evidence that DNA-PKcs acts as a regulator of the ATR-CHK1 pathway both through regulation of RPA/ATR and through direct activation of CHK1 at serine 345 (Serrano et al., 2013) (Khanna et al., 2013).

This led us to explore the cytotoxicity of V158411 in a glioblastoma cell line M059J which has a well characterised defect in DNA-PKcs and its paired cell line M059J-Fus1 in which functional DNA-PKcs has been restored by transfer of chromosome 8. The DNA-PKcs expressing cells were approximately 10-fold more sensitive to a 24 hour continuous exposure to single-agent V158411. To determine whether this interesting difference in sensitivity of the M059J cell line pair was unique to V158411 or a class-effect with other CHK1 inhibitors, the cytotoxicity of two other commercially available CHK1 inhibitors, AZD7762 and PF00477736, was compared in the M059J and M059J-Fus1. PF00477736 was similarly more cytotoxic to the M059J-Fus1 cell with a 3-fold lower LC_{50} than the M059J cells. There was, however, no difference in sensitivity between the cells with AZD7762. This might be explained by the observation that unlike the selective CHK1 inhibitors V158411 and PF00477736, AZD7762 is dual CHK1/CHK2 inhibitor.

A possible alternative explanation for the sensitivity complicating factor in the interpretation of these data is that the M059J-Fus1 cells were created by the transfer of chromosome 8 (the gene for *DNA-PKcs* is located on 8q11) these cells also express cMyc (located on 8q24). CHK1 inhibitors have previously been shown to be active as single agents in myc-amplified neuroblastomas and

lymphomas (Hoglund et al., 2011a, Hoglund et al., 2011b, Murga et al., 2011, Ferrao et al., 2011, Walton et al., 2012). So the increased sensitivity of the M059J-Fus1 cell line may be due to increased expression of myc leading to increased sensitivity to V158411. However, since the V3 cells, lacking DNA-PKcs, were also resistant to V158411, and they do not differ from parental AA8 cells in their Myc status, it is likely that DNA-PKcs itself is contributing to the sensitivity.

To explore this further the effects of the DNA-PKcs inhibitor NU7441 on the sensitivity of the paired glioblastoma cells to V158411 were investigated. As expected NU7441 had no effect in the M059J cells; however, it did confer resistance to V158411 in the M059J-Fus1 cells implicating the kinase activity of DNA-PKcs in the sensitivity to CHK1 inhibition. What exactly this role is remains to be identified. The data regarding the differential sensitivity of Ku80 and DNA-PKcs defective CHO cells would suggest that it is not related to its NHEJ function. DNA-PKcs has been implicated in the stabilization of c-Myc and, as described above, amplified Myc is associated with sensitivity to CHK1 inhibition (An et al., 2008).

To investigate the relationship between CHK1 and DNA-PKcs further the expression of the genes was examined in publically available archived mRNA microarrays. Analysis of data from mRNA expression arrays comparing normal tissue and tumour tissue from different tumour sites showed that in one dataset (CLL) there was no significant difference between CHK1 or DNA-PKcs expression in normal and tumour tissue. In another dataset (breast cancer) there was a discordant relationship with CHK1 being over-expressed in tumour tissue and DNA-PKcs being under-expressed. However, in three datasets from

patients with pancreatic cancer, NSCLC and HCC increased CHK1 and DNA-PKcs mRNA levels were seen in tumour tissue compared to normal tissue. Of greatest interest in the dataset from with liver disease and HCC, there was increasing dysregulation of both DNA-PKcs and CHK1 with the advancing stage of disease from normal liver tissue through to very advanced HCC. There was concordance between the mRNA expression levels, with samples with increased CHK1 levels also having increased DNA-PK levels.

The interesting relationship between CHK1 and DNA-PKcs in the HCC dataset led us to examine the sensitivity of a panel of 6 liver cancer cell lines to V158411 with or without the DNA-PKcs inhibitor 1 μM NU7441 24 hour co-treatment in clonogenic assays. The cells displayed a spectrum of sensitivity to V158411 and in all cases there was a modicum of protection by NU7441, which was significant in the case of the Huh7 cells.

To further explore if there is a relationship between V158411 cytotoxicity and DNA-PKcs; the baseline expression of DNA-PKcs, IR-induced activation of DNA-PKcs autophosphorylation at serine^{2096} and the baseline expression of CHK1 along with gemcitabine-induced autophosphorylation at serine^{296} was explored in the main cell line panel and the panel of 6 liver cancer cell lines.

There was no correlation between baseline CHK1 and DNA-PKcs expression or between the induced phosphorylation of CHK1^{serine296} and induced DNA-PKcs^{serine2096} phosphorylation. Furthermore, there was no correlation between the LC_{50} for V158411 in individual cell lines and the basal expression of either CHK1, DNA-PKcs or the induced phosphorylation of CHK1^{serine296} in the cell

lines. However, there was a correlation between the LC_{50} for V158411 and the induced phosphorylation of DNA-PKcs^{serine2096} 1 hour after 10 Gy IR.

This does not fit with our hypothesis, based on the work from CHO cells and M059J cells that cells that the lack of functional DNA-PKcs confers resistance to CHK1 inhibitors. It would seem more likely that DNA-PKcs acts as an important regulator of the ATR-CHK1 pathway, and that is not simply its presence or absence that confers sensitivity to CHK1 inhibitors, but its time-sensitive inducible function that plays a critical role in the efficacy of CHK1 inhibitors.

Chapter 7 Conclusion

The first priority of the work presented here was to develop a means to measure the extent of CHK1 inhibition so that suitable concentrations of V158411 could be selected for subsequent experiments and to identify a potential biomarker that could be used to measure the pharmacodynamic effect of CHK1 inhibitors in clinical trials.

Total CHK1 expression, CHK1^{serine296} phosphorylation and CHK1^{serine345} phosphorylation was investigated in western blots using lysates from cancer cell lines and a number of assays validated. The choice of a biomarker for use with single agent V158411 is more difficult; CHK1^{serine296} autophosphorylation was reduced by a 1 hour exposure to V158411, but as the baseline level of CHK1^{serine296} phosphorylation is very low the sensitivity of such a test is reduced and is not practical for clinical trial biomarker use.

The selection of a potential biomarker for use in combination with cytotoxic therapy or in an *ex vivo* stimulation assay is more straight forward. CHK1^{serine296} autophosphorylation was reliably induced by a short (1 hour) exposure to cytotoxic (1 μM gemcitabine). This increase was abrogated in a concentration-dependent fashion by 50, 150 and 500 nM V158411 respectively. A 1 hour treatment with gemcitabine or V158411 increased CHK1^{serine345} phosphorylation; combination of the agents was additive, but not synergistic. Hence, CHK1^{serine345} phosphorylation is probably less helpful as a biomarker in combination studies.

CHK1^{serine345} phosphorylation was reliably increased in the presence of V158411. As this is not a downstream event of CHK1 inhibition, it cannot be

used a proof-of-mechanism biomarker, but could be used as a measure of CHK1 inhibition, if other factors such as the phosphorylation of serine^{345} (e.g. ATR after DNA damage) could be controlled. Other downstream targets of CHK1 were explored in preliminary studies that are not presented in this thesis. Cdc25A expression was not found to change in a reliable or specific fashion following short 1 hour exposures to cytotoxic agents (1 μM gemcitabine or 10 mM hydroxyurea) or with 50, 150 or 500 nM V158411. An ELISA assay for Wee1 phosphorylation as a downstream assay of CHK1 function was also explored during this project. Unfortunately the assay was not sensitive during early work, but with further development could be an alternative downstream biomarker of CHK1 inhibition.

The mechanism of cytotoxicity for single agent V158411 was only partly determined by this work. It appears to be potentially related to CHK1 inhibition, as siRNA knockdown of *CHK1* in MCF7 cells was cytotoxic in clonogenic assays. V158411 as a single agent reliably reduced the fraction of cells in G_2 of the cell cycle. However, whether the cytotoxicity of V158411 is related to the role of CHK1 in cell cycle regulation at the S and G_2 cell cycle checkpoints, or via an alternative mechanism is unclear. Further mechanistic exploration of this is required. The effect of V158411 at the S phase checkpoint could be more reliably determined by using a staining technique such as BrdU-labelling to accurately quantify the proportion of cells in S phase.

The work to determine the specificity of V158411 was hampered by the non-viability of the *CHK1* siRNA knockdown. Alternative strategies to explore the specificity of V158411 would be the development of an inducible kinase-dead *CHK1* cell line, or a cell line with a mutation at the serine^{296} phosphorylation site

or a cell line mimicking a constitutively phosphorylated (and therefore activated) CHK1^{serine296}.

This work shows that V158411 has significant single agent activity. The LC_{50} of V158411 in MCF7 breast cancer cells was 113 nM despite there only being 45% inhibition of Chk1^{serine296} phosphorylation with 150 nM V158411. In K562 CML cells the LC_{50} was 152 nM with approximately 50% inhibition of Chk1^{serine296} phosphorylation with 150 nM. This suggests that only partial CHK1 inhibition results in significant cytotoxicity or that cytotoxicity is not entirely dependent on CHK1 inhibition. Germline *CHK1* +/- mice do not have tumours that lose the second allele (Liu et al., 2000). This suggests that *CHK1* is a haploinsufficient tumour suppressor gene. However, Lam et al demonstrated that haploinsufficiency in *CHK1* heterozygotes leads to cells accumulate DNA damage following inappropriate S phase entry and a failure to restrain entry into mitosis (Lam et al., 2004). This raises the concern that the use of a CHK1 inhibitor may cause problems in normal tissue, and may lead to significant toxicity limiting the therapeutic window.

A potential hypothesis for the mechanism of single agent cytotoxicity of V158411 can be based on data by Drew (Drew et al., 2011). They showed that inhibition of DNA repair for 24 hours (with the PARP inhibitor AG014699 10 μM in HCC1937 cells) led to an equivalent level of DNA damage (as quantified by γH2AX foci) as to the exposure of cells to 2 Gy of ionising radiation. This suggests that the level of spontaneous DNA damage is high in all cells. In cancer cells, with an absent G_1 checkpoint, the exposure to V158411 for 24 hours leads to cells continuing through the G_2 checkpoint without stopping to

facilitate DNA repair. This results in the acquisition of significant levels of DNA damage accounting for the single agent cytotoxicity of V158411.

There is relatively sparse pre-clinical data in the literature on the cytotoxicity of other CHK1 inhibitors used as single agents. Some activity has been seen in cancer cell lines with 300 nM XL9844 for 24 hours, 100 nM AZD7762 for 25 hours, and 500 nM SCH 900776 for 24 hours, though with all compounds more cell lines showed minimal cytotoxicity than were sensitive (Matthews et al., 2007, Mitchell et al., 2010b, Montano et al., 2012). However, in light of the single agent activity seen in this work (12 cell lines with an LC_{50} between 100 nM and 1000 nM) and in work performed by Vernalis in triple–negative breast, ovarian, lymphoma and leukaemia cell lines (Bryant et al., 2014a, Bryant et al., 2014b), further work to assess the efficacy of single agent V158411 in animal models and then potentially in early phase clinical trials should be considered.

The work outlined in this thesis did not show synergistic cytotoxicity when V158411 was combined with gemcitabine or cisplatin. This is despite there being significant inhibition of CHK1 activity (as determined by $CHK1^{serine296}$ phosphorylation) and abrogation of cisplatin-mediated cell cycle arrest (in HCT116 cells). This is in contrast to work with many other CHK1 inhibitors, where there is enhancement of cytotoxicity due to CHK1 inhibition in combination with a range of cytotoxic agents. There is pre-clinical and early phase clinical trial data demonstrating potential synergism between AZD7762 and gemcitabine (Zabludoff et al., 2008, McNeely et al., 2010, Seto et al., 2013, Sausville et al., 2014), and SCH 900776 and gemcitabine (Montano et al., 2012, Guzi et al., 2011, Daud et al., 2010).

Cisplatin has been used in other pre-clinical studies in combination with CHK1 inhibitors with mixed results. Bunch and Eastman showed chemosensitisation of cisplatin in CHO and breast cancer cell lines with UCN-01 and ICP-1 (Bunch and Eastman, 1996, Eastman et al., 2002). However, Wagner and Karnitz failed to demonstrate any chemosensitisation with UCN-01 and AZD7762 in HeLa cells (Wagner and Karnitz, 2009).

One potential explanation for the lack of chemopotentiation is that the concentrations of both V158411 and gemcitabine were cytotoxic as single agents, additivity was seen, but not synergism. Other studies have not always used clonogenic assays to assess cytotoxicity and it is sometimes unclear whether the data has been normalised to ensure that potentiation rather than additivity is being seen.

This is not to say that V158411 may not show synergism with other conventional cytotoxics. This would require additional *in vivo* and *in vitro* studies. It may be that V158411 needs to be present for longer than 24 hours following exposure to a conventional cytotoxic, though the work described in Section 4.3 with single agent V158411 suggested that a shorter duration exposure to a higher concentration of V158411 was more cytotoxic than a longer exposure to a lower concentration of V158411. Following the work of Calvo, using LY2603618 in combination with pemetrexed +/- cisplatin showing significant chemopotentiation; it would be interesting to explore in *in vitro* studies whether V158411 showed any chemopotentiation with this combination (Calvo et al., 2014).

The data that V158411 may act as a radiosensitiser are encouraging (see Section 4.7). V158411 was shown to significantly abrogate IR-mediated G_2 cell cycle arrest and significantly potentiated the cytotoxicity of IR in (MCF7 and HCT116 wild type and $p53^{-/-}$ cells). However, there are significant challenges using agents as radiosensitisers in *in vivo* studies and in clinical studies. In clinical practice, palliative radiotherapy is sometimes given as a single fraction (8 Gy for instance in cases of isolated bone metastases) or when a patient is too frail to attend on consecutive days for radiotherapy. However, most radiation regimens, both curative and palliative, involve multiple fractions (normally doses of 0.5-2 Gy per fraction) of radiotherapy given on consecutive days. An additional problem with using single palliative fractions of radiotherapy in combination trials with novel agents, is that the aim of such treatment is normally to palliate symptoms in patients nearing the end of their life and that output measures to evaluate efficacy are rare.

In an early phase drug-only trial, it is normal to wait for 3-6 weeks to observe toxicity; however, when combining a novel agent with radiotherapy the potential that the novel therapy has potentiated the side effects of radiotherapy means that the delay has to be considerably longer (Zaidi et al., 2009). Radiation experts recommend waiting at least 6 weeks between cohorts to detect problems like acute lung toxicity from radiation. The implications of this are that radiosensitisation trials are generally slow to recruit and complete. It is very difficult to detect true late side effects from novel cytotoxics in combination with radiation in an early phase clinical trial, as cardiac side effects such as accelerated coronary artery disease are only seen after a number of years and the prognosis for most patients in early phase clinical trials is around 12 weeks.

V158411 is an intravenous compound, some other CHK1 inhibitors are bioavailable as oral compounds, XL9844, GNE-900, and CCT244747, GDC-0425 and GDC-0575 (Matthews et al., 2007, Blackwood et al., 2013, Walton et al., 2012). Oral CHK1 inhibitors would be more suitable to use in combination with radiotherapy. Common radical or high-dose palliative radiotherapy regimens normal involve daily fractions of radiotherapy for 4 to 6 weeks. Administering a daily intravenous infusion would not be practical over a 4 to 6 week period, but a once or twice a day oral inhibitor would be accepted by patients and doctors alike.

The data presented in Chapter 5 suggested that there was no relationship between single agent V158411 cytotoxicity, chemo-sensitisation or radio-sensitisation and p53 status. This may be because loss of G_1 cell cycle checkpoint control is very common in cancer; p53 is only one of a number of elements of the G_1 cell cycle checkpoint control pathway that may lost or non-functional leading to a dependence in cancer cells on the S and G_2 checkpoints (Massague, 2004). A further implication of this is that p53 status is not likely to be a suitable biomarker for patient stratification. Nevertheless it may be useful to investigate the relationship between the clinical outcome and p53 status of the diagnostic biopsy. This approach has been employed by the investigators in the Phase 1 clinical trial of SCH 900776 in combination with gemcitabine, though no correlation between p53 status and outcome has been presented in the data that has been released thus far (Daud et al., 2010).

Data published by Dai suggested that inhibition of the Ras/MEK/ERK pathway with a small molecular inhibitor (AZD6244 – a MEK 1/2 inhibitor) conferred sensitivity to the CHK1 inhibitor UCN-01 (Dai et al., 2002). Myc amplification

was shown to confer sensitivity to CHK1 inhibition in lymphomas (Hoglund et al., 2011a) and in neuroblastomas (Walton et al., 2012). Further pre-clinical work exploring whether the relative sensitivity and resistance of the cell lines to V158411 might be correlated with myc, Ras, MEK, and ERK expression would be useful. Exploratory examination of Ras, MEK, ERK and myc mRNA and protein expression levels in tumour samples from patients in early phase clinical trials may also be informative if this could be correlated with clinical outcome data.

The data presented in Chapter 6 shows that other elements of the DNA damage response may also play a role in determining the sensitivity to V158411. Of great interest from is that CHO cells lacking functional DNA-PKcs were relatively resistant to single agent V158411. In the glioblastoma cell line pair M059J cells lacking functional DNA-PKcs were more resistant to V158411 than M059J-Fus1 cells. Co-treatment with a DNA-PKcs inhibitor (NU7741) made the M059J-Fus1 cells more resistant to V158411. This phenomenon was seen with AZD7762 and PF00477736 suggesting that this is not an effect limited to V158411, but a class effect with CHK1 inhibitors. This suggests that in the absence of functional DNA-PKcs cells are resistant to CHK1-mediated cytotoxicity. Analysis of archived mRNA data from normal tissue and tumours suggested that both CHK1 and DNA-PKcs mRNA levels were commonly both up-regulated/dysregulated in tumour samples compared to normal tissues.

The data suggests that the LC_{50} of V158411 on its own in cancer cell lines may correlate to the inducible (2 Gy IR) phosphorylation of DNA-PKcs^{serine2096}. Cell lines with a low level of inducible DNA-PKcs^{serine2096} phosphorylation were more sensitive to V158411 in clonogenic assays. Conversely, high levels of inducible

DNA-PKcs^{serine2096} phosphorylation were associated with relative resistance to V158411. This is in contrast to the data suggesting that loss of DNA-PKcs or the presence of a DNA-PKcs inhibitor correlates with resistance to CHK1-mediated cytotoxicity. DNA-PKcs a role in regulation and control of the CHK1-ATR pathway (as proposed in Figure 6-2), but this relationship is likely to be complex.

This data suggests that it may be useful to attempt to correlate the PK and efficacy data from early phase clinical trials with the potential data from an *ex vivo* assessment of the inducible phosphorylation of DNA-PKcs^{serine2096} on patient material. Exploratory examination of other components of the NHEJ pathway including such as Ku70, Ku80, as well as total CHK1 and DNA-PKcs mRNA levels and protein expression levels in tumour samples from patients in early phase clinical trials may also be informative.

The only single agent CHK1 inhibitor early phase clinical trial to date has been with the oral CHK1 inhibitor LY2606368. No pre-clinical data with this compound has been published. The first-in-human Phase I clinical trial of V158411 was due to have a single-agent run in phase, with V158411 delivered on Day 1 and Day 8 of a cycle 0, prior to the delivery of V158411 in combination with conventional cytotoxics. A single agent V158411 alone arm should be considered either as a stand-alone Phase 1 clinical trial or as an additional arm on the existing combination trial as it is currently proposed. This would give the recommended Phase II dose (RP2D) of V158411 alone for use in future trials.

A protocol for the first-in-human Phase I clinical trial of V158411 in combination with single agent carboplatin or gemcitabine or the combination of gemcitabine

and carboplatin has been prepared and Vernalis are actively looking to partner the project.

There will obviously be concern about potential cardiac toxicity with any first-in-man CHK1 inhibitor trials, including V158411. Cardiac toxicity seen with AZD7762, which led to the clinical development of the compound being abandoned (Sausville et al., 2014, Seto et al., 2013). Cardiac toxicity had been seen in the pre-clinical animal toxicity work.

As other early phase clinical trials have not reported any cardiac toxicity it is likely that the cardiac toxicity seen with AZD7762 is not a class effect and specific to the compound. AZD7762 is not a selective CHK1 inhibitor and has activity against a number of other kinase targets. The inhibition of receptor tyrosine kinases (RTKs) is known to be associated with cardiac toxicity (Force and Kolaja, 2011).

However, it would be prudent to have strict inclusion criteria for entrants into clinical trials excluding any patients with potentially increased cardiac risk. Increased cardiac monitoring for patients in early phase clinical trials including baseline ECHO/MUGA, serial ECGs and cardiac troponin monitoring should also be considered.

Following on from the work presented here on the choice of a suitable biomarker, there is also the issue of the type of biomarker material for animal studies and early phase clinical trials. There has to be balance between the technical difficulty in obtaining biomarker material, whether obtaining material is burdensome to the patient and the suitability of the material for biomarker work. The sampling of blood is technically easy, tolerable to the patient, but presents

a problem for developing a biomarker for a cell cycle checkpoint inhibitor, as most PBMCs are not actively cycling, but in G_0. Hair follicles have been used (Fong et al., 2009), plucking and obtaining good quality hair follicles can be time consuming and the preparation of material is fiddly, time-consuming whilst yielding only small volumes of material.

With respect to solid biopsy material, biopsies of normal skin tissue to use as a surrogate tissue are technically relatively easy to collect and process. Using normal skin as a surrogate tissue has been used as a biomarker in radiotherapy trials (Qvarnstrom et al., 2004). Repeated biopsies of skin may be unacceptable to some patients. Often the 'gold-standard' tissue to collect is a sample of the patient's tumour. This may carry a morbidity and even a mortality risk and depending on the location tumour be technically challenging. An additional problem is tumour heterogeneity; the sample biopsied may not be representative of the whole tumour (Chan and Bristow, 2010). For these reasons, repeated biopsies of patient's tumours are not normally acceptable to the patient or physician.

However, the antibodies used in this work were only validated in western blotting. Western blotting could be performed in PBMCs and material from hair follicles, but is not suitable for other material. New antibodies for CHK1^{serine296} are now available; and it would be interesting to explore whether these could be used in other applications. If the antibodies were shown to be suitable for immunohistochemistry (IHC) then it may be possible to look for CHK1^{serine296} phosphorylation following cytotoxic therapy, with and without a CHK1 inhibitor, in either tumour or normal skin biopsy tissue in mice or patients receiving early phase clinical trials.

If the newer antibodies worked in flow cytometry, it opens up the possibility that in future studies, changes in CHK1^{serine296} phosphorylation in circulating tumour cells (CTCs), could be explored using imaging flow cytometry (eg: Imagestream platform). The potential pitfalls of such an approach are that CTCs are not present in all cancer patients and in those patients who do have CTCs they can vary widely in number (Nole et al., 2008). There is also concern as to whether CTCs truly represent the biology of the primary tumour.

In conclusion V158411 is a novel CHK1 inhibitor that shows potential as both a single agent drug and in combination with radiotherapy. A phase I trial should seek to determine the single agent MTD of V158411 and the MTD in combination with ionising radiation. There is no evidence to select patients for clinical trials based on the p53 status of their tumour, but it would be useful to correlate this information and data on other elements of the DNA repair pathway against efficacy in early phase clinical trials. Further development of CHK1^{serine296} phosphorylation as a biomarker for use in clinical trials is also warranted.

References

ABULAITI, A., FIKARIS, A. J., TSYGANKOVA, O. M. & MEINKOTH, J. L. 2006. Ras induces chromosome instability and abrogation of the DNA damage response. *Cancer Res,* 66**,** 10505-12.

ACHARYA, S., WILSON, T., GRADIA, S., KANE, M. F., GUERRETTE, S., MARSISCHKY, G. T., KOLODNER, R. & FISHEL, R. 1996. hMSH2 forms specific mispair-binding complexes with hMSH3 and hMSH6. *Proc Nat Academy Sciences,* 93**,** 13629-34.

ALLALUNIS-TURNER, M. J., ZIA, P. K., BARRON, G. M., MIRZAYANS, R. & DAY, R. S., 3RD 1995. Radiation-induced DNA damage and repair in cells of a radiosensitive human malignant glioma cell line. *Radiat Res,* 144**,** 288-93.

AN, J., YANG, D. Y., XU, Q. Z., ZHANG, S. M., HUO, Y. Y., SHANG, Z. F., WANG, Y., WU, D. C. & ZHOU, P. K. 2008. DNA-dependent protein kinase catalytic subunit modulates the stability of c-Myc oncoprotein. *Mol Cancer,* 7**,** 32.

ANNUNZIATA, C. M. & O'SHAUGHNESSY, J. 2010. Poly (adp-ribose) polymerase as a novel therapeutic target in cancer. *Clin Cancer Res,* 16**,** 4517-26.

AYLON, Y., LIEFSHITZ, B. & KUPIEC, M. 2004. The CDK regulates repair of double-strand breaks by homologous recombination during the cell cycle. *EMBO J,* 23**,** 4868-75.

BADEA, L., HERLEA, V., DIMA, S. O., DUMITRASCU, T. & POPESCU, I. 2008. Combined gene expression analysis of whole-tissue and microdissected pancreatic ductal adenocarcinoma identifies genes specifically overexpressed in tumor epithelia. *Hepato-gastroenterology,* 55**,** 2016-27.

BAHASSI, E. M., OVESEN, J. L., RIESENBERG, A. L., BERNSTEIN, W. Z., HASTY, P. E. & STAMBROOK, P. J. 2008. The checkpoint kinases CHK1 and CHK2 regulate the functional associations between hBRCA2 and Rad51 in response to DNA damage. *Oncogene,* 27**,** 3977-85.

BENNETT, C. B., SNIPE, J. R. & RESNICK, M. A. 1997. A persistent double-strand break destabilizes human DNA in yeast and can lead to G2 arrest and lethality. *Cancer Res,* 57**,** 1970-80.

BLACKWOOD, E., EPLER, J., YEN, I., FLAGELLA, M., O'BRIEN, T., EVANGELISTA, M., SCHMIDT, S., XIAO, Y., CHOI, J., KOWANETZ, K., RAMISCAL, J., WONG, K., JAKUBIAK, D., YEE, S., CAIN, G., GAZZARD, L., WILLIAMS, K., HALLADAY, J., JACKSON, P. K. & MALEK, S. 2013. Combination drug scheduling defines a "window of opportunity" for chemopotentiation of gemcitabine by an orally bioavailable, selective CHK1 inhibitor, GNE-900. *Mol Cancer Ther,* 12**,** 1968-80.

BLASINA, A., HALLIN, J., CHEN, E., ARANGO, M. E., KRAYNOV, E., REGISTER, J., GRANT, S., NINKOVIC, S., CHEN, P., NICHOLS, T., O'CONNOR, P. & ANDERES, K. 2008. Breaching the DNA damage checkpoint via PF-00477736, a novel small-molecule inhibitor of checkpoint kinase 1. *Mol Cancer Ther,* 7**,** 2394-404.

BOUWMAN, P. & JONKERS, J. 2012. The effects of deregulated DNA damage signalling on cancer chemotherapy response and resistance. *Nat Rev Cancer,* 12**,** 587-98.

BREGA, N., MCARTHUR, C., BRITTEN, S., WONG, S., WANG, E., WILNER, K., BLASINA, A., SCHWARTZ, G. K., GALLO, J. & TSE, A. N. 2010. Phase 1 clinical trial of gemcitablne (GEM) in combination with PF-00477736 (PF-736), a selective inhibitor of CHK1 kinase. *ASCO Annual Meeting 2010.* Chicago.

BRYANT, C., RAWLINSON, R., MASSEY, A. J. 2014a. CHK1 inhibition as a novel theraputic strategy for treating triple-negative breast and ovarian cancers. *BMC cancer.* 14, 570-584

BRYANT, C., SCRIVEN, K. & MASSEY, A. J. 2014b. Inhibition of the checkpoint kinase Chk1 induces DNA damage and cell death in human Leukemia and Lymphoma cells. *Mol Cancer,* 13**,** 147.

BUNCH, R. T. & EASTMAN, A. 1996. Enhancement of cisplatin-induced cytotoxicity by 7-hydroxystaurosporine (UCN-01), a new G2-checkpoint inhibitor. *Clin Cancer Res,* 2**,** 791-7.

BURDAK-ROTHKAMM, S. & PRISE, K. M. 2009. New molecular targets in radiotherapy: DNA damage signalling and repair in targeted and non-targeted cells. *Eur J Pharmacol,* 625**,** 151-5.

BUSCHTA-HEDAYAT, N., BUTERIN, T., HESS, M. T., MISSURA, M. & NAEGELI, H. 1999. Recognition of nonhybridizing base pairs during nucleotide excision repair of DNA. *Proc Nat Academy Sci,* 96**,** 6090-5.

CALVO, E., CHEN, V. J., MARSHALL, M., OHNMACHT, U., HYNES, S. M., KUMM, E., DIAZ, H. B., BARNARD, D., MERZOUG, F. F., HUBER, L., KAYS, L., IVERSEN, P., CALLES, A., VOSS, B., LIN, A. B., DICKGREBER, N., WEHLER, T. & SEBASTIAN, M. 2014. Preclinical

analyses and phase I evaluation of LY2603618 administered in combination with Pemetrexed and cisplatin in patients with advanced cancer. *Invest New Drugs*.

CARLESSI, L., DE FILIPPIS, L., LECIS, D., VESCOVI, A. & DELIA, D. 2009. DNA-damage response, survival and differentiation in vitro of a human neural stem cell line in relation to ATM expression. *Cell Death Differ,* 16**,** 795-806.

CARRASSA, L., SANCHEZ, Y., ERBA, E. & DAMIA, G. 2009. U2OS cells lacking CHK1 undergo aberrant mitosis and fail to activate the spindle checkpoint. *J Cell Mol Med,* 13**,** 1565-76.

CHAN, N. & BRISTOW, R. G. 2010. "Contextual" Synthetic Lethality and/or Loss of Heterozygosity: Tumor Hypoxia and Modification of DNA Repair. *Clin Cancer Res,* 16**,** 4553-60.

CHEN, B. P., LI, M. & ASAITHAMBY, A. 2012. New insights into the roles of ATM and DNA-PKcs in the cellular response to oxidative stress. *Cancer Lett,* 327**,** 103-10.

CHEN, P., LUO, C., DENG, Y., RYAN, K., REGISTER, J., MARGOSIAK, S., TEMPCZYK-RUSSELL, A., NGUYEN, B., MYERS, P., LUNDGREN, K., KAN, C. C. & O'CONNOR, P. M. 2000. The 1.7 A crystal structure of human cell cycle checkpoint kinase CHK1: implications for CHK1 regulation. *Cell,* 100**,** 681-92.

CHEN, Y. & SANCHEZ, Y. 2004. CHK1 in the DNA damage response: conserved roles from yeasts to mammals. *DNA Repair (Amst),* 3**,** 1025-32.

CLARKE, C. A. & CLARKE, P. R. 2005. DNA-dependent phosphorylation of CHK1 and Claspin in a human cell-free system. *Biochem J,* 388**,** 705-12.

COLE, K. A., HUGGINS, J., LAQUAGLIA, M., HULDERMAN, C. E., RUSSELL, M. R., BOSSE, K., DISKIN, S. J., ATTIYEH, E. F., SENNETT, R., NORRIS, G., LAUDENSLAGER, M., WOOD, A. C., MAYES, P. A., JAGANNATHAN, J., WINTER, C., MOSSE, Y. P. & MARIS, J. M. 2011. RNAi screen of the protein kinome identifies checkpoint kinase 1 (CHK1) as a therapeutic target in neuroblastoma. *Proc Natl Acad Sci,* 108**,** 3336-41.

COURAGE, C., BUDWORTH, J. & GESCHER, A. 1995. Comparison of ability of protein kinase C inhibitors to arrest cell growth and to alter cellular protein kinase C localisation. *Br J Cancer,* 71**,** 697-704.

CURTIN, N. J. 2012. DNA repair dysregulation from cancer driver to therapeutic target. *Nature Rev Cancer,* 12**,** 801-17.

D'ADDA DI FAGAGNA, F., REAPER, P. M., CLAY-FARRACE, L., FIEGLER, H., CARR, P., VON ZGLINICKI, T., SARETZKI, G., CARTER, N. P. & JACKSON, S. P. 2003. A DNA damage checkpoint response in telomere-initiated senescence. *Nature,* 426**,** 194-8.

DAEMEN, A., WOLF, D. M., KORKOLA, J. E., GRIFFITH, O. L., FRANKUM, J. R., BROUGH, R., JAKKULA, L. R., WANG, N. J., NATRAJAN, R., REIS-FILHO, J. S., LORD, C. J., ASHWORTH, A., SPELLMAN, P. T., GRAY, J. W. & VAN'T VEER, L. J. 2012. Cross-platform pathway-based analysis identifies markers of response to the PARP inhibitor olaparib. *Breast Cancer Res Treat,* 135**,** 505-17.

DAI, Y., CHEN, S., PEI, X. Y., ALMENARA, J. A., KRAMER, L. B., VENDITTI, C. A., DENT, P. & GRANT, S. 2008. Interruption of the Ras/MEK/ERK signaling cascade enhances CHK1 inhibitor-induced DNA damage in vitro and in vivo in human multiple myeloma cells. *Blood,* 112**,** 2439-49.

DAI, Y., LANDOWSKI, T. H., ROSEN, S. T., DENT, P. & GRANT, S. 2002. Combined treatment with the checkpoint abrogator UCN-01 and MEK1/2 inhibitors potently induces apoptosis in drug-sensitive and -resistant myeloma cells through an IL-6-independent mechanism. *Blood,* 100**,** 3333-43.

DART, D. A., ADAMS, K. E., AKERMAN, I. & LAKIN, N. D. 2004. Recruitment of the cell cycle checkpoint kinase ATR to chromatin during S-phase. *J Biol Chem,* 279**,** 16433-40.

DAUD, A., SPRINGETT, G., MENDLESON, D., MUNSTER, P., GOLDMAN, J., STROSBERG, J., KATO, G., NESHEIWAT, T., ISAACS, R. & ROSEN, L. 2010. A Phase I dose-escalation study of SCH-900776, a selective inhibitor of checkpoint 1 (CHK1), in combination with gemcitabine (Gem) in subjects with advanced solid tumours. *ASCO Annual Meeting 2010.* Chicago.

DE VOS, M., SCHREIBER, V. & DANTZER, F. 2012. The diverse roles and clinical relevance of PARPs in DNA damage repair: current state of the art. *Biochem Pharmacol,* 84**,** 137-46.

DEES, E. C., BAKER, S. D., O'REILLY, S., RUDEK, M. A., DAVIDSON, S. B., AYLESWORTH, C., ELZA-BROWN, K., CARDUCCI, M. A. & DONEHOWER, R. C. 2005. A phase I and pharmacokinetic study of short infusions of UCN-01 in patients with refractory solid tumors. *Clin Cancer Res,* 11**,** 664-71.

DING, M., ZHANG, E., HE, R. & WANG, X. 2013. Newly developed strategies for improving sensitivity to radiation by targeting signal pathways in cancer therapy. *Cancer Sci,* 104**,** 1401-10.

DREW, Y., MULLIGAN, E. A., VONG, W. T., THOMAS, H. D., KAHN, S., KYLE, S., MUKHOPADHYAY, A., LOS, G., HOSTOMSKY, Z., PLUMMER, E. R., EDMONDSON, R. J. & CURTIN, N. J. 2011. Therapeutic potential of poly(ADP-ribose) polymerase inhibitor AG014699 in human cancers with mutated or methylated BRCA1 or BRCA2. *J Nat Cancer Institute,* 103**,** 334-46.

DUENSING, A., TENG, X., LIU, Y., TSENG, M., SPARDY, N. & DUENSING, S. 2006. A role of the mitotic spindle checkpoint in the cellular response to DNA replication stress. *J Cell Biochem,* 99**,** 759-69.

DUROCHER, D. & JACKSON, S. P. 2001. DNA-PK, ATM and ATR as sensors of DNA damage: variations on a theme? *Curr Opin Cell Biol,* 13**,** 225-31.

EASTMAN, A., KOHN, E. A., BROWN, M. K., RATHMAN, J., LIVINGSTONE, M., BLANK, D. H. & GRIBBLE, G. W. 2002. A novel indolocarbazole, ICP-1, abrogates DNA damage-induced cell cycle arrest and enhances cytotoxicity: similarities and differences to the cell cycle checkpoint abrogator UCN-01. *Mol Cancer Ther,* 1**,** 1067-78.

EL-DEIRY, W. S. 2003. The role of p53 in chemosensitivity and radiosensitivity. *Oncogene,* 22**,** 7486-95.

FERGUSON, A. M., WHITE, L. S., DONOVAN, P. J. & PIWNICA-WORMS, H. 2005. Normal cell cycle and checkpoint responses in mice and cells lacking Cdc25B and Cdc25C protein phosphatases. *Mol Cell Biol,* 25**,** 2853-60.

FERRAO, P. T., BUKCZYNSKA, E. P., JOHNSTONE, R. W. & MCARTHUR, G. A. 2011. Efficacy of CHK inhibitors as single agents in MYC-driven lymphoma cells. *Oncogene*.

FONG, P., BOSS, D., YAP, T., TUTT, A., WU, P., MERGUI-ROELVINK, M., MORTIMER, P., SWAISLAND, H., LAU, A., O'CONNOR, M., ASHWORTH, A., CARMICHAEL, J., KAYE, S., SCHELLENS, J. & DE BONO, J. 2009. Inhibition of Poly(ADP-Ribose) Polymerase in Tumors from BRCA Mutation Carriers. *N Engl J Med,* 361.

FORCE, T. & KOLAJA, K. L. 2011. Cardiotoxicity of kinase inhibitors: the prediction and translation of preclinical models to clinical outcomes. *Nat Rev Drug Discov,* 10**,** 111-26.

GILAD, O., NABET, B. Y., RAGLAND, R. L., SCHOPPY, D. W., SMITH, K. D., DURHAM, A. C. & BROWN, E. J. 2010. Combining ATR suppression with oncogenic Ras synergistically increases genomic instability, causing synthetic lethality or tumorigenesis in a dosage-dependent manner. *Cancer Res,* 70**,** 9693-702.

GUTIERREZ, A., JR., TSCHUMPER, R. C., WU, X., SHANAFELT, T. D., ECKEL-PASSOW, J., HUDDLESTON, P. M., 3RD, SLAGER, S. L., KAY, N. E. & JELINEK, D. F. 2010. LEF-1 is a prosurvival factor in chronic lymphocytic leukemia and is expressed in the preleukemic state of monoclonal B-cell lymphocytosis. *Blood,* 116**,** 2975-83.

GUZI, T. J., PARUCH, K., DWYER, M. P., LABROLI, M., SHANAHAN, F., DAVIS, N., TARICANI, L., WISWELL, D., SEGHEZZI, W., PENAFLOR, E., BHAGWAT, B., WANG, W., GU, D., HSIEH, Y., LEE, S., LIU, M. & PARRY, D. 2011. Targeting the Replication Checkpoint Using SCH 900776, a Potent and Functionally Selective CHK1 Inhibitor Identified via High Content Screening. *Mol Cancer Ther,* 10**,** 591-602.

HALLIWELL, B. 2007. Oxidative stress and cancer: have we moved forward? *Biochem J,* 401**,** 1-11.

HANAHAN, D. & WEINBERG, R. A. 2011. Hallmarks of cancer: the next generation. *Cell,* 144**,** 646-74.

HANDE, K. R. 1998. Etoposide: four decades of development of a topoisomerase II inhibitor. *Eur J Cancer,* 34**,** 1514-21.

HARPER, J. V., ANDERSON, J. A. & O'NEILL, P. 2010. Radiation induced DNA DSBs: Contribution from stalled replication forks? *DNA Repair (Amst),* 9**,** 907-13.

HIROSE, Y., BERGER, M. S. & PIEPER, R. O. 2001. Abrogation of the Chk1-mediated G(2) checkpoint pathway potentiates temozolomide-induced toxicity in a p53-independent manner in human glioblastoma cells. *Cancer Res,* 61**,** 5843-9.

HO, A. L., BENDELL, J. C., CLEARY, J. M., SCHWARTZ, G., BURRIS, H. A., OAKES, P., AGBO, F., BARKER, P. N., SENDEROWICZ, A. M. & SHAPIRO, G. I. 2011. Phase 1, open-label, dose-escalation study of AZD7762 in combination with irinotecan (irino) in patients (pts) with advanced solid tumours. *ASCO Annual Meeting 2011.*

HOEIJMAKERS, J. H. 2001. Genome maintenance mechanisms for preventing cancer. *Nature,* 411**,** 366-74.

HOEIJMAKERS, J. H. 2009. DNA damage, aging, and cancer. *N Engl J Med,* 361**,** 1475-85.

HOGLUND, A., NILSSON, L. M., MURALIDHARAN, S. V., HASVOLD, L. A., MERTA, P., RUDELIUS, M., NIKOLOVA, V., KELLER, U. & NILSSON, J. A. 2011a. Therapeutic implications for the induced levels of CHK1 in myc-expressing cancer cells. *Clin Cancer Res,* 17**,** 7067-79.

HOGLUND, A., STROMVALL, K., LI, Y., FORSHELL, L. P. & NILSSON, J. A. 2011b. CHK2 deficiency in Myc overexpressing lymphoma cells elicits a synergistic lethal response in combination with PARP inhibition. *Cell Cycle,* 10**,** 3598-607.

HOTTE, S. J., OZA, A., WINQUIST, E. W., MOORE, M., CHEN, E. X., BROWN, S., POND, G. R., DANCEY, J. E. & HIRTE, H. W. 2006. Phase I trial of UCN-01 in combination with topotecan in patients with advanced solid cancers: a Princess Margaret Hospital Phase II Consortium study. *Ann Oncol,* 17**,** 334-40.

HUANG, P., CHUBB, S., HERTEL, L. W., GRINDEY, G. B. & PLUNKETT, W. 1991. Action of 2',2'-difluorodeoxycytidine on DNA synthesis. *Cancer Res,* 51**,** 6110-7.

IRVING, J. A. & HALL, A. G. 2001. Mismatch repair defects as a cause of resistance to cytotoxic drugs. *Expert Rev Anticancer Therapy,* 1**,** 149-58.

JAMIL, S., MOJTABAVI, S., HOJABRPOUR, P., CHEAH, S. & DURONIO, V. 2008. An essential role for MCL-1 in ATR-mediated CHK1 phosphorylation. *Mol Biol Cell,* 19**,** 3212-20.

JEGGO, P. A. & LOBRICH, M. 2007. DNA double-strand breaks: their cellular and clinical impact? *Oncogene,* 26**,** 7717-9.

JIN, J., SHIROGANE, T., XU, L., NALEPA, G., QIN, J., ELLEDGE, S. J. & HARPER, J. W. 2003. SCFbeta-TRCP links CHK1 signaling to degradation of the Cdc25A protein phosphatase. *Genes Dev,* 17**,** 3062-74.

KAELIN, W.G. 2005 The concept of synthetic lethality in the context of anticancer therapy. *Nature Rev Cancer,* 5, 689-698

KASTAN, M. B., ZHAN, Q., EL-DEIRY, W. S., CARRIER, F., JACKS, T., WALSH, W. V., PLUNKETT, B. S., VOGELSTEIN, B. & FORNACE, A. J., JR. 1992. A mammalian cell cycle checkpoint pathway utilizing p53 and GADD45 is defective in ataxia-telangiectasia. *Cell,* 71**,** 587-97.

KAWABE, T. 2004. G2 checkpoint abrogators as anticancer drugs. *Mol Cancer Ther,* 3**,** 513-9.

KEEPERS, Y. P., PIZAO, P. E., PETERS, G. J., VAN ARK-OTTE, J., WINOGRAD, B. & PINEDO, H. M. 1991. Comparison of the sulforhodamine B protein and tetrazolium (MTT) assays for in vitro chemosensitivity testing. *Eur J Cancer,* 27**,** 897-900.

KHANNA, A., KAUKO, O., BOCKELMAN, C., LAINE, A., SCHRECK, I., PARTANEN, J. I., SZWAJDA, A., BORMANN, S., BILGEN, T., HELENIUS, M., POKHAREL, Y. R., PIMANDA, J., RUSSEL, M. R., HAGLUND, C., COLE, K. A., KLEFSTROM, J., AITTOKALLIO, T., WEISS, C., RISTIMAKI, A., VISAKORPI, T. & WESTERMARCK, J. 2013. CHK1 Targeting Reactivates PP2A Tumor Suppressor Activity in Cancer Cells. *Cancer Res,* 73**,** 6757-69.

KHANNA, K. K. & JACKSON, S. P. 2001. DNA double-strand breaks: signaling, repair and the cancer connection. *Nat Genet,* 27**,** 247-54.

KING, C., DIAZ, H., BARNARD, D., BARDA, D., CLAWSON, D., BLOSSER, W., COX, K., GUO, S. & MARSHALL, M. 2014. Characterization and preclinical development of LY2603618: a selective and potent CHK1 inhibitor. *Invest New Drugs,* 32**,** 213-26.

KINSELLA, T. J. 2009. Coordination of DNA mismatch repair and base excision repair processing of chemotherapy and radiation damage for targeting resistant cancers. *Clin Cancer Res,* 15**,** 1853-9.

KOBERLE, B., GRIMALDI, K. A., SUNTERS, A., HARTLEY, J. A., KELLAND, L. R. & MASTERS, J. R. 1997. DNA repair capacity and cisplatin sensitivity of human testis tumour cells. *Int J Cancer.,* 70**,** 551-5.

KREAHLING, J. M., FOROUTAN, P., REED, D., MARTINEZ, G., RAZABDOUSKI, T., BUI, M. M., RAGHAVAN, M., LETSON, D., GILLIES, R. J., ALTIOK, S., 2013. Wee1 inhibition by MK-1775 leads to tumor inhibition and enhances efficacy of gemcitabine in human sarcomas. PLOSone. 8, 1, 1-8

KREMPLER, A., DECKBAR, D., JEGGO, P. A. & LOBRICH, M. 2007. An imperfect G2M checkpoint contributes to chromosome instability following irradiation of S and G2 phase cells. *Cell Cycle,* 6**,** 1682-6.

KUFE, D., SPRIGGS, D., EGAN, E. M. & MUNROE, D. 1984. Relationships among Ara-CTP pools, formation of (Ara-C)DNA, and cytotoxicity of human leukemic cells. *Blood,* 64**,** 54-8.

KYSELA, B., CHOVANEC, M. & JEGGO, P. A. 2005. Phosphorylation of linker histones by DNA-dependent protein kinase is required for DNA ligase IV-dependent ligation in the presence of histone H1. *Proc Natl Acad Sci U S A,* 102**,** 1877-82.

LAM, M. H., LIU, Q., ELLEDGE, S. J., ROSEN, J. M. 2004. CHK1 is haploinsufficient for multiple functions critical to tumor suppression. *Cancer Cell*. 6, 45-59

LARA, P. N., JR., MACK, P. C., SYNOLD, T., FRANKEL, P., LONGMATE, J., GUMERLOCK, P. H., DOROSHOW, J. H. & GANDARA, D. R. 2005.

The cyclin-dependent kinase inhibitor UCN-01 plus cisplatin in advanced solid tumors: a California cancer consortium phase I pharmacokinetic and molecular correlative trial. *Clin Cancer Res,* 11**,** 4444-50.

LEE, J., KUMAGAI, A. & DUNPHY, W. G. 2001. Positive regulation of Wee1 by CHK1 and 14-3-3 proteins. *Mol Biol Cell,* 12**,** 551-63.

LEVINE, A. J. 1997. p53, the cellular gatekeeper for growth and division. *Cell,* 88**,** 323-31.

LI, J. & STERN, D. F. 2005. Regulation of CHK2 by DNA-dependent protein kinase. *J Biol Chem,* 280**,** 12041-50.

LINDAHL, T. 1993. Instability and decay of the primary structure of DNA. *Nature,* 362**,** 709-15.

LIU, Q., GUNTUKU, S., CUI, X. S., MATSUOKA, S., CORTEZ, D., TAMAI, K., LUO, G., CARATTINI-RIVERA, S., DEMAYO, F., BRADLEY, A., DONEHOWER, L. A. & ELLEDGE, S. J. 2000a. CHK1 is an essential kinase that is regulated by ATR and required for the G(2)/M DNA damage checkpoint. *Genes Dev,* 14**,** 1448-59.

LIU, S., OPIYO, S. O., MANTHEY, K., GLANZER, J. G., ASHLEY, A. K., AMERIN, C., TROKSA, K., SHRIVASTAV, M., NICKOLOFF, J. A. & OAKLEY, G. G. 2012. Distinct roles for DNA-PK, ATM and ATR in RPA phosphorylation and checkpoint activation in response to replication stress. *Nucleic Acids Res,* 40**,** 10780-94.

LIU, X., MATSUDA, A. & PLUNKETT, W. 2008. Ataxia-telangiectasia and Rad3-related and DNA-dependent protein kinase cooperate in G2 checkpoint activation by the DNA strand-breaking nucleoside analogue 2'-C-cyano-2'-deoxy-1-beta-D-arabino-pentofuranosylcytosine. *Mol Cancer Ther,* 7**,** 133-42.

LIU, Y., VIDANES, G., LIN, Y. C., MORI, S. & SIEDE, W. 2000b. Characterization of a Saccharomyces cerevisiae homologue of Schizosaccharomyces pombe CHK1 involved in DNA-damage-induced M-phase arrest. *Mol Gen Genet,* 262**,** 1132-46.

LOBRICH, M. & JEGGO, P. A. 2007. The impact of a negligent G2/M checkpoint on genomic instability and cancer induction. *Nat Rev Cancer,* 7**,** 861-9.

LOPEZ, F. J., CUADROS, M., CANO, C., CONCHA, A. & BLANCO, A. 2012. Biomedical application of fuzzy association rules for identifying breast cancer biomarkers. *Medical & biological engineering & computing,* 50**,** 981-90.

MACK, P. C., GANDARA, D. R., LAU, A. H., LARA, P. N., JR., EDELMAN, M. J. & GUMERLOCK, P. H. 2003. Cell cycle-dependent potentiation of cisplatin by UCN-01 in non-small-cell lung carcinoma. *Cancer Chemother Pharmacol,* 51**,** 337-48.

MAHANEY, B. L., MEEK, K. & LEES-MILLER, S. P. 2009. Repair of ionizing radiation-induced DNA double-strand breaks by non-homologous end-joining. *The Biochemical journal,* 417**,** 639-50.

MAILAND, N., FALCK, J., LUKAS, C., SYLJUASEN, R. G., WELCKER, M., BARTEK, J. & LUKAS, J. 2000. Rapid destruction of human Cdc25A in response to DNA damage. *Science,* 288**,** 1425-9.

MARTIN, A. & CLYNES, M. 1993. Comparison of 5 microplate colorimetric assays for in vitro cytotoxicity testing and cell proliferation assays. *Cytotechnology,* 11**,** 49-58.

MASSAGUE, J. 2004. G1 cell-cycle control and cancer. *Nature,* 432**,** 298-306.

MATTHEWS, D. J., YAKES, F. M., CHEN, J., TADANO, M., BORNHEIM, L., CLARY, D. O., TAI, A., WAGNER, J. M., MILLER, N., KIM, Y. D., ROBERTSON, S., MURRAY, L. & KARNITZ, L. M. 2007. Pharmacological abrogation of S-phase checkpoint enhances the anti-tumor activity of gemcitabine in vivo. *Cell Cycle,* 6**,** 104-10.

MATTHEWS, T. P., KLAIR, S., BURNS, S., BOXALL, K., CHERRY, M., FISHER, M., WESTWOOD, I. M., WALTON, M. I., MCHARDY, T., CHEUNG, K. M., VAN MONTFORT, R., WILLIAMS, D., AHERNE, G. W., GARRETT, M. D., READER, J. & COLLINS, I. 2009. Identification of inhibitors of checkpoint kinase 1 through template screening. *J Medicinal Chemistry,* 52**,** 4810-9.

MAUDE, S. L. & ENDERS, G. H. 2005. Cdk inhibition in human cells compromises chk1 function and activates a DNA damage response. *Cancer Res,* 65**,** 780-6.

MCNEELY, S., CONTI, C., SHEIKH, T., PATEL, H., ZABLUDOFF, S., POMMIER, Y., SCHWARTZ, G. & TSE, A. 2010. Chk1 inhibition after replicative stress activates a double strand break response mediated by ATM and DNA-dependent protein kinase. *Cell Cycle,* 9**,** 995-1004.

MITCHELL, C., PARK, M., EULITT, P., YANG, C., YACOUB, A. & DENT, P. 2010a. Poly(ADP-ribose) polymerase 1 modulates the lethality of CHK1 inhibitors in carcinoma cells. *Mol Pharmacol,* 78**,** 909-17.

MITCHELL, J. B., CHOUDHURI, R., FABRE, K., SOWERS, A. L., CITRIN, D., ZABLUDOFF, S. D. & COOK, J. A. 2010b. In vitro and in vivo radiation sensitization of human tumor cells by a novel checkpoint kinase inhibitor, AZD7762. *Clin Cancer Res,* 16**,** 2076-84.

MONTANO, R., CHUNG, I., GARNER, K. M., PARRY, D. & EASTMAN, A. 2012. Preclinical development of the novel CHK1 inhibitor SCH900776 in combination with DNA-damaging agents and antimetabolites. *Mol Cancer Ther,* 11**,** 427-38.

MORENO-HERRERO, F., DE JAGER, M., DEKKER, N. H., KANAAR, R., WYMAN, C. & DEKKER, C. 2005. Mesoscale conformational changes in the DNA-repair complex Rad50/Mre11/Nbs1 upon binding DNA. *Nature,* 437**,** 440-3.

MORGAN, M. A., PARSELS, L. A., ZHAO, L., PARSELS, J. D., DAVIS, M. A., HASSAN, M. C., ARUMUGARAJAH, S., HYLANDER-GANS, L., MOROSINI, D., SIMEONE, D. M., CANMAN, C. E., NORMOLLE, D. P., ZABLUDOFF, S. D., MAYBAUM, J. & LAWRENCE, T. S. 2010. Mechanism of radiosensitization by the CHK1/2 inhibitor AZD7762 involves abrogation of the G2 checkpoint and inhibition of homologous recombinational DNA repair. *Cancer Res,* 70**,** 4972-81.

MOUMEN, A., MASTERSON, P., O'CONNOR, M. J. & JACKSON, S. P. 2005. hnRNP K: an HDM2 target and transcriptional coactivator of p53 in response to DNA damage. *Cell,* 123**,** 1065-78.

MUKHERJEE, B., KESSINGER, C., KOBAYASHI, J., CHEN, B. P., CHEN, D. J., CHATTERJEE, A. & BURMA, S. 2006. DNA-PK phosphorylates histone H2AX during apoptotic DNA fragmentation in mammalian cells. *DNA Repair (Amst),* 5**,** 575-90.

MURGA, M., CAMPANER, S., LOPEZ-CONTRERAS, A. J., TOLEDO, L. I., SORIA, R., MONTANA, M. F., D'ARTISTA, L., SCHLEKER, T., GUERRA, C., GARCIA, E., BARBACID, M., HIDALGO, M., AMATI, B. & FERNANDEZ-CAPETILLO, O. 2011. Exploiting oncogene-induced replicative stress for the selective killing of Myc-driven tumors. *Nat Struct Mol Biol,* 18**,** 1331-5.

MURRAY, A. W. 1995. The genetics of cell cycle checkpoints. *Current opinion Gen Dev,* 5**,** 5-11.

MURRAY, A. W. 2004. Recycling the cell cycle: cyclins revisited. *Cell,* 116**,** 221-34.

NAEGELI, H. & SUGASAWA, K. 2011. The xeroderma pigmentosum pathway: decision tree analysis of DNA quality. *DNA Repair (Amst),* 10**,** 673-83.

NIKJOO, H., O'NEILL, P., WILSON, W. E. & GOODHEAD, D. T. 2001. Computational approach for determining the spectrum of DNA damage induced by ionizing radiation. *Radiation Res,* 156**,** 577-83.

NOLE, F., MUNZONE, E., ZORZINO, L., MINCHELLA, I., SALVATICI, M., BOTTERI, E., MEDICI, M., VERRI, E., ADAMOLI, L., ROTMENSZ, N.,

GOLDHIRSCH, A. & SANDRI, M. T. 2008. Variation of circulating tumor cell levels during treatment of metastatic breast cancer: prognostic and therapeutic implications. *Ann Oncol,* 19**,** 891-7.

NOLL, D., MCGREGOR MASON, T., MILLER, P.S. 2006 Formation and repair of interstrand cross-links in DNA. *Chemical reviews.* 106(2), 277-301.

O'CONNOR, T. R. & LAVAL, J. 1991. Human cDNA expressing a functional DNA glycosylase excising 3-methyladenine and 7-methylguanine. *Biochemical Biophysical Res Comm,* 176**,** 1170-7.

PARSELS, L. A., MORGAN, M. A., TANSKA, D. M., PARSELS, J. D., PALMER, B. D., BOOTH, R. J., DENNY, W. A., CANMAN, C. E., KRAKER, A. J., LAWRENCE, T. S. & MAYBAUM, J. 2009. Gemcitabine sensitization by checkpoint kinase 1 inhibition correlates with inhibition of a Rad51 DNA damage response in pancreatic cancer cells. *Mol Cancer Ther,* 8**,** 45-54.

PARSELS, L. A., QIAN, Y., TANSKA, D. M., GROSS, M., ZHAO, L., HASSAN, M. C., ARUMUGARAJAH, S., PARSELS, J. D., HYLANDER-GANS, L., SIMEONE, D. M., MOROSINI, D., BROWN, J. L., ZABLUDOFF, S. D., MAYBAUM, J., LAWRENCE, T. S. & MORGAN, M. A. 2011. Assessment of CHK1 phosphorylation as a pharmacodynamic biomarker of CHK1 inhibition. *Clin Cancer Res,* 17**,** 3706-15.

PATIL, M., PABLA, N. & DONG, Z. 2013. Checkpoint kinase 1 in DNA damage response and cell cycle regulation. *Cell Mol Life Sci,* 70**,** 4009-21.

PAULOVICH, A. G., TOCZYSKI, D. P. & HARTWELL, L. H. 1997. When checkpoints fail. *Cell,* 88**,** 315-21.

PEASLAND, A., WANG, L. Z., ROWLING, E., KYLE, S., CHEN, T., HOPKINS, A., CLIBY, W. A., SARKARIA, J., BEALE, G., EDMONDSON, R. J. & CURTIN, N. J. 2011. Identification and evaluation of a potent novel ATR inhibitor, NU6027, in breast and ovarian cancer cell lines. *Brit J Cancer,* 105**,** 372-81.

PENG, C. Y., GRAVES, P. R., THOMA, R. S., WU, Z., SHAW, A. S. & PIWNICA-WORMS, H. 1997. Mitotic and G2 checkpoint control: regulation of 14-3-3 protein binding by phosphorylation of Cdc25C on serine-216. *Science,* 277**,** 1501-5.

PEREZ, R. P., LEWIS, L. D., BEELEN, A. P., OLSZANSKI, A. J., JOHNSTON, N., RHODES, C. H., BEAULIEU, B., ERNSTOFF, M. S. & EASTMAN, A. 2006. Modulation of cell cycle progression in human tumors: a pharmacokinetic and tumor molecular pharmacodynamic study of cisplatin plus the CHK1 inhibitor UCN-01 (NSC 638850). *Clin Cancer Res,* 12**,** 7079-85.

PETERSEN, L., HASVOLD, G., LUKAS, J., BARTEK, J. & SYLJUASEN, R. G. 2010. p53-dependent G(1) arrest in 1st or 2nd cell cycle may protect human cancer cells from cell death after treatment with ionizing radiation and CHK1 inhibitors. *Cell Prolif,* 43**,** 365-71.

PINEDO, H. M. & PETERS, G. F. 1988. Fluorouracil: biochemistry and pharmacology. *J Clin Oncology,* 6**,** 1653-64.

PLUNKETT, W., HUANG, P. & GANDHI, V. 1995. Preclinical characteristics of gemcitabine. *Anti-cancer drugs,* 6 Suppl 6**,** 7-13.

POMMIER, Y., KOHLHAGEN, G., WU, C. & SIMMONS, D. T. 1998a. Mammalian DNA topoisomerase I activity and poisoning by camptothecin are inhibited by simian virus 40 large T antigen. *Biochemistry,* 37**,** 3818-23.

POMMIER, Y., POURQUIER, P., FAN, Y. & STRUMBERG, D. 1998b. Mechanism of action of eukaryotic DNA topoisomerase I and drugs targeted to the enzyme. *Biochimica et biophysica acta,* 1400**,** 83-105.

POWELL, S. N., DEFRANK, J. S., CONNELL, P., EOGAN, M., PREFFER, F., DOMBKOWSKI, D., TANG, W. & FRIEND, S. 1995. Differential sensitivity of p53(-) and p53(+) cells to caffeine-induced radiosensitization and override of G2 delay. *Cancer Res,* 55**,** 1643-8.

PREVO, R., FOKAS, E., REAPER, P. M., CHARLTON, P. A., POLLARD, J. R., MCKENNA, G., BRUNNER, T. B., 2014. The novel ATR inhibitor VE-821 increases sensitivity of pancreatic cancer cells to radiation and chemotherapy. *Cancer Bio Ther*, 13, 1072-1081

QVARNSTROM, O. F., SIMONSSON, M., JOHANSSON, K. A., NYMAN, J. & TURESSON, I. 2004. DNA double strand break quantification in skin biopsies. *Radiother Oncol,* 72**,** 311-7.

RAYMOND, E., FAIVRE, S., WOYNAROWSKI, J. M. & CHANEY, S. G. 1998. Oxaliplatin: mechanism of action and antineoplastic activity. *Sem Oncology,* 25**,** 4-12.

REDON, C. E., NAKAMURA, A. J., ZHANG, Y. W., JI, J. J., BONNER, W. M., KINDERS, R. J., PARCHMENT, R. E., DOROSHOW, J. H. & POMMIER, Y. 2010. Histone {gamma}H2AX and Poly(ADP-Ribose) as Clinical Pharmacodynamic Biomarkers. *Clin Cancer Res,* 16**,** 4532-42.

REINHARDT, H. C. & YAFFE, M. B. 2009. Kinases that control the cell cycle in response to DNA damage: CHK1, CHK2, and MK2. *Curr Opin Cell Biol,* 21**,** 245-55.

RIXE, O., ORTUZAR, W., ALVAREZ, M., PARKER, R., REED, E., PAULL, K. & FOJO, T. 1996. Oxaliplatin, tetraplatin, cisplatin, and carboplatin: spectrum of activity in drug-resistant cell lines and in the cell lines of the National Cancer Institute's Anticancer Drug Screen panel. *Biochemical pharmacology,* 52**,** 1855-65.

ROGAKOU, E. P., PILCH, D. R., ORR, A. H., IVANOVA, V. S. & BONNER, W. M. 1998. DNA double-stranded breaks induce histone H2AX phosphorylation on serine 139. *J Biol Chem,* 273**,** 5858-68.

RUSSELL, K. J., WIENS, L. W., DEMERS, G. W., GALLOWAY, D. A., PLON, S. E. & GROUDINE, M. 1995. Abrogation of the G2 checkpoint results in differential radiosensitization of G1 checkpoint-deficient and G1 checkpoint-competent cells. *Cancer Res,* 55**,** 1639-42.

SAFFHILL, R., MARGISON, G. P. & O'CONNOR, P. J. 1985. Mechanisms of carcinogenesis induced by alkylating agents. *Biochimica et biophysica acta,* 823**,** 111-45.

SANCHEZ, Y., WONG, C., THOMA, R. S., RICHMAN, R., WU, Z., PIWNICA-WORMS, H. & ELLEDGE, S. J. 1997. Conservation of the CHK1 checkpoint pathway in mammals: linkage of DNA damage to Cdk regulation through Cdc25. *Science,* 277**,** 1497-501.

SANCHEZ-PALENCIA, A., GOMEZ-MORALES, M., GOMEZ-CAPILLA, J. A., PEDRAZA, V., BOYERO, L., ROSELL, R. & FAREZ-VIDAL, M. E. 2011. Gene expression profiling reveals novel biomarkers in nonsmall cell lung cancer. *Int J Cancer,* 129**,** 355-64.

SAUSVILLE, E., LOROSSO, P., CARDUCCI, M. A., BARKER, P. N., AGBO, F., OAKES, P. & SENDEROWICZ, A. M. 2011. Phase 1dose-escalationstudy of AZD7762 in combination with gemcitabine (gem) in patients (pts) with advanced solid tumours. *ASCO Annual Meeting 2011.*

SAUSVILLE, E., LORUSSO, P., CARDUCCI, M., CARTER, J., QUINN, M. F., MALBURG, L., AZAD, N., COSGROVE, D., KNIGHT, R., BARKER, P., ZABLUDOFF, S., AGBO, F., OAKES, P. & SENDEROWICZ, A. 2014. Phase I dose-escalation study of AZD7762, a checkpoint kinase inhibitor, in combination with gemcitabine in US patients with advanced solid tumors. *Cancer Chemother Pharmacol,* 73**,** 539-49.

SAUSVILLE, E. A., ARBUCK, S. G., MESSMANN, R., HEADLEE, D., BAUER, K. S., LUSH, R. M., MURGO, A., FIGG, W. D., LAHUSEN, T., JAKEN, S., JING, X., ROBERGE, M., FUSE, E., KUWABARA, T. & SENDEROWICZ, A. M. 2001. Phase I trial of 72-hour continuous infusion UCN-01 in patients with refractory neoplasms. *J Clin Oncol,* 19**,** 2319-33.

SEHL, M. E., LANGER, L. R., PAPP, J. C., KWAN, L., SELDON, J. L., ARELLANO, G., REISS, J., REED, E. F., DANDEKAR, S., KORIN, Y., SINSHEIMER, J. S., ZHANG, Z. F. & GANZ, P. A. 2009. Associations between single nucleotide polymorphisms in double-stranded DNA repair pathway genes and familial breast cancer. *Clin Cancer Res,* 15**,** 2192-203.

SERRANO, M. A., LI, Z., DANGETI, M., MUSICH, P. R., PATRICK, S., ROGINSKAYA, M., CARTWRIGHT, B. & ZOU, Y. 2013. DNA-PK, ATM and ATR collaboratively regulate p53-RPA interaction to facilitate homologous recombination DNA repair. *Oncogene,* 32**,** 2452-62.

SETO, T., ESAKI, T., HIRAI, F., ARITA, S., NOSAKI, K., MAKIYAMA, A., KOMETANI, T., FUJIMOTO, C., HAMATAKE, M., TAKEOKA, H., AGBO, F. & SHI, X. 2013. Phase I, dose-escalation study of AZD7762 alone and in combination with gemcitabine in Japanese patients with advanced solid tumours. *Cancer Chemother Pharmacol,* 72**,** 619-27.

SHAO, R. G., CAO, C. X., ZHANG, H., KOHN, K. W., WOLD, M. S. & POMMIER, Y. 1999. Replication-mediated DNA damage by camptothecin induces phosphorylation of RPA by DNA-dependent protein kinase and dissociates RPA:DNA-PK complexes. *EMBO J,* 18**,** 1397-406.

SHAPIRO, G. I. & HARPER, J. W. 1999. Anticancer drug targets: cell cycle and checkpoint control. *J Clin Invest,* 104**,** 1645-53.

SHARMA, S., SINGH, M. & SHARMA, P. L. 2011. Beneficial effect of insulin in hyperhomocysteinemia and diabetes mellitus-induced vascular endothelium dysfunction: role of phosphoinositide dependent kinase and protein kinase B. *Mol Cell Biochem,* 348**,** 21-32.

SHERR, C. J. 1996. Cancer cell cycles. *Science,* 274**,** 1672-7.

SHEWACH, D. S. & LAWRENCE, T. S. 2007. Antimetabolite radiosensitizers. *J Clin Oncology,* 25**,** 4043-50.

SHIBATA, A., CONRAD, S., BIRRAUX, J., GEUTING, V., BARTON, O., ISMAIL, A., KAKAROUGKAS, A., MEEK, K., TAUCHER-SCHOLZ, G., LOBRICH, M. & JEGGO, P. A. 2011. Factors determining DNA double-strand break repair pathway choice in G2 phase. *EMBO J,* 30**,** 1079-92.

SHILOH, Y. 2003. ATM and related protein kinases: safeguarding genome integrity. *Nat Rev Cancer,* 3**,** 155-68.

SHILOH, Y. 2006. The ATM-mediated DNA-damage response: taking shape. *Trends Biochem Sci,* 31**,** 402-10.

SHRIVASTAV, M., DE HARO, L. P. & NICKOLOFF, J. A. 2008. Regulation of DNA double-strand break repair pathway choice. *Cell Res,* 18**,** 134-47.

SIDDIK, Z. H. 2003. Cisplatin: mode of cytotoxic action and molecular basis of resistance. *Oncogene,* 22**,** 7265-79.

SKEHAN, P., STORENG, R., SCUDIERO, D., MONKS, A., MCMAHON, J., VISTICA, D., WARREN, J. T., BOKESCH, H., KENNEY, S. & BOYD, M. R. 1990. New colorimetric cytotoxicity assay for anticancer-drug screening. *J Natl Cancer Inst,* 82**,** 1107-12.

SORENSEN, C. S., HANSEN, L. T., DZIEGIELEWSKI, J., SYLJUASEN, R. G., LUNDIN, C., BARTEK, J. & HELLEDAY, T. 2005. The cell-cycle checkpoint kinase CHK1 is required for mammalian homologous recombination repair. *Nat Cell Biol,* 7**,** 195-201.

SORENSEN, C. S., SYLJUASEN, R. G., FALCK, J., SCHROEDER, T., RONNSTRAND, L., KHANNA, K. K., ZHOU, B. B., BARTEK, J. & LUKAS, J. 2003. CHK1 regulates the S phase checkpoint by coupling the physiological turnover and ionizing radiation-induced accelerated proteolysis of Cdc25A. *Cancer Cell,* 3**,** 247-58.

SYLJUASEN, R. G., SORENSEN, C. S., NYLANDSTED, J., LUKAS, C., LUKAS, J. & BARTEK, J. 2004. Inhibition of CHK1 by CEP-3891 accelerates mitotic nuclear fragmentation in response to ionizing Radiation. *Cancer Res,* 64**,** 9035-40.

TAKATA, M., SASAKI, M. S., SONODA, E., MORRISON, C., HASHIMOTO, M., UTSUMI, H., YAMAGUCHI-IWAI, Y., SHINOHARA, A. & TAKEDA, S. 1998. Homologous recombination and non-homologous end-joining pathways of DNA double-strand break repair have overlapping roles in the maintenance of chromosomal integrity in vertebrate cells. *EMBO J,* 17**,** 5497-508.

TAO, Y., LETEUR, C., YANG, C., ZHANG, P., CASTEDO, M., PIERRE, A., GOLSTEYN, R. M., BOURHIS, J., KROEMER, G. & DEUTSCH, E. 2009. Radiosensitization by Chir-124, a selective CHK1 inhibitor: effects of p53 and cell cycle checkpoints. *Cell Cycle,* 8**,** 1196-205.

TEOULE, R. 1987. Radiation-induced DNA damage and its repair. *Int J Rad Bio,* 51**,** 573-89.

THERASSE, P., ARBUCK, S.G., EISENHAUER, E.A., WANDERS, J., KAPLAN, R.S., RUBINSTEIN, L., VERWEIJ, J., GLABBEKE, M., OOSTEROM, A.T., CHRISTIAN, M.C., GWYTHER, S.G.. 2000. New guidelines to evaluate the response to treatment in solid tumors. *J Nat Cancer Inst*. 92, 205–216

TRICKER, A. R., & PREUSSMANN, R. 1991. Carcinogenic N-nitrosamines in the diet: occurrence, formation, mechanisms and carcinogenic potential. *Mutation Res*. 259, 277-289

TSE, A. N., CARVAJAL, R. & SCHWARTZ, G. K. 2007a. Targeting checkpoint kinase 1 in cancer therapeutics. *Clin Cancer Res,* 13**,** 1955-60.

TSE, A. N., RENDAHL, K. G., SHEIKH, T., CHEEMA, H., AARDALEN, K., EMBRY, M., MA, S., MOLER, E. J., NI, Z. J., LOPES DE MENEZES, D. E., HIBNER, B., GESNER, T. G. & SCHWARTZ, G. K. 2007b. CHIR-124, a novel potent inhibitor of CHK1, potentiates the cytotoxicity of topoisomerase I poisons in vitro and in vivo. *Clin Cancer Res,* 13**,** 591-602.

TSUZUKI, T., SAKUMI, K., SHIRAISHI, A., KAWATE, H., IGARASHI, H., IWAKUMA, T., TOMINAGA, Y., ZHANG, S., SHIMIZU, S., ISHIKAWA, T. & ET AL. 1996. Targeted disruption of the DNA repair methyltransferase gene renders mice hypersensitive to alkylating agent. *Carcinogenesis,* 17**,** 1215-20.

TUBBS, J. L., PEGG, A. E. & TAINER, J. A. 2007. DNA binding, nucleotide flipping, and the helix-turn-helix motif in base repair by O6-alkylguanine-DNA alkyltransferase and its implications for cancer chemotherapy. *DNA repair,* 6**,** 1100-15.

VALKO, M., RHODES, C. J., MONCOL, J., IZAKOVIC, M. & MAZUR, M. 2006. Free radicals, metals and antioxidants in oxidative stress-induced cancer. *Chemico-biological interactions,* 160**,** 1-40.

VAN ATTIKUM, H. & GASSER, S. M. 2005. ATP-dependent chromatin remodeling and DNA double-strand break repair. *Cell Cycle,* 4**,** 1011-4.

VAN MAANEN, J. M., RETEL, J., DE VRIES, J. & PINEDO, H. M. 1988. Mechanism of action of antitumor drug etoposide: a review. *J Nat Cancer Inst,* 80**,** 1526-33.

VANCE, S., LIU, E., ZHAO, L., PARSELS, J. D., PARSELS, L. A., BROWN, J. L., MAYBAUM, J., LAWRENCE, T. S. & MORGAN, M. A. 2011. Selective radiosensitization of p53 mutant pancreatic cancer cells by combined inhibition of CHK1 and PARP1. *Cell Cycle,* 10**,** 4321-9.

VILENCHIK, M. M. & KNUDSON, A. G. 2003. Endogenous DNA double-strand breaks: production, fidelity of repair, and induction of cancer. *Proc Natl Acad Sci U S A,* 100**,** 12871-6.

VOGELSTEIN, B., LANE, D. & LEVINE, A. J. 2000. Surfing the p53 network. *Nature,* 408**,** 307-10.

WAGNER, J. M. & KARNITZ, L. M. 2009. Cisplatin-induced DNA damage activates replication checkpoint signaling components that differentially affect tumor cell survival. *Mol Pharmacol,* 76**,** 208-14.

WALTON, M. I., EVE, P. D., HAYES, A., VALENTI, M., DE HAVEN BRANDON, A., BOX, G., BOXALL, K. J., AHERNE, G. W., ECCLES, S. A., RAYNAUD, F. I., WILLIAMS, D. H., READER, J. C., COLLINS, I. & GARRETT, M. D. 2010. The preclinical pharmacology and therapeutic activity of the novel CHK1 inhibitor SAR-020106. *Mol Cancer Ther,* 9**,** 89-100.

WALTON, M. I., EVE, P. D., HAYES, A., VALENTI, M. R., DE HAVEN BRANDON, A. K., BOX, G., HALLSWORTH, A., SMITH, E. L., BOXALL, K. J., LAINCHBURY, M., MATTHEWS, T. P., JAMIN, Y., ROBINSON, S. P., AHERNE, G. W., READER, J. C., CHESLER, L., RAYNAUD, F. I., ECCLES, S. A., COLLINS, I. & GARRETT, M. D. 2012. CCT244747 is a novel potent and selective CHK1 inhibitor with oral efficacy alone and in combination with genotoxic anticancer drugs. *Clin Cancer Res,* 18**,** 5650-61.

WANG, F. Z., FEI, H. R., CUI, Y. J., SUN, Y. K., LI, Z. M., WANG, X. Y., YANG, X. Y., ZHANG, J. G. & SUN, B. L. 2014. The checkpoint 1 kinase inhibitor LY2603618 induces cell cycle arrest, DNA damage response and autophagy in cancer cells. *Apoptosis,* 19**,** 1389-98.

WANG, S. W., NORBURY, C., HARRIS, A. L. & TODA, T. 1999. Caffeine can override the S-M checkpoint in fission yeast. *J Cell Sci,* 112 (Pt 6)**,** 927-37.

WEINSTEIN, J. N. & LORENZI, P. L. 2013. Cancer: Discrepancies in drug sensitivity. *Nature,* 504**,** 381-3.

WEISS, G. J., DONEHOWER, R. C., IYENGAR, T., RAMANATHAN, R. K., LEWANDOWSKI, K., WESTIN, E., HURT, K., HYNES, S. M., ANTHONY, S. P. & MCKANE, S. 2013. Phase I dose-escalation study to examine the safety and tolerability of LY2603618, a checkpoint 1 kinase inhibitor, administered 1 day after pemetrexed 500 mg/m(2) every 21 days in patients with cancer. *Invest New Drugs,* 31**,** 136-44.

WURMBACH, E., CHEN, Y. B., KHITROV, G., ZHANG, W., ROAYAIE, S., SCHWARTZ, M., FIEL, I., THUNG, S., MAZZAFERRO, V., BRUIX, J., BOTTINGER, E., FRIEDMAN, S., WAXMAN, S. & LLOVET, J. M. 2007. Genome-wide molecular profiles of HCV-induced dysplasia and hepatocellular carcinoma. *Hepatology,* 45**,** 938-47.

XIA, Z., DICKENS, M., RAINGEAUD, J., DAVIS, R. J. & GREENBERG, M. E. 1995. Opposing effects of ERK and JNK-p38 MAP kinases on apoptosis. *Science,* 270**,** 1326-31.

XIE, K. C. & PLUNKETT, W. 1996. Deoxynucleotide pool depletion and sustained inhibition of ribonucleotide reductase and DNA synthesis after treatment of human lymphoblastoid cells with 2-chloro-9-(2-deoxy-2-fluoro-beta-D-arabinofuranosyl) adenine. *Cancer Res,* 56**,** 3030-7.

YANG, H., YOON, S. J., JIN, J., CHOI, S. H., SEOL, H. J., LEE, J. I., NAM, D. H. & YOO, H. Y. 2011. Inhibition of checkpoint kinase 1 sensitizes lung cancer brain metastases to radiotherapy. *Biochemical Biophysical Res Comm,* 406**,** 53-8.

YOSHIYAMA, K. O., SAKAGUCHI, K. & KIMURA, S. 2013. DNA damage response in plants: conserved and variable response compared to animals. *Biology (Basel),* 2**,** 1338-56.

YOUNG, C. W. & HODAS, S. 1964. Hydroxyurea: Inhibitory Effect on DNA Metabolism. *Science,* 146**,** 1172-4.

ZABLUDOFF, S. D., DENG, C., GRONDINE, M. R., SHEEHY, A. M., ASHWELL, S., CALEB, B. L., GREEN, S., HAYE, H. R., HORN, C. L., JANETKA, J. W., LIU, D., MOUCHET, E., READY, S., ROSENTHAL, J. L., QUEVA, C., SCHWARTZ, G. K., TAYLOR, K. J., TSE, A. N., WALKER, G. E. & WHITE, A. M. 2008. AZD7762, a novel checkpoint kinase inhibitor, drives checkpoint abrogation and potentiates DNA-targeted therapies. *Mol Cancer Ther,* 7**,** 2955-66.

ZACHOS, G., BLACK, E. J., WALKER, M., SCOTT, M. T., VAGNARELLI, P., EARNSHAW, W. C. & GILLESPIE, D. A. 2007. CHK1 is required for spindle checkpoint function. *Dev Cell,* 12**,** 247-60.

ZAIDI, S. H., HUDDART, R. A. & HARRINGTON, K. J. 2009. Novel targeted radiosensitisers in cancer treatment. *Curr Drug Discov Technol,* 6**,** 103-34.

ZENVIRT, S., KRAVCHENKO-BALASHA, N. & LEVITZKI, A. 2010. Status of p53 in human cancer cells does not predict efficacy of CHK1 kinase inhibitors combined with chemotherapeutic agents. *Oncogene*.

ZHANG, C., YAN, Z., PAINTER, C. L., ZHANG, Q., CHEN, E., ARANGO, M. E., KUSZPIT, K., ZASADNY, K., HALLIN, M., HALLIN, J., WONG, A., BUCKMAN, D., SUN, G., QIU, M., ANDERES, K. & CHRISTENSEN, J. G. 2009. PF-00477736 mediates checkpoint kinase 1 signaling pathway and potentiates docetaxel-induced efficacy in xenografts. *Clin Cancer Res,* 15**,** 4630-40.

ZHAO, H. & PIWNICA-WORMS, H. 2001. ATR-mediated checkpoint pathways regulate phosphorylation and activation of human CHK1. *Mol Cell Biol,* 21**,** 4129-39.

ZHOU, B. B. & ELLEDGE, S. J. 2000. The DNA damage response: putting checkpoints in perspective. *Nature,* 408**,** 433-9.